Rock-forming Minerals in Thin Section

Rock-forming Minerals in Thin Section

H. Pichler

Professor of Mineralogy, Petrology and Geochemistry
University of Tübingen
Germany

and

C. Schmitt-Riegraf

Lecturer in Mineralogy
University of Münster
Germany

Translated by

L. Hoke

Institute of Geological and Nuclear Sciences
New Zealand

CHAPMAN & HALL
London · Weinheim · New York · Tokyo · Melbourne · Madras

Published by Chapman & Hall, 2–6 Boundary Row, London SE1 8HN, UK

Chapman & Hall, 2–6 Boundary Row, London SE1 8HN, UK

Chapman & Hall GmbH, Pappelallee 3, 69469 Weinheim, Germany

Chapman & Hall USA, 115 Fifth Avenue, New York, NY 10003, USA

Chapman & Hall Japan, ITP-Japan, Kyowa Building, 3F, 2-2-1 Hirakawacho, Chiyoda-ku, Tokyo 102, Japan

Chapman & Hall Australia, 102 Dodds Street, South Melbourne, Victoria 3205, Australia

Chapman & Hall India, R. Seshadri, 32 Second Main Road, CIT East, Madras 600 035, India

English language edition 1997

Original German edition *Gesteinsbildende Minerale im Dünnschliff*

Softcover reprint of the hardcover 2nd edition 1993

Typeset in 9/10 pt Times by Best-set Typesetter Ltd, Hong Kong

ISBN-13:978-94-010-7145-1 e-ISBN-13:978-94-009-1443-8
DOI:10.1007/978-94-009-1443-8

A catalogue record for this book is available from the British Library

Library of Congress Catalog Card Number: 96-86163

Contents

Colour plate section appears between pages 134 and 135

Part C Appendices

Preface to the English edition

The use of a polarizing microscope is still an essential tool for every earth scientist who does petrographic work. No student in mineralogy, petrography and petrology, geology and mining geology should leave university without knowledge of this fundamental method for determining minerals and rocks, which in 1850 revolutionized our science and placed it on firm foundations.

In German geological literature, this is the first short comprehensive teaching book about using a microscope in the identification of minerals for at least fifty years. The classic German works of this kind, such as those by Weinschenk (1915) and Chudoba (1932), opened up polarizing microscopy to earlier generations, including one of the authors (H.P.) These have long been out of print and outdated. Therefore, in order to close this gap and to provide future earth scientists with guidelines in practical microscopy, we have compiled these notes, which have been used and developed over many years at the Mineralogical Institute in Tübingen. In writing this book the following guidelines were used:

1. The contents focus on rock-forming minerals. In our selection, we have been generous and have also included some rare minerals, such as perovskite, pyrochlore, koppite, cancrinite, etc. We selected those minerals that are familiar, occur in rocks of central Europe, and that are well represented in rock collections. The rare minerals occur in volcanic and subvolcanic rocks of the Kaiserstuhl, the Hegau, Schwäbische Alb and in the Laacher volcanic areas of Germany.

2. We give emphasis to the common minerals. They are shown in the tables in bold letters; the less common and not so important minerals are shown in normal type. Rare minerals and also special rock-forming minerals which belong to salt and clay-rich rocks and soils are not covered in this book; we refer the reader to more specialized books, in particular Tröger (1982, 1969). The Tröger edition (1969), unfortunately out of print, is recommended as an essential reference book.

3. Important data are presented in table form. The tables at the end of the book complement the more descriptive text, which the microscope user should use in the identification of minerals. Tables 6 and 7a–7d are particularly useful.

4. In order to make it easier for the beginner we start off with the principles of polarization microscopy. This part is short and places emphasis on the practical applications. The microscope user should know which observations can and should be made in plane-polarized light and which ones in crossed polarized light; how to determine the optical character of the optical elongation; what straight, symmetric and inclined extinctions are, and how to make observations in the conoscopic path of light. Comprehending indicatrix models requires knowledge of the relationship between crystal symmetry and its optical characteristics. All these points are covered in the first part of this book. Literature for further reading about polarization microscopy is listed in the Bibliography. In particular we recommend the clearly written, very practical small book by Müller and Raith (1987).

5. Importance of paragenesis. The coexistence of certain minerals in assemblages is characteristic for most rocks. For instance, as a general rule, if a volcanic rock contains a mineral of the sodalite group then quartz will not be present. However, minerals such as nepheline, leucite, aegirine-augite and melanite can be expected. Consideration of possible paragenesis can help in the search and identification of minerals.

6. Photomicrographs and black and white diagrams. We have tried to show all minerals described here either as a drawing (by C. S.-R.) or as a photomicrograph (by Manfred Pfleghaar).

We are pleased that, through this translation, it has been possible to bring this book to the attention of the English-speaking mineralogy community.

Hans Pichler
Cornelia Schmitt-Riegraf
Tübingen

Preface to the German second edition

Apart from some improvements to the text and updating the optical data, some black-and-white photomicrographs were replaced by better ones, photographed by C. S.-R. In addition some new figures showing crystal forms and optical parameters, which for a number of minerals were missing in the first edition, were added; the number of illustrations has been increased to a total of 114.

We are grateful to all colleagues who have sent us suggestions for improvements. We look forward to further suggestions and comments.

Hans Pichler
Cornelia Schmitt-Riegraf
Tübingen and Münster

Symbols and abbreviations

$\parallel$	Parallel
n	Refraction
n_ω (= n_o)	Index of refraction of ordinary light waves
n_ε (= n_e)	Index of refraction of extraordinary light waves
$n_\alpha < n_\beta < n_\gamma$ (= $n_X < n_Y < n_Z$)	Main refraction indices
Δ	Maximum double refraction
$\oplus$	Optimum positive
$\ominus$	Optimum negative
MZ (+)	Main positive zone/positive character of elongation
MZ (–)	Main negative zone/negative character of elongation
$2V_\alpha$ (= $2V_x$)	Axis angle round the negative centre line
$2V_\gamma$ (= $2V_z$)	Axis angle round the positive centre line
$\gamma \wedge c$	Angle between γ and c
#	Cleavage
nm	Nanometer
Opt. ch.	Optical character

Crystallographical terms

Crystallographical graph axes	a, b, c
cub.	Cubic
hex.	Hexagonal
trig.	Trigonal
tetr.	Tetragonal
rhomb.	Orthorhombic
monocl.	Monoclinic
tricl.	Triclinic
ps.-cub.	Pseudo-cubic
ps.-hex.	Pseudo-hexagonal

Abbreviations of mineral names in illustrations and tables

Ab	Albite
Ae	Aegirine-augite
Ak	Actinolite
An	Anorthite
Ap	Apatite
Bi	Biotite
Cc	Calcite
Ch	Chalcedony
Chl	Chlorite
Cpx	Clinopyroxene
Co	Cordierite
Ep	Epidote
Gl	Volcanic glass
Go	Goethite
Gr	Garnet
Ha	Hauyne
Hbl	Hornblende
Kf	K-feldspar
Ky	Kyanite
LG	Lithium-mica
Mu	Muscovite
Ne	Nepheline
Ol	Olivine
Opx	Orthopyroxene
Or	Orthoclase
Pl	Plagioclase
Py	Pyroxene
Q	Quartz
So	Sodalite
St	Staurolite
TA	Titanaugite
Ze	Zeolite

Part A Optical Crystallography

1 The polarizing microscope

1.1 Microscope components and their function

The polarizing microscope is a specialized magnification instrument. It is equipped with two polarizers which enable minerals to be examined under plane-polarized light, for their birefringence and refraction characteristics.

Modern microscopes are of a box-like construction equipped with the optical parts as shown in Fig. 1. The polarizer converts unpolarized light, which is emitted from the microscope's light, source and which vibrates in numerous directions, into polarized light, which vibrates within a single plane. The vibration direction of the plane-polarized light traditionally has an E–W privileged direction parallel to the horizontal line of the cross-hairs in the ocular. As polarized light, it travels through the thin mineral section and undergoes a number of changes which can be examined either with or without an analyser. This is a second polarizer with the privileged direction in N–S orientation (parallel to the vertical line of the cross-hairs in the ocular). If an object is viewed with the analyser inserted, it is said to be viewed under crossed nicols or crossed polars. In older microscopes the privileged directions of the polarizer and analyser can be reversed.

Below the rotatable microscope stage is the condensing unit (Fig. 2). In the case of orthoscopic observations at low magnifications, the upper condensing lens is not used and is swung out of the path of light. When working at high magnifications (using a ×10 objective lens or higher) or looking at interference figures in the conoscopic path of light, the upper condensing lens is used.

Care must be taken to ensure that the condensing lens is positioned directly below the object, thus providing optimum illumination. At low magnifications and during orthoscopic viewing,

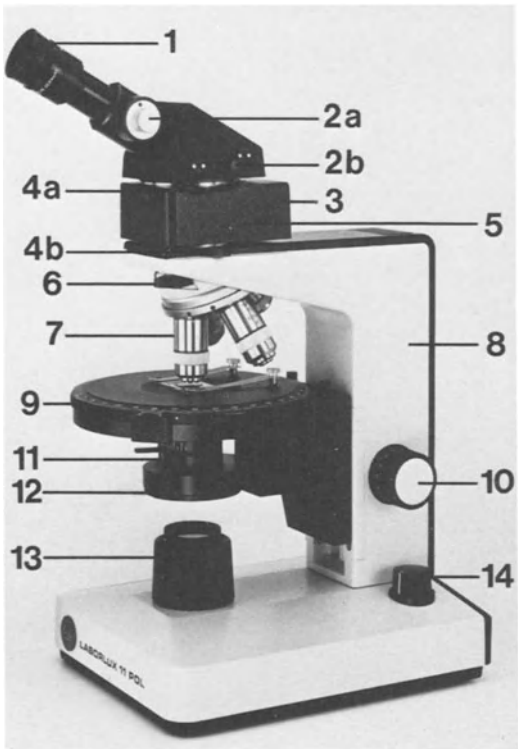

Fig. 1 Components of a student microscope (LABOR-LUX 11 POL, Leitz).

1	Ocular with cross-hair and adjustable eye-piece.
2a	Iris diaphragm.
2b	Amici Bertrand lens.
3	Analyser (withdrawal, far side of microscope).
4a,b	Mechanism to slot in, exchange or remove the microscope tube.
5	Intermediate tubus piece.
6	Compensator slot.
7	Objective.
8	Microscope stand.
9	Circular rotatable stage with a vernier index and a pair of stage clips.
10	Combined coarse and fine adjustment to set the position of the stage.
11	Condensing lens and iris diaphragm.
12	Rotatable polarizer.
13	Microscope light source with adjustable aperture.
14	Adjustment of light.

the condensing lens might have to be slightly lowered to achieve the best illumination.

The substage assembly consisting of condenser lenses and an iris diaphragm are used to provide the best illumination for the object. The iris diaphragm (Fig. 2) may be opened or closed as desired by the turn of a lever. In orthoscopic light it is kept at a narrower setting than in conoscopic light.

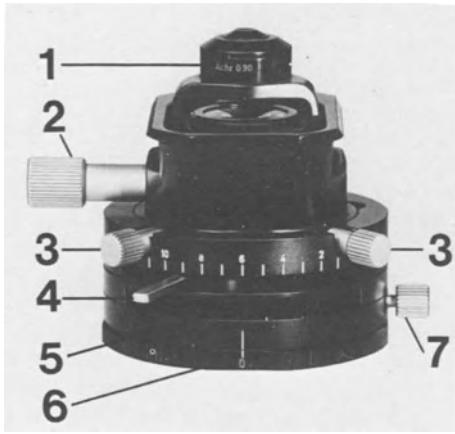

Fig. 2 Example of a substage polarizer and condensing lens set-up.

1 Exchangeable condensing lens head.
2 Adjustment levers for swinging the condensing lens into and out of the path of light.
3 Centring screws for adjusting the condensing lens.
4 Lever to adjust the iris diaphragm.
5 Slot for inserting the λ/4 plate for circular polarization.
6 Rotatable polarizer.
7 Screw to control the position of the polarizer.

The rotatable microscope stage should rotate freely around the microscope axis and be calibrated so that degrees of rotation can be determined on a vernier index. This allows precise angular measurements to be made.

Modern microscopes tend to have several objective lenses that can be rotated into the path of light. Generally three objectives suffice for a student microscope: a low-power objective (×2.5 or 4) provides a good overall view of the thin section, whereas at medium (×10) and high (×40, 45 or 63) magnification more detailed observations can be made, such as determination of the extinction angle, cleavage intersection angle and indicatrix observations in the conoscopic light path.

The engravings on the objective lenses (Fig. 3) give the following characteristics: 160/0.17 means that the achromatic objective has a free working distance of 160 mm and the thin section must have a cover glass which is 0.17 mm thick. The engraving 25/0.50 gives the magnification (×25) and the aperture width of 0.5 mm. Letters such as NPI (not present in Fig. 3) give additional information (NPI = plane chromatic); an additional P means that the objective is tension free.

The ocular increases the convergence of light rays from the objective lens so that the real image can be seen. It should have a pair of mutually perpendicular cross-hairs, which mark the two privileged directions of the polarizer and analyser.

The Bertrand lens is used when the object is viewed in the conoscopic light path. This lens tends to be positioned above the analyser on the right-hand side (Fig. 1) and can be inserted into the light path as desired.

The different light paths for orthoscopic and conoscopic observations are shown in Table 1.

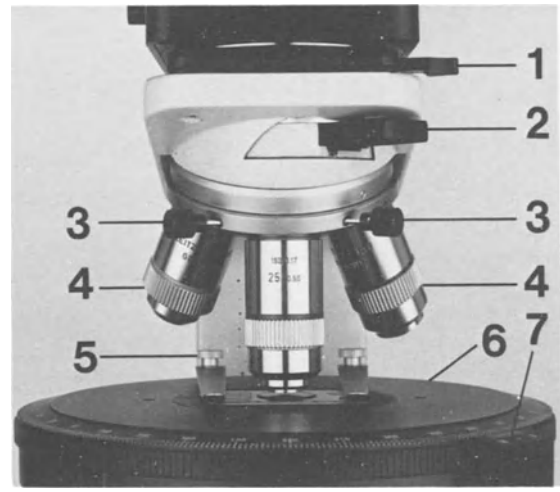

Fig. 3 Objectives (LABORLUX 11 POL, Leitz).

1 Lever to fix or loosen the intermediate microscope tube.
2 Microscope tube slot with inserted compensator.
3 Centring screw for objective.
4 Objective showing engravings (explanation in text).
5 Springs to hold the thin section in position.
6 Rotatable microscope stage with degree markings engraved around its edge.
7 Nonius to read off rotations of the microscope stage to $\frac{1}{10}°$ accuracy.

1.2 Accessory equipment

Transformer

Power for the light source is supplied via a transformer.

Accessories

Accessory anisotropic plates and wedges are used to determine the direction and size of vibration of light in the crystal when viewed under crossed nicols. They possess two mutually perpendicular privileged directions; the one corresponding to the larger index n_γ, which is the slow direction, is marked while n_α is perpendicular to it and corresponds to the smaller index and hence faster direction.

Three accessories are commonly used in optical mineralogy:

1. **λ-plate** (**first-order red** or **gypsum plate**; Fig. 4(a)). Its birefringence and thickness are such that it produces a retardation (λ) of 551 nm, equivalent to the red I interference colour (red of the 1st order).
2. The **quartz wedge** (Fig. 4(b)) produces increasingly higher retardations (interference colours up to the 4th order) as its thicker parts successively move into the light path (Fig. 1, no. 6) and is sensitive within 0–4λ.
3. The variable **rotating compensator** is generally used only in research microscopes. It permits a very accurate determination of the change in retardation.

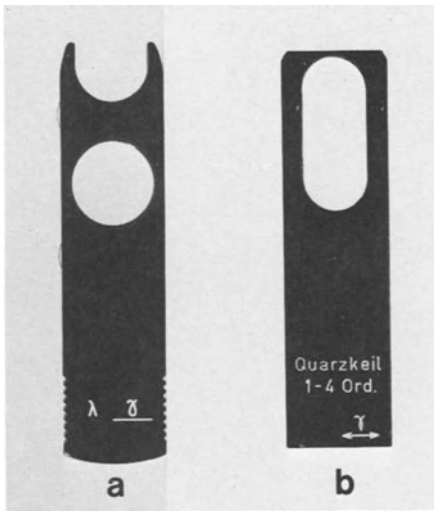

Fig. 4 Compensator accessory plate and wedge to determine the privileged vibration directions (company photo, Leitz).

(a) λ-plate (red I, gypsum plate).

(b) Quartz wedge 0–4λ.

If no compensation wedges or plates are used care should be taken not to get dust precipitating into the slot.

Ocular

People wearing glasses should use a special ocular. For measurements of the size of an object, an ocular with a micrometer should be used. It has to be calibrated by using a micrometer on the microscope stage.

1.3 Adjustment of the microscope

The adjustment of the polarizers will be described in section 2.1.2.3.

1.3.1 Centring the condensing lens

Prior to use the microscope must be checked to ensure that the object is properly and evenly illuminated. If this is not the case (Fig. 5(a)), then the condensing lens must be centred in the following way:

1. The light source aperture at the foot of the microscope is closed down.
2. The condensing lens is inserted into the path of light.
3. The substage assembly is slightly racked up or down until the edge of the illuminated field is in focus (Fig. 5(b)).
4. If the illuminated field is not centred (Fig. 5(b)) then the condensing lens adjustment screws are used (Fig. 2, no. 3) until the illuminated field is exactly in the centre of the viewing field (Fig. 5(d)).
5. Condensing lens is swung out.
6. The light source aperature is opened so that the full field of view is illuminated right up to its edges (Fig. 5(f)).

1.3.2 Centring the objective

An object is centred when it remains at the cross-hair intersection during a 360° rotation of the stage. If this is not the case the objective needs to be centred in the following way:

1. A small conspicuous mineral grain is aligned with the cross-hair intersection (Fig. 6(a)).
2. If the mineral grain describes a circle during rotation of the stage, then the objective is not centred (Fig. 6(b)).

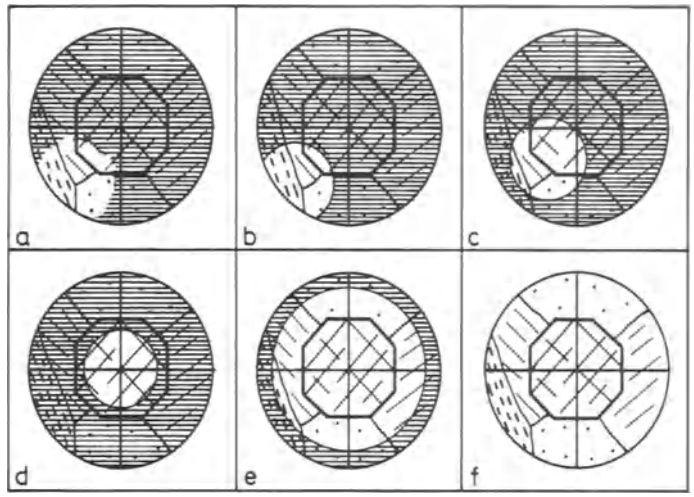

Fig. 5 Centring the condensing lens.

(a) Decentring: with the condensing lens in the light path and the light source aperture closed down the illuminated field is not aligned with the intersection of the cross-hairs.

(b) Adjustment of the condensing lens, so that the edge of the illuminated field is in focus and sharp.

(c), (d) Rotating the condensing lens adjustment screws, so that the illuminated field is centred and brought into alignment with the intersection of the cross-hairs.

(e), (f) Opening the aperture of the light source.

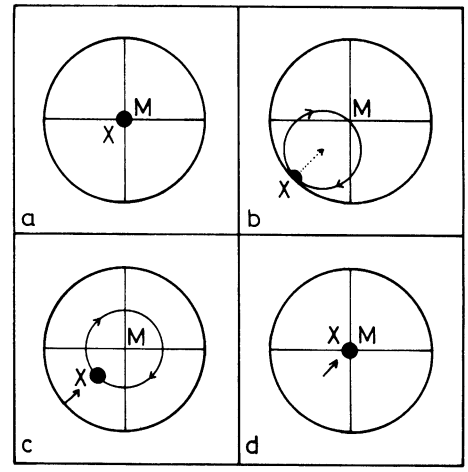

Fig. 6 Centring the objective.

(a) A mineral grain X is aligned with the intersection of the cross-hairs.

(b) Decentred: the mineral grain X describes a circle when rotating the stage. Note is taken of the centre of the circle.

(c) Using the objective centring screws the intersection of the cross-hairs is brought into alignment with the centre of the circle, by moving the grain when it is furthest from the cross-hair intersection by half the X–M distance between it and the cross-hair intersection towards the cross-hair intersection.

(d) By adjusting the thin section the grain is aligned with the cross-hair intersection M. Further centring might be necessary.

3. The cross-hair intersection is brought to coincide with the centre of the circle described by the mineral grain by turning the centring screws on the objective. This is best done by moving the mineral grain when it is furthest from the cross-hair intersection (X position) by half the distance between X and the cross-hair intersection M in the direction of M (Fig. 6(c)).

4. The grain is brought into alignment with the cross-hair intersection by moving the thin section. If it remains in its position then the objective is centred. If not, continue the procedure described above until the objective is centred.

2 Orthoscopic observations

2.1 Observations with one polarizer

2.1.1 Light impervious (opaque) minerals and substances

Minerals in thin section which appear dark to black under the microscope when viewed with uncrossed polarizers are called opaque. In very thin thin sections and also in certain orientations some opaque minerals are transparent to light, particularly at their edges, and show a weak brightening into dark, reddish, brownish or smokey greyish colours. Rock-forming opaque minerals are predominantly comprised of ore minerals, graphite and carbonaceous substances.

Some minerals in this group, such as chromite, hematite, ilmenite and others, in thin section can appear opaque as well as slightly transparent in dark colours. Because of their slight transparency they should be listed in Part B, section 2 (transparent isotropic minerals) or in Part B, section 3 (optically uniaxial minerals). Here, however, with the exception of chromite, we treat them as opaque minerals.

Reflected light microscopy on polished thin sections is necessary to identify opaque minerals (e.g. Schneiderhöhn, 1952; Ramdohr, 1975; Mücke, 1989). Magnetite (Fe_3O_4) and ilmenite ($FeTiO_3$) can be differentiated by transmitted light microscopy only if they occur as euhedral (idiomorphic) crystals showing their characteristic crystal morphology. Rather than using the wrong mineral name, the term opaque mineral should be used.

2.1.2 Transparent minerals and substances

2.1.2.1 Characteristic crystal shapes

The shape, habit and orientation of a crystal in thin section can provide us with its crystal symmetry. Amorphous substances, such as glass or opal, are without development of crystal faces. Cubic minerals tend to appear in equant polyhedral to spherical shapes with square, hexagonal and octahedral cross-sections (Fig. 7(a)). Distortion due to growth irregularities and corrosion is common (e.g. sodalite group, Figs 53, 55, 56). Minerals belonging to the uniaxial crystal system tend to be long to short columnar or prismatic or they are fibrous or acicular in longitudinal sections and are commonly square, rectangular, rhomboidal, triangular, hexagonal or octagonal in cross-section (Fig. 7(b)–(d)).

Biaxial minerals, in cases where they are

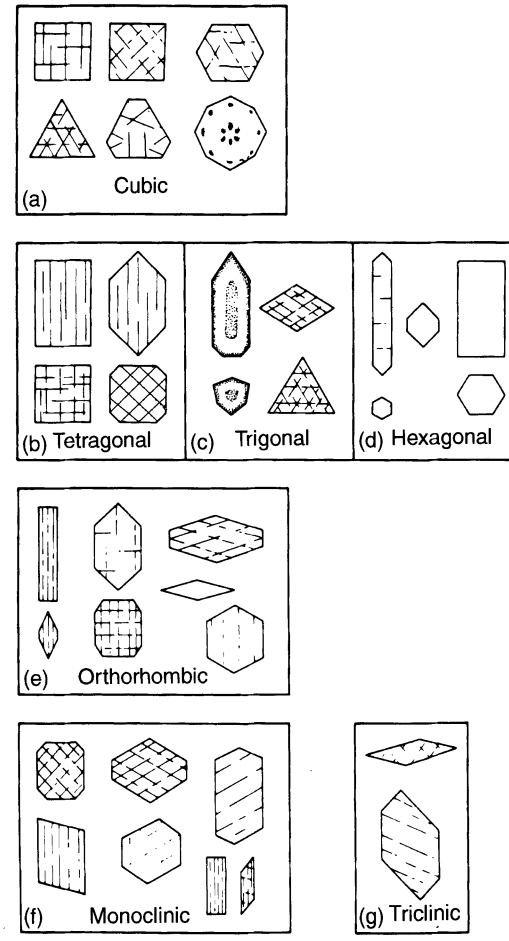

Fig. 7 Characteristic section of idiomorphic minerals.

(a) Isotropic (cubic) minerals.

(b)–(d) Uniaxial (tetragonal, trigonal, hexagonal) minerals.

(e)–(g) Biaxial (orthorhombic, monoclinic and triclinic) minerals.

From Müller and Raith (1987), after Chudoba (1932).

euhedral, tend to be prismatic or tabular. In rhombic crystals cross-sections tend to be of bladed columnar shape. Monoclinic and triclinic minerals commonly show tabular cross-sections (e.g. feldspars). Cross-sections of rhombic and monoclinic crystals tend to have rectangular or octahedral shapes (Fig. 7(e),(f)).

2.1.2.2 Cleavage

Observations of crystal cleavage is an important diagnostic tool. The breaking of a crystal along its crystallographic planes produces a cleavage which can be perfect, clear or poor. Perfect cleavage forms straight clean surfaces in the crystal which penetrate the whole crystal (e.g. in micas, Fig. 8(a)). If the cleavage trace is not penetrative but abruptly stops then it is referred to as clear cleavage (e.g. amphiboles, Fig. 8(b)). In cases where the cleavage is not straight and is irregular following a general direction (e.g. in garnet, Fig. 8(c)) then the cleavage is termed poor. The density of cleavage traces has no influence on this nomenclature.

In a single mineral section different cleavage sets can be developed, more or less equally, which form characteristic intersection angles (amphiboles 124° and 56° respectively, pyroxenes nearly 90°; Figs 143, 118). When measuring the cleavage intersection angle, the orientation of the mineral grain within the thin section plane has to be considered because this has an effect on the size of the angle. Ideally, the cleavage traces should be oriented perpendicular to the thin section plane. This can be determined by slightly moving the microscope stage up and down, and selecting only those cleavage sets where the defocusing of the cleavage set is symmetric relative to the cleavage trace rather than moving to one side. In colourless minerals cleavage traces can be seen better by slightly closing the iris diaphragm and defocusing the image.

Cleavage traces in minerals are important reference systems in minerals, because they follow crystallographic planes and therefore are diagnostic in determining the orientation of the mineral grain within the thin section. For instance, if only one cleavage set is developed in a pyroxene grain, then it can be concluded that the mineral section is oriented parallel to the crystallographic c-axis or at an acute angle to c. However, if both cleavage sets are developed with intersection angles of 90°, then the pyroxene section is oriented approximately or exactly perpendicular to the c-axis.

2.1.2.3 Colour and pleochroism

Minerals in thin section are either colourless or show varying colour intensities. Colour in idiochromatic minerals is an important diagnostic feature. Colours get fainter and more difficult to recognize the thinner the thin section. Important idiochromatic minerals are rutile, pyroxene, amphibole, mica, chlorite, tourmaline and others. Chemical variations in a single mineral can be reflected in a colour change and can lead to a zoned colour change (e.g. sphene) or a patchy colour distribution (e.g. andalusite, kyanite, corundum).

In coloured anisotropic crystals light is absorbed differently depending on the crystal direction. This produces different colours and intensity of colour for the grain in different orientations under plane-polarized light. The colour change phenomenon is called **pleochroism**.

The orientation-dependent absorption can be weak to very strong. In the former case it can be too weak to be discernible with the human eye. The effect of the pleochroism decreases the thinner the thin section. The presence or absence of pleochroism is a very important diagnostic feature (e.g. to differentiate between amphiboles and pyroxenes).

Adjustment of the polarizer can be carried out by looking at a mineral with straight extinction (e.g. anhydrite). The cleavage trace is oriented parallel to the cross-hairs, then both polarizer and analyser are rotated simultaneously until the crystal shows maximum extinction.

2.1.2.4 Refractive index: relief, chagrin, and the Becke line

Light rays incident at an oblique angle upon an interface between two different media will generally give rise to refracted rays. These are dependent on the speed of light within the media

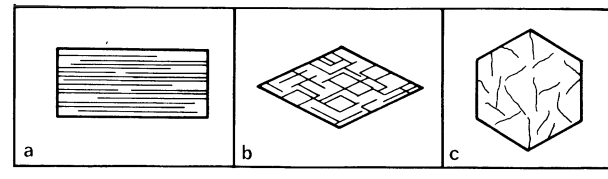

Fig. 8 Perfect (a), clear (b) and faint (c) cleavage.
(a) Mica.
(b) Amphibole.
(c) Garnet.
After Chudoba (1932).

concerned. According to Snell's law, the speed of light within a medium (v) is inversely proportional to the refractive indices of the medium (n) and hence with decreasing travel time the refractive indices increase.

The refractive index of a vacuum is n = 1 and hence all minerals have n > 1, because the speed of light through minerals is considerably less than through a vacuum. If the investigated mineral has a considerably higher refractive index than the minerals it is surrounded by then it will appear with a higher **relief** (positive or high relief) (Fig. 9(a)). The opposite is the case if the investigated mineral has a lower refractive index than the material it is surrounded by and it will show a negative or low relief ('depressions' in a thin section; Fig. 9(b)). Under the microscope using uncrossed polarizers one can observe some grains which stand out and others which are sunken in spite of all grains lying within a plane. Estimating the degree of relief is important in the identification of minerals. Table 1 shows five major subgroups of minerals with characteristic degrees of relief.

After the relief and birefringence of a specific mineral has been identified Table 6 can be used to narrow down further the mineral identification to only a few options. Roughness of mineral surfaces are sometimes referred to as its **chagrin** (French = scarred skin). A rough and wrinkled surface can be observed in those minerals only where the refractive index considerably differs from the mounting media. A strong relief can be enhanced by a strong chagrin. The chagrin of a mineral is observed best when the iris diaphragm is closed down and an objective lens of ×10 to ×25 is used.

The greater the contrast in refractive indices between adjacent grains the clearer are the grain boundaries which are defined by a black rim next to a bright rim, referred to as the **Becke line**. This can be best seen using a ×10 to ×25 objective lens and viewing the mineral slightly out of focus. The Becke line disappears on focusing the image. During focusing and defocusing of the image the Becke line moves from one grain into the adjacent grain. The following rule applies: when the microscope is lowered below the position of maximum focus the Becke line moves towards the medium with the higher refractive index (Fig. 10). The reverse is the case when the microscope stage is racked up with the Becke line moving into the mineral with the lower refractive index.

Through observations of movements of the Becke line the relative difference between refractive indices can be determined between adjacent minerals, particularly if the mineral to be determined borders on to a mineral of known index.

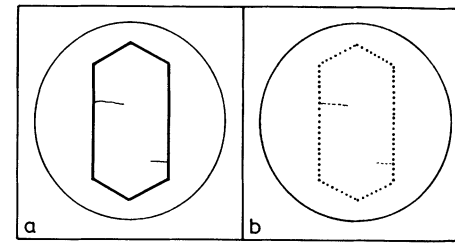

Fig. 9 Mineral with higher (a) and lower (b) refractive index relative to its surrounding mineral or the mounting material.

(a) Clear positive relief; mineral stands out like an island.

(b) No relief, negative relief; mineral forms a depression in the thin section.

2.2 Observations under crossed polars

2.2.1 Passage of light through isotropic media

Materials through which monochromatic light travels with the same speed, regardless of its direction of vibration, are called isotropic media, such as minerals of the isometric system (trans-

Table 1 Differences in refractive indices in the more important minerals

	'Depressions' (negative relief in thin section)	No relief	Medium relief	Strong relief	Extreme relief
n	<1.55	1.55–1.6	1.60–1.70	1.70–1.80	>1.8
Examples	nepheline, zeolite	quartz, feldspar	apatite, mica, carbonate	pyroxene, amphibole, olivine	zircon, rutile, sphene

parent cubic minerals), glass and amorphous minerals. Isotropic media viewed under crossed polars do not show interference colours but appear black and viewed in a conoscopic light path do not show an axial figure (Part A, section 3). To this group belong rock-glass, rare amorphous minerals (such as opal) and all crystals of cubic symmetry.

In addition, we include within this group those minerals that show a very weak birefringence and are non-cubic, such as leucite, which commonly occurs as twinned paramorphs after its cubic high-temperature form.

Deviations from this normal optical behaviour of isotropic minerals are referred to as **optical anomalies**. With the analyser in the light path they appear as patchily distributed brighter areas (e.g. certain garnets), as very weakly birefringent lamellar areas or as regular patterns which are characteristic and diagnostic for certain cubic minerals.

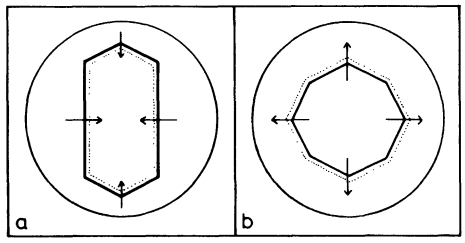

Fig. 10 Becke line (shown as dotted line).

(a) Mineral with a higher relief than its surroundings. With lowering the microscope stage, the Becke line moves into the mineral.

(b) Mineral with a lower relief than its surroundings. With raising of the microscope stage, the Becke line moves out of the mineral.

2.2.2 Passage of light through anisotropic media

2.2.2.1 Birefringence and polarization

General

The **wavelength** λ of a light ray can be defined as the distance between two adjacent points in a transversal wave which experiences vibrations of the same amount and direction. Such points are said to be in phase (Fig. 11). The trace of the vibration plane is perpendicular to the direction of travel of the wave. The speed of light passing through isotropic crystals (cubic) or amorphous media is equal in all directions but the travel time is reduced by a factor determined by the refractive index of the media. In anisotropic media a light ray may travel with considerably different speed in different directions of vibration within a crystal. The light ray is split into two linear polarized waves which travel with different speeds (and hence different refractive indices). The two planes of vibration are perpendicular to each other. This phenomenon is referred to as **birefringence**. It is strongly dependent on the orientation of the crystal. The maximum difference between the two refractive indices in a crystal is referred to as maximum birefringence (Δ).

Different coinciding electromagnetic (transverse) waves of the same vibration direction and same travel time can either be added or subtracted, or they cancel each other out (Fig. 12). The interaction of coinciding waves is referred to as **interference**. Additive or constructive interfer-

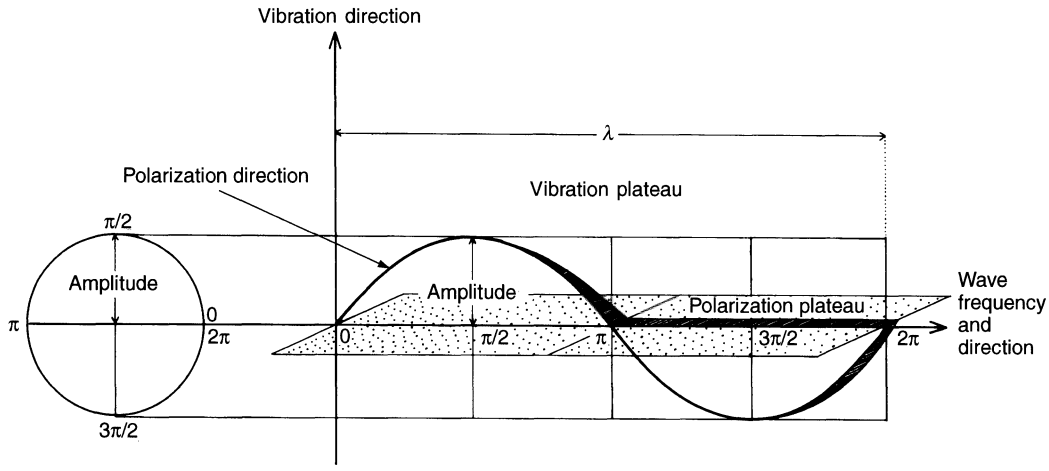

Fig. 11 Harmonic vibration of an (electromagnetic) transverse wave, also showing vibration and polarization planes.

ence occurs, if the two interfering waves are in phase; that is, if their path difference is $\Gamma = 1\lambda, 2\lambda, 3\lambda$, etc. then their wave amplitudes add up (Fig. 12(a)). If the path difference of two interfering waves is $\Gamma = 1/2\lambda, 3/2\lambda, 5/2\lambda$, etc., then they are exactly out of phase and the two waves annihilate each other (Fig. 12(b)). In cases where the interfering waves are neither in nor out of phase the resulting amplitude can be either bigger or smaller than the original amplitude (Fig. 12(c)).

If crossed polarized light passes through a transparent anisotropic mineral, then the light is split into two waves vibrating perpendicular to each other (with different refractive indices $n_{\alpha'}$ and $n_{\gamma'}$). In those cases where the vibration directions are different from those of the analyser (A–A) and polarizer (P–P) the crystal appears in bright light (Fig. 13(a)). As the two waves pass from the polarizer to the analyser they slightly vary in phase and interfere variably dependent on their path difference. In the four diagonal positions (45°, 135°, etc.) the interference is optimal and maximum brightness is achieved.

In contrast, if the two vibration directions of the waves in the crystal are parallel to the vibration directions of the polarizer and analyser respectively, then the crystal appears dark and is in total optical extinction (Fig. 13(b)). If the mineral is rotated out of this position, then the mineral will progressively get brighter with increasing interference in the analyser, until it reaches maximum brightness in the diagonal position. If the section is rotated further then maximum extinction is reached again in the 90° position and also in the 180° and 270° positions.

As commonly observed, a crystal may not show evenly distributed extinction, but partial extinction, with parts appearing brighter. All transitions between the two endmembers are possible. If during rotation of the section the extinction sweeps across the crystal then we refer to it as **undulatory extinction**, which is commonly observed in tectonic quartz (Fig. 84).

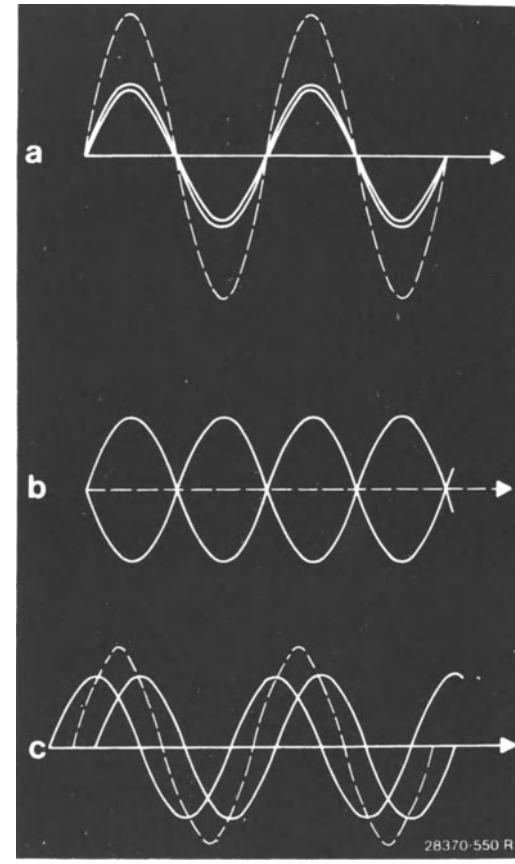

Fig. 12 Superposition (interference) of light waves of the same amplitude.

(a) Retardation $\Gamma = 1, 2\lambda$, etc.

(b) Retardation $\Gamma = \frac{1}{2}\lambda, \frac{3}{2}\lambda$, etc.

(c) Retardation $\Gamma = \frac{1}{4}\lambda, \frac{3}{4}\lambda$, etc.

From Patzelt (1974).

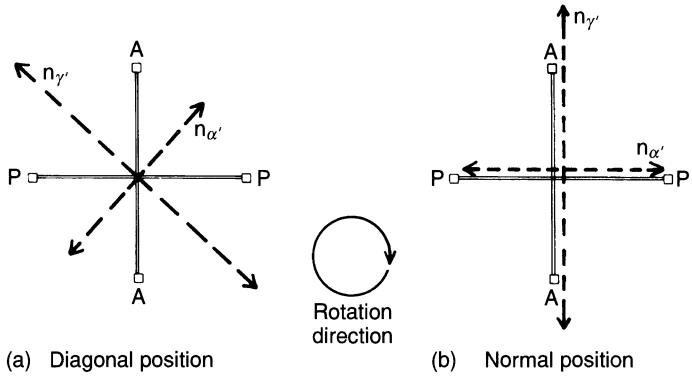

(a) Diagonal position (b) Normal position

Fig. 13 Main vibration directions ($n_{\alpha'}$ and $n_{\gamma'}$) in an anisotropic mineral with straight extinction.
P–P, A–A = vibration directions of the polarizer and analyser.

(a) Diagonal position (45°, 135°, etc.) = brightest position.

(b) Vertical position (0°, 90°, etc.) = darkest position.

Normal interference colours

Visible light represents a relatively limited band of wavelengths within the electromagnetic spectrum with wavelengths ranging from 380 to 780 nm (Fig. 14). The two extreme wavelength endmembers are in a 1:2 ratio to each other; hence a mineral with a 380 nm retardation under crossed polars in short-wavelength visible light will behave like an λ-plate and in long-wavelength visible light like a λ/2 plate. Constructive and destructive wave interference or elimination of component wavelengths of the white light causes **interference colours**.

In cases where the retardation is very small and only up to 300 nm the interfering waves are only slightly offset to each other with all component wavelengths being weakened equally. This results in a slight difference in colour from the original white light and grey to grey-white colours.

In the medium retardation range (300–1300 nm) certain component wavelengths are totally eliminated whereas others undergo positive interference. In this range strong clear colours dominate, ranging from orange to deep red, indigo-blue, sky-blue, green to yellow (first- and lower second-order). These colours are repeated but are somewhat weakened in the upper second- and lower third-order.

At an even higher retardation (>1300 nm) an increasing number of equally distributed λ in the spectra are eliminated, leading to an increased fading of the colours, which ultimately pass into the white of the upper order.

The interference colours are periodically repeated, but have subtle colour variations. The colour sequence is subdivided into orders. Each order represents a 551 nm retardation range, with the 1st order ranging from 0 to 551 nm 2nd order from 551 to 1102 nm, etc. Particularly important is the deep red of the 1st order (551 nm red), which is used in a λ-plate (gypsum plate; Part A, section 1.2) as compensator.

Using compensators to determine the interference colours

The gypsum plate (red 1st) is an accessory device used for determining the interference colours. For example: A bright blue interference colour is observed. The question arises if this is a 2nd or 3rd order blue. In higher orders no blue colours occur. Using the gypsum plate the following possibilities have to be anticipated: if the blue is of the 3rd order, addition by 1λ would cause the interference colour to change to pale purple of the 4th order, subtraction by 1λ would produce a sky-blue colour of the 2nd order. However, if the initial blue is of the 2nd order, then addition would result in a 3rd order dark blue and subtraction in a 1st order pale-grey interference colour.

Colour addition occurs either in the 45° or 135° position, and subtraction in the 135° or 45° respectively. The gypsum plate is inserted when the

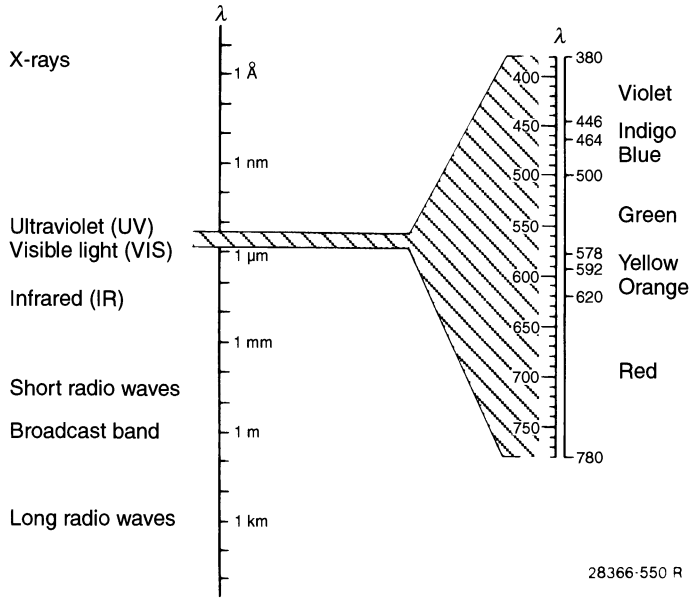

Fig. 14 Spectrum of electromagnetic waves (from Patzelt, 1974).

section is in the 45° and then in the 135° position. Subtraction in theory could lead to negative retardation values, but the smaller retardation value is always subtracted from the larger one. In the case of 1st order yellow, 551 – 400 = 151 results in a dark-grey interference colour.

When dealing with minerals with grey interference colours of the 1st order (e.g. quartz, feldspar, nepheline or apatite) then the use of a gypsum plate leads to blue colours of the 2nd order in the case of addition, and subtraction results in 1st order yellow. Again, the smaller retardation is subtracted from the larger one.

In cases of high interference colours greater than 4th and 5th orders, a quartz wedge (Part A, section 1.2) is used instead of the gypsum plate (red 1st).

Anomalous interference colours

Changes in the birefringence as a function of λ is called **dispersion**. This can occur in three different ways: interference colours that are higher than normal, lower than normal or anomalous.

If the birefringence is higher for the short wavelengths of light than for the long wavelengths, higher interference colours result; in this case ($n_{\gamma'}$–$n_{\alpha'}$) for purple > ($n_{\gamma'}$–$n_{\alpha'}$) for red. Instead of grey-white and white-yellow interference colours of the 1st order, bright blue and yellow colours typical for the 2nd order are observed: red 1st appears as bright red normally characteristic for 2nd order red, 2nd order green is brighter and darker and is more like that of the 3rd order. Examples of minerals with higher then normal interference colours are epidote and clinozoisite. Epidote shows bright-blue 1st order colours which pass straight into bright yellow.

Lower than normal interference colours occur when the birefringence for the long wavelengths of light is higher than for the short wavelengths; in this case ($n_{\gamma'}$–$n_{\alpha'}$) for purple < ($n_{\gamma'}$–$n_{\alpha'}$) for red. Instead of interference colours of the 1st order, grey and brown colours appear: instead of 1st order grey, grey-blue can be observed, 1st order yellow changes to leather-brown, 1st order red into dull brown-red. This is characteristic for tourmaline and $MgFe^{2+}$-chlorite.

Anomalous interference colours occur when the birefringence is positive ⊕ for one end of the light spectrum and negative ⊖ for the other end, representing the ($n_{\gamma'}$–$n_{\alpha'}$) $1 \lesseqgtr 0$ case. Instead of 1st order grey, 1st order ink-blue to purple colours are typical. Minerals with anomalous interference colours are, for instance, vesuvianite, melilite and Fe^{2+}Mg-chlorite.

Dispersion in the extinction position

This is common in monoclinic and triclinic minerals where the extinction positions for the long and short light wavelengths are different. Therefore a complete extinction cannot be achieved and even in the darkest position some colour can be seen. For example, if a mineral section is in the extinction position for 1st order red, then some blue light still manages to get through, resulting in a grey-blue colour of the mineral. The opposite is the case when the mineral is in the extinction position for blue light, then some red and yellow light will get through, resulting in brown-red colours (e.g. in certain clinopyroxenes cut parallel to the {010} plane).

2.2.2.2 The indicatrix model

General

The optical characteristics of crystals are better understood by using a three-dimensional model of the index of refraction, referred to as the **indicatrix**. It is either the shape of a sphere or ellipsoid where the surface of the indicatrix is proportional to the crystal's refractive indices which vary for different wavelengths (Figs 15, 16).

In the simplest case the indicatrix is a perfect sphere (e.g. all cubic crystals) in which the refraction does not change with the vibration direction of the light within the crystal. In minerals of lower symmetry the indicatrix has the shape of a two- or three-axial ellipsoid, which has a certain orientation relative to the crystallographic axis (a, b, c).

The three axes of the ellipsoid are labelled X, Y, and Z with their half-lengths proportional to their respective refractive indices n_α, n_β and n_γ (= n_x, n_y, n_z). For a three-axial indicatrix: $n_\alpha < n_\beta < n_\gamma$.

With the aid of the indicatrix model the physical behaviour of a light ray inside the crystal can be illustrated in three dimensions. One imagines that the light ray runs through the centre of the indicatrix. A section through the indicatrix perpendicular to the direction of travel of the light ray is either of the shape of a sphere or that of an ellipse. In the latter case the axes of the ellipse represent the vibration directions of the two perpendicular transverse waves. The half-lengths of the axes of the ellipse are proportional to the respective refractive indices $n_{\gamma'}$ and $n_{\alpha'}$. The wave which vibrates parallel to the longer axis of the ellipse has the higher refractive index ($n_{\gamma'}$) and hence the smaller speed of travel. The wave which vibrates parallel to the shorter axis of the ellipse has the smaller refractive index ($n_{\alpha'}$) and a faster travel time.

The indicatrices of hexagonal, trigonal and tetragonal crystal systems

Their symmetry defines $a_1 = a_2 = a_3 \neq c$ and $a = b \neq c$ respectively. Therefore the main or principal refractive indices are equal ($n_\alpha = n_\beta$ for optically

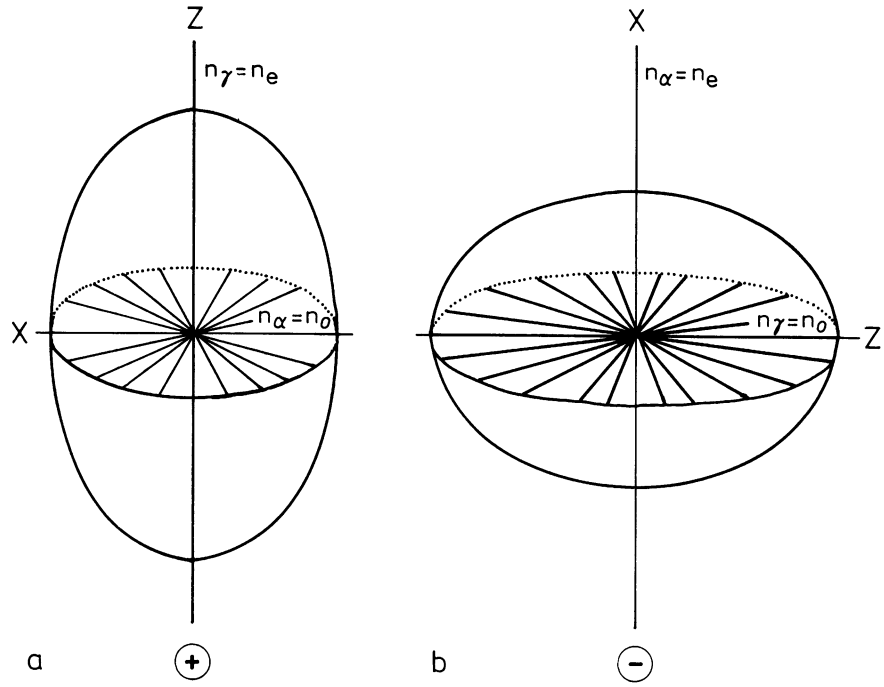

Fig. 15 Indicatrix ellipsoid for optically uniaxial crystals (rotation ellipsoid).
(a) Optically uniaxial positive.
(b) Optically uniaxial negative.

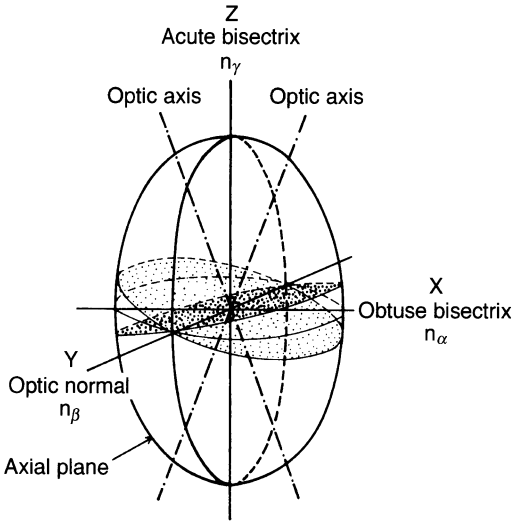

Fig. 16 Three-axial ellipsoidal indicatrix for an optically biaxial positive crystal showing both optic axes and circular sections (dotted pattern).

positive and $n_\beta = n_\gamma$ for optically negative minerals. The indicatrix is a two-axial ellipsoid (rotation ellipsoid) with the half-axial lengths $n_\alpha < n_\gamma$ (Fig. 15(a),(b)). The axis of rotation is the optic axis. Sections oriented perpendicular to it through the indicatrix are circles. The light ray that travels parallel to the optic axis behaves as if in an isotropic medium. Minerals of hexagonal, tetragonal and trigonal symmetry have only one optic axis (also referred to as the axis of isotropy) and are therefore classed as **optically uniaxial**.

Optically uniaxial minerals cut perpendicular to the optic axis or cut in any other orientation always show that one axis of the intersection ellipse is of equal length. Its half-length is proportional to the index of refraction of the ordinary ray (n_o or n_ω). Independent of the direction of incidence of light, the ordinary ray has the same refractive index and behaves as if travelling through an isotropic medium. The other wave is called the extraordinary ray ($n_{e'}$, or n_E or n_ε) with variable indices of refraction dependent on the direction of incidence of light. In a section perpendicular to the optic axis and the vibration direction parallel to Z or X, n_e represents the maximum value with $n_e = n_\gamma$ or $n_e = n_\alpha$ (Fig. 15(a),(b)) (In all other sections the deviation from the extreme value is expressed as $n_{e'}$ ($n_{\varepsilon'}$) and $n_{\gamma'}$, $n_{\alpha'}$ respectively.)

For the hexagonal, trigonal and tetragonal crystal systems the following rule applies: **n_e is always parallel to the c-axis (and hence parallel to the optic axis), n_o always lies in a circle perpendicular to it** (Fig. 15(a),(b)).

This leads to two options determined by the relative size of the two refractive indices n_e and n_o:

1. $\mathbf{n_e > n_o}$ is equivalent to $n_e = n_\gamma$ and $n_o = n_\alpha$. Therefore $n_e - n_o > 0$. The actual size of the maximum birefringence (Δ) is defined by the maximum difference between the refractive indices of the extraordinary and ordinary rays and hence $\Delta(\Delta = n_e - n_o)$ is greater then zero and positive.

   Uniaxial crystals with n_γ parallel to c (and therefore Z parallel to c) are **optically uniaxial positive**. Their indicatrix is an ellipsoid which is stretched along the optic axis or rotation axis (Fig. 15(a)).

   Example: quartz with $n_e = n_\gamma = 1.5533$
   $n_o = n_\alpha = 1.5442$
   $\oplus\Delta \quad = 0.0091$

2. $\mathbf{n_e < n_o}$ is equivalent to $n_e = n_\alpha$ and $n_o = n_\gamma$. Therefore $n_e - n_o < 0$. Uniaxial crystals with n_α parallel to c (and X parallel to c) are referred to as **optically uniaxial negative**. Their indicatrix is oblate in the direction of the optic axis and stretched perpendicular to it (Fig. 15(b)).

   Example: calcite with $n_e = n_\alpha = 1.4865$
   $n_o = n_\gamma = 1.6584$
   $\ominus\Delta \quad = 0.1719$

The indicatrices of minerals of lower symmetry (rhombic, monoclinic and triclinic)

Here the indicatrix is a three-axial ellipsoid with the axes X, Y, Z and three principal indices of refraction ($n_\alpha < n_\beta < n_\gamma$; Fig. 16).

Two extreme cases are examined, one where the light ray enters the crystal parallel to (||) Z and the other where it is || X. In the former case the two transversal waves vibrate || X and || Y with refractive indices of n_α and n_β respectively (Fig. 16). In the second case the vibration directions are || Z and || Y with refractive indices of n_γ and n_β respectively (Fig. 16). If in both cases the perpendicular wave becomes increasingly inclined until in the first case it is || X and in the second case || Z, then $n_{\alpha'}$ becomes larger in the first case and $n_{\gamma'}$ smaller in the second case. In both cases at certain directions of the incident ray where $n_{\alpha'} = n_\beta$ and $n_{\gamma'} = n_\beta$ respectively, there is no birefringence and both intersection ellipses are circles. In a tri-axial indicatrix the axes perpendicular to the two circular sections are called optic axes or axes of isotropy. The crystals of the lower symmetry systems are biaxial (Fig. 16). Both optic axes lie in the XZ principal intersection plane which is referred to as the optical axial plane (AE). Y is referred to as the optic perpendicular which is always perpendicular to the optical axial plane. The angle between the two optic axes is called **axial angle 2V** with its semi-value V. Z and X halve the axial angle and are called **medium lines** or **bisectrix**. The first medium line or acute bisectrix halves the acute angle between the optic axes, the obtuse angle is bisected by the obtuse bisectrix. With regard to the bisectrix two cases can be distinguished:

1. Z is the acute bisectrix, X is the obtuse one: **optically biaxial positive**. The angle $2V_\gamma$ is always < 90°, $2V_\alpha$ is always > 90° (Fig. 17, left).
2. X is the acute bisectrix, Z is the obtuse one: **optically biaxial negative**. The angle $2V_\alpha < 90°$, $2V_\gamma > 90°$ (Fig. 17, right).

In the case where both axial angles are equal and therefore 90°, the crystal is referred to as being **neutral**. Optical neutral crystals can occur in solid solution series, where one endmember is optically positive and the other negative (e.g. olivine series, Fig. 115). In such cases changes in the size of the axial angle are related to chemical changes of the mineral.

Orientation of the indicatrix in the low symmetry classes enable three cases to be distinguished:

1. In rhombic crystals the X,Y,Z axes coincide with the a,b,c crystallographic axes and the triaxial indicatrix has rhombic symmetry. How the indicatrix axes relate to a,b and c depends on the mineral (there are six different orientations possible). All sections perpendicular to (100), (010) and (001) always show straight extinction (Part A, section 2.2.2.4) (e.g. orthopyroxene).

   Shape and orientation of the indicatrix within a crystal are dependent on the following parameters: a) wavelength (all optical characteristics which depend on wavelength are called dispersion); b) chemical composition; c) pressure and/or temperature. A classic example for dispersion is brookite (TiO_2, rhombic): in red light the optical axial plane (AE) lies in (001). With reducing wavelength, 2V decreases and in yellow-green light 2V = 0° (uniaxial). Even smaller wavelengths result in increasing axial angles and in violet light AE lies in (010).
2. In monoclinic crystals only one axis of the indicatrix coincides with one of the crystallographic axes, which is always the b-axis. The two other indicatrix axes are not crystallographically fixed but lie oblique to the crystallographic axes a and c. This results in oblique extinction (Part A, section 2.2.2.4) (e.g. clinopyroxenes; Fig. 126).

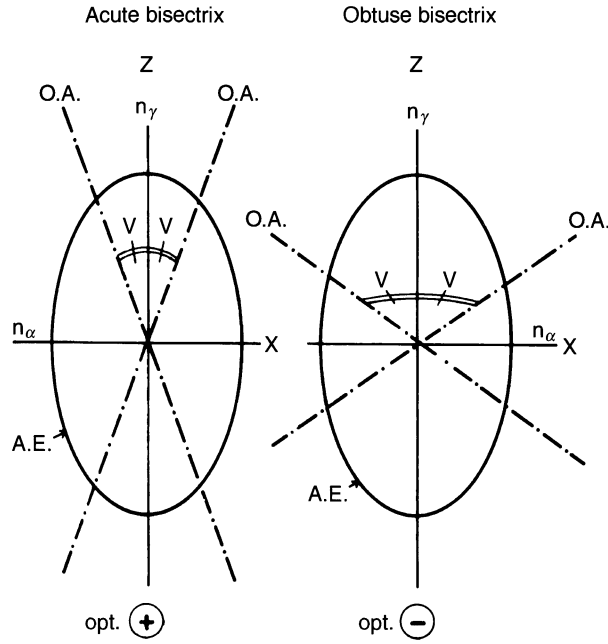

Fig. 17 Section through the axial plane of an elliptical indicatrix for optically biaxial crystals. O.A. = optic axis, A.E. = optic axial plane, V = half the optic axial angle 2V. Left: n_γ in the acute bisectrix ($2V_\gamma < 90°$), optically biaxial ⊕. Right: n_γ in the obtuse bisectrix ($2V_\gamma > 90°$), optically biaxial ⊖.

2.2.2.3 Optical character of elongation

The principal zone (**main zone** (MZ) or **elongation zone**) is equal to the elongation direction in a mineral. In minerals of characteristic and fixed crystal shape the optical character of the main zone (determined by the vibration directions of $n_{\gamma'}(n_{z'})$ and $n_{\alpha'}(n_{x'})$) is very important for identification. This applies to all cases where it is difficult to get a clear conoscopic axial image. Minerals of variable crystal shape, like those that are sometimes elongated parallel to one or the other axis (e.g. calcite or anatase), do not have a clear optical elongation.

Only elongated mineral sections of hexagonal, trigonal, tetragonal and rhombic symmetry classes are suitable for determining the optical character of the elongation. In elongated sections of monoclinic and triclinic crystals, which show oblique extinction, it is difficult to determine the optical character of the main zone. It is only possible if the extinction angle is less than 20° (e.g. amphibole, but not clinopyroxene).

Methodology

The mineral section is viewed under crossed polars and rotated into the 45° diagonal position (NE–SW orientation) where it appears in its brightest colours. The compensator red 1st (gypsum plate) is inserted. The n_γ direction is engraved on the accessory plate (Fig. 4(a)). It is oriented perpendicular to the length of the accessory plate; n_α is oriented parallel to its length. Two cases are possible:

1. n_γ gypsum is ∥ $n_{\gamma'}$ crystal and n_α gypsum is ∥ $n_{\alpha'}$ crystal ≙ MZ(+).
2. n_γ gypsum is ∥ $n_{\alpha'}$ crystal and n_α gypsum ∥ $n_{\gamma'}$ crystal ≙ MZ(−).

In the first case the retardation increases and causes a colour-change towards blue to greenish-yellow (if the initial birefringence colour is grey of the 1st order); in general the interference colours shift towards higher orders. The process is called **addition** = **positive main zone** (MZ) = (+) (Fig. 18(1)).

In the second case the retardation colour decreases, changing from grey of the 1st order to grey to orange-yellow of the 1st order; therefore the interference colours decrease = **subtraction** = **negative main zone** = (−) (Fig. 18(2)). In general the retardation of the gypsum plate (551 nm) is added to or subtracted from the interference colour of the mineral. With this simple device one can easily determine if $n_{\gamma'}$ or $n_{\alpha'}$ vibrate parallel to the longitudinal crystal direction. Furthermore, with the exception of platy crystals, the orientation of the indicatrix within the crystal can be fixed (Fig. 18).

If there is uncertainty as to whether or not the diagonal crystal position produces addition or subtraction, then rotate the section into the next diagonal position, which is at 90° from the starting position (orientation NW–SE). If negative

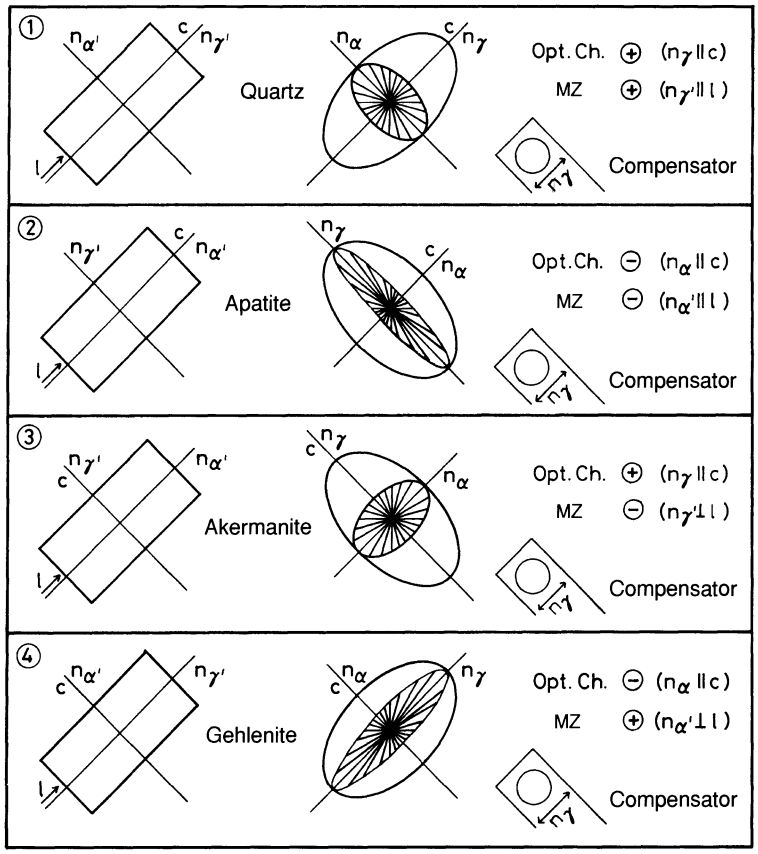

Fig. 18 Determination of the vibration direction $n_{\gamma'}$ and $n_{\alpha'}$ and orientation of the indicatrix in optically uniaxial crystals in longitudinal section (= principal zone or main zone MZ). Minerals with low birefringence have been chosen as examples.

(1) Prismatic crystals: the c-axis is parallel to the longitudinal axis of the crystal.
Case 1:
$n_{\gamma'}$ crystal ∥ n_γ compensator, $n_{\alpha'}$ crystal ∥ n_α compensator.
Interference colours increase (blue): MZ (+), optically uniaxial ⊕.

(2) Prismatic crystals: the c-axis is ∥ to the longitudinal axis of the crystal.
Case 2:
$n_{\alpha'}$ crystal ∥ n_γ compensator.
$n_{\gamma'}$ crystal ∥ n_α compensator.
Interference colours decrease (subtract/yellow): MZ (–), optically uniaxial ⊖.

(3) Platy crystals: c-axis is perpendicular to the elongation direction of the crystal.
Case 1:
$n_{\alpha'}$ crystal ∥ n_γ compensator.
$n_{\gamma'}$ crystal ∥ n_α compensator.
Interference colours decrease (subtract/yellow): MZ (–), optically uniaxial ⊕.

(4) Platy crystals: the c-axis is perpendicular to the elongation direction of the crystal!
Case 2:
$n_{\gamma'}$ crystal ∥ n_γ compensator.
$n_{\alpha'}$ crystal ∥ n_α compensator.
Interference colours increase (addition/blue): MZ (+), optically uniaxial ⊖.
The optical character has to be determined in the conoscopic light path.

colours or subtraction occurs, then addition or positive colours are produced for the first diagonal position and vice versa.

In minerals with 3rd or even higher order interference colours, any positive or negative colour shift is very difficult to determine. It is better to use a quartz wedge instead of the red 1st compensator. This has the effect, in the case of addition, of making colours of the higher orders became fainter. They become stronger if subtraction occurs. It also helps to apply the quartz wedge to thin wedge-shaped crystal edges. With insertion of a quartz wedge, colours move out of the grain in the case of addition; this is best seen by following the red colour. In the case of subtraction colour bands migrate towards or into the crystal and get stronger, shifting towards colours of lower orders.

Attention should be paid to several further considerations. Where the retardation of a mineral is smaller then 551 nm, then, in the case of subtraction, colours initially decrease down to black of the 1st order and then increase again (for explanation see Part A, section 2.2.2.1). In strongly coloured minerals addition and subtraction are difficult to determine and it is best to apply the quartz wedge technique to crystal edges.

The sign of the main zone and the optical character of a mineral coincide in prismatic crystals (Fig. 18(1)) whereas they differ in uniaxial platy crystals (Fig. 18(1),(2)). In biaxial crystals it can differ: it is the same in positive crystals with n_γ parallel or at a small angle to the main zone (MZ) and also in negative crystals with n_α parallel or at a small angle to MZ (examples are natrolite, Fig. 199, and andalusite, Fig. 223). It is different in negative crystals with n_γ parallel or at a small angle to MZ and in positive crystals with n_α parallel or at a small angle to MZ (example: amphibole, Figs 146, 147, 152). The character of the MZ changes in all biaxial minerals, depending on the orientation of the section, where n_β vibrates within MZ. MZ is (+) in the case where n_α–n_β lie within the section and it is (–) when n_γ–n_β lie in the section (e.g. olivine, Fig. 112).

2.2.2.4 Parallel, symmetric and oblique extinction

Crystal symmetry and extinction

Where the axes of the indicatrix coincide with the crystallographic axis (a,b,c), which is the case in all minerals of higher symmetry classes (hexagonal, trigonal, tetragonal and orthorhombic), the vibration directions of both waves are parallel or symmetric to the morphological reference systems provided by the mineral (crystallographic faces, edges, cleavage, twinning-plane, etc.). If any of these reference lines are aligned parallel to the N–S or E–W direction of the cross-hairs, then one observes total extinction under crossed polars: **parallel extinction** in 0°, 90°, 180°, 270° and 360° positions (Fig. 19(a),(b)). A crystal shows **symmetric extinction** if one vibration direction lies exactly between two equally developed morphological reference lines or cleavage systems (Fig. 19(b),(d)) (e.g. halving the angle between the rhombic cleavage set developed in calcite). Symmetric extinction only occurs if the section is cut exactly perpendicular to the cleavage intersection. If this is not the case, then even in minerals of higher symmetry classes, exact

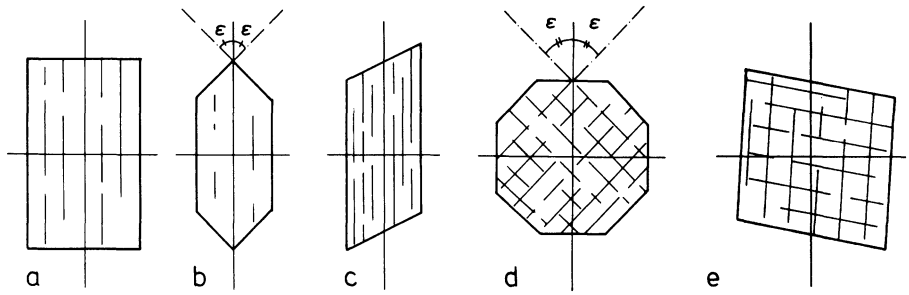

Fig. 19 Extinction in anisotropic crystals.

(a) Parallel extinction.

(b) Parallel and symmetric extinction: parallel extinction in respect to the cleavage set which runs parallel to the longitudinal axis of the crystal, symmetric extinction with respect to the perpendicular crystal faces (angle ε).

(c) Oblique extinction: the section cuts a monoclinic crystal parallel to (010).

(d) Symmetric extinction.

(e) Oblique extinction.

symmetric extinction is not observed. The latter particularly applies to orthorhombic crystals. On the other hand all monoclinic crystals show straight extinction in all orientations within the zone [010]. This is a limitation one must be aware of. Nevertheless, the determination of the type of extinction is one of the quickest methods to determine in minerals of the higher or lower symmetry classes (e.g. orthopyroxene or clinopyroxene). The possibility of finding an orthopyroxene which shows oblique extinction is three times less than in a clinopyroxene.

Oblique extinction (Fig. 19(c),(e))

This occurs when the vibration direction of the light is at an oblique angle to crystallographic reference planes. This obliqueness occurs in minerals of the lower symmetry classes (monoclinic, triclinic) and varies between the different crystal systems. In the monoclinic system there are certain orientations where extinction is parallel or symmetric (e.g. clinopyroxene in sections parallel to (100) show parallel extinction and basal sections parallel to (001) show symmetric extinction).

2.2.2.5 Twinning

General

Many minerals do not just consist of a single crystal but are made up of more then one individual intergrowth, forming double or multiple twins. Where the c-axes of the twinned crystals are parallel, the extinction will be the same in both twins. Twinning in quartz with parallel c-axes is very common but tends to go unrecognized under the microscope. Where the longitudinal axes of the twinned crystals are at an angle to each other (e.g. interpenetrating staurolite twins), then the extinction in all sections which are not parallel to the twining plane are different in the individual twinned crystals. The same is true for twinned monoclinic and triclinic crystals (Figs 144(b),(c), 179). Multiple twinning is particularly common in triclinic feldspars where it is diagnostic (Figs 180, 185, 188).

3 Observations under conoscopic light

3.1 Introduction

The orthoscopic image is one where the mineral is viewed perpendicular to the path of light, whereas under conoscopic light the mineral is viewed simultaneously from different angles in a cone of light using the maximum aperture. Conditions for viewing a mineral in the conoscopic light path are:

1. Objective 40, 50 or 63 POL.
2. Condensing lens is swung into the light path. The aperture must be fully open.
3. Crossed polars.
4. Amici Bertrand lens (Fig. 1) is swung into the light path; for small crystals the iris diaphragm is used.

An anisotropic mineral under conoscopic light produces interference figures. In conoscopic light the mineral and its optical characteristics are seen in all directions within a cone of light. Within the light cone light waves travel in various directions, each with two waves vibrating perpendicular to each other, with speed, retardation and vibration directions being equal in certain cases and unequal in others. The **isochrome** circles represent the emergence of rays from the mineral of the same retardation and hence the same birefringence colours, and the dark **isogyre cross** marks those areas where there is extinction (Fig. 20) and where the wave vibration directions are parallel to the polarizers. The shape and symmetry of the isochromes and isogyres vary with the orientation of the mineral. The interference figure changes when the microscope stage is rotated because the travel time of the rays changes, as do the retardation and vibration directions, depending on orientation. No changes occur in the case where the mineral is uniaxial and viewed perpendicular to its optic axis. Isotropic minerals do not produce conoscopic images. One isogyre can be lost from the field of view where the position of the optic axis falls outside the field of view.

3.2 Conoscopic examination of optically uniaxial crystals

3.2.1 Conoscopic images of uniaxial crystals in different orientations

The interference figure is a black isogyre cross in an uniaxial crystal when it is oriented so that the optic axis is perpendicular to the plane of the microscope stage. The wedge-shaped ends of the isogyres are referred to as **homodromes** (smaller end) and **antidromes** (broader end) (Fig. 20) (the homodromes point to the position of the optic axis). The presence of an isogyre cross in optic uniaxial crystals equates to an extinction position in the orthoscopic light path (different in optically isotropic minerals). The intersection point of the isogyres, where they are thinnest, marks where the optic axis in the crystal pierces the field of view (= **melatope**). The isogyre cross splits the field of view into four sectors (I–IV, Fig. 20) which contain coloured concentric rings (isochromes).

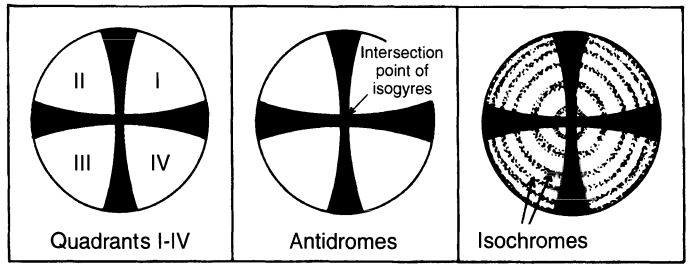

Fig. 20 Conoscopic images of optically uniaxial crystals in sections approximately perpendicular to the optic axis. The optic axis pierces the image at the intersection point of the two black isogyres. The concentric colour rings (isochromes, shown in dotted pattern) are spaced with increasing density from each other and increasing interference colours away from the centre. While rotating the stage the image does not change.

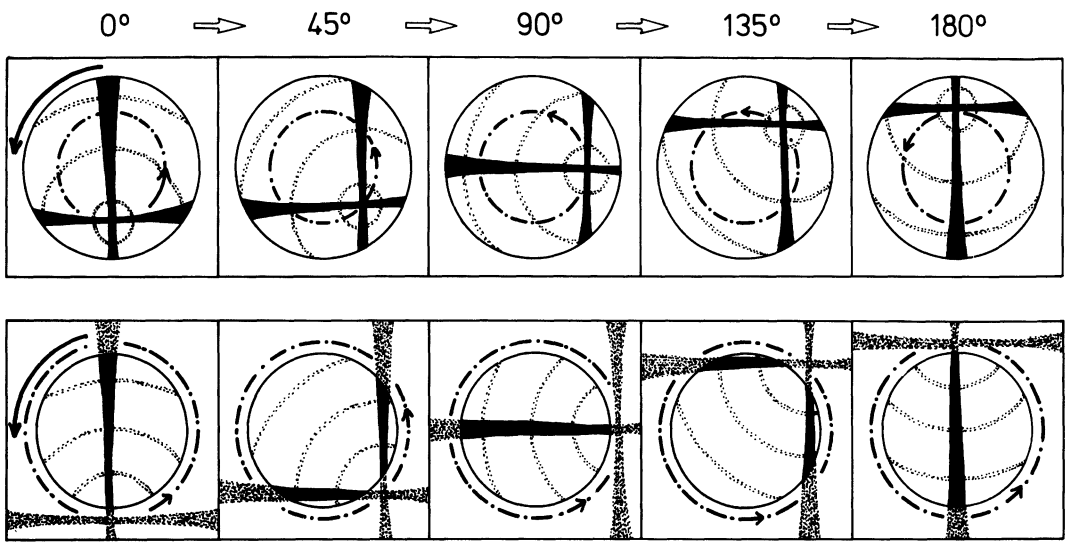

Fig. 21 Conoscopic images of optically uniaxial crystals in sections of different orientation and rotation positions. The isochromes are shown in a dotted pattern.

Upper row: section approximately perpendicular to the optic axis; the isogyres form a cross (melatope) which remains in the field of view when rotating the microscope stage.

Lower row: section at an oblique angle to the optic axis; the melatope is outside the field of view.

Thick arrow: direction of rotation of the microscope stage (anticlockwise). Broken arrow: rotation of the conoscopic image (anticlockwise).

If the mineral has been sectioned exactly perpendicular to the optic axis, then the melatope and the isogyre cross do not change their position when rotating the stage. If the section is at a small angle to the perpendicular to the optic axis, then the isogyre cross changes position when rotating the stage (Fig. 21, upper row).

In mineral sections cut at a large angle to the optic axis, the melatope can lie and rotate along a circle outside the field of view. The diameter of this circle depends on the angle to the optic axis. The isogyres remain parallel to the N–S and E–W orientation respectively and move in and out of the field of view (Fig. 21, lower row), which is quite different to optically biaxial minerals. The narrower end (homodrome) of the isogyres is always in the direction of the melatope. When restricted to images of the thicker end of the isogyre (antidrome), inexperienced observers can easily confuse the image with that of an optically biaxial crystal.

Sections oriented approximately parallel to the optic axis, show wide and diffuse isogyre patterns. In sections parallel to the optic axis a broad black cross appears, which opens quickly even at small rotations of the stage (Fig. 22); again this can easily lead to confusion with biaxial conoscopic images.

3.2.2 Determination of the optical character of uniaxial crystals

The compensator red I (gypsum plate) is inserted while viewing the mineral in the conoscopic light path. Where quadrants I and III show addition in their interference colours by one order (551 nm), the mineral has **positive** character. In the case of quartz, which shows grey-white colours of the 1st order, the accessory plate produces blue colours of the 2nd order. In quadrants II and IV, the colours decrease by one order, e.g. they become a 1st order yellow (subtraction). In minerals where the opposite is the case (e.g. apatite or nepheline), the minerals have **negative** optical character (Fig. 23). Here the accessory plate produces yellow in quadrants I and III and blue in II and IV.

Observation of addition or subtraction in a quadrant depends on the vibration directions of the ordinary and extraordinary rays (n_o, n_e). This can be best illustrated in a Becke's 'Skiodromsphere' (for more detail see e.g. Müller and Raith 1987).

In minerals with high interference colours it can be difficult to decide if addition or subtraction occurs when inserting the red I compensator.

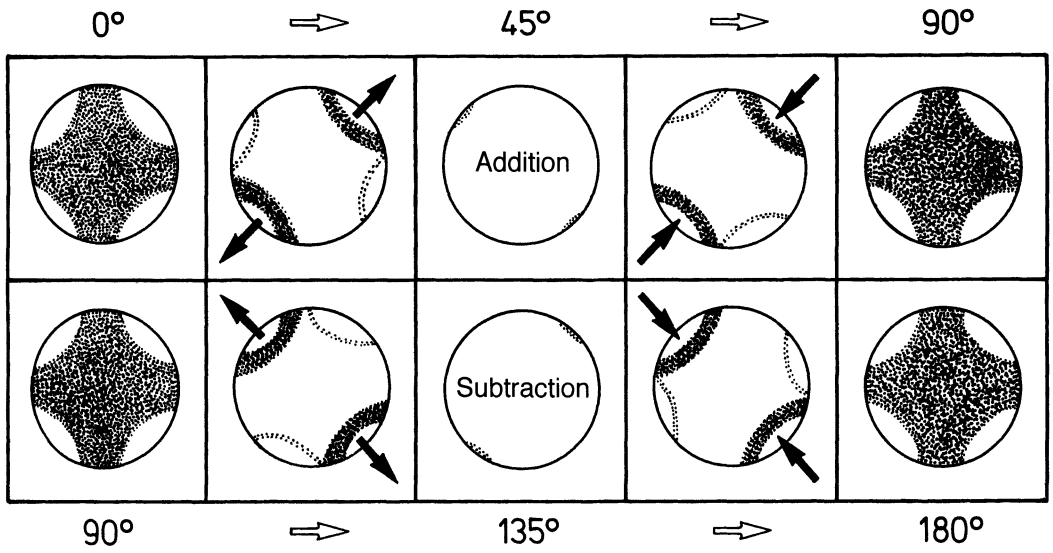

Fig. 22 Conoscopic images of optically uniaxial crystals in section approximately parallel to the optic axis during 180° rotation of the microscope stage. Isochromes are shown in the dotted pattern. Addition of colours in the 45° position and subtraction of colours in the 135° position apply to a uniaxial positive optical character. The opposite is the case in uniaxial negative crystals.

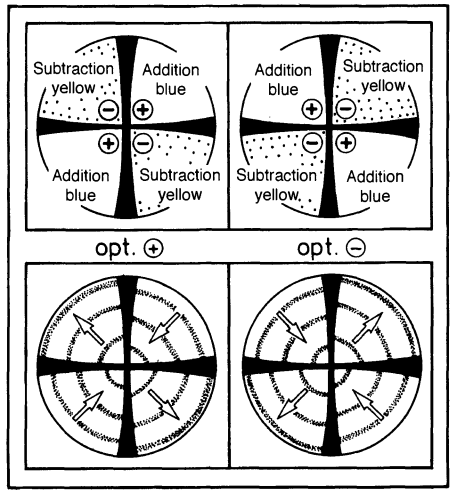

Fig. 23 Determination of the optical character of a uniaxial crystal with low birefringence colours in sections approximately perpendicular to the optic axis.

Top row: determination with the aid of the compensator red I. Left: addition with colours of a higher order in quadrants I and III = optic ⊕. Right: subtraction of colours in quadrants I and III = optic ⊖.

Lower row: Determination with the aid of the quartz wedge in minerals with higher birefringence colours. Left: isochromes in quadrants I and III move towards the centre = optic ⊕. Right: isochromes move away from the centre in quadrants I and III = optic ⊖.

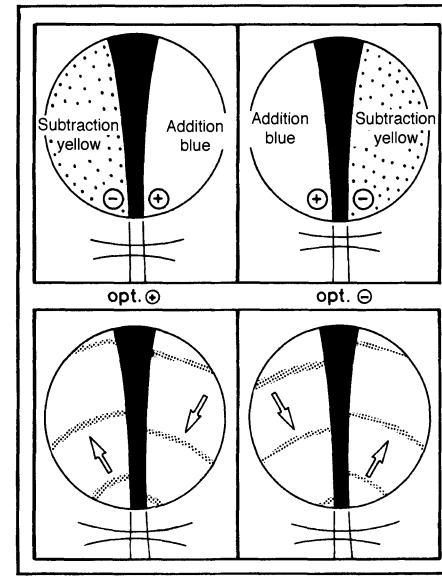

Fig. 24 Determination of the optical character in uniaxial crystals with low birefringence colours in sections oblique to the optic axis.

Top row: determination with the aid of the compensator red I. Left: addition of colours in quadrant I and subtraction in quadrant II = optic ⊕. Right: subtraction of colours in I and addition in quadrant II = optic ⊖.

Lower row: determination with the aid of a quartz wedge in minerals with higher birefringence colours. Left: isochromes move towards the centre in quadrant I = optic ⊕. Isochromes move away from the centre in quadrant I = optic ⊖.

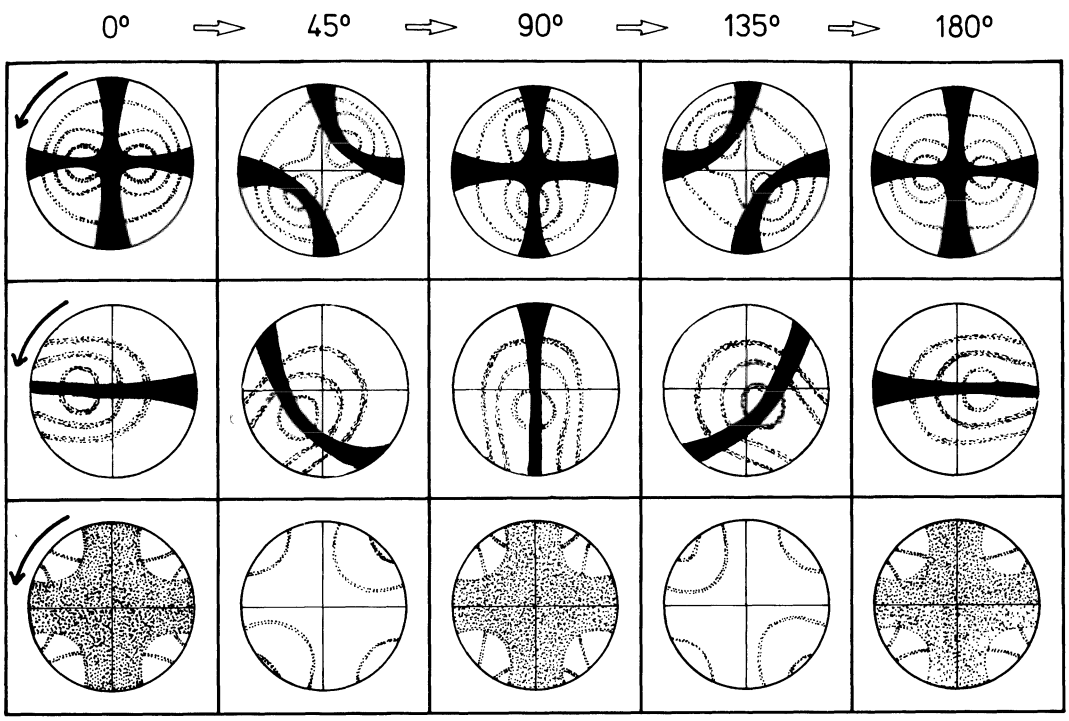

Fig. 25 Conoscopic images of optically biaxial crystals in different orientations and rotation positions. Isochromes are shown in the dotted pattern.

Upper row: sections oriented perpendicular to the acute bisectrix (2V ~ 40°); the melatope remains in the field of view.

Middle row: section oriented perpendicular to one of the optic axes (2V ~ 80°); one melatope is in the field of view. Isogyres swing back and forth.

Lower row: section perpendicular to the obtuse bisectrix and parallel to the optic axial plane. The isogyre cross is wide and rapidly expands and moves outside the field of view.

Black arrow: direction of rotation of both the microscope stage and the conoscopic image is anticlockwise.

It is better to use a quartz wedge (Fig. 23). In a mineral with optical positive character the colour rings in quadrants I and III move inwards towards the centre (= addition) and in quadrants II and IV they move outwards (subtraction). If the opposite is the case then the mineral has optical negative character (colour rings in quadrants I and III move outwards and in II and IV inwards).

Determination of the optical character as described above can easily be done in sections perpendicular or nearly perpendicular to the optic axis (Fig. 24). However, if the section is oriented parallel to the optic axis, then one follows the procedure illustrated in Fig. 22. If addition is observed in the 45° position (i.e. the isogyres have moved out of the field of view in quadrants I and III) then the mineral is optically positive. If subtraction occurs in this position then the mineral is optically negative.

3.3 Determination of the optical character of biaxial minerals in the conoscopic light path

3.3.1 Conoscopic images of biaxial minerals in different orientations

Under conoscopic light, biaxial minerals present an isochromatic system of elliptical curves with the optic axes and isogyres intersecting at their focal points (Fig. 25, upper row). The thinnest parts of the isogyres mark the points where the optic axes pierce through. The convex part of the isogyres always point towards the acute bisectrix (2V < 90°), and the concave side towards the obtuse bisectrix (2V > 90°).

Minerals sectioned perpendicular to the acute bisectrix show both isogyres in the field of view, if axial angles are small- or medium-sized. In the

0°, 90°, 180° etc. positions the isogyres form a black cross similar to uniaxial crystals (Fig. 25, upper row). However, the isogyres differ slightly from those observed in uniaxial crystals with the thinner isogyre showing two constrictions (piercing points of the two optic axes, with the isogyre resembling the optic axial plane) and the second isogyre being much thicker. During rotation of the microscope stage the cross opens up and the isogyres become two hyperbolas which are furthest apart from each other in the diagonal positions (45°, 135°, etc.). In mineral sections oriented at a high angle to the acute bisectrix or perpendicular to one of the optic axes the optic angle becomes very large and only one isogyre can be seen in the field of view. It is straight and oriented either N–S or W–E in the 90° position (Fig. 25, middle row). During rotation into diagonal positions the isogyres are variably bent and thin in places. The point of maximum curvature always points towards the acute bisectrix.

In sections perpendicular to the obtuse bisectrix viewed in the 90° position the isogyres form a wide cross which rapidly opens when rotating the stage and disappears from the field of view after a 15°–25° rotation (Fig. 25, bottom row). A similar conoscopic image is observed in sections parallel to the optic axial plane. Here the isogyres disappear from the field of view after a 10° rotation. Such sections can lead to erroneous identification of the mineral as uniaxial.

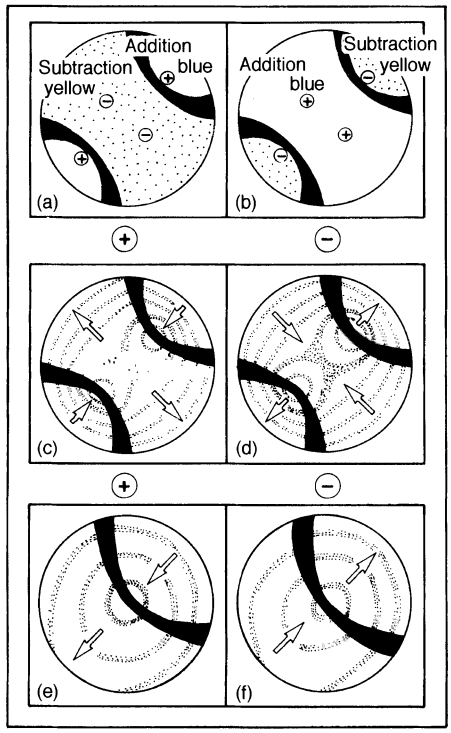

Fig. 26 Determination of the optical character of biaxial crystals.

(a)–(d) Section perpendicular to the acute bisectrix.

(e), (f) Section approximately perpendicular to one of the optic axes.

(a), (b) Mineral with low birefringence: determination with the red I compensator.

(c)–(f) Mineral with high birefringence: determination with the quartz wedge.

(a), (c), (e) opt. ⊕; (b), (d), (f) opt. ⊖.

3.3.2 Identification of the optical character of biaxial crystals

The conoscopic image is viewed in the diagonal position and then the compensator red I is inserted. If only one isogyre can be seen in the field of view then it is positioned so that its convex side points towards the SW (Fig. 26(e),(f)). If in a biaxial mineral of low birefringence colours, blue colours (addition) are observed on the concave side of the isogyre, and yellow colours (subtraction) on the convex side, then it is optically positive. In the opposite case, with subtraction and reduced colours on the concave side and addition and blue colours on the convex side, the mineral is optically negative (Fig. 26(a)(b)).

For minerals with high birefringence colours the quartz wedge is used rather then the red I compensator. On inserting the quartz wedge the isochromes move according to the illustration in Fig. 26 ((c)–(f)).

In sections where no melatope pierces the conoscopic image an unambiguous uniaxial or biaxial identification of a mineral is very difficult and requires a lot of experience. Therefore, such sections are best avoided; it is best to choose those that show low birefringence colours in the diagonal position.

Note:

- Conoscopic observations are best done in sections that show minimal birefringence colours.
- Determine birefringence in sections that show maximum interference colours.

3.3.3 Estimation of the optic axial angle 2V

The curvature of the isogyres is a measure of the size of 2V (Fig. 27). If one or both isogyres are in a diagonal position, then the optic angle can be determined according to the instructions given in

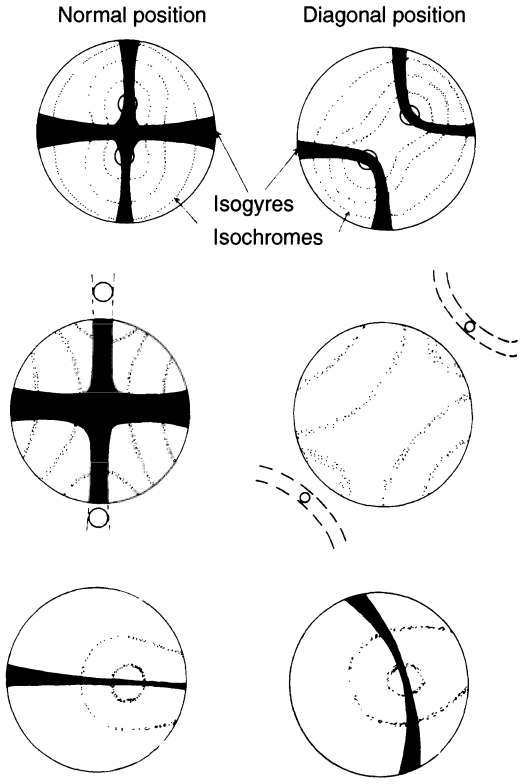

Fig. 27 Conoscopic images of optically biaxial minerals with varying axial angles. Left: 0°, 90° positions, etc.; right: diagonal 45° position, etc.

Upper row: small axial angle; view perpendicular to the acute bisectrix.

Middle row: large axial angle; view of one bisectrix.

Lower row: large axial angle; section approximately perpendicular to one of the optic axes.

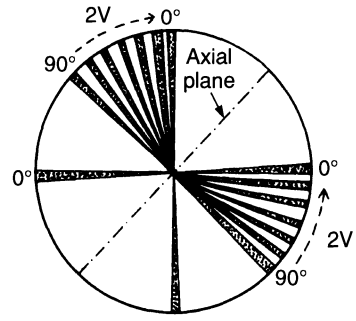

Fig. 28 Bending of isogyres as a measure of the size of the optic axial angle 2V in a section perpendicular to one of the optic axes in a diagonal position.

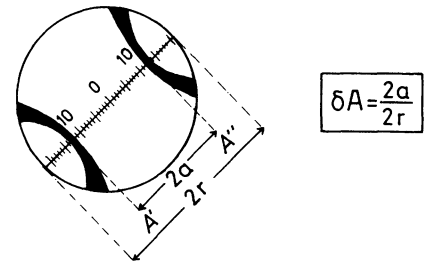

Fig. 29 Determination of 2V by measuring A′–A″ with the aid of a micrometer (Rittmann, 1963). In the example presented here 2r = 43 and 2a = 25; δA = 0.58. In Fig. 30 for n = 1.70 V = 17° and hence 2V = 34°.

Fig. 28. If the isogyres are straight then 2V is approximately 90°.

3.3.4 Determination of optic axial angles 2V in oblique section

If the optic axial angle is small, then it can be measured directly (without a universal stage). This method works for micas in basal section. One condition is that both isogyres can be observed in the field of view under conoscopic light. This means that section orientation should be approximately perpendicular to the acute bisectrix (Rittmann 1963).

Both isogyres are placed in diagonal positions and then the diameter 2r and the distance between the two points of maximum curvature 2a are measured (Fig. 29). The following equation applies:

$$\delta A = 2a/2r,$$

$$\sin V = \frac{\delta A \cdot U}{n}$$

where n = refractive index of the mineral (average value n_β taken from Table 7) and U = numerical aperture (Fig. 30, U = 0.85). δA is determined by dividing the two measurements 2r and 2a, the value n is obtained from Table 7 and 2V is read off Fig. 30.

Example: for muscovite (n = 1.6), δA is determined with 0.78 and V = 24.5°, $2V_x$ = 49°; for biotite (n = 1.65), δA is calculated as 0.16 and hence V = 4.8° with $2V_x$ = 9.6°.

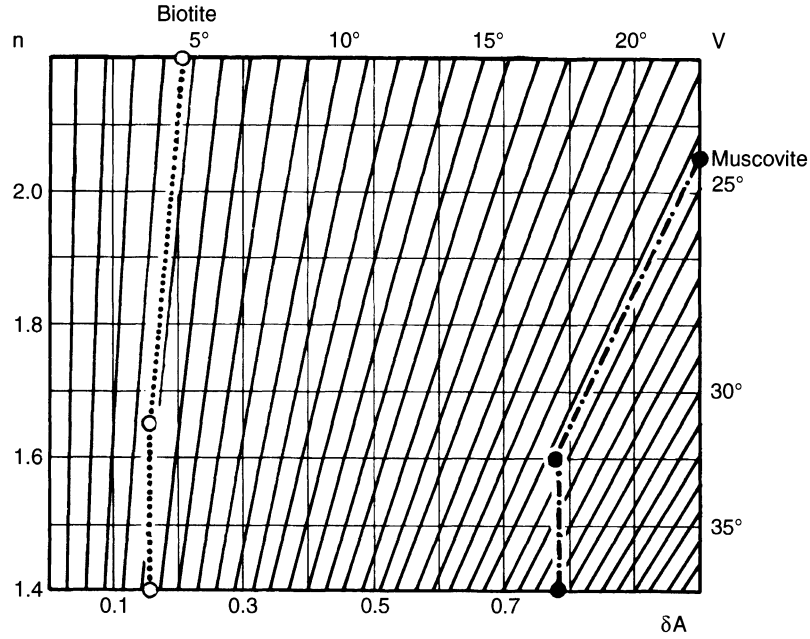

Fig. 30 Diagram for the determination of the half optic axial angle (V) for objectives with the numerical aperture of 0.85 (Rittmann, 1963). δA is plotted against n. The oblique lines represent V. See example for biotite and muscovite in the text.

Summary 1: Mineral identification with the polarizing microscope

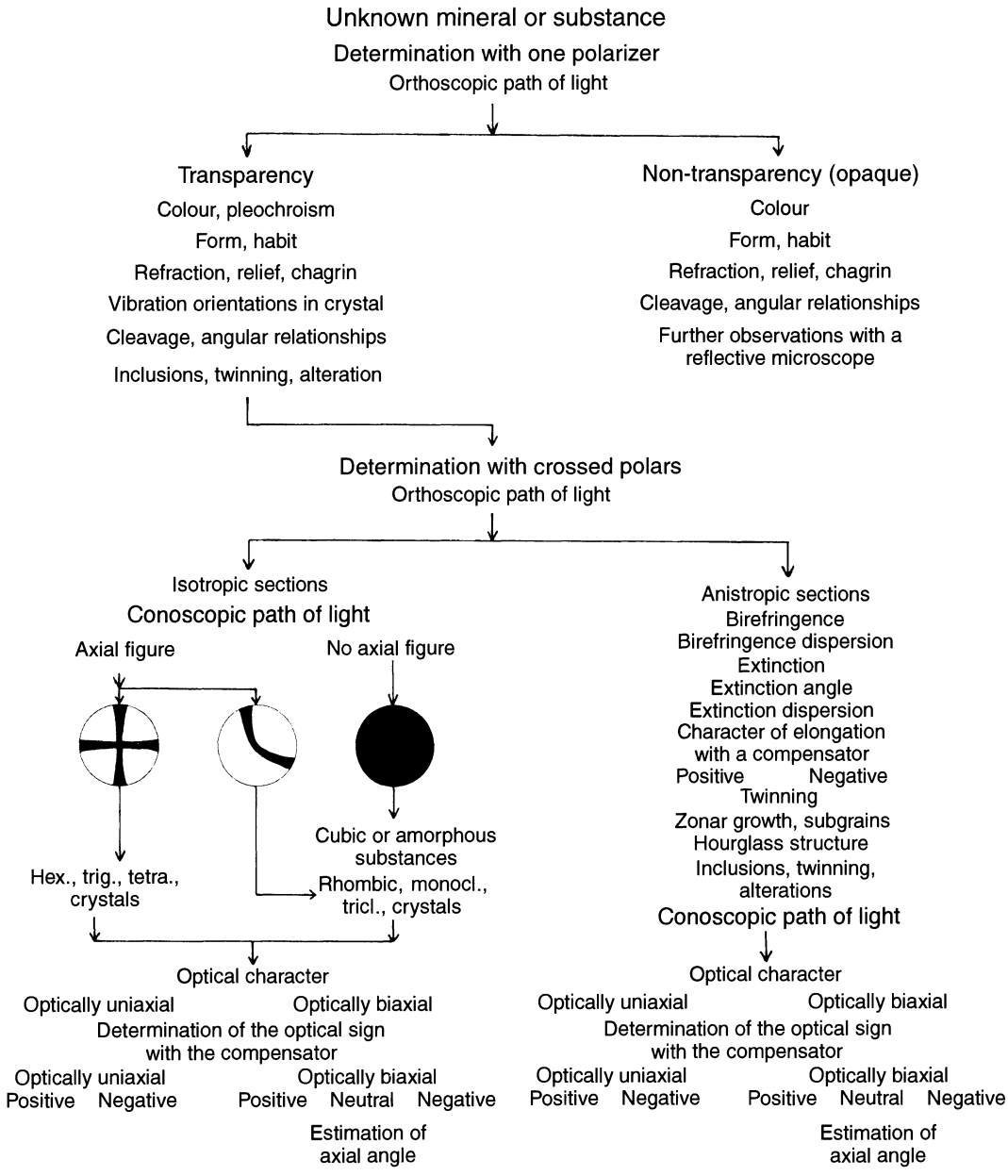

Summary 2: Protocol of mineral identification in thin section

Protocol

Thin section number _____ Rock type _____

Mineral number	1	2	3	4	5	6	7	8
Determinations with only one polarizer								
Habit								
Cleavage								
Estimate of the refraction								
Colour								
Pleochroism								
Determinations with crossed polars								
Isotropic/anisotropic								
Twinning								
Extinction angle								
Birefringence								
Uniaxial/biaxial optical character								
Optic axial angle 2V								
Main optical zone (optical orientation)								
Special optical phenomena (e.g. zoning, anomalies, etc.)								
Mineral name								

Part B Optical Mineralogy

1 Opaque minerals and substances

A precise optic identification is only possible with a reflecting light microscope.

1.1 Magnetite

Fe_3O_4 cubic–hexoctahedral

General features: most important and common accessory ore mineral. Belongs to the spinel group. In volcanic rocks it tends to occur as **titanomagnetite**, where one part of Fe is replaced by Ti (Fe_2TiO_4).

Thin-section characteristics

Form: square, rare triangular or hexagonal sections (Fig. 31), commonly as irregularly shaped aggregates; also developed as skeletal crystals.

Colour: black; in submicroscopic grains viewed in oblique reflected light smoky-grey to dark brown.

Refraction: extremely high ($n \approx 2.4$); however, it is not transparent, and cannot therefore be used for identification.

Distinguishing features: graphite has less defined, smeared grain boundaries and commonly forms flaky parallel grains; magnetite can be distinguished from ilmenite only if the latter shows skeletal forms and/or is altered to leucoxene.

Alteration: quite resistant. Oxidized to hematite (e.g. on the surface of lava flows). Titanomagnetite weathers to leucoxene by hydrothermal and hydrous alteration; that leads to Fe loss.

Occurrence: accessory mineral in most igneous rocks. It is more common in basic rocks (up to 5%) than in acidic rocks. In volcanic rocks two generations can be developed: as idiomorphic grains and as disseminated grains in the groundmass. Its presence in volcanic glasses can cause a brown coloration. In magmatic rocks it can occur as a deuteric mineral, formed by the breakdown of water-bearing minerals (biotite and hornblende) during the late stages of magma crystallization (opacite rims around biotite and hornblende; Part B, sections 4.3.3, 4.4.4.2, and Fig. 150). In metamorphic rocks it is common in low- to high-grade rocks, typically as idiomorphic grains (e.g. in chlorite schist and as small grains in hornfels). It occurs in almost all clastic sediments; locally enriched in alluvial deposits.

Paragenesis: very common. In igneous rocks commonly found together with ilmenite.

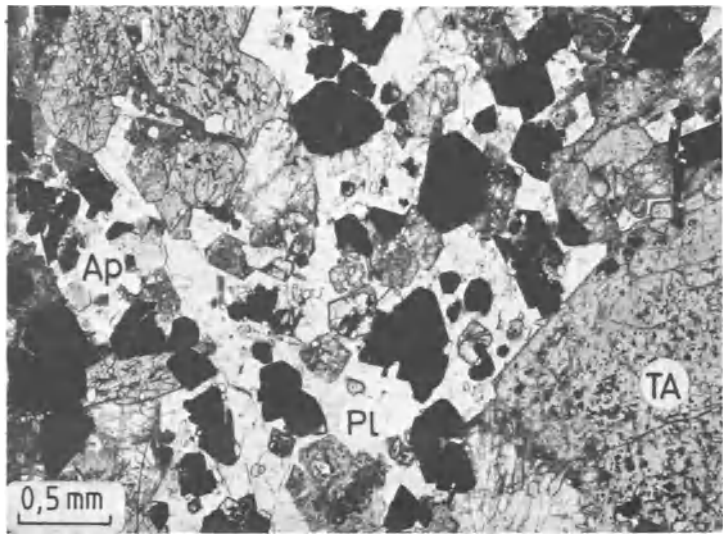

Fig. 31 Idiomorphic magnetite grains in a nepheline monzogabbro (essexite). Doupov (Duppau), CR. Uncrossed polarizers.

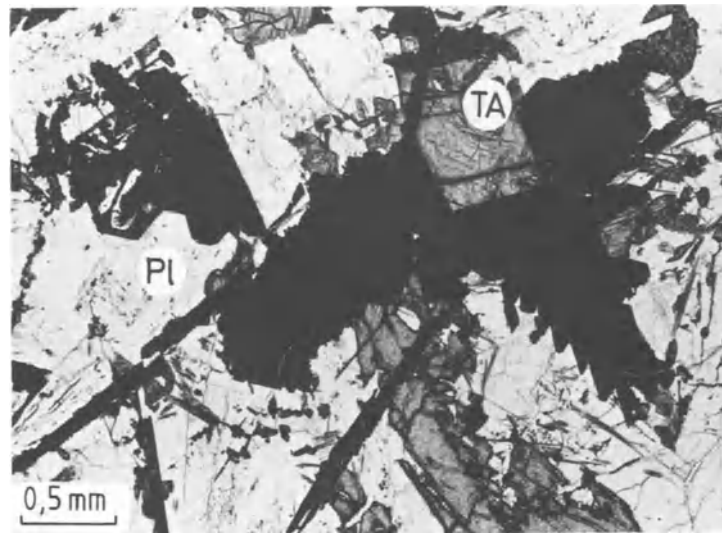

Fig. 32 Skeletal ilmenite in kersantite. Steinmauer, southeast of Heppenheim, Odenwald, Germany. Uncrossed polarizers.

Fig. 33 Skeletal ilmenite crystal showing leucoxene alteration (white parts in the crystal).

1.2 Ilmenite

$FeTiO_3$ trigonal–rhombohedral

General features: the most important and common accessory ore mineral after magnetite.

Thin-section characteristics

Form: thin flakes; dendritic aggregates; skeletal (Figs 32, 33).

Colour: opaque; in very thin sections deep transparent brown.

Refraction: extremely high (n = 2.33–2.51). In crossed polarized light clear anisotropic characteristics, optically uniaxial in very thin flakes.

Distinguishing features: from magnetite and other opaque minerals it can be distinguished only if present in skeletal form or by its characteristic alteration into leucoxene.

Alteration: fairly stable mineral. Hydrothermal and hydrous alterations along rims or complete replacement into leucoxene (= alteration of ilmenite and titanoilmenite into a fine-grained, dark-red aggregate of rutile, anatase, sphene, hematite). Sometimes a laminar intergrowth between ilmenite and magnetite can be developed and is more clearly seen in altered than in fresh grains.

Occurrence: it occurs together with magnetite as an accessory mineral in almost all igneous rocks. In basic plutonic rocks it is commonly found as titanomagnetite (Part B, section 1.1). It occurs in metamorphic rocks (e.g. in amphibolites) in detrital sediments and sedimentary rocks.

Paragenesis: very common. In igneous rocks commonly found together with magnetite.

1.3 Hematite

Fe_2O_3 trigonal–scalenohedral

Thin-section characteristics

Form: thin plates (0001), fine scales, fibrous (kidney iron ore; Colour plate 1), dusty aggregates, oolitic or granular.

Colour: in thin sections of normal thickness it is opaque and in very thin sections flakes are transparent, showing a slight pleochroism from brown-red to yellow-red (to grey-yellow). This dark colour makes optical determinations difficult.

Refraction and birefringence:

$$\begin{array}{ll} n_e & = 2.87 - 2.94 \\ n_o & = 3.15 - 3.22 \\ \hline \ominus\Delta & = 0.28 \end{array}$$

Extremely high refraction and birefringence.

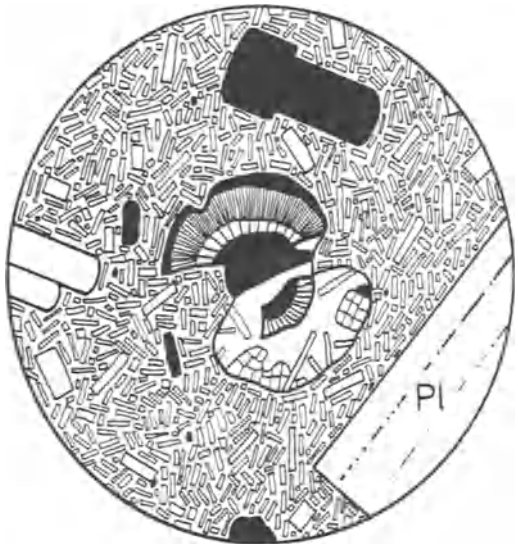

Fig. 34 Hematite in radial fibrolitic form, kidney form. Andesite from the Mojanda volcano, northern Ecuador. Uncrossed polarizers.

Distinguishing features: goethite and lepidolite are of a lighter brown colour, ilmenite tends to be skeletal with leucoxene alterations and brown; aenigmatite forms part of very characteristic and different paragenesis.

Occurrence: as a secondary mineral in igneous rocks (Fig. 34) and as pseudomorphs after magnetite (Part B, section 1.1) (e.g. as disseminated aggregate in fly-ash and in surface layers of lava flows). It forms during the oxidation of disseminated magnetite as a result of hydrothermal alteration in volcanic glasses, e.g. in Permian palaeorhyolites (quartz porphyry) which show a characteristic red colouring. Hematite also occurs as a very fine pigment in a variety of sedimentary rocks (red coloration) and it is found in low- to medium-grade metamorphic rocks.

Paragenesis: not typical.

1.4 Pyrite

FeS_2 cubic–didodecahedral

Thin-section characteristics

Form: square, triangular and hexagonal sections (Figs 35, 36), also granular.

Colour: opaque, in oblique reflected light brass-yellow.

Distinguishing features: from magnetite, ilmenite and pyrrhotite only by reflected light microscopy.

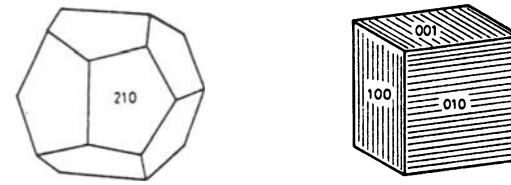

Fig. 35 Typical form of pyrite. Pentagon-dodecahedron (pyritohedron) or cube with characteristic stripes.

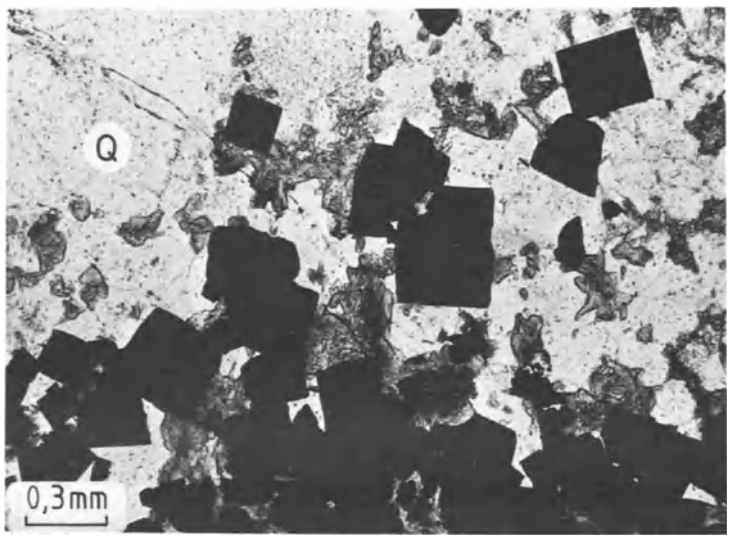

Fig. 36 Idiomorphic pyrite cubes in a Precambrian sandstone. Republic of South Africa. Uncrossed polarizers.

Alteration: weathers easily, altering to limonite, etc.

Occurrence: an accessory mineral in igneous rocks; an impregnation mineral in hydrothermally altered rocks (e.g. as a result of fumerole activity); also in metamorphic rocks (Fig. 36), in bituminous-rich limestones, and in black shales.

Paragenesis: not typical.

1.5 Pyrrhotite

FeS dihexagonal–dipyramidal

Thin-section characteristics

Form: granular or in irregular-shaped aggregates.

Colour: opaque, in reflected light bronze-coloured to brown.

Distinguishing features: from other ore minerals only with the aid of a reflecting light microscope.

Occurrence: primary accessory mineral in mafic to ultramafic plutonic rocks (diorites and peridotites). Rare in volcanic rocks. Also in low- to high-grade metamorphic rocks.

Paragenesis: with olivine, ortho- and clinopyroxene, plagioclase magnetite and ilmenite.

1.6 Graphite

C dihexagonal–dipyramidal

General features: carbon-bearing organic sedimentary material is changed into graphite during metamorphism.

Thin-section characteristics

Form: commonly as thin flakes and scales after (0001), occasionally as grains, also with egg-shaped cross-sections. Parallel alignment with or without folding and smeared edges are typical (Fig. 37). Grain boundaries tend to be irregular, because graphite gets smeared during the process of thin-section making.

Cleavage: tabular crystals with perfect cleavage along (0001), which cannot be seen under the microscope.

Colour: opaque, non-transparent and therefore dark black; grey-green translucent, only in the thinnest flakes.

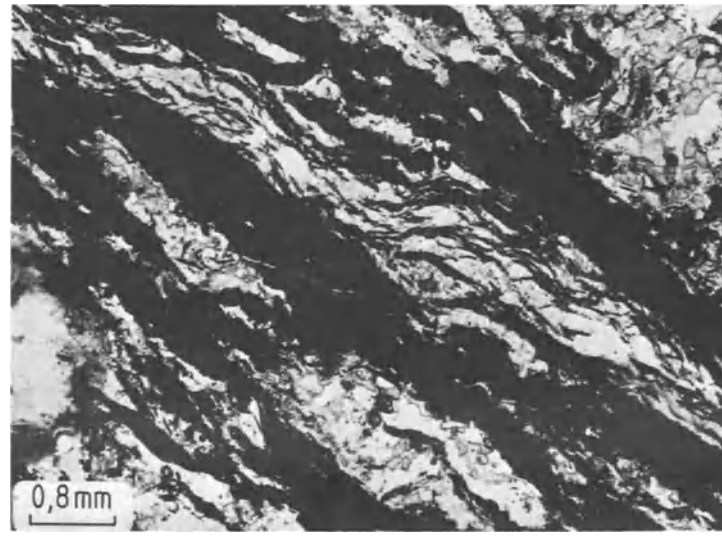

Fig. 37 Disseminated graphite. Graphitic phyllite. East of Baños, Eastern Cordillera, Ecuador. Uncrossed polarizers.

Refraction: n = 1.5– >2.0, very variable.

Distinguishing features: smeared edges are characteristic and help to distinguish it from other opaque minerals except molybdenite.

Alteration: none.

Occurrence: only in certain metamorphic rocks such as graphite-rich phyllites and graphite-rich gneisses (e.g. Bayerischer Wald, Germany). In augen gneisses.

Paragenesis: with quartz, K-feldspar, albite, mica, chlorite and rutile.

1.7 Carbonaceous substances

C amorphous

Thin-section characteristics

Form: commonly as finely distributed and disseminated dusty grains or as irregular and amorphous masses.

Colour: opaque, dirty-brown shine; in very thin sections brown to grey translucent.

Refraction: n = 1.5–1.9, very variable.

Distinguishing features: under the microscope it cannot be distinguished from disseminated ore minerals.

Alteration: during metamorphism at temperatures greater than 200–250 °C it changes into graphite.

Occurrence: rock-forming as coal, black shale or coal shale. As a dark pigment in a variety of sedimentary rocks, particularly in pelites (e.g. black shales, slates) and also in limestones (e.g. coal–limestones).

Paragenesis: with quartz, calcite and clay minerals.

2 Optically isotropic (also pseudo-cubic) minerals and amorphous substances

2.1 Perovskite

(Ca, Na, Fe^{2+}, Ce, Sr) (Ti, Nb)O_3 pseudo-cubic (rhombic-dipyramidal)

General features: rare mineral, commonly found in SiO_2-undersaturated basaltic igneous rocks together with melilite.

Thin-section characteristics

Form: cubic and triangular cross-sections; rare skeletal crystals.

Cleavage: cubic after {100} only developed in larger crystals.

Twinning: polysynthetic after {111}, rare simple twins after {110} and {100}, only visible in larger crystals.

Colour: variable; predominantly violet-grey, brown-red, amber to bright yellow, rarely green to colourless. Concentric colour distribution possible. Very small crystals appear opaque because of their total light reflectance.

Refraction: extremely high, n = 2.30–2.38.

Special characteristics: paramorph, under crossed polars all larger crystals show polysynthetic twinning, as do leucite crystals (Part B, section 2.5), and anomalous low birefringence colours (axial angle $2V_\gamma \sim 90°$).

Distinguishing features: picotite and melanite have considerable lower refraction; rutile occurs in a different paragenesis. Easily confused with dysanalyte and pyrochlore because of similar refraction and colour, and hence best identified by microprobe analysis.

Distinguishing features: commonly unaltered.

Occurrence: forms as an early crystal phase in silica undersaturated, Ca-rich igneous rocks (Fig. 38), in particular in melilite-bearing volcanic rocks (e.g. melilite-bearing nephelinite of Hegau, Schwäbische Alb, Kaiserstuhl, Germany), in dykes (alnoite), kimberlites, rare in nephelinites and leucitites without melilite.

Paragenesis: with melilite, nepheline, sodalite group, also leucite and magnetite; never with ilmenite.

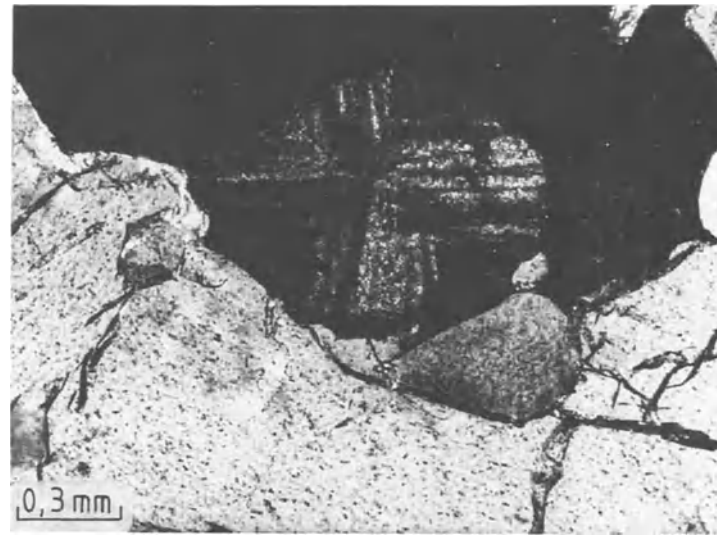

Fig. 38 Granular perovskite with clear relief and very dark colour. Pyroxene melilitite, Ilimaussaq, West Greenland. Uncrossed polarizers.

2.2 Spinel group

Spinel $MgAl_2O_4$ cubic–hexaoctahedral
Hercynite $FeAl_2O_4$
Picotite $(Mg, Fe)(Al, Fe, Cr)_2O_4$
Chromite $FeCr_2O_4$.

General features: divided into three subgroups: Aluminospinel or spinel s.s. (spinel, hercynite, pleonaste), ferrospinel (magnetite; Part B, section 1.1) and chromiumspinel (picotite and chromite).

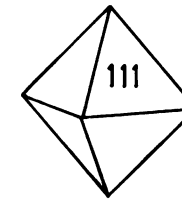

Fig. 39 Spinel with typical octahedral form.

Thin-section characteristics

Form: euhedral hexagonal (Fig. 39), with square and triangular cross-sections, also anhedral as rounded and angular grains (Colour plate 2).

Cleavage: not visible in thin section. Exception: spinel s.s. in forsterite-bearing marbles show a well-developed cleavage after {100}.

Twinning: common after {111}, not clearly visible in thin section.

Colour:

Spinel:	Hercynite:	Picotite:	Chromite:
colourless, pale pink, pale blue; green-grey if Fe^{2+}-rich (pleonaste).	dark green, bright emerald green (Colour plate 2).	yellowish and brownish.	dark brown to nearly opaque, at thinned-out grain edges dark brown to red-brown translucent.

Refraction:

Spinel:	Hercynite:	Picotite:	Chromite:
n = 1.72–1.74	n = 1.78–1.80	n = 2.0	n = 2.05–2.16

Differences in colour and refraction are due to varying chemical composition. High refraction produces a strong positive relief (Fig. 40), often with dark rims around grains.

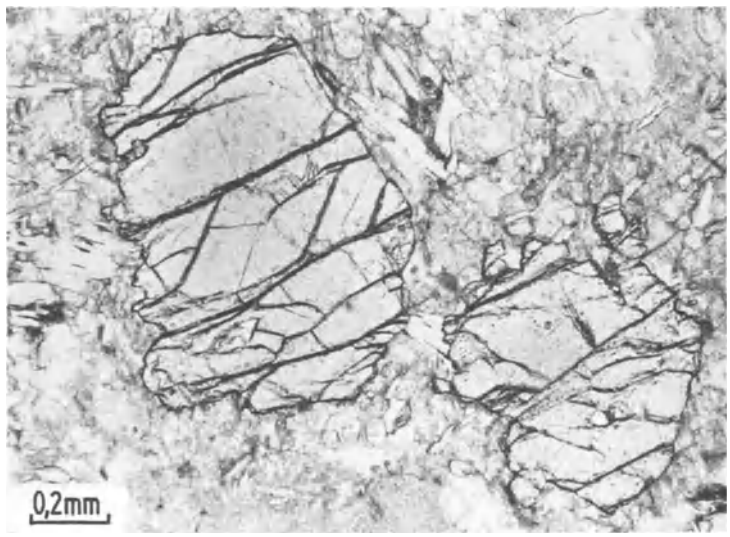

Fig. 40 Mg-spinel with cleavage after {100} in forsterite-bearing marble. Notice the clear relief. Hrubý Jeseník, Moravia, CR. Uncrossed polarizers.

Distinguishing features: similar to garnet, distinguished from it by triangular cross-sections and absence of optical anomalies.

Alteration: none.

Occurrence: spinel s.s. is rare. Occurs in granulites and some contact metamorphic aureole rocks. The Fe^{2+} variety (**pleonaste**) can occur as an early euhedral phase in basalts (e.g. gabbro from Radautal, Harz Mts, Germany) and also as an accessory mineral in dolomitic marbles and siliceous marbles. **Hercynite** occurs in Ti-rich ultrabasic igneous rocks and also in cordierite-bearing gneisses. **Picotite** predominantly occurs as inclusions in olivine in alkali-basalts and related volcanic rocks, also in olivine aggregates and in granular form in serpentinites. **Chromite** is the earliest phase to crystallize in basalts, and therefore occurs in peridotites, melilites, limburgites, pyroxenites, picrites and also in gabbros and norites.

Paragenesis: spinel s.s., with almandine, cordierite and corundum, and with calcite, dolomite and serpentine;
picotite, with olivine;
chromite, with olivine, serpentine and titanaugite;

2.3 Pyrochlore and koppite

$(Na, Ca)_2(Nb, Ti, Ta)_2O_6(OH, F, O)$ cubic–hexaoctahedral

Thin-section characteristics

Form: commonly fine-grained, as euhedral-octahedral grains (Fig. 41).

Cleavage: none.

Colour:

Pyrochlore:	Koppite:
red-brown to dark brown to black.	brown, red to nearly colourless.

Distinguishing features: under the microscope it is not possible to distinguish between pyrochlore, koppite, perovskite, chromite, picotite and melanite. Rutile and cassiterite occur in different parageneses.

Alteration: none.

Occurrence: very rare. In foid-bearing pegmatites, in sanidinites; koppite in carbonatites (e.g. from Schelingen, Kaiserstuhl, Germany).

Paragenesis: with calcite, apatite and phlogopite.

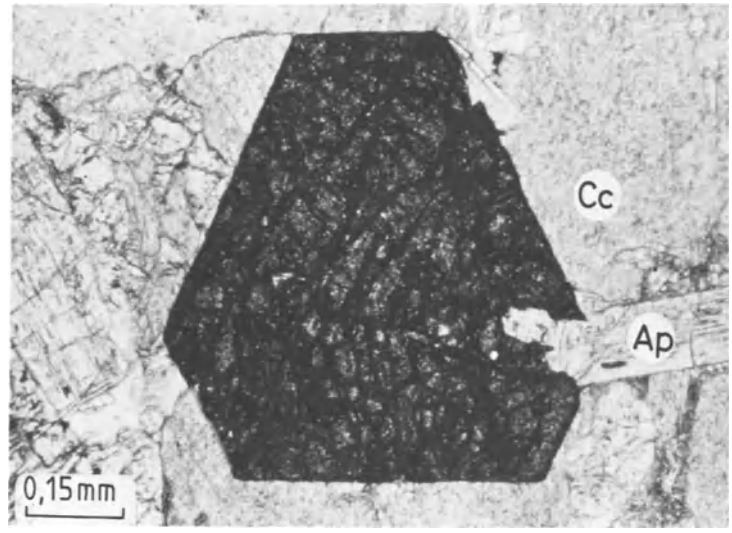

Fig. 41 Koppite (euhedral) in koppite-bearing carbonatite. Schelingen, Kaiserstuhl, Germany. Uncrossed polarizers.

2.4 Garnet group

$R_3^{2+}Z_2^{3+}[SiO_4]_3$ cubic–hexa-octahedral

General features: most common in metamorphic rocks where they form isomorphic mixtures of their endmembers (Table 2).

Table 2 Composition of the most important endmembers of the garnet group

R^{2+}	Z^{3+} Al	Fe	Cr
Mg	pyrope		
Fe	almandine		
Mn	spessartine		
Ca	grossularite	andradite	uvarovite

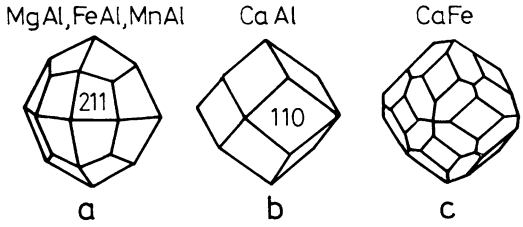

Fig. 42 Crystal form differs according to the chemical composition of garnets: (a) icositetrahedral: pyrope, almandine, spessartine; (b) rhombic-dodecahedral: grossularite; (c) combination of (a) and (b): andradite.

The garnet group can be divided into two subgroups based on different ionic radii of Mg, Fe, Mn on the one hand and Ca on the other:

1. Pyralspite = pyrope (Mg, Al), almandine (Fe, Al) and spessartine (Mn, Al)
2. Grandites or ugrandites = grossularite (Ca, Al), andradite (Ca, Fe) and uvarovite (Ca, Cr). This subgroup also includes melanite (= andradite with 5–15 wt% TiO_2).

Thin-section characteristics

Form: frequently euhedral (almandine, grossularite, Fig. 42), but also occurs as subhedral rounded or irregular unhedral grains (pyrope, Fig. 43). Square and hexagonal cross-sections after the rhombic dodecahedra {110} or icositetrahedra {211}. The latter habit predominantly occurs in felspathoid rocks and the rhombic dodecahedral form is frequent in mica schists.

Cleavage: none, {110} cleavage sometimes present. Rare parallel or irregular fractures in stressed crystals (Fig. 44).

Colour: colourless in thin sections of normal thickness. Pale pinkish colours are typical in pyralspites and pale-green to yellow and brown-green colours in the grandites. Stronger colours are typical for melanites (brown, commonly zonal variations) and in uvarovites (bright emerald green).

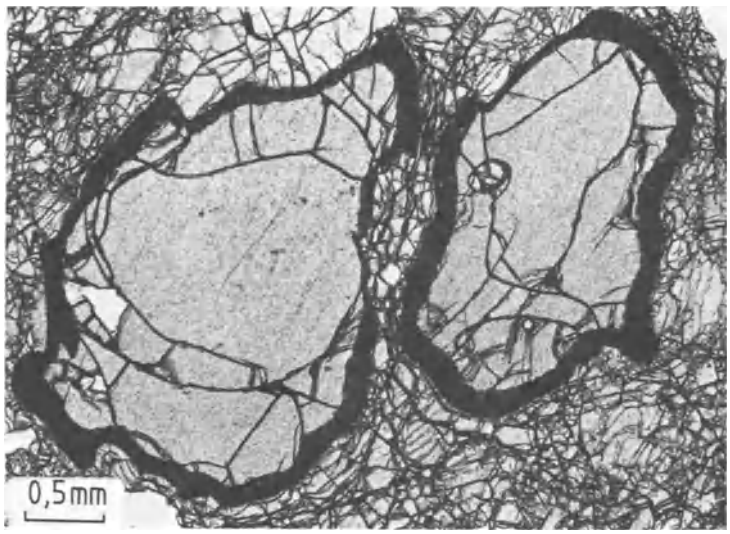

Fig. 43 Pyrope with a kelyphitic rim in garnet olivine rock. Val Gorduno, Canton Ticino, Switzerland. Uncrossed polarizers.

Refraction:

Pyrope	n = 1.720 – 1.760
Almandine	n = 1.770 – 1.820
Spessartine	n = 1.790 – 1.810
Grossularite	n = 1.735 – 1.770
Andradite	n = 1.850 – 1.890
Uvarovite	n = 1.838 – 1.870
Melanite	n = 1.860 – 2.000

The high refraction gives rise to a high relief, with a rough, grooved surface and dark edges. Even small crystals clearly stand out from their surrounding minerals.

Special characteristics: grossularite, andradite and uvarovite tend to show anomalous birefringence, particularly in larger crystals (Fig. 45) with grey interference colours of the first order (Δ up to 0.008, typically optically biaxial $\ominus$, but also biaxial with $2V = 90°$). Zonar growth is common. In metamorphic rocks prophyroblastic garnets can show a sieve texture with other minerals distributed in a diffuse or zonal pattern in the garnet (poikiloblastic texture, Fig. 44). Snowball garnets form as a result of synmetamorphic deformation during porphyroblastic growth, producing heliocentric inclusions (Fig. 46).

Distinguishing features: garnet is easily recognized under the microscope. Presence of anomalous birefringence colours can make the identification more difficult. If grains are very small they can be mistaken for minerals from the spinel group. However, spinel-group minerals

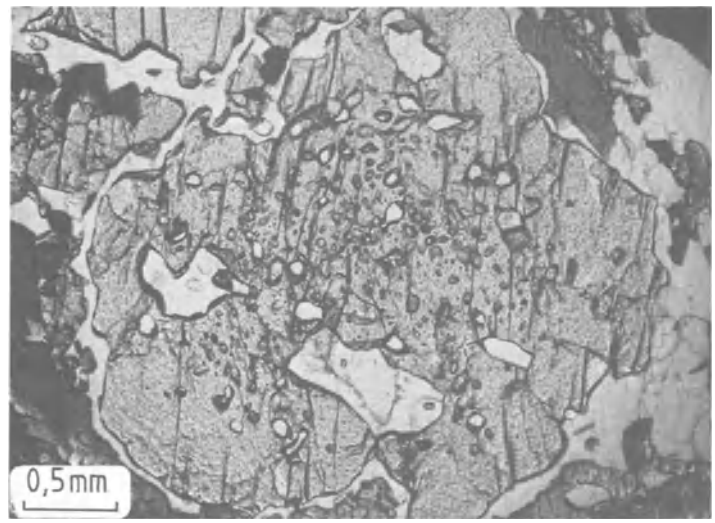

Fig. 44 Poikiloblastic almandine with tectonically induced parallel fractures. Garnet amphibolite. Xenolith in the volcanic complex of Doña Juana, southern Colombia. Uncrossed polarizers.

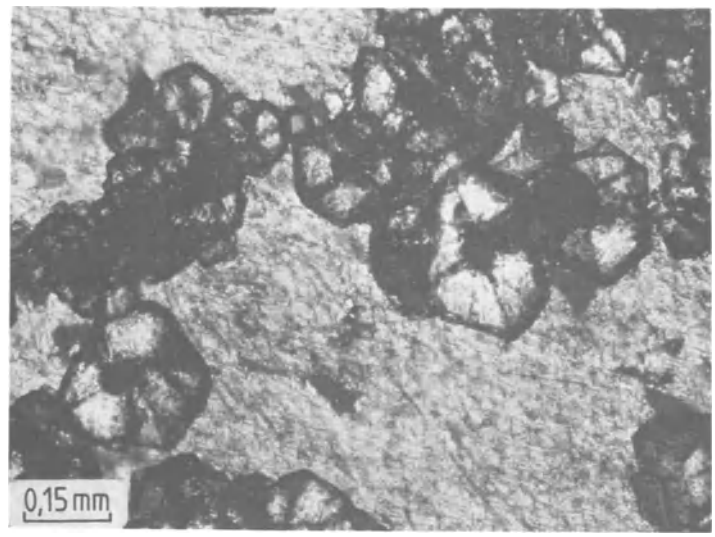

Fig. 45 Euhedral uvarovite with anomalous birefringence colours in a calcite matrix. Magog, Quebec, Canada. Crossed polars.

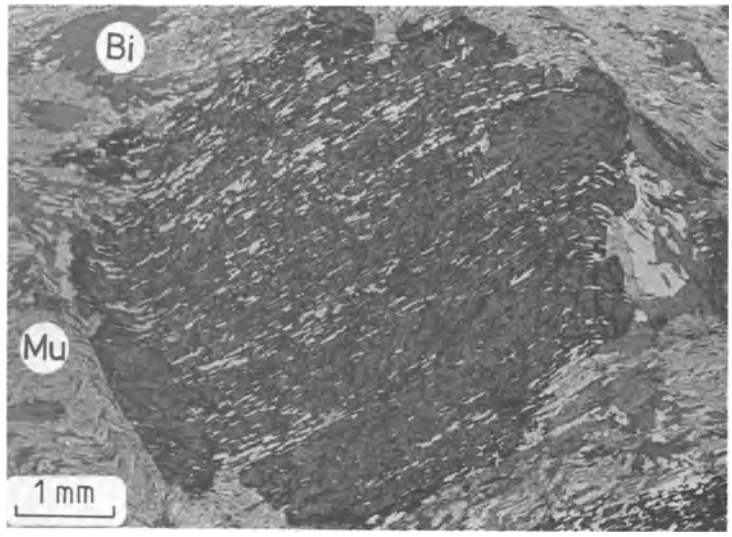

Fig. 46 Poikiloblastic almandine with heliocentric inclusions. Deformed garnet-biotite-muscovite schist with rotated garnet. Lukmanier Pass, Switzerland. Uncrossed polarizers.

tend to be green in colour with octahedral habits. Representatives of the grandite subgroup can be confused with periclase in marbles; melanite is similar to picotite and perovskite, but the latter has a much higher refraction.

Identification of the endmember compositions with the aid of a microscope alone is not possible and one has to resort to microprobe analysis.

Alteration: radial replacement of pyrope or pyrope-rich almandine by hornblende and picotite (kelyphitic rim) can occur in garnet and olivine-bearing rocks (Fig. 43). Kelyphitic rims of hornblende, plagioclase and quartz around garnet in amphibolites and eclogites are common; they probably form during retrograde metamorphism at lower pressures. Low-grade diaphthoritic metamorphic alterations sometimes aided by hydrothermal alterations can lead to replacement of garnet by chlorite (or biotite, sericite or epidote).

2.4.1 Pyrope

$Mg_3Al_2[SiO_4]_3$

Form: commonly shows round cross-sections with kelyphitic rims (Fig. 43).

Occurrence: in high-pressure (high-temperature) paragenesis in peridotite, serpentinite, kimberlite, eclogite. Placer deposits (e.g. Bohemian massive or as 'Kaprubin' in South Africa).

Paragenesis: with olivine, serpentinite, pyroxene (omphacite in eclogite) and phlogopite.

2.4.2 Almandine

$Fe_3Al_2[SiO_4]_3$

Occurrence: most common garnet. Occurs on a regional scale in metamorphic Al-rich rocks (Fig. 44) and is found throughout most metamorphic rocks from phyllites to high-grade gneisses. In amphibolites almandine tends to contain appreciable amounts of pyrope and grossularite. It is rare in igneous rocks (e.g. granites, granodiorites and calc-alkaline volcanic rocks) due to resorption of Al-rich contact rocks into the magma.

Paragenesis: in mica schist with biotite, muscovite, chlorite, quartz, kyanite and staurolite.

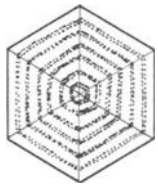

Fig. 47 Characteristic zoning pattern in grossularite.

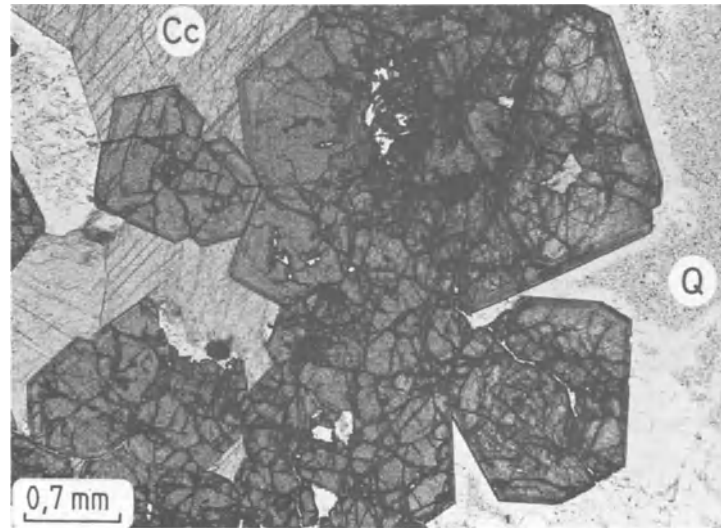

Fig. 48 Euhedral, zoned grossularite in a contact aureole. San Leone, Sardinia. Uncrossed polarizers.

2.4.3 Grossularite

$Ca_3Al_2[SiO_4]_3$

Form: granular euhedral grains.

Colour: colourless to pale green.

Special characteristics: optical anomalies and zonal growth patterns are common (Figs 47, 48).

Occurrence: a contact- and regional metamorphic mineral in calcareous and marly rocks. In siliceous carbonates and marbles. Also occurs in rocks which have undergone calcium metasomatism; in the case of metasomatic addition of iron, andradite forms instead of grossularite, which belongs to the ugrandite series and is typical of skarn formations.

Paragenesis: with diopside, wollastonite vesuvianite and calcite.

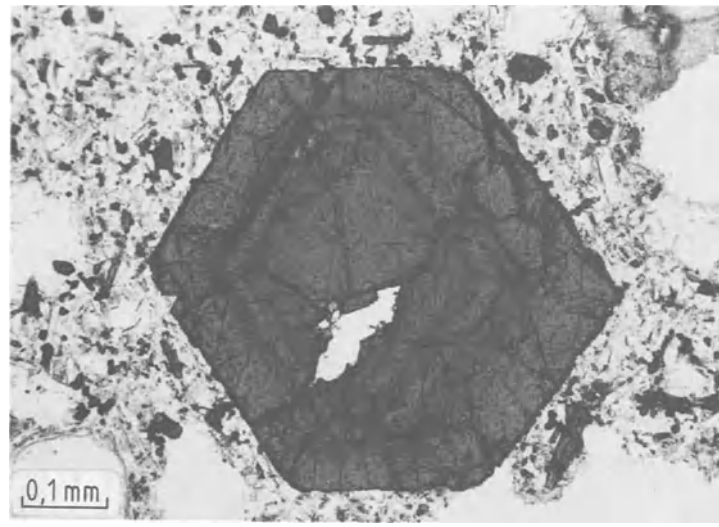

Fig. 49 Zoned melanite in phonolite. Niederrotweil, Kaiserstuhl, Germany. Uncrossed polarizers.

2.4.4 Melanite

$Ca_3Fe_2[(Si, Ti)O_4]_3$

Colour: bright to dark brown; intensity of colour and birefringence increase with increasing TiO_2 content. Growth zones are common.

Occurrence: accessory mineral in alkali and Na-rich silica undersaturated volcanic rocks (phonolite to tephrite and foidite and related pyroclastic derivatives, e.g. Kaiserstuhl (Fig. 49) and Laacher volcanic area, Germany) and in equivalent plutonic rocks.

Paragenesis: with nepheline, leucite, minerals of the sodalite group, aegirine-augite and sanidine.

2.5 Leucite

$K[AlSi_2O_6]$ cubic hexoctahedral and tetragonal-dipyramidal

General features: most common and characteristic feldspathoid in K-rich and silica deficient volcanic rocks replacing the potassium feldspar component:

$$K[AlSi_3O_8]–SiO_2 \rightarrow K[AlSi_2O_6].$$

The cubic high-temperature form of leucite crystallizes at temperatures in excess of 605 °C. At lower temperatures it forms pseudo-cubic paramorphous crystals after the high-temperature form, and optically anisotropic polysynthetic twinning is typical (Figs 50(c), 51).

Thin-section characteristics

Form: typically occurs in euhedral crystals, in trapezohedron form {211} (Fig. 50(a)) with octahedral or rounded cross-sections. Skeletal forms are not uncommon.

Fig. 50 Characteristic forms of leucite.
(a),(b) Leucite with inclusions.
(c) Euhedral deltoid-icositetrahedron with typical laminar twins.

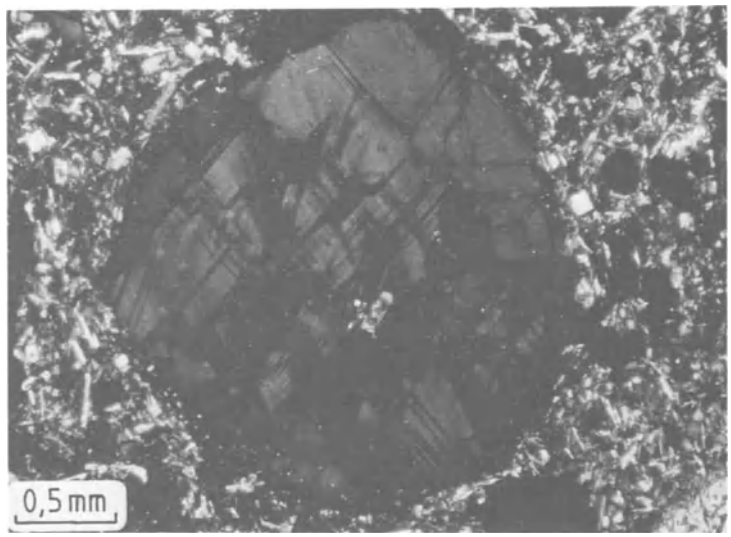

Fig. 51 Euhedral leucite phenocryst showing characteristic twin lamellae. Nepheline-nosean leucitite (schorenbergite). Rieden, Laacher volcanic area, Germany. Crossed polars.

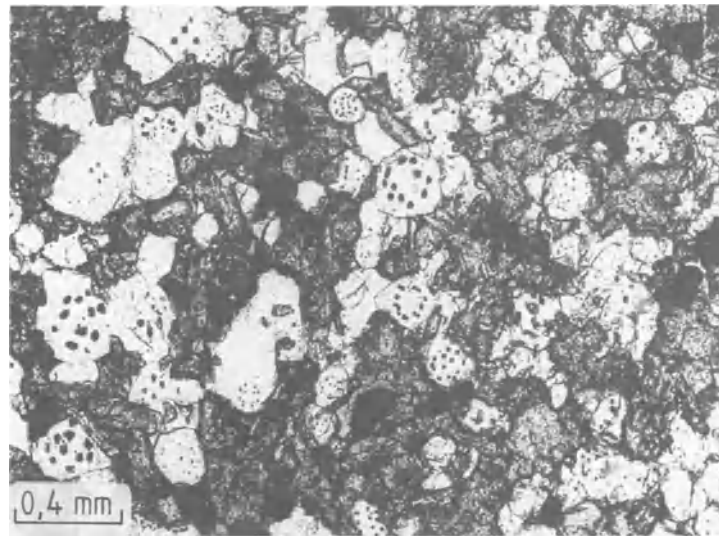

Fig. 52 Euhedral leucite with inclusions in leucitite. Capo di Bove, Colli Albani, Italy. Uncrossed polarizers.

Cleavage: imperfect on {110}, not visible under the microscope.

Twinning: fine lamellar twinning parallel to {110} (Figs 50(c), 51).

Colour: colourless.

Refraction and birefringence:

$n_e = 1.509$
$n_o = 1.508$
$\oplus\Delta = 0.001$

Very low, negative relief; in polysynthetic twins extremely low birefringence (compensator red I necessary for identification); identification of very small grains is very difficult (grey to black interference colours of the 1st order).

Special characteristics: commonly two leucite generations can occur in a rock: large, partly glomerophyrically intergrown crystals and small, rounded leucite crystals in the groundmass with concentrically and radially aligned inclusions (in most cases glass) (Figs 50(a),(b); 52).

Distinguishing features: easily confused with analcite, which has a lower birefringence, is xenomorphic and inclusions-free; chabasite has very low birefringence, anomalous subgrains with a well-developed cleavage parallel to {1011} and shows rhombohedral habit; tridymite is optically uniaxial positive; rock-glass in general shows a higher relief and is devoid of cleavage and crystal forms.

Alteration: late magmatic hydrothermal Na-rich fluids can alter leucite into pseudo-leucite by metasomatic Na/K-exchange (= fine-grained intergrowth of alkali feldspar and leucite), or into analcite pseudomorphs.

Occurrence: in K-rich silica-undersaturated young volcanic rocks (e.g. the leucite tephrites and leucitites from Mt Vesuvius, the Colli Albani, from northern Lazio, from the Laacher volcanic area in Germany and other areas); it never occurs in plutonic or metamorphic rocks.

Paragenesis: never found together with quartz. Commonly found with nepheline, minerals from the sodalite group, aegirine-augite, olivine, clinopyroxene, melanite and rock-glass.

2.6 Sodalite group

Sodalite $Na_8[Cl_2|(AlSiO_4)_6]$ cubic–hexatetrahedral
Nosean $Na_8[SO_4|(AlSiO_4)_6]$
Hauyne $(Na,Ca)_{8-4}[(SO_4)_{2-1}|(AlSiO_4)_6]$

General features: isotypic crystals of the feldspathoids, which occur in Na-rich silica-undersaturated magmatic rocks.

Thin-section characteristics

Form: six, eight and ten-sided cross-sections are very common, and they can be slightly distorted. Rounded corners and corroded, curved and embayed faces are typical (Figs 53, 55). In volcanic rocks grains are predominantly euhedral, and in plutonic rocks xenomorphic (sodalite, Fig. 54).

Cleavage: weak parallel to {110}.

Twinning: parallel to {111}.

Colour: in nosean and hauyne the colours may vary within a single crystal in a patchy or striped fashion.
Sodalite: typically colourless, rare pale grey.
Nosean: colourless to grey-brown, rarely pale blue.
Hauyne: pale blue, purple or bluish green.

Refraction: very low, negative relief.
Sodalite n = 1.483–1.490
Nosean n = 1.488–1.495
Hauyne n = 1.496–1.508

Special characteristics: in nosean and hauyne dark rims and zonar exsolution inclusions of submicroscopic Fe-sulphides and Fe-oxides are concentrically arranged or define linear patterns (Figs 53, 56, 57).

Distinguishing features: the different sodalite-group minerals are not easily distinguished from each other under the microscope. Tröger describes some microchemical tests carried out on uncovered thin sections to help with further identification (Tröger, 1969). Smaller grains tend to remain unrecognized, particularly when they occur as colourless microliths within the matrix. They can be mistaken for analcite and leucite. Leucite tends to show polysynthetic twinning and/or is rich in inclusions. Analcite tends to be restricted to cavities.

Alteration: late magmatic hydrothermal alteration produces fibrolitic zeolite aggregates, predominantly natrolite, growing and propagating from cracks. Weathering leads to sericite formation and alteration into kaolinite, during which initially the rock shows a brick-red colour due to fine-grained disseminated limonite.

Fig. 53 Nosean and hauyne showing characteristic alignment of inclusions along growth zones (exsolved Fe-ore) and corroded edges.

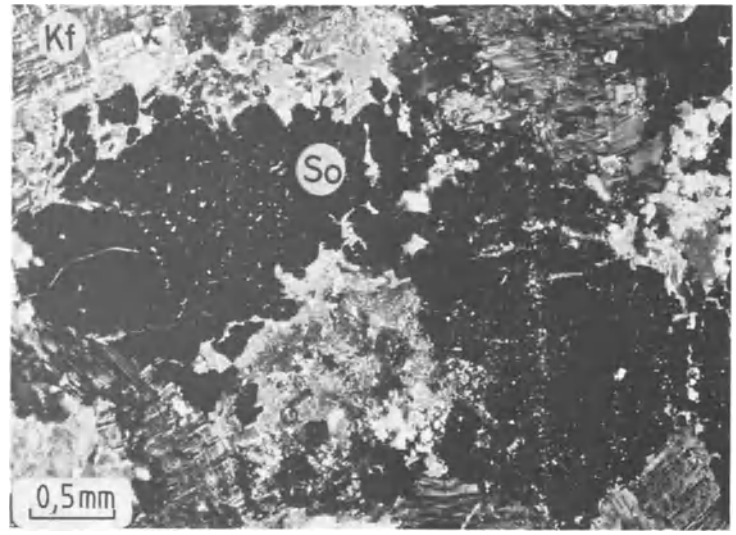

Fig. 54 Euhedral sodalite (isotropic) next to sericitized microcline with typical microcline twinning. Sodalite syenite (ditroite). Ditro, Transylvania, Romania. Crossed polars.

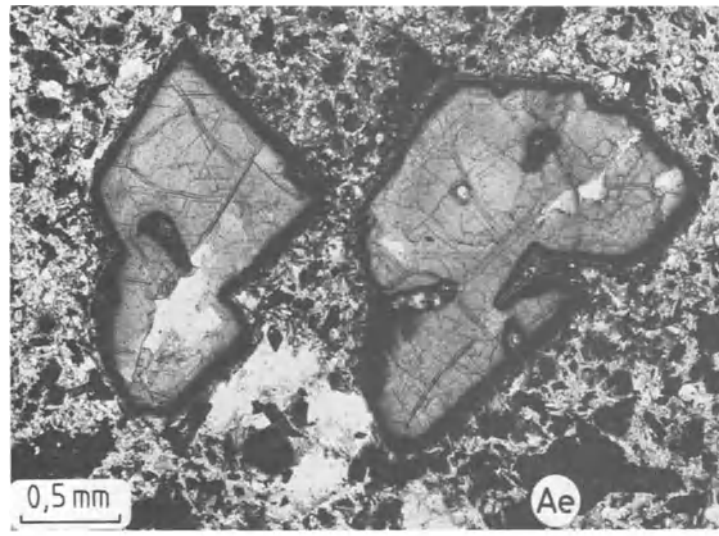

Fig. 55 Euhedral, corroded nosean phenocryst with dark edges. Nosean phonolite (selbergite). Rieden, Laacher volcanic area, Germany. Uncrossed polarizers.

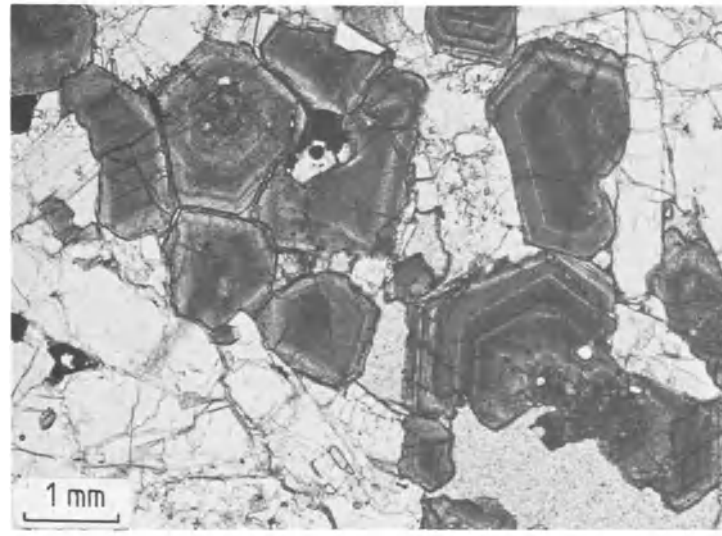

Fig. 56 Euhedral, partly corroded and zoned hauyne phenocrysts surrounded by K-feldspar. Hauyne syenite. Laacher volcanic area, Germany. Uncrossed polarizers.

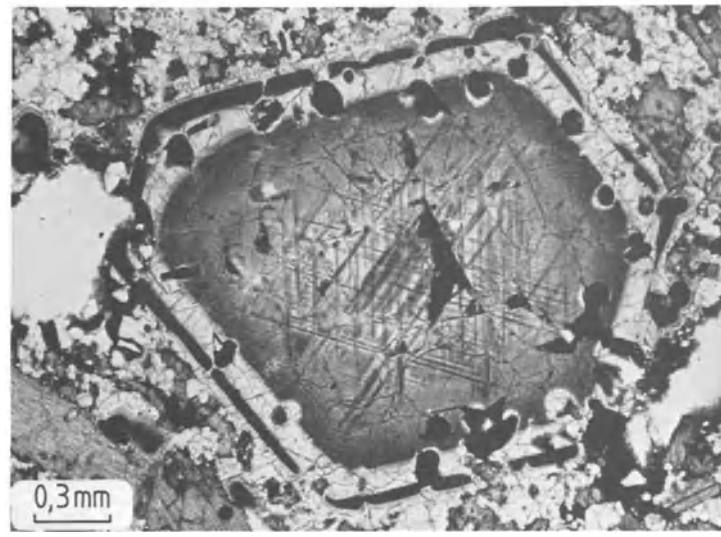

Fig. 57 Euhedral hauyne phenocryst with dark edges and fine ore inclusions in the centre. Hauyne tephrite, Monte Vulture, Apulia, southern Italy. Uncrossed polarizers.

Occurrence: sodalite is the most common representative of this group. It can be rock-forming in Na-rich and silica-undersaturated plutonic and volcanic rocks (e.g. sodalite-syenite, sodalite-monzosyenite, sodalite-phonolite, etc.). Nosean and hauyne are restricted to volcanic rocks and are common in phonolites and tephrites, and also in foidites and rare in hauynites.

Paragenesis: sodalite-group minerals are never found together with quartz. However, they occur with nepheline, leucite, aegirine-augite, melanite, olivine, Ti-augite and rock-glass.

2.7 Analcite

$Na[AlSi_2O_6] \cdot H_2O$ cubic–hexaoctahedral.

General features: it is a post-magmatic mineral which predominantly occurs in cavities and fractures in volcanic rocks.

Thin-section characteristics

Form: commonly xenomorph or as eight-sided or rounded grains.

Cleavage: not good, parallel to (001), rarely visible in large crystals.

Twinning: under the microscope rarely visible; lamellar parallel to (001) and (110).

Colour: colourless.

Refraction and birefringence:

$n_e = 1.486$
$n_o = 1.487$
$\ominus\Delta = 0.001$

Very low, negative relief; common as isotropic interstitial material; larger crystals tend to show anomalous weak birefringence colours, optically uniaxial to biaxial ⊖ with small axial angle.

Special characteristics: in single crystals weak birefringence similar to leucite.

Distinguishing features: easily mistaken for leucite, particularly if the latter is without its characteristic inclusions. Chabazite has higher birefringence colours; sodalite shows weak cleavage traces parallel to {110}; opal has no cleavage; tridymite has lower birefringence colours.

Alteration: into natrolite as a result of CO_2 flushing and reaction with quartz and kaolinite.

Occurrence: rare, as a late magmatic mineral together with foids in the ground matrix of volcanic rocks (e.g. analcite basalts of the Cyclope islands/Aetna). Intergranular as interstitial material between plagioclase and clinopyroxene in basalts (e.g. Vogelsberg basalt, Germany). Alteration product of other foids, particularly leucite. In fractures and cavities (Fig. 58), together with

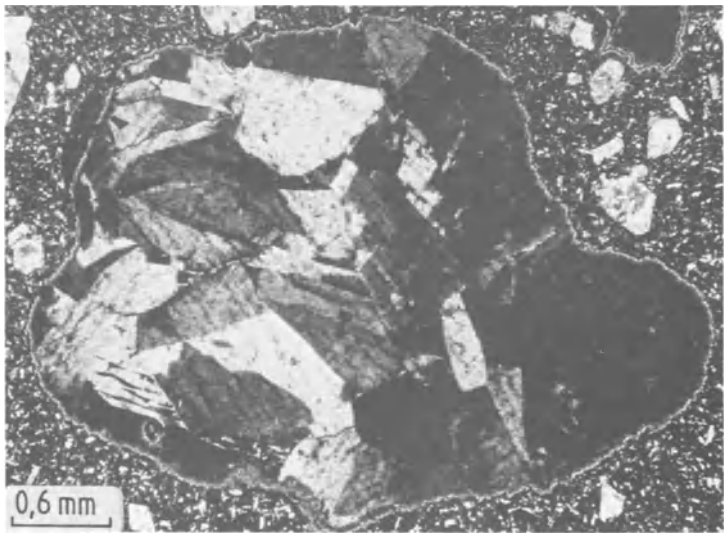

Fig. 58 Paramorphous analcite filling an amygdale in an alkaline hawaiite. Cyclope Islands near Catania, Sicily. Crossed polars.

zeolite. In low-grade metamorphic basaltic rocks as mineral of the zeolite facies.

Paragenesis: magmatic, never together with quartz, but with nepheline, leucite and Ti-augite. In zeolite-facies rocks and with heulandite, stilbite and laumontite.

2.8 Cristobalite

SiO_2 pseudo-cubic (tetragonal–trapezohedral)

General features: easily overlooked, rare silica mineral in cavities in acidic volcanic rocks. Paramorphous transition of cubical high-cristobalite into tetragonal low-cristobalite at decreasing temperatures.

Thin-section characteristics

Form: platy, in cavities of volcanic rocks in round aggregates; fibrous or as needles forming part of devitrification spherolites together with alkali feldspars (Fig. 65); like chalcedony in lussatite and lussatine.

Twinning: commonly parallel to (111).

Cleavage: none.

Colour: colourless.

Refraction and birefringence:

$n_e = 1.484$
$n_o = 1.487$
$\ominus\Delta = 0.003.$

Very low relief and birefringence, optically uniaxial ⊖, abnormal biaxial ⊖ ($2V_\alpha = 25°$).

Character of elongation: lussatite: (+), Lussatine: (–).

Extinction: tends to be straight.

Distinguishing features: tridymite is biaxial ⊕ and tends to be platy; chalcedony has higher birefringence colours, quartz is uniaxial ⊕; and also nepheline has a higher relief and birefringence (Fig. 59). Chabazite shows anomalous subgrains and has a better developed cleavage and occurs in a different paragenesis.

Alteration: none.

Occurrence: rare mineral, almost exclusively restricted to fractures and cavities in silica-oversaturated volcanic rocks, and also as devitrification mineral; also occurs as a contact-metamorphic mineral in sanidine-facies rocks.

Paragenesis: with rock-glass, tridymite and alkali feldspar.

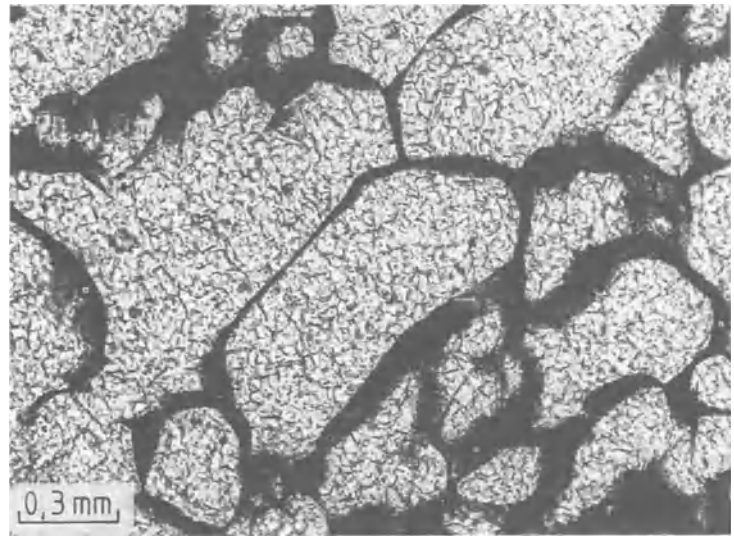

Fig. 59 Low-cristobalite with typical subgrain texture in a glace (industrial fire-resistant product). Uncrossed polarizers.

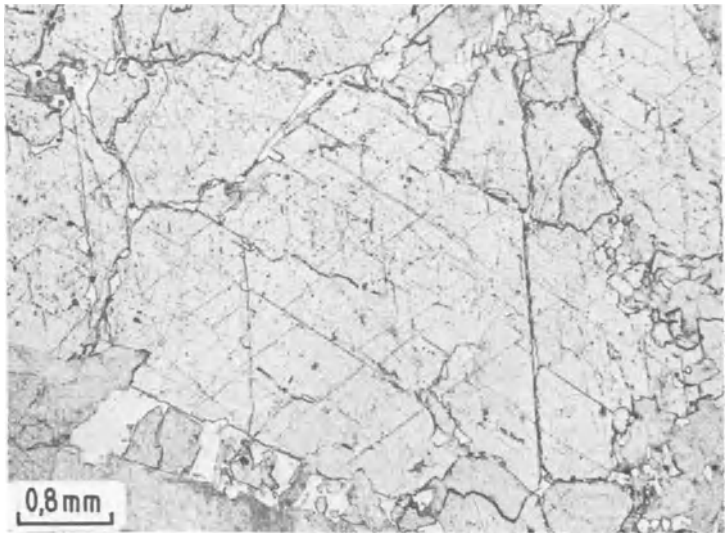

Fig. 60 Fluorite with two intersecting cleavage planes at 70° and 110°. Fluorite-bearing granite. Wölsendorf, Oberpfalz, Bavaria, Germany. Uncrossed polarizers.

2.9 Fluorite

CaF_2 cubic–hexaoctahedral

Thin-section characteristics

Form: usually anhedral, interstitial mineral, rarely euhedral with square shapes {001}.

Cleavage: perfect octahedral {111}, cleavage traces are either intersecting at 70° and 110° angles respectively (Fig. 60), or as three intersecting lines at 60° and 120° angles.

Colour: colourless, often bluish or purple with zonar or spotted colour patterns.

Refraction: n = 1.434, very low, negative relief; isotropic.

Special characteristics: purple colour zonation due to varying radioactive traces of uranium and thorium. In purple-coloured fluorite coloured haloes around radioactive inclusions are typical.

Distinguishing features: isotropic, low refractive index, usually zoned with perfect cleavage traces.

Alteration: none.

Occurrence: rare, as a trace mineral (e.g. in Li-rich granites, greisen and pegmatites). More commonly found in association with hydrothermal deposits. Also found as cementing material in sandstone and in biogenic dolomite.

Paragenesis: with topaz, tourmaline, quartz and hematite.

2.10 Amorphous minerals, glass and cryptocrystalline material

2.10.1 Limonite

$FeOOH \cdot nH_2O$ amorphous

General features: breakdown product of Fe-bearing minerals. Mainly comprised of cryptocrystalline goethite (α-FeOOH, Part B, section 4.27) and lepidocrocite (γ-FeOOH) with variable water content.

Thin-section characteristics

Form: amorphous, shapeless, interstitial material, oolitic, crusty, detrital or earthy, radially fibrous and in concentric layers.

Colour: orange-brown to red-brown; dendritic forms are opaque.

Refraction: n = 2.0–2.1, very high refractive index; isotropic (rare with anomalous low birefringence colours).

Distinguishing features: crystalline goethite has a high birefringence and straight extinction.

Alteration: breakdown in microcrystalline hematite.

Occurrence: alteration product of oxidized Fe-bearing minerals, in most rocks; common as a pigment.

Paragenesis: not characteristic.

2.10.2 Opal

$SiO_2 + nH_2O$ amorphous

Thin-section characteristics

Form: amorphous, colloidal masses filling interstitial spaces and grape- and kidney-shaped aggregates (Fig. 61).

Cleavage: none, only irregular shrinkage fractures.

Colour: colourless to yellow or red (due to Fe-hydrate).

Refraction: n = 1.44–1.46, exceptionally low relief; isotropic, occasionally anomalous tension-induced birefringence (due to water loss).

Distinguishing features: rock-glass, analcite and members of the sodalite group have a higher refractive index. Fluorite shows excellent cleavage, and chabazite shows weak birefringence.

Alteration: during alteration and diagenesis opal is replaced by chalcedony.

Occurrence: a secondary mineral in young rocks. Absent in plutonic and metamorphic rocks. In volcanic rocks present as water-clear hyalite in grape- or kidney-shaped aggregates that grow in fractures and cavities in acidic and basic lavas and pyroclastic rocks. Opal is formed as a result of hydrothermal and water interaction with the silicate component of the rock. It also occurs in sinter precipitates of geothermal springs and geysers. During weathering of silicates, silica-gel forms which crystallizes as opal, impregnating the rock. Opal is a rock-forming mineral in diatomite and radiolarite as an organogenic product.

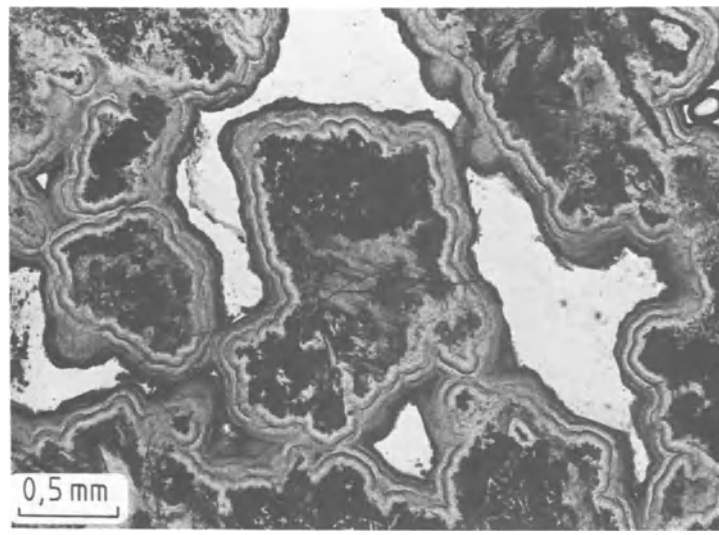

Fig. 61 Grape- to kidney-shaped opal as colloidal interstitial mass filling cavities in a young volcanic rock from western Anatolia, Turkey. Uncrossed polarizers.

2.10.3 Rock-glass

Variable chemistry amorphous

General features: metastable, product of rapidly cooled or quenched melts. Restricted to volcanic rocks and dykes.

Thin-section characteristics

Form: amorphous.

Cleavage: none. Commonly irregular spherical cracks (perlitic texture) formed during shrinkage while cooling (Fig. 62).

Colour: colourless, pale yellow to pale brown, rarely pale coffee-brown (basaltic glass); colour due to submicroscopic inclusions of magnetite and ilmenite.

Refraction and birefringence:

Rhyolite glass	n = 1.48 – 1.51
Palaeorhyolite glass (pitchstone)	n = 1.49 – 1.51
Dacite glass	n = 1.50 – 1.53
Trachyte glass	n = 1.49 – 1.53
Andesite glass	n = 1.49 – 1.53
Basaltic glass (tachylyte, sideromelane)	n = 1.53 – 1.58
Leucittephrite glass	n = 1.51 – 1.61

The refractive index varies according to chemistry; isotropic, tension-induced birefringence colours are produced around inclusions.

Special characteristics: Natural glasses often show flow textures (e.g. obsidian) or shard textures typical for ignimbrites (Fig. 63) with phenocrysts surrounded in a flow-like fashion by a shard-rich matrix. However, this is not a result of flow but of welding together of hot rock particles and melt, with the melt being squeezed out by the overburden. Also characteristic are the spheroidal perlitic shrinkage cracks (Fig. 62).

Distinguishing features: difficult to recognize in those cases where the glass is colourless and occurs as interstitial material in small quantities (Fig. 64). Opal and fluorite have lower refractive indexes. Analcite, leucite and members of the sodalite group show crystal forms and also cleavage.

Alteration: devitrification propagates from fractures. The glass is replaced by fine crystalline patchy aggregates (texture) comprised of those minerals which would have formed if the magma had cooled more slowly. Spherolite occurs in acidic glass, where it forms radially arranged fibres of quartz or low-cristobalite and alkali feldspar, nucleating from crystal faces and other inclusions in the glass (Figs 65, 66). The same quench crystals, are rare in basic glasses, where they are called variolites, and consist of plagioclase and pyroxene. In some glasses skeletal and dendritic microcrystals form during cooling or/and devitrification (Fig. 68). Basic glasses of older volcanoes (e.g. Devonian to lower Carboniferous diabase, spilite) show a green colour, e.g. they are partly altered into oxidized chlorite (delessite). Hydrothermally altered glasses contain zeolites, in particular natrolite. Weathering of acidic glasses produces

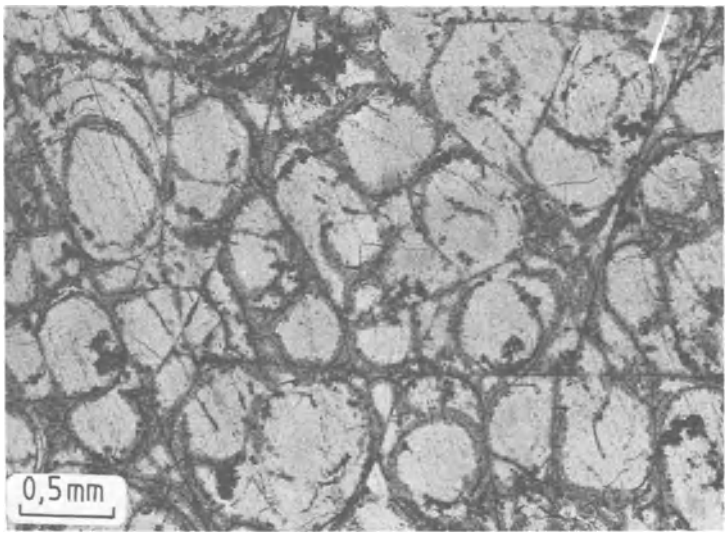

Fig. 62 Volcanic glass with perlitic cracks. Vitrophyric Permian palaeorhyolite (quartz porphyry). Schletta, Sachsen. Uncrossed polarizers.

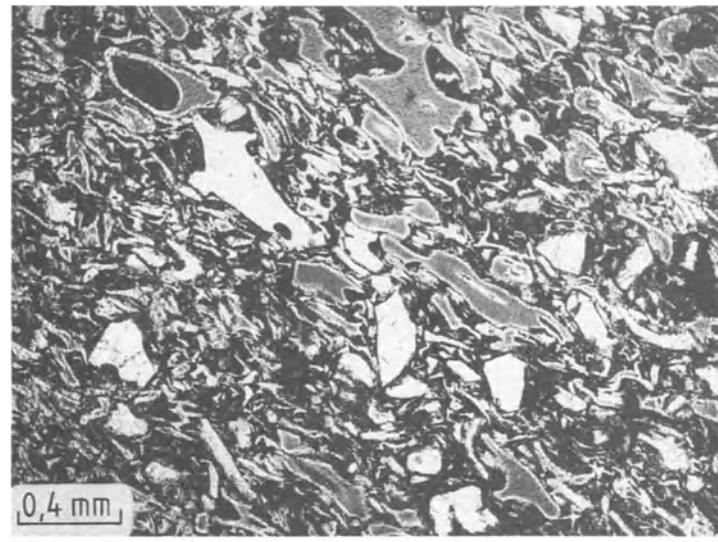

Fig. 63 Volcanic glass with typical ignimbrite texture: glass shards. Rhyodacitic ignimbrite. Alota, eastern Cordillera, SW Bolivia. Uncrossed polarizers.

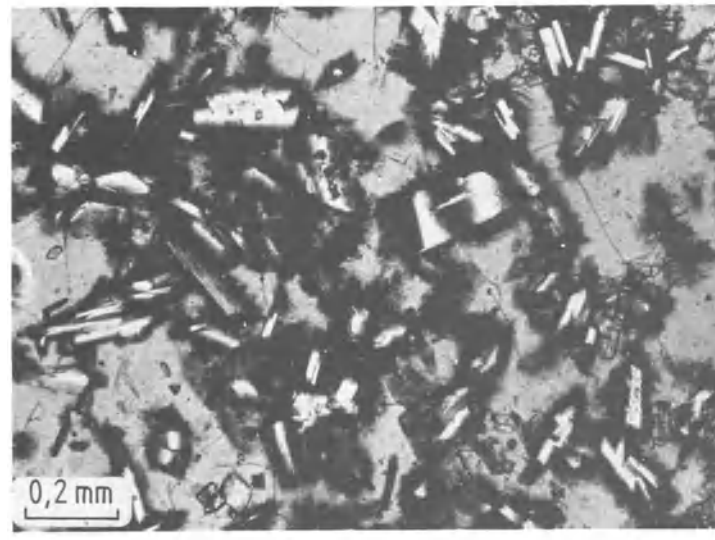

Fig. 64 Pale-brown basaltic glass filling interstitial space in an alkali-olivine basalt. Onset of recrystallization around plagioclase and titanaugite phenocrysts. Lanzarote, Canary Islands. Uncrossed polarizers.

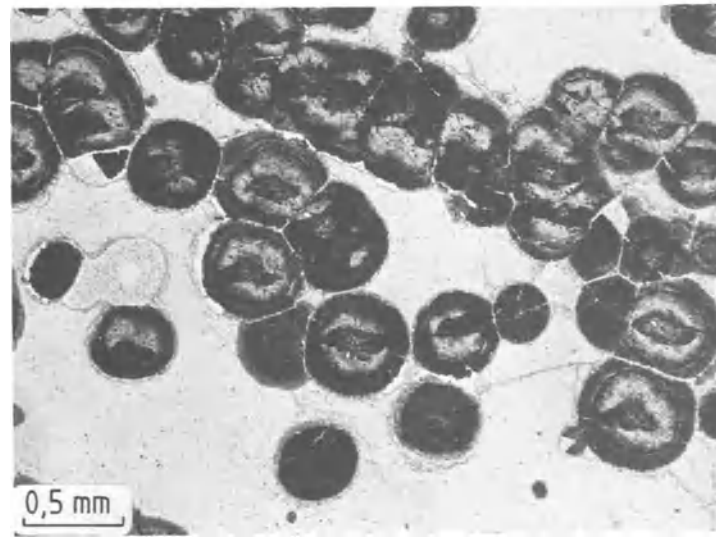

Fig. 65 Acidic volcanic rock with spheroidal devitrification texture. Rhyolitic obsidian. Hliník, Slovakia. Uncrossed polarizers.

Fig. 66 Acidic volcanic glass with spherolites (devitrification to alkali feldspar and low-cristobalite). Rhyolite. Kremnica, Slovakia. Uncrossed polarizers.

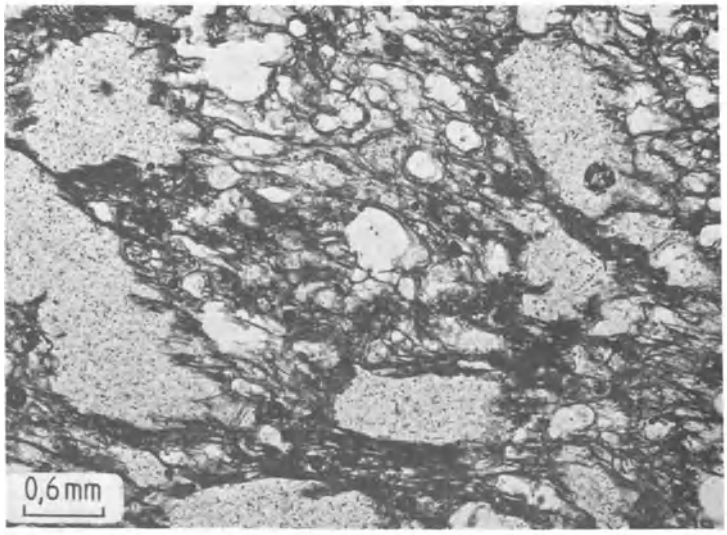

Fig. 67 Volcanic glass with bubbly pumiceous texture. Dacitic pumice. Mojanda volcano, northern Ecuador. Uncrossed polarizers.

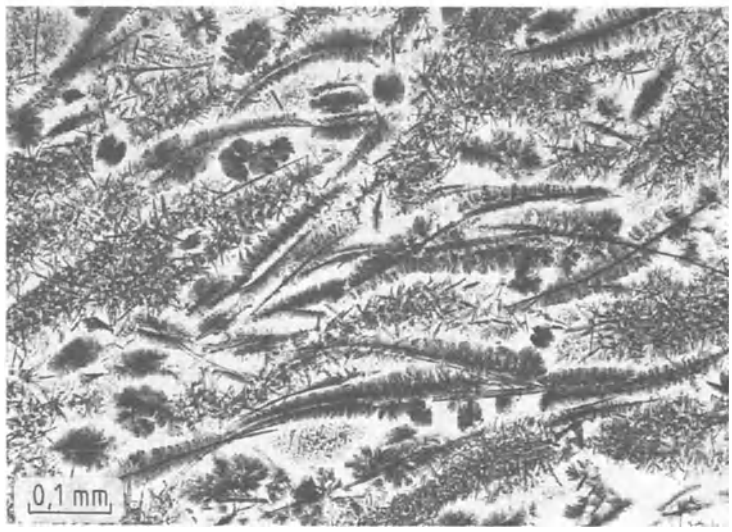

Fig. 68 Fern-like devitrification microlites (green hornblende?) in a Tertiary largely devitrified glass. Arran Island, Scotland. Uncrossed polarizers.

kaolinite and basic glasses alter to nontronite, montmorillonite or halloysite.

Volcanic glasses are distinguished from each other by their water content, and how fresh they are:

Obsidian:	1–2% H_2O:	fresh.
Perlite:	3–4%: H_2O	shows perlitic cracks from which devitrification textures propagate; low birefringence (use compensator red I).
Pitchstone:	4–8% H_2O:	older volcanic glass (e.g. from the Permian in Saxony) largely devitrified.

Occurrence: natural glasses are the product of rapidly cooling magmas; hence they are absent in plutonic rocks. Glass can be present in dykes which cooled close to the surface. In lavas and ignimbrites it is common as matrix material: volcanic glass (obsidian), pumice (Fig. 67), slag and ash. With increasing SiO_2 and Al_2O_3 content the melt viscosity increases and therefore the chance of glass formation also increases (about 90% of all glasses are from acidic magmas). Higher iron and magnesium and reduced silica content reduce the viscosity. Therefore glass is more common in acidic volcanic rocks than in basic rocks (as interstitial material, Fig. 64). A high glass content is present in the hyalo-basanite (limburgite) of the Kaiserstuhl, Germany.

Paragenesis: in acidic volcanic rocks with quartz, sanidine, plagioclase, biotite and hornblende. In basic volcanic rocks with plagioclase, clinopyroxenes/titanaugite, olivine, leucite, nepheline, minerals of the sodalite group and melanite.

3 Optically uniaxial minerals

3.1 Minerals which are optically uniaxial positive

3.1.1 Rutile

TiO_2 ditetragonal–dipyramidal

General features: widely distributed as small grains in metamorphic rocks. Most common TiO_2 polymorph (rutile, brookite and anatase).

Thin-section characteristics

Form: columnar to needle-shaped parallel to [001] (Figs 69, 70), also granular, occasionally forming a grid-like pattern (sagenite texture, Fig. 71).

Cleavage: perfect parallel to {110}, (100) moderate.

Twining: common on (101) elbow-shaped, and on (301) heart-shaped.

Colour: yellow to red-brown (dependent on Fe content); weak pleochroism; as inclusions in biotite, radioactive trace content can produce pleochroic haloes. Small crystals and hair-like rutile needles appear black due to the high total reflection.

Refraction and birefringence:

$n_e = 2.899 - 2.901$
$n_o = 2.605 - 2.613$
$\oplus\Delta = 0.286 - 0.296$

Rutile has the second highest refractive index and birefringence of all minerals (mother-of-pearl white, 16th order). High birefringence colours are obscured by strong colour. Optically uniaxial ⊕, sometimes anomalously biaxial.

Optic axial angle: small in anomalous biaxial crystals.

Character of elongation: (+).

Extinction: tends to be straight.

Distinguishing features: very dark rutile can be differentiated from an opaque ore mineral by putting the front condenser lens into the viewing path, which brings out the translucent nature of rutile. Sphene and brookite are optically biaxial; zircon tends to be colourless with low refractive index; limonite is isotropic; hematite is red-brown to dark red in thin flakes.

Reactions: none.

Occurrence: common in many metamorphic rocks as an accessory mineral (e.g. in shales, quartzites, mica schists, gneiss, amphibolites, glaucophan schists, eclogites). Occurs as small grains in magmatic and plutonic rocks; rarely as exsolution mineral of opaque Fe-rich phases in foid-bearing plutonic rocks and granites. Its secondary occurrence is as an exsolution mineral in Ti-bearing biotite as fine needles or twinned (= sagenite, Fig. 71). Rutile inclusions appear in

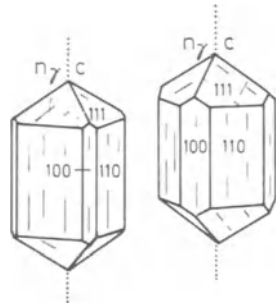

Figs 69 and **70** Crystal form and optical characteristics of rutile (left) and cassiterite (right).

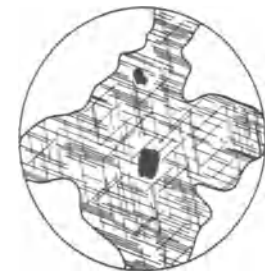

Fig. 71 Grid network of rutile in biotite.

quartz as fine hair-like needles. Larger crystals occur in granite-pegmatites and quartz veins.

Parageneses: with kyanite, cordierite, corundum and spinel; with biotite and quartz.

3.1.2 Cassiterite

SnO_2 ditetragonal–dipyramidal

Thin-section characteristics

Form: predominantly granular, also short columns (Fig. 70) or long needles.

Cleavage: good, parallel to (100), under the microscope visible only as faint traces.

Twinning: simple twins, rare coarse lamellar twins parallel to (101).

Colour: rare colourless to grey, commonly yellow, reddish or brown; weak pleochroism with zonar, patchy or striped colour distribution (Fig. 72).

Refraction and birefringence:

n_e	= 2.093 – 2.100
n_o	= 1.990 – 2.010
$\oplus\Delta$	= 0.096 – 0.098

Very high refraction and birefringence (strong colours tend to obscure birefringence colours), high relief; optically uniaxial positive, rarely anomalously biaxial.

Optic axial angle: rare anomalous biaxial with $2V_\gamma = 10°$ (max. 38°).

Character of elongation: (+).

Extinction: tends to be straight.

Special characteristics: can give rise to pleochroic haloes in adjacent minerals; irregular colour distribution.

Distinguishing features: rutile has a higher refraction and birefringence and a stronger pleochroism; orthite has a lower refraction and birefringence.

Reactions: none.

Occurrence: trace mineral in granite. Main occurrence is in pegmatitic-pneumatolytic dykes, and in greisen.

Paragenesis: with quartz, K-feldspar, lithium mica, tourmaline, topaz, fluorite and rutile.

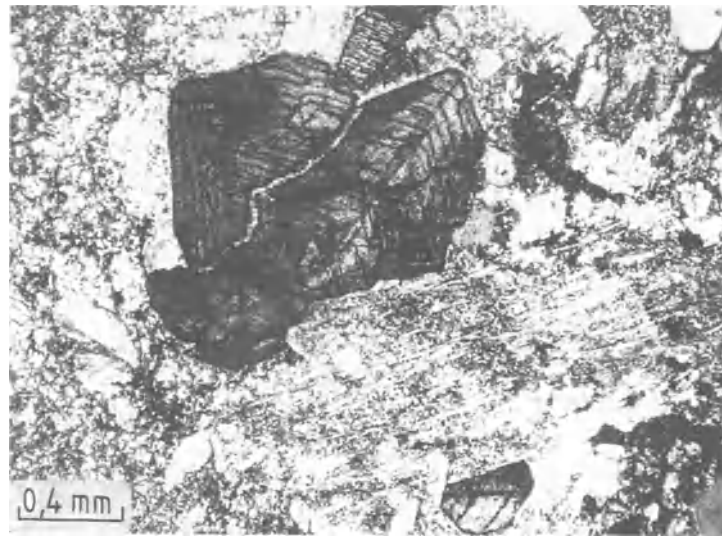

Fig. 72 Idiomorphic cassiterite with zonar coloration. Greisen. Altenberg, Erzgebirge, Germany. Uncrossed polarizers.

3.1.3 Zircon

$Zr[SiO_4]$ ditetragonal-dipyramidal

General features: accessory mineral in many rocks.

Thin-section characteristics

Form: short to long columns parallel to {110} or {100} (Fig. 73), also as rounded and granular grains in metamorphic rocks.

Cleavage: {110} imperfect.

Twinning: rare, on {111}.

Colour: colourless, rare pale brown, green or pink, often radioactive (with pleochroic haloes in coloured silicates), strongly pleochroic in coloured grains.

Refraction and birefringence:

n_e	= 1.961 – 2.015
n_o	= 1.922 – 1.960
$\oplus\Delta$	= 0.042 – 0.065

High refraction, strong relief with dark rims, high birefringence colours with lively red, blue and green interference colours of the 2nd and 3rd order (Colour plate 3). Optically uniaxial ⊕. Because of radioactive-induced lattice deformation the refraction can be as low as n = 1.826 and the birefringence as low as Δ = 0.000 (= amorphous, metamict malacone).

Optic axial angle: often anomalously biaxial with $2V_\gamma = 10°$.

Character of elongation: (+).

Extinction: tends to be straight.

Special characteristics: clear zoning is common. Pleochroic haloes are particularly clearly visible when zircon occurs as an inclusion in strongly coloured minerals (biotite, hornblende, tourmaline, etc.). Inclusions in zircon of magnetite, biotite, cassiterite, quartz, tourmaline or glass or fluid inclusions are common. Inclusions can cause a grey coloration.

Distinguishing features: from sphene, by its bright interference colours; from rutile and cassiterite by colour (colourless); monazite shows a clear cleavage and is optically biaxial, and also has a low refractive index. Also xenotime has a lower refraction, anatase is optical uniaxial ⊖, and orthite has a lower refractive index and lower birefringence colours.

Alteration: very strong resistance but because of radioactive decay it becomes isotropic (metamict).

Occurrence: one of the first mineral phases to form in acidic magmas, in granites and also quartz diorites. In volcanic rocks occurs as inclusions in biotite and hornblende. In basic magmas Zr is built into the lattice of pyroxene, and hence zircons are rare in these rocks. Zircon is very common in nepheline syenite to monzosyenite and in pegmatites. It is a diagnostic detrital mineral in sedimentary rocks (heavy mineral), and an accessory mineral in metamorphic rocks.

Paragenesis: with quartz, K-feldspar, plagioclase, biotite and hornblende; in nepheline syenite with nepheline, apatite, biotite and K-feldspar.

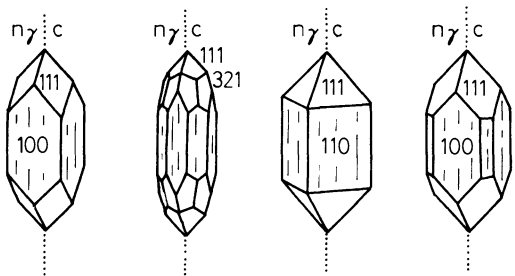

Fig. 73 Crystal form and optical characteristics of zircons of four different habits.

3.1.4 Xenotime

$Y[PO_4]$ ditetragonal–dipyramidal

General features: rare, accessory mineral.

Thin-section characteristics

Form: short columnar (Fig. 74), also granular.

Cleavage: {110} good, visible only in larger crystals.

Twinning: rare parallel to (101).

Colour: colourless to brownish, also red; occasionally weak pleochroism from pale pink to pale yellow or from yellow via grey-brown to pale yellow-green; small magnetite inclusions result in darkening.

Refraction and birefringence:

n_e	= 1.816 – 1.827
n_o	= 1.721 – 1.720
$\oplus\Delta$	= 0.095 – 0.107

High refraction with clear relief and very high birefringence (higher than zircon). Similar interference colours to carbonate, but masked by crystal colour; optically uniaxial ⊕.

Character of elongation: (+).

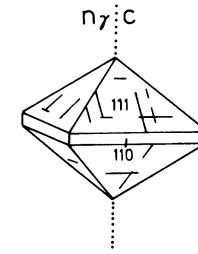

Fig. 74 Crystal form and optical characteristics of xenotime.

Extinction: straight.

Special characteristics: when as an inclusion forms pleochroic haloes.

Distinguishing features: early crystallization phase in granites, aplites, pegmatites, nepheline-syenites and orthogneisses. It is alteration resistant and is therefore preserved as a heavy detrital mineral in sand and sandstones.

Paragenesis: with brown zircon (hyacinth), ilmenite, rutile and cassiterite.

3.1.5 Melilite group

Åkermanite $Ca_2Mg[Si_2O_7]$ tetragonal–scalenohedral
Gehlenite $Ca_2Al[Al_1Si)_2O_7]$

General features: there is isomorphic solid solution between the two endmembers, åkermanite and gehlenite. Occurrence restricted to silica undersaturated magmas. Melilite is not a feldspathoid but considered to be a desolidified pyroxene and belongs to the dark components of a rock.

Thin-section characteristics

Form: square and elongate cross-sections (Figs 75–77). Åkermanite, thin plates after {001}; gehlenite, short columns parallel to {100} and thick plates after {001}.

Cleavage: åkermanite, (001), not good; gehlenite, (001) and {110}, not good.

Twinning: interpenetrating twins.

Colour: åkermanite, colourless; gehlenite, colourless, rare pale honey-yellow to brown with weak pleochroism.

Refraction and birefringence:

Åkermanite		Gehlenite	
n_e	= 1.639	n_e	= 1.658
n_o	= 1.631	n_o	= 1.669
$\oplus\Delta$	= 0.008	$\ominus\Delta$	= 0.011

Medium high refraction, low birefringence (with grey to maximum straw-yellow interference colours of the 1st order; in cases where $\Delta \approx 0.000$

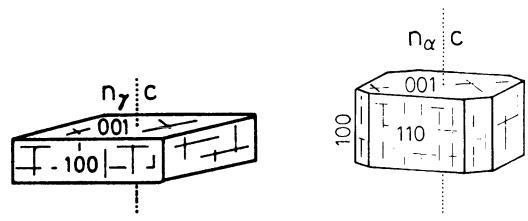

Fig. 75 Crystal form and optical characteristics of åkermanite (left) and gehlenite (right).

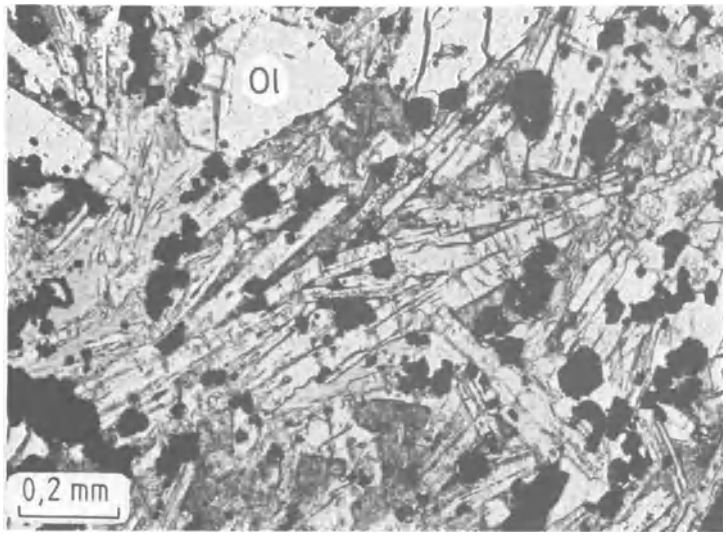

Fig. 76 Thin åkermanite laths, together with olivine and ore (chromite). Olivine-melilite nephelinite. Kappishäusern near Urach, Schwäbische Alb, Germany. Uncrossed polarizers.

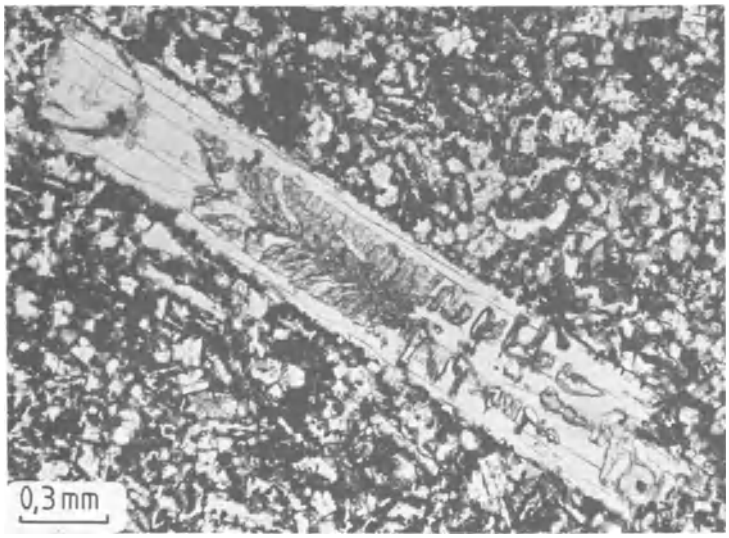

Fig. 77 Idiomorphic melilite (åkermanite) laths with characteristic rod-like inclusions. Melilite nephelinite, Jusi, Schwäbische Alb, Germany. Uncrossed polarizers.

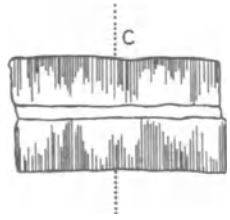

Fig. 78 Typical rod-like structure in melilite with central dividing line.

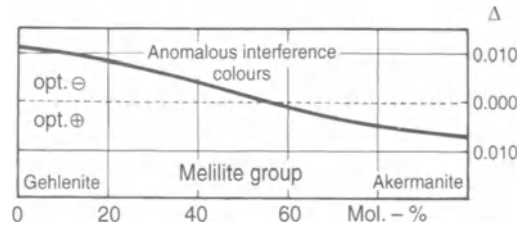

Fig. 79 Birefringence and the anomalous interference colours depend on the chemical composition of the melilite crystal.

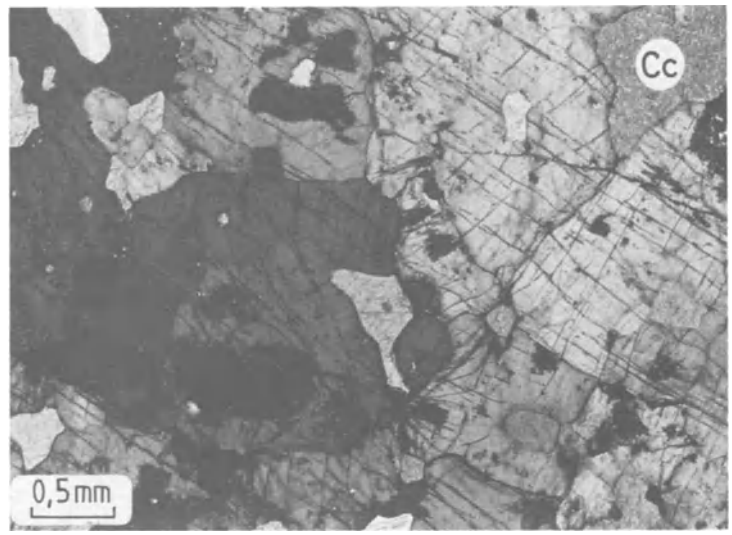

Fig. 80 Gehlenite crystals with calcite as interstitial mineral. Thick platy grains with weak cleavage (001) and {110}. Contact metamorphic marble. Le Selle-Sea, near Predazzo, Trentino, northern Italy. Crossed polars.

anomalous blue or leather-brown interference colours.

Character of elongation: opposite to the optical character (Fig. 18).

Extinction angle: generally straight.

Special characteristics: may contain characteristic rod-like inclusions such as zeolite fibres parallel to the c-axis and projecting into the crystal from the (001) plane as far as the middle line. Can contain glass as inclusions (Figs 77, 78). There is a continuous transition from the optically negative gehlenite to the optically positive åkermanite, during which Δ constantly decreases and is 0.000 at $Ak_{52}Ge_{48}$ and then increases again with increasing åkermanite content (Fig. 79). Melilite with $\Delta = 0.000$ is common in lavas, where it has lavender-blue and bright-brown interference colours due to its strong dispersion.

Distinguishing features: glass is isotropic; nepheline has a low refraction; apatite often shows hexagonal cross-sections and never has anomalous interference colours; vesuvianite has a higher refraction; and zoisite is optically biaxial positive.

Alteration: alters easily. Hydrothermal alteration into zeolite: growth of nearly isotropic fibres of mordentite, nucleating along the basal planes of the crystal, which give rise to a rod-like texture (Figs 77, 78). Weathers into carbonate.

Occurrence: in strongly silicata-undersaturated magmas (e.g. melilite nephelinites of the Schwäbische Alb, Germany; melilite leucitite in the Colli Albani, Italy). Rare in dykes as alnoite (Alnö Island, Sweden). In contact aureoles of plutonic with marly calcareous rocks pure gehlenite porphyroblast can form (e.g. dolomitic marble of the monzonite area, Predazzo, Southern Alps (Fig. 80)). Synthetic pure åkermanite forms in blast-furnace slag.

Paragenesis: never together with quartz. In volcanic rocks next to nepheline, leucite, perovskite, pyroxene and olivine. In plutonic rocks with perovskite, pyroxene, olivine, monticellite, nepheline, biotite and melanite. In dykes with perovskite, pyroxene, olivine, hauyne, biotite and primary carbonate.

3.1.6 SiO_2 group

Cristobalite, (Fig. 59)

3.1.6.1 Quartz

SiO_2 trigonal–trapezohedral (low-quartz)

General features: the second most common and purest mineral on earth. There are two modifications, a high- and a low-temperature quartz (α-quartz = high-quartz, and β-quartz = low-quartz;

Fig. 81). High-quartz crystallizes from melts >573 °C and transforms into the low-temperature paramorphoses.

Thin-section characteristics

Form: typically occurs as trigonal low-quartz; granular, hypidiomorphic to xenomorphic. In volcanic rocks paramorphic hexagonal high-quartz with hexagonal cross-sections and resorbed rims is typical (Figs 82, 83).

Cleavage: none, only irregular, curved fractures.

Twinning: very common, but rarely visible under the microscope.

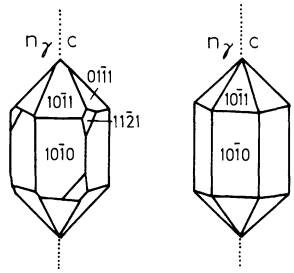

Fig. 81 Crystal forms and optical characteristics of low-quartz (left) and high-quartz (right).

Refraction and birefringence:

n_e = 1.5533
n_o = 1.5442
⊕Δ = 0.0091

Low refraction and birefringence with grey to white interference colours of the 1st order (in the case of yellow colours the thin section is too thick); uniaxial ⊕, and anomalous biaxial ⊕.

Optic axial angle: strained quartz can give an anomalous biaxial figure with $2V_\gamma = 0–10°$.

Character of elongation: (+), but it can be determined only in planes parallel to the prism planes.

Extinction: generally straight.

Special characteristics: undulatory extinction is common as a result of subgrains forming in response to strain (Fig. 84). Each subgrain has a slightly different orientation from the neighbouring grains. Subgrains tend to be biaxial with a slight difference in the orientation of the acute bisectrix.

Mortar-texture: fine-grained polygonal quartz aggregates recrystallize around larger grains; recrystallization postdates ductile deformation; there is irregular, random orientation in the recrystallized grains.

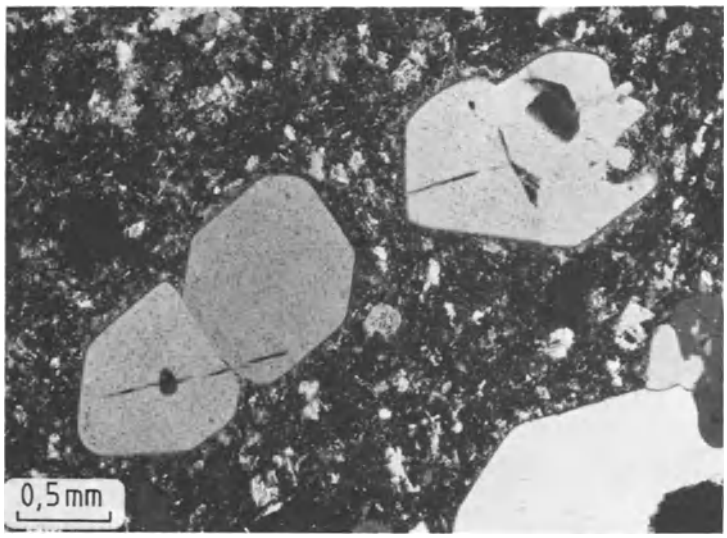

Fig. 82 Rounded quartz phenocrysts, euhedral high-temperature form, in a matrix of recrystallized rhyolite. Permian palaeo-rhyolite (quartz porphyry). Nahe area, Germany. Crossed polars.

Laminar undulatory extinction can mimic relict texture of former dynamic deformation, e.g. quartz ribbons. Fluid and gas inclusions (commonly H_2O and CO_2) can occur. They can be arranged along fractures and growth zones.

Distinguishing features: absence of cleavage, lack of alteration, low relief; twinning easily recognizable. Nepheline never forms such clear crystals and also is optically ⊖, similar to beryl. Among the biaxial crystals quartz is easily mistaken for cordierite. However, the latter has an optic axial angle 2V of a minimum of 35°, whereas 2V biaxial quartz never exceeds 10°. Cordierite as well as inclusion-free feldspar tends to form crystals which are not as free of alterations as quartz. K-feldspar has a lower refractive index.

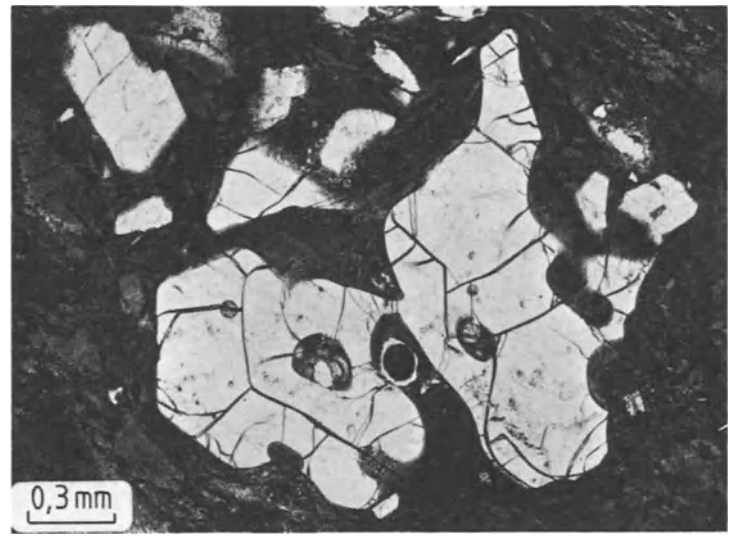

Fig. 83 Strongly resorbed quartz in ignimbrite. Rhyodacitic ignimbrite. Soniquera, eastern Cordillera, SW Bolivia. Crossed polars.

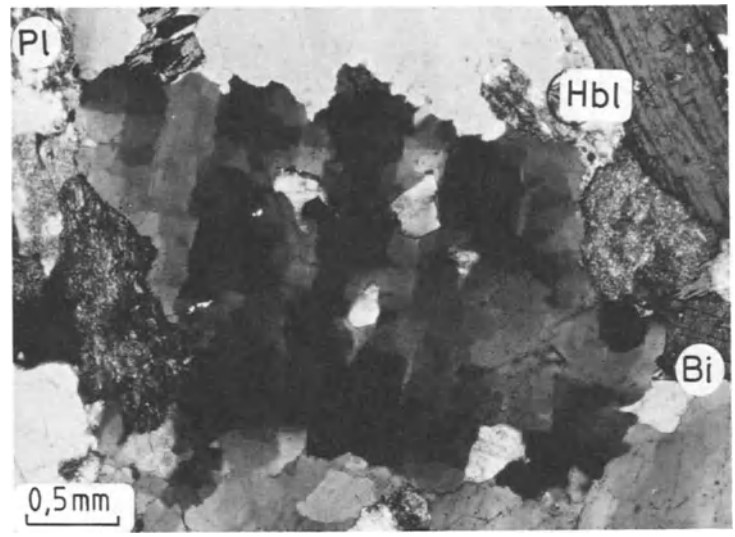

Fig. 84 Anhedral quartz forming an intergranular matrix in a metagranodiorite. Undulatory extinction has resulted in response to strain. Plagioclase and other minerals are also shown. Erratic boulder, Baltic Sea coastline, near Kiel. Crossed polars.

The white to grey interference colours of the 1st order are taken as a measure to determine the thickness of thin sections (30 μm). The refractive index of quartz (n_o) is the safest reference for determining the refraction of other unknown minerals.

Alteration: none.

Occurrence: in all magmatic rocks which are silica saturated, therefore ubiquitous in magmatic rocks. Dark-coloured rocks which are rich in mafic minerals generally have very little, if any, free quartz, whereas more light-coloured rocks, such as gabbroic and tholeitic basalts, have up to 5% vol., and granites/rhyolites up to 35% vol. quartz. Generally, the amount of quartz increases with decreasing darkness of the rock. Magmatic rocks with more than 35% vol. quartz have probably not undergone secondary SiO_2 metasomatism. In pegmatites and some other acidic plutonic rocks quartz can occur systematically intergrown with feldspar; this is referred to as graphic intergrowth. In the case of an irregular intergrowth we speak about a granophyric texture. In rhyolitic to dacitic volcanic rocks (lavas and ignimbrites) corrosion features due to remelting can be seen in the quartz phenocrysts (Fig. 83). These resorption features reflect rapid physical changes in pressure and temperature which can lead to disequilibrium between the quartz phenocrysts and the melt. Quartz resists alteration and is therefore concentrated in detrital sediments, forming sandstones, etc. It occurs sometimes together with chalcedony and opal (Part B, section 2.10.2) as matrix material in silica-rich sediments, as secondary diagenetic mineral in organic radiolarite, hornfels and jasper-concretions. It also occurs in sedimentary limestones, marls and evaporites as idiomorphic, often long-prismatic secondary mineral.

Quartz is present in metamorphic rocks of all metamorphic grades, ranging from phyllite to gneiss. It responds to shear deformation by preferred crystallization and ribbon formation (Fig. 85). Polygonal quartz textures form during static recrystallization. In some gneisses in which plagioclase is being replaced by K-feldspar myrmekite textures are developed that rim the feldspar, with quartz growing in worm-like fashion perpendicular to the interface.

Paragenesis: quartz only crystallizes in silica-oversaturated rocks and therefore never coexists with felspathoids. Occasionally quartz is found in silica-undersaturated rocks, together with corundum, spinel and olivine. This is interpreted as the result of a change in the chemistry of the magma, as phases that do not react with the melt crystallize (e.g. olivine) and the silica content in the melt increases. Resorption rims of olivine give testimony of such chemical changes in the melt.

In granites, quartz crystallizes together with microcline, albite and biotite, and also with green hornblende and sphene. In acidic volcanic rocks it often occurs together with corroded K-feldspar, plagioclase, biotite, brown hornblende and rock-glass.

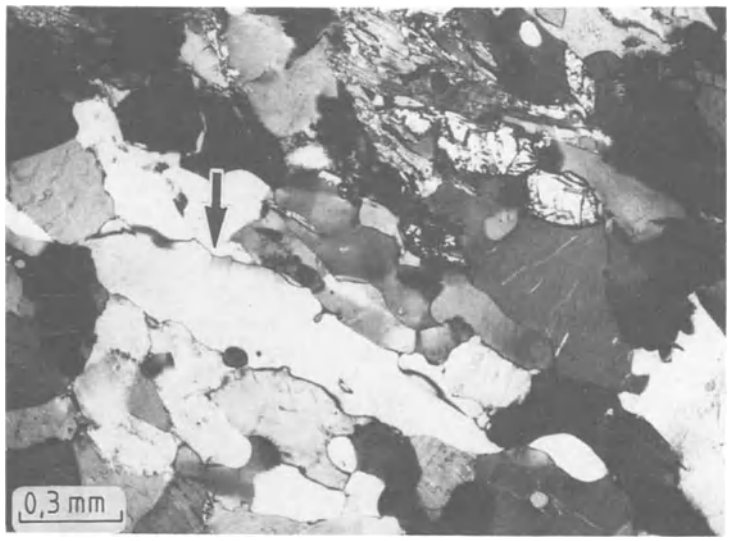

Fig. 85 Ribbon quartz (arrow), as a result of high shear strain. Granulite. Meidling Valley, Lower Austria. Crossed polars.

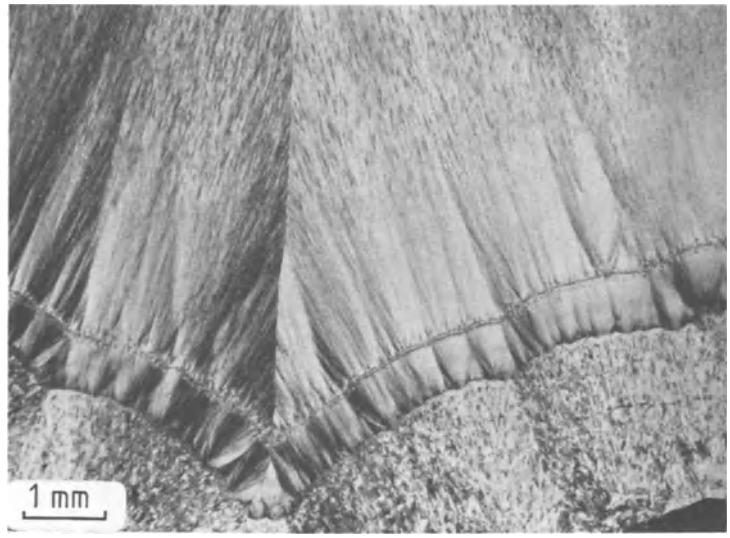

Fig. 86 Microfibrous radial chalcedony. Secondary mineral in a cavity in a Tertiary basalt. Eskifjördur, eastern Iceland. Crossed polars.

3.1.6.2 Chalcedony

SiO_2 trigonal–trapezohedral

General features: crypto- to microcrystalline, fibrous form of low-quartz; product of dehydrated opal.

Thin-section characteristics

Form: fibrous (Fig. 86), star-shaped, spherolitic, often forming pseudomorphs after other minerals or filling voids in fossils. The fibre direction is parallel to the c-axis.

Cleavage: none.

Colour: colourless.

Refraction and birefringence:

n_e = 1.538 – 1.543
n_o = 1.530 – 1.533
$\oplus\Delta$ = 0.008 – 0.010

Low refraction and birefringence, slightly lower than quartz; optically uniaxial ⊕. Often anomalously biaxial with $2V_\gamma = 0–25°$.

Character of elongation: Chalcedony s.s. (–), quarzine (+).

Extinction: commonly straight.

Distinguishing features: very characteristic; possibly confused with fibrous natrolite, but this has a lower refraction.

Alteration: very robust.

Occurrence: secondary mineral. In volcanic rocks fills fractures and cavities (e.g. in melaphyres of the Saar–Nahe area in Germany), forming agate. Pseudomorph and silicification mineral particularly in fossil wood and other fossils. In concretions in flint.

Paragenesis: opal and zeolites.

3.1.6.3 Tridymite

SiO_2 pseudo-hexagonal (rhombic-disphenoidal)

General features: difficult to recognize; rare; fills cavities in acidic volcanic rocks.

Thin-section characteristics

Form: thin platy to flaky, in cavities as aggregate of hexagonal flakes, arranged like roof tiles, or as wedge-shaped trillings; also as xenomorphic grains.

Cleavage: feeble, rarely visible.

Twinning: common, wedge-shaped crystals of two or more individuals, trillings.

Colour: colourless.

Refraction and birefringence:

n_γ	= 1.481
n_β	= 1.478
n_α	= 1.477
$\oplus\Delta$	= 0.004

Low relief and weak birefringence, almost always biaxial ⊕, because only the rhombic paramorph is stable at normal (STP) conditions. $2V_\gamma = 40–90°$.

Character of elongation: (–).

Extinction: tends to be straight.

Distinguishing features: analcite and leucite tend to show abnormal subgrains; sodalite is isotropic; zeolite shows higher refractive indices and higher birefringence colours; nepheline has a higher relief and is uniaxial ⊖; cristobalite is uniaxial ⊖; and fluorite has a well-developed cleavage.

Alteration: none.

Occurrence: rare, easily overlooked. Typically occurs in acidic to intermediate volcanic rocks (rhyolite to andesite, trachyte, latite and obsidian) in cavities and fractures. As contact-metamorphic mineral in 'sanidinite facies'.

Paragenesis: with rock-glass and cristobalite.

3.1.7 Chabazite

$Ca[Al_2Si_2O_{12}]\cdot 6H_2O$ ditrigonal–scalenohedral

General features: uniaxial representative of the zeolite group.

Thin-section characteristics

Form: rhombohedral (pseudo-cubic; Figs 87, 88), almost always idiomorphic, rarely xenomorphic granular or polygonal aggregates.

Cleavage: good to poor after rhombohedra.

Colour: colourless.

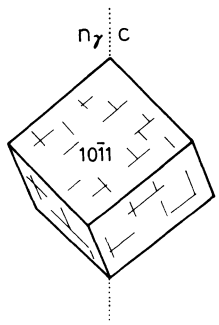

Fig. 87 Crystal form and optical characteristics of chabazite.

Refraction and birefringence:

n_e	= 1.478 – 1.490	n_γ	= 1.488
n_o	= 1.480 – 1.485	n_β	= 1.485
$\oplus\ominus\Delta$	= 0.002 – 0.005	n_α	= 1.485
		$\oplus\Delta$	= 0.003

Extremely low birefringence and negative relief (grey interference colours of the 1st order); uniaxial ⊕ as well as ⊖, also biaxial ⊕.

Optic axial angle: commonly anomalously optically biaxial ⊕ with $2V_\gamma = 0–30°$.

Extinction angle: symmetric to crystal outlines and to cleavage.

Special characteristics: can show abnormal subgrains.

Distinguishing features: its cubic habit means it can easily be distinguished from the other more fibrous zeolites. Analcite tends to be isotropic; crystobalite often contains subgrains; gmelinite has lower birefringence colours; apophyllite, nosean and hauyne have a higher relief.

Alteration: none.

Occurrence: in cavities and fractures in basaltic rocks (e.g. in basalts, phonolites, etc.). Also in cavities in granites, granodiorites and other plutonic rocks.

Paragenesis: with phillipsite, thomsonite, calcite and analcite.

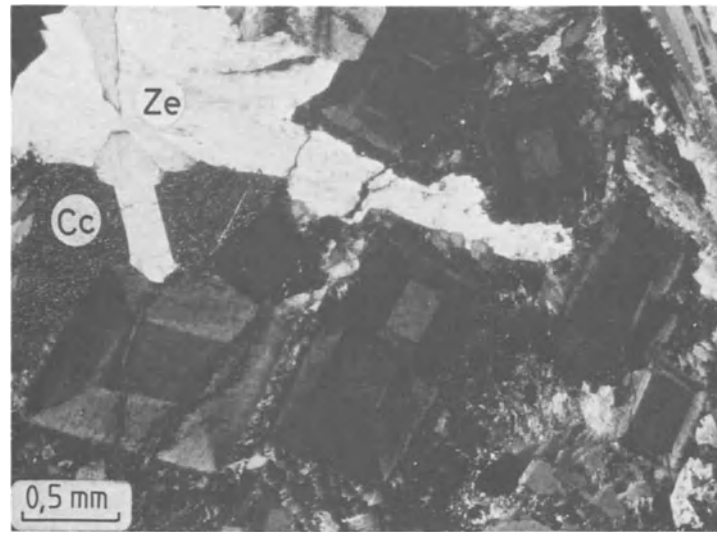

Fig. 88 Cubic zeolite with zonar growth rings and very low refraction (chabazite). Secondary mineral in cavity in alkali-olivine basalt. Capo Pássero, SE Sicily. Crossed polars.

3.2 Minerals with uniaxial negative character

Hematite (Part B, section 1.3)

3.2.1 Anatase

TiO_2 ditetragonal–dipyramidal

Thin-section characteristics

Form: often granular, rarely dipyramidal or thin tabular (Fig. 89).

Cleavage: distinct after {111} and (001).

Colour: yellow, brownish or dark blue to black with a weak pleochroism, common patchy or zonar colouring.

Refraction and birefringence:

$n_e = 2.488$
$n_o = 2.561$
$\ominus\Delta = 0.073$

Very high refraction and birefringence (strong relief and bright interference colours of the 3rd order); optically uniaxial ⊖, rarely anomalously biaxial.

Optic axial angle: if anomalously biaxial, $2V_\alpha$ very small.

Character of elongation: (–).

Extinction: straight.

Distinguishing features: zircon, rutile and sphene are optically uniaxial to biaxial ⊕.

Alteration: none.

Occurrence: a diagenetic mineral in sediments, alteration product of TiO_2-bearing minerals in weathered rocks. An accessory mineral in magmatic and metamorphic rocks; in granitic pegmatites.

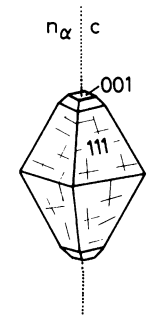

Fig. 89 Crystal form and optical characteristics of anatase.

3.2.2 Trigonal carbonate group

Calcite	$CaCO_3$	ditrigonal–scalenohedral
Dolomite	$CaMg(CO_3)_2$	trigonal–rhombohedral
Magnesite	$MgCO_3$	ditrigonal–scalenohedral
Siderite	$FeCO_3$	ditrigonal–scalenohedral

General features: the calcite group (calcite, magnesite, siderite) and dolomite are the most important rock-forming minerals of carbonate sedimentary rocks.

3.2.2.1 Calcite

Thin-section characteristics

Form: massive, xenomorphic, granular, as rock-forming mineral; also star-shaped spherolitic, fibrous, oolitic or pisolitic, and mimicks organic fossil structures. Common as sutured granular or as polygonal (in marble) aggregates.

Cleavage: perfect rhombohedral cleavage $\{10\bar{1}1\}$ with an intersection angle of adjacent planes at 75°. Not visible in fine granular aggregates.

Twinning: glide twins are very common (polysynthetic translation lamellar twinning) on $(01\bar{1}2)$ parallel to the long rhombic diagonal or parallel to its sides (Fig. 90); commonly lamellar twinning is so dense that grey interference colours of the 1st order occur.

Colour: colourless and transparent.

Refraction and birefringence:

n_e	= 1.486
n_o	= 1.658
$\ominus\Delta$	= 0.172

Extreme birefringence according to orientation of crystal (sections parallel to the c-axis show mother-of-pearl white of the 10th order); strong chagrin change according to crystal orientation; optically uniaxial ⊖; commonly anomalously biaxial ⊖.

Optic axial angle: in metamorphic rocks commonly deformation-induced twinning giving rise to biaxial optical characteristics with $2V_\alpha = 4–14°$ (25°).

Extinction: symmetric relative to rhombohedral cleavage planes.

Special characteristics: the great difference between the refractive indices and n_o creates a pleochroism-like feature, referred to as chagrin change (it is colourless in the n_e vibration direction). However, in the direction of n_o the relief is stronger with a strong chagrin, causing the section to appear much darker than in the n_e direction. This is characteristic for all rhombohedral carbonates. Crystals which are optically biaxial do not show complete extinction but patchy bluish interference colours.

Distinguishing features: without a universal stage it cannot be distinguishable from other carbonates. Staining techniques and solubility in acids are good tests. Rock-forming dolomite in rocks tends to be idiomorphic, contrary to calcite, and rarely shows lamellar twinning along $(02\bar{2}1)$, whereas calcite commonly is twinned after $(01\bar{1}2)$.

Alteration: very robust with changing pressures and temperatures, but during weathering it is easily dissolved.

Occurrence: very common. Rare as a major mineral in alkaline magmas (carbonatites; e.g. Kaisterstuhl, Fig. 91) and as a hydrothermal mineral in ore deposits; fills cavities in rocks (Fig. 92) (e.g. Saar–Nahe area, Germany). Occurs as a retrograde reaction mineral in magmatic rocks during breakdown of anorthite-rich plagioclase and in sediments as concretions from organisms such as corals, sponges and foraminifera-rich marls, etc. (Figs 93, 94). Inorganic precipitation from oversaturated solutions leads to very fine-grained carbonates, oolites and travertine. Matrix-forming in clastic sediments (e.g. calcareous sandstones). In metamorphic rocks calcite occurs in marbles.

Paragenesis: not diagnostic. In cavities together with zeolites.

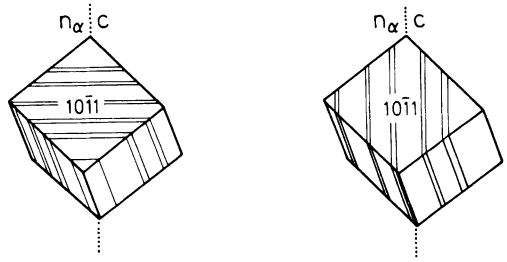

Fig. 90 Crystal form and optical characteristics of calcite (left) and dolomite (right), illustrating different orientations of polysynthetic twinning.

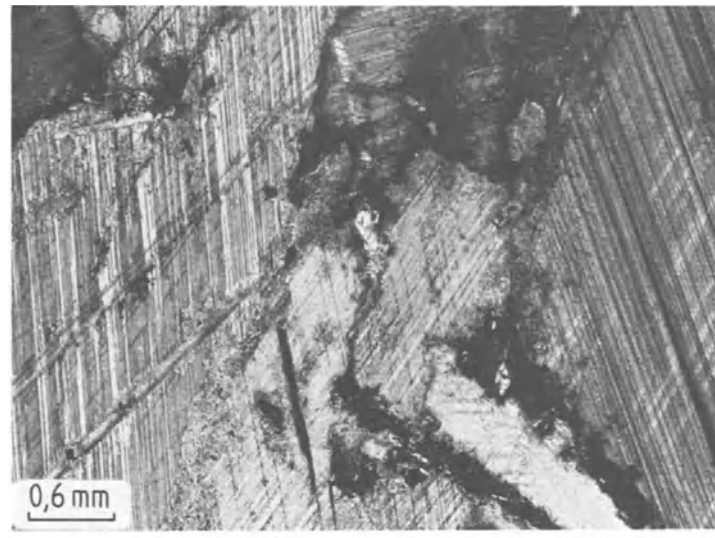

Fig. 91 Primary calcite with well-developed cleavage and translation lamellar twinning. Koppite-carbonatite. Schelingen, Kaiserstuhl, Germany. Uncrossed polarizers.

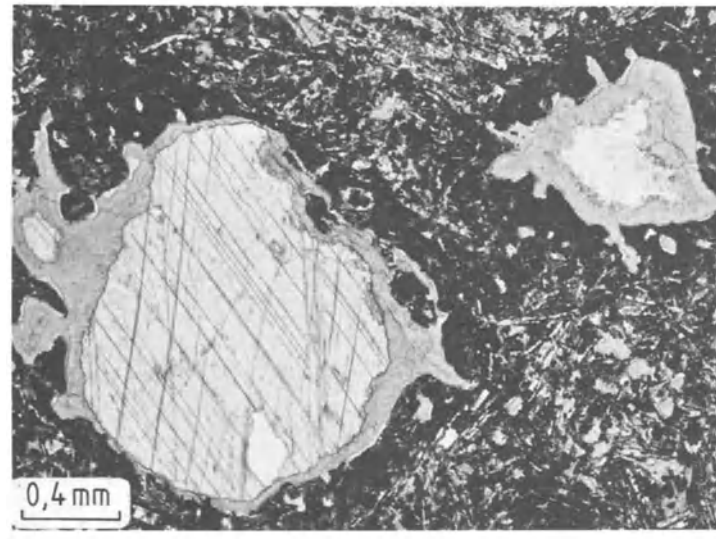

Fig. 92 Secondary calcite and faint-green saponite filling cavity. Note the perfect rhombohedral cleavage and also the stronger relief compared to saponite. Spilite. Gumpertsreuth, near Hof, Bavaria, Germany. Uncrossed polarizers.

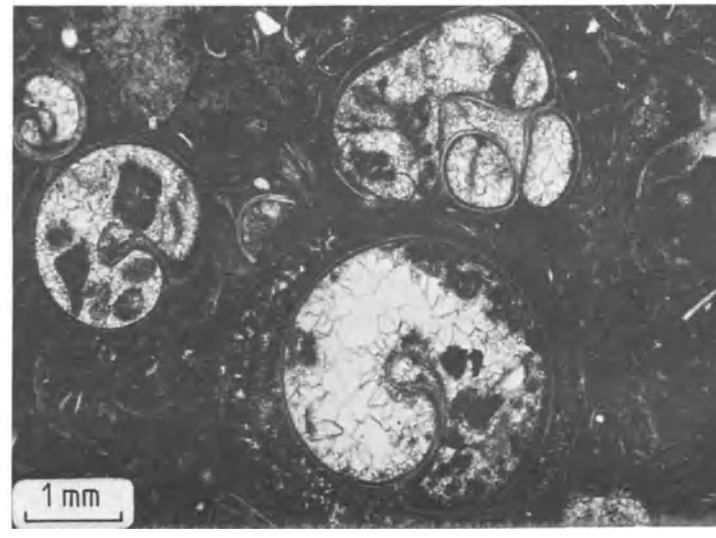

Fig. 93 Organically formed calcite (gastropod shell and other fossils) (sparite) with calcite cement (micrite). Miocene limestone (Hydrobia-limestone) from the Mainz Basin. Crossed polars.

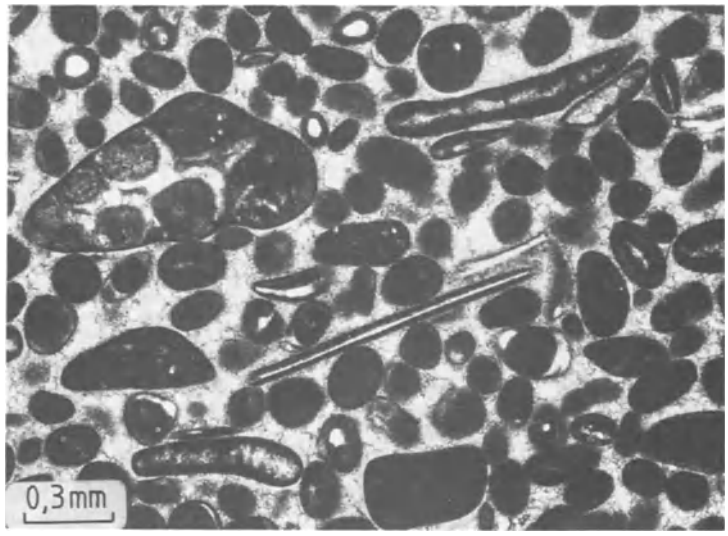

Fig. 94 Jurassic oolite with microfossils. Organically formed calcite and ooides in calcite cement (pseudosparite). Schwäbische Alb, Germany. Uncrossed polarizers.

3.2.2.2 Dolomite

Thin-section characteristics

Form: rhombohedral, in carbonaceous rocks idiomorphic in contrast to coexisting calcite; detrital grains in marble are xenomorphic to hypidiomorphic.

Cleavage: perfect, after rhombohedral $\{10\bar{1}1\}$, with the intersection of adjacent sides of the rhombohedron at $73^3/_4°$. Crystals can be cleaved parallel to the basal plane (0001).

Twinning: not as common as in calcite, lamellar twinning on $(02\bar{2}1)$. Twinning lamellae are parallel to the short rhombohedral diagonal (Fig. 90).

Colour: colourless to pale, rarely grey or brownish (Fe-bearing).

Refraction and birefringence:

	Fe-free	Fe-bearing
n_e	= 1.500	– 1.520
n_o	= 1.679	– 1.703
$\ominus\Delta$	= 0.179	– 0.183

Low to intermediate refraction and very high birefringence (mother-of-pearl white of the higher orders); optically uniaxial $\ominus$.

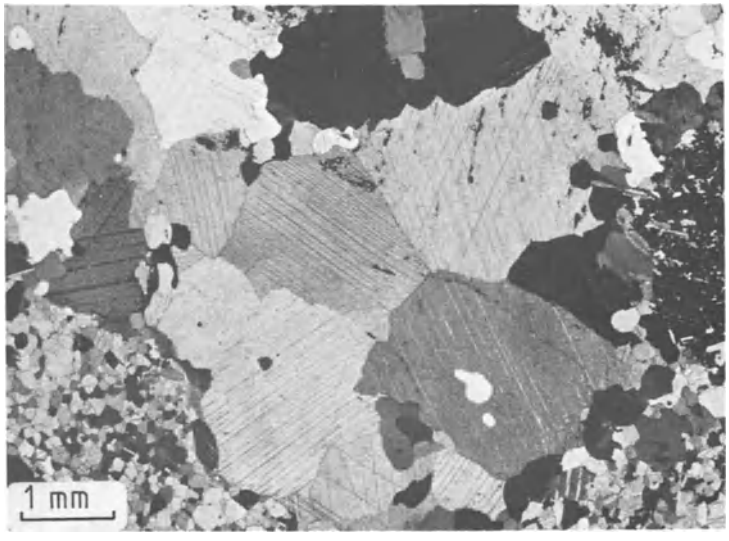

Fig. 95 Hypidiomorphic dolomite crystal with typical rhombohedral cleavage. Dolomitic marble. Campolungo, Ticino, Switzerland. Crossed polars.

Extinction: symmetrically relative to cleavage traces.

Distinguishing features: difficult to distinguish from the other carbonates without the aid of a universal stage. Staining techniques and solubility in acids are good tests. The twinning lamellae are oriented parallel to the short diagonal of the rhombohedron; the thin lamellae of calcite are oriented at right angles and tend to show grey interference colours of the 1st order.

Alteration: very robust, not easily affected by weathering.

Occurrence: in hydrothermal deposits, as veinlets in ore deposits, in cavities in altered basaltic volcanic rocks also occurs as sugar-grained dolomitic marble (Fig. 95), as well as in the form of beautiful rhombohedral porphyroblasts in talc and chlorite schist.

Paragenesis: not typical.

3.2.2.3 Magnesite

Thin-section characteristics

Form: hypidiomorphic to xenomorphic aggregates, rare as idiomorphic crystals; also granular, fibrous or compact porcelain- or gel-like masses.

Cleavage: perfect on rhombohedral planes $\{10\bar{1}1\}$.

Twinning: rare lamellar pressure twins on $(01\bar{1}2)$.

Colour: colourless, grey to pale, brownish if Fe-bearing.

Refraction and birefringence:

	Fe-free	Fe-bearing
n_e	= 1.509	– 1.563
n_o	= 1.700	– 1.782
$\ominus\Delta$	= 0.191	– 0.219

Low to intermediate refraction and extremely high birefringence (mother-of-pearl white of the higher orders); optically uniaxial ⊖.

Extinction: symmetric relative to cleavage planes.

Distinguishing features: difficult to distinguish from the other carbonates without the aid of a universal stage. Staining techniques and solubility in acids are good tests.

Alteration: very robust mineral.

Occurrence: hydrothermal to metasomatic, forming coarse tabular masses, locally mined. Also occurs as idiomorphic porphyroblasts in talc and chlorite schist. It is alteration product in serpentinites, forming gel-like fracture-filling masses. It forms pseudomorphs after olivine (Fig. 96).

Paragenesis: as gel-magnesite together with opal.

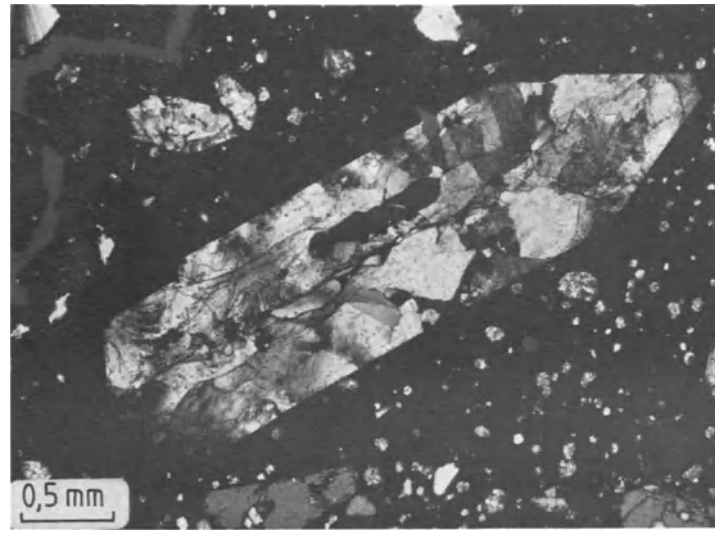

Fig. 96 Magnesite replacing olivine in an olivine-bearing melilitic tuff. Urach, Schwäbische Alb, Germany. Crossed polars.

3.2.2.4 Siderite

Thin-section characteristics

Form: idiomorphic (fine- to coarse-grained), commonly hypidiomorphic to xenomorphic granular or oolitic.

Cleavage: perfect on $\{10\bar{1}1\}$.

Twinning: lamellar twinning on $(01\bar{1}2)$; lamellar pressure twins are very rare, but very common in dolomite and calcite.

Colour: colourless to pale yellow-brown.

Refraction and birefringence:

$n_e = 1.633$
$n_o = 1.875$
$\ominus\Delta = 0.242$

Medium to high refraction and extremely high birefringence (highest among the carbonate group), clearly developed 'pseudo-dichroism'; optically uniaxial ⊖.

Extinction: symmetrically relative to the cleavage planes.

Distinguishing features: difficult to distinguish from the other carbonates without the aid of a universal stage. Staining techniques and solubility in acids are good tests. Sphene and cassiterite are optically ⊕.

Alterations: oxidation into ice flower-like dendritic aggregates of goethite (limonite).

Occurrence: as veins in orebodies; as hydrothermal and metasomatic alteration product of carbonate and dolomite, forming coarse-grained, tabular, locally mined bodies.

Paragenesis: not characteristic.

3.2.3 Corundum

Al_2O_3 trigonal–scalenohedral

Thin-section characteristics

Form: idiomorphic with tabular habit, of commonly hexagonal shape (Fig. 97); columnar, barrel-shaped, massive granular crystals (emery).

Cleavage: none; parting on $\{10\bar{1}1\}$ and $\{0001\}$ intersecting at an angle of 94°.

Twinning: lamellar on $\{10\bar{1}1\}$, simple twinning on $\{0001\}$ and $\{10\bar{1}1\}$.

Colour: colourless; occasionally characteristic patchy, stripy or zonar reddish or brownish coloration with pleochroism (n_o: purple red, violet, blue; n_e: yellow, grey-green, pale blue; Colour plate 4).

Refraction and birefringence:

$n_e = 1.760 - 1.764$
$n_o = 1.768 - 1.772$
$\ominus\Delta = 0.008$

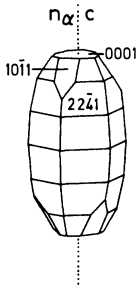

Fig. 97 Crystal form and optical characteristics of corundum.

High refraction with a strong relief and low birefringence (grey interference colours of the 1st order, similar to quartz); optically uniaxial ⊖.

Optic axial angle: can be anomalously biaxial ⊖, with $2V_\alpha = 5–7°$ (to >30°).

Character of elongation: (–), rare (+).

Extinction: tends to be straight.

Special characteristics: can show irregular bluish pleochroism, which is diagnostic.

Distinguishing features: chrysoberyl is optically biaxial ⊕; vesuvianite has anomalous interference colours; apatite has a lower refractive index and tends to be idiomorphic; tourmaline has birefringence colours of a higher order and is also strongly pleochroic.

Alteration: retrograde alteration into an aggregate of white mica.

Occurrence: during resorption of Al-rich wall rocks into a magma, corundum–spinel xenoliths can form (norites, tholeites) if resorption is complete, larger single corundum crystals can survive (very rare). It is very rare in nepheline syenite pegmatites; in syenite together with scapolite and nepheline and feldspars. It also occurs in Al-rich contact-metamorphic rocks of low silica content; in silica-poor regional metamorphic rocks in general, and in metamorphosed bauxite (e.g. emery-rock, Island of Naxos, Greece).

Paragenesis: in magmatites with spinel, cordierite, garnet, sillimanite and andalusite; in metamorphic rocks with cordierite, spinel, tourmaline or andalusite, kyanite, sillimanite, muscovite and rutile; in emery with magnetite, ilmenite, hematite, quartz and rutile.

3.2.4 Vesuvianite

$Ca_{10}(Mg, Fe)_2Al_4[(OH)_4|(SiO_4)_5|Si_2O_7)_2]$ ditetragonal–dipyramidal

Thin-section characteristics

Form: idiomorphic, short prisms (Fig. 98), commonly xenomorphic granular; rarely needle-shaped to spherulitic aggregates.

Cleavage: poor on (110).

Colour: colourless, sometimes yellowish, pale green or brownish; commonly zoned or patchy; very rarely it shows a weak pleochroism.

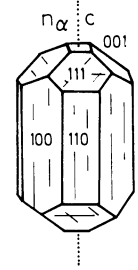

Fig. 98 Crystal form and optical characteristics of vesuvianite.

Refraction and birefringence:

n_e	= 1.701 – 1.732
n_o	= 1.705 – 1.738
⊖Δ	= 0.004 – 0.006

High refractive index with a strong relief and low birefringence colours (interference colours of the 1st order), commonly anomalous lower interference colours; optically uniaxial ⊖, except the very rare variety wiluite is optically ⊕; also anomalously biaxial ⊖.

Optic axial angle: in anomalously biaxial ⊖ cases $2V_\alpha = 17–33°$.

Character of elongation: (–), also (+) in wiluite.

Extinction: tends to be straight.

Special characteristics: optically different growth zones and anomalous patches, anomalous interference colours (lavender-blue, leather-brown, grey-green or purple; Colour plate 5); in section along its long axis, hourglass texture.

Distinguishing features: zoisite and clinozoisite are optically biaxial ⊕ and can be confused with wiluite; melilite and apatite have lower refractive indices; andalusite has a considerably greater axial angle; can be confused with grossularite.

Alteration: very rare, e.g. into prehnite.

Occurrence: in contact-metamorphic siliceous limestone and marble, derived from marls and marly limestone, also in equivalent metamorphic rocks.

Paragenesis: with fassaite, grossularite, wollastonite, calcite, epidote and sphene.

3.2.5 Tourmaline

$Na(Fe^{2+}, Mg, Al)_3\,(Al, Fe^{3+})_6[(OH, F, O)_4|(BO_3)_3|Si_6O_{18}]$ ditrigonal–pyramidal

General features: the tourmaline group forms a solid solution series between the two endmembers schorl (Fe) and dravite (Mg).

Thin-section characteristics

Form: short columnar (Fig. 99(a),(b)), needle-shaped, spherulitic, in radiating groups of columnar and acicular crystals (Fig. 100), rarely granular. Typically rounded triangular cross-sections (Fig. 99(c)); in pegmatites poikilitic intergrowth with quartz. In metamorphic rocks it can form microlites, which are easily overlooked.

Cleavage: none; irregular parting approximately perpendicular to the long axis.

Colour: always coloured; blue-grey to olive-brown, green, pale-yellow to ochre. Strong characteristic pleochroism (Fig. 101), with the ordinary ray being more strongly absorbed than the extraordinary ($n_e < n_o$), which results in strong colours perpendicular to the c-axis and pale colours parallel to c (Fig. 99(b)). A zonar colour change (blue and brown) is common.

Refraction and birefringence:

n_e	= 1.635 – 1.650
n_o	= 1.660 – 1.671
⊖Δ	= 0.025 – 0.035

High refraction with a positive relief, slightly varying according to composition. Intermediate

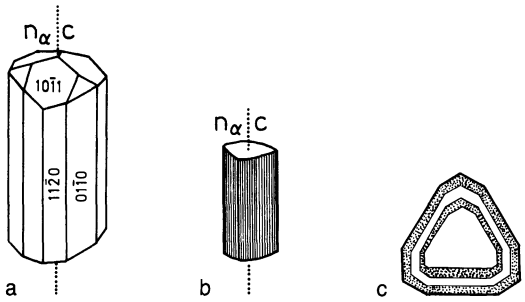

Fig. 99 (a) Crystal form and optical characteristics of tourmaline.

(b) Tourmaline with characteristic stripes parallel to its optic axis.

(c) Section through a tourmaline crystal perpendicular to the crystallographic c-axis, showing the characteristic rounded triangular cross-section and zonar growth.

birefringence colours (maximum interference colours ranging from the upper 1st order to the middle part of the 2nd order, often masked by the strong pleochroism); optically uniaxial ⊖, rarely anomalously biaxial.

Optic axial angle: deformed crystals tend to be anomalously biaxial with a small axial angle ($2V_\alpha \sim 5°$).

Character of elongation: (–).

Special characteristics: basal sections do not show any pleochroism. Colour zonation is common (Fig. 101). Zircon inclusions have haloes which are strongly pleochroic.

Distinguishing features: corundum has a higher refractive index; andalusite and staurolite are optically biaxial and have lower birefringence;

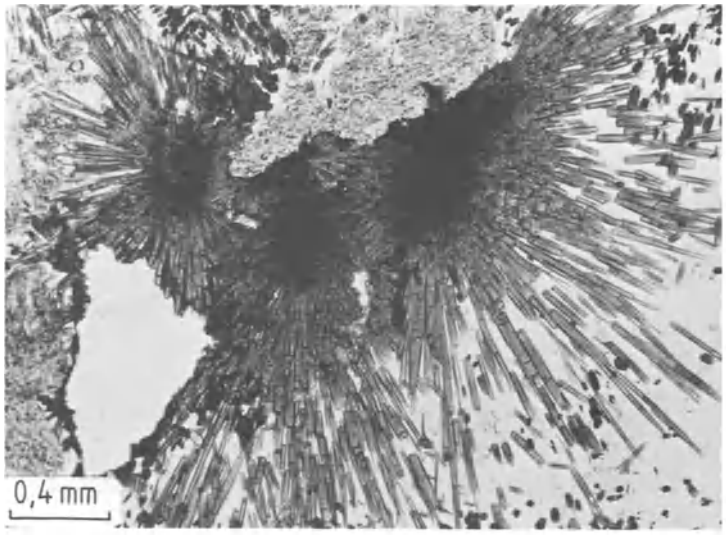

Fig. 100 Radiating tourmaline stars, with green pleochroism and irregular parting approximately perpendicular to the optical c-axis. Tourmaline granite. Luxulyan, Cornwall, Great Britain. Uncrossed polarizers.

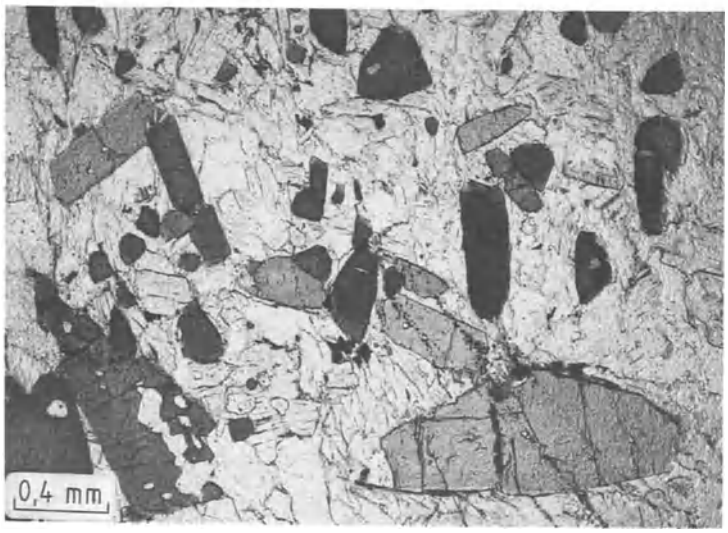

Fig. 101 Tourmaline crystal with typical curved triangular cross-sections and showing strong pleochroism. Tourmaline gneiss. Erratic boulder, Baltic Sea coastline, near Kiel, Germany. Uncrossed polarizers.

biotite shows a perfect cleavage perpendicular to the c-axis; alkali-hornblende does not have straight extinction.

Alteration: none; next to quartz the most stable mineral.

Occurrence: whenever boron is present in granites and pegmatites tourmaline will be present (schorl represents biotite); crystallization immediately after the main phase of crystallization of acidic melts adjacent to the contact rocks (tourmalitization at the expense of biotite), as pneumatolytically formed mineral in contact metamorphism, in hornfels and pelitic rocks. Absent in volcanic rocks. Tourmaline occurs in most granite pegmatites and quartz–tourmaline veins and is a common mineral in most medium- to high-grade metamorphic rocks. It is common as detritus in sedimentary rocks, authogenic in carbonates and as secondary mineral in sandstones.

Paragenesis: with topaz, beryl, lepidolite, cassiterite, spodumene, fluorite and apatite.

3.2.6 Apatite

$Ca_5[(F, OH, Cl)|(PO_4)_3]$ hexagonal–dipyramidal

General features: important accessory mineral in almost every magmatic rock. Most important phosphorous-bearing mineral.

Thin-section characteristics

Form: short to thin and columnar, stretched along the c-axis; in basal section hexagonal outlines (Figs 102(a),(b); 103), typically idiomorphic and surrounded by quartz, biotite and hornblende, etc., also granular; in phosphorites star-shaped to cryptocrystalline, spherulitic and oolitic.

Cleavage: poor on (0001) and {10$\bar{1}$0}. Basal parting (Fig. 102(c)).

Colour: colourless; often with oriented inclusions; concentric growth patterns; brownish or blue-grey, or orange, weakly pleochroic colours.

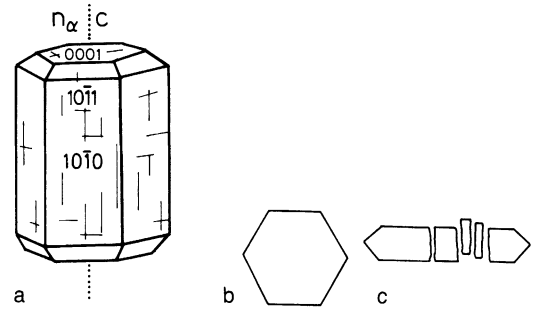

Fig. 102 (a) Crystal form and optical characteristics of apatite.

(b) Hexagonal basal section perpendicular to the c-axis.

(c) Section along length of crystal showing basal parting with partly displaced fragments.

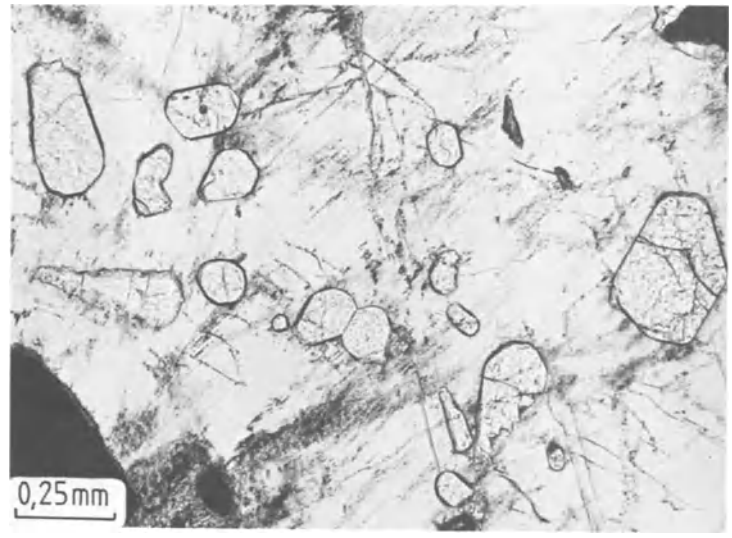

Fig. 103 Idiomorphic apatites with strong, clear relief forming inclusions in microcline. Nepheline syenite. Laugen valley near Larvik, southern Norway. Uncrossed polarizers.

Refraction and birefringence:

$n_e = 1.631$
$n_o = 1.634$
$\ominus\Delta = 0.003$

Medium high refractive index with positive relief relative to quartz and feldspar; low birefringence (colours of the 1st order); optically uniaxial ⊖, rarely anomalously biaxial.

Optic axial angle: occasionally weakly anomalously biaxial with $2V_\alpha = 0–20°$.

Character of elongation: (–).

Extinction: straight.

Special characteristics: rare anomalous subgrains. Inclusions in biotite and hornblende give rise to pleochroic haloes.

Distinguishing features: can be mistaken for nepheline, which is also optically uniaxial ⊖. However, apatite has a much higher relief, and tends to be idiomorphic and unaltered, whereas nepheline tends to be xenomorphic, pale coloured and altered; beryl and quartz have lower refractive indices and different appearances; melilite tends to show anomalous interference colours; sillimanite is biaxial and has a higher birefringence, and shows good parting fractures; topaz is optically biaxial ⊕ and has a higher birefringence.

Alteration: none, always fresh.

Occurrence: one of the first minerals to crystallize from a magma, an accessory mineral (0.1–1%) in almost all magmatic rocks. More common in dark Na- and K-rich magmatic rocks and their derivatives (nepheline syenite, nepheline monzosyenite, olivine nephelinite, etc.) and even more common in carbonatites and lamprophyres. Apatite also occurs in pegmatites (with Li-bearing mica, beryl, etc.). In sedimentary rocks it occurs as rounded grains; it is rock-forming in phosphorites (as kidney ore structures) as globular oolitic aggregates. In metamorphic rocks apatite is stable over a wide pressure–temperature range.

Paragenesis: ubiquitous mineral

3.2.7 Beryl

$Al_2Be_3[Si_6O_{18}]$ dihexagonal-dipyramidal

Thin-section characteristics

Form: short to long columns along [0001] (Fig. 104), commonly xenomorphic to idiomorphic, granular; inclusion-rich; in tectonites cataclastic fragments (Fig. 105).

Cleavage: poor on (0001), not visible under the microscope.

Colour: colourless, rare pleochroism from pale blue (n_γ) to pale green (n_α).

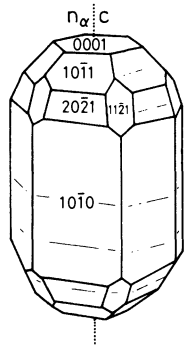

Fig. 104 Crystal form and optical characteristics of beryl.

Birefringence and refraction:

$n_e = 1.565 – 1.599$
$n_o = 1.569 – 1.610$
$\ominus\Delta = 0.004 – 0.009$

Medium strong refraction and very weak birefringence (grey colours of the 1st order), can be anomalously biaxial if tectonized.

Optic axial angle: in anomalously biaxial ⊖ cases $2V_\alpha = 0–6°$.

Character of elongation: (–).

Distinguishing features: easily overlooked and mistaken for quartz, which has a lower refraction and a slightly higher birefringence, is uniaxial ⊕ and has a ⊕ elongation; apatite shows a distinctly higher relief; nepheline has a different paragenesis and lower refraction; topaz is optically biaxial ⊕ with a higher refraction.

Alteration: rare, nucleating from margins and fractures. Hydrothermal alteration leads to muscovite.

Occurrence: typically occurs in pegmatites as pneumatolytic mineral in granites, rarely in nepheline syenites and also rarely in regional metamorphic mica schist and marbles.

Paragenesis: with quartz, tourmaline, topaz, Li-mica and cassiterite.

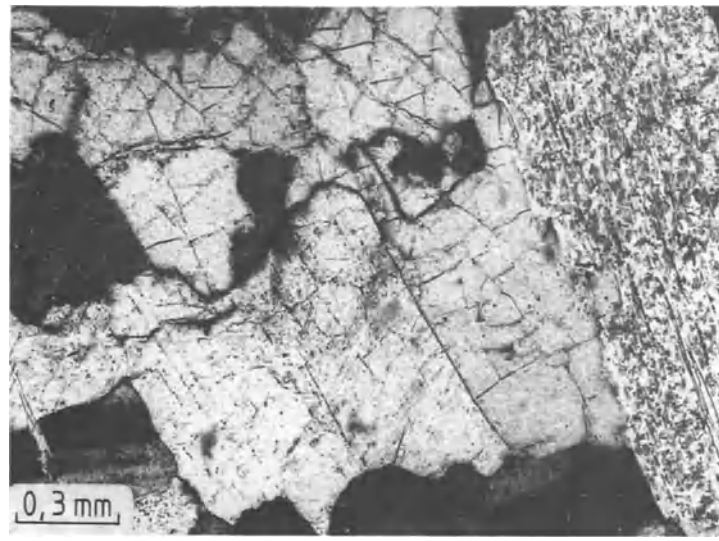

Fig. 105 Tectonized beryl crystal with cataclastic mosaic texture. Unknown locality. Crossed polars.

3.2.8 Nepheline

$Na_3[AlSiO_4]_4$ hexagonal–pyramidal

General features: next to leucite nepheline is the most important feldspathoid and is particularly common in silica-undersaturated, Na-rich magmatic rocks, where it replaces the albite component:
$Na[AlSi_3O_8] - 2SiO_2 \rightarrow Na[AlSiO_4]$.
Nepheline can contain up to 37 mol % $KAlSiO_4$ and up to 20 mol % of isomorphic albite.

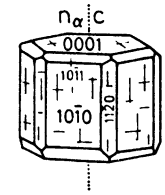

Fig. 106 Crystal form and optical characteristics of nepheline.

Thin-section characteristics

Form: commonly as xenomorphic interstitial phase, which precipitates very late during the crystallization from a melt. It also occurs as idiomorphic short columnar crystals with hexagonal {0001} and rectangular [0001] cross-sections (Figs 106, 107).

Cleavage: on $\{10\bar{1}0\}$ and on (0001), not visible under the microscope.

Twinning: rare on $\{10\bar{1}0\}$.

Colour: colourless; in plutonic rocks it tends to form a milky coloured exsolution of the kalsilite component (this variety is called **elaeolite**). It shows clouding at crystal margins.

Refraction and birefringence:

n_e	= 1.526 – 1.542
n_o	= 1.529 – 1.546
$\ominus\Delta$	= 0.003 – 0.005

The refraction and birefringence are characteristically low; it has no relief relative to canada balsam, and has grey to greyish-blue interference colours of the 1st order; it is optically uniaxial ⊖, occasionally optically biaxial. In very thin thin-section the birefringence can be seen only with the red I compensator.

Optic axial angle: rarely anomalously biaxial ⊖ with $2V_\alpha = 0–6°$.

Character of elongation: (–).

Extinction: tends to be straight.

Special characteristics: can show anomalous subgrains; in volcanic rocks crystals can be zoned, and there can be inclusions of aegirine-augite, greenish sericite and Fe-oxides.

Distinguishing features: if nepheline occurs as interstitial material only it is often difficult to identify. Quartz and tridymite are both optically ⊕ and always fresh; apatite and beryl have much higher refractive indices; sanidine has oblique extinction, is twinned and has good cleavage; melilite has a higher refraction; scapolite has a

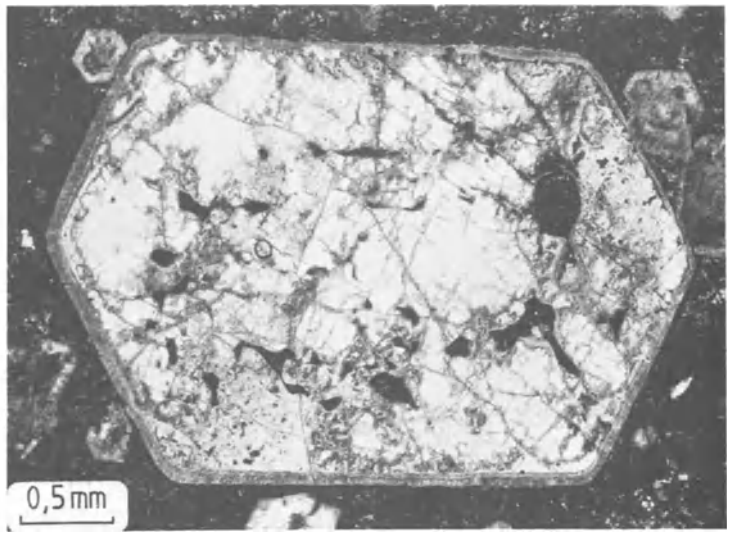

Fig. 107 Idiomorphic nepheline with hexagonal symmetry containing inclusions and showing alterations around the rim into fibrous zeolite. Other crystals present are hauyne (small crystal in the top right corner). Phononephelinite. Katzenbuckel, Odenwald, Germany. Uncrossed polarizers.

good cleavage and is tetragonal; zeolites have lower refraction.

Alteration: it alters easily, into sodalite, analcite and rarely into cancrinite, and into fibrous zeolite (in particular natrolite and the dendritic hydronephelite) by hydrothermal and pneumatolitic influences. Under the influence of CO_2-rich solutions it alters into sericite (pseudomorphs of sericite/muscovite are called liebenerite).

Occurrence: in alkali magmatic rocks which are silica undersaturated; particularly in nepheline phonolites to nepheline tephrites, nephelinites, nepheline syenites and nepheline monzosyenites, essexites, etc. Next to leucite it occurs subordinately in K-rich volcanic rocks (e.g. leucite tephrites). Nepheline tends to crystallize from a magma together with the alkali feldspars as one of the last phases to crystallize. This gives rise to the commonly hypidiomorphic to xenomorphic form. Exceptions to this are the idiomorphic nepheline phenocrysts in phonolites or phononephelinites of the Katzenbuckel in the Odenwald, Germany (Fig. 107; two nepheline generations).

Paragenesis: it never occurs together with quartz. Typically it occurs with other foid representatives (e.g. from the sodalite group), as well as leucite, aegirine-augite, melanite, melilite, olivine, Ti-augite, Ti-biotite, apatite, cancrinite and feldspars.

3.2.9 Scapolite group

Marialite $Na_8[(Cl_2, SO_4, CO_3)|(AlSi_3O_8)_6]$ tetragonal–dipyramidal
Meionite $Ca_8[(Cl_2, SO_4, CO_3)_2|(Al_2Si_2O_8)_6]$

General features: both endmembers of this group form a solid-solution series, similar to the plagioclase group. The pure endmembers do not occur in nature. Scapolite is a very rare mineral.

Thin-section characteristics

Form: granular, columnar (Fig. 108), stalk-like (Fig. 110).

Cleavage: good on (100), not so good {110}; in cross-section the two cleavage planes intersect at right angles (Fig. 109). In columnar crystals parting is on (001) (Fig. 110).

Colour: colourless; inclusions often cause clouding.

Refraction and birefringence:

	Marialite	Meionite
n_e	= 1.531 – 1.541	1.556 – 1.564
n_o	= 1.539 – 1.550	1.590 – 1.600
$\ominus\Delta$	= 0.004 – 0.005	0.034 – 0.038

Refraction and birefringence clearly increase from marialite to meionite. Marialite has grey interference colours of the 1st order, and meionite of the 2nd order (bright violet); optically uniaxial.

Fig. 108 Crystal form and optical characteristics of scapolite.

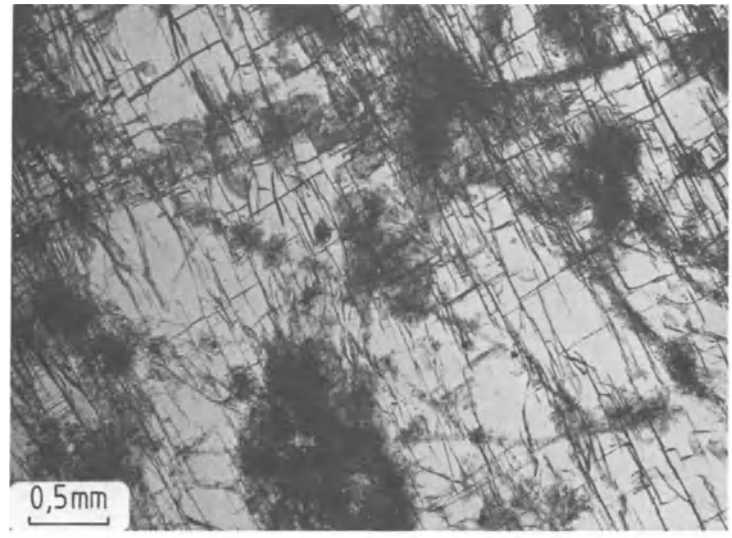

Fig. 109 Scapolite showing two sets of fractures intersecting at right angles and hydrothermally induced alteration into zeolite. Oedegården near Bamle, Telemark, Norway. Crossed polars.

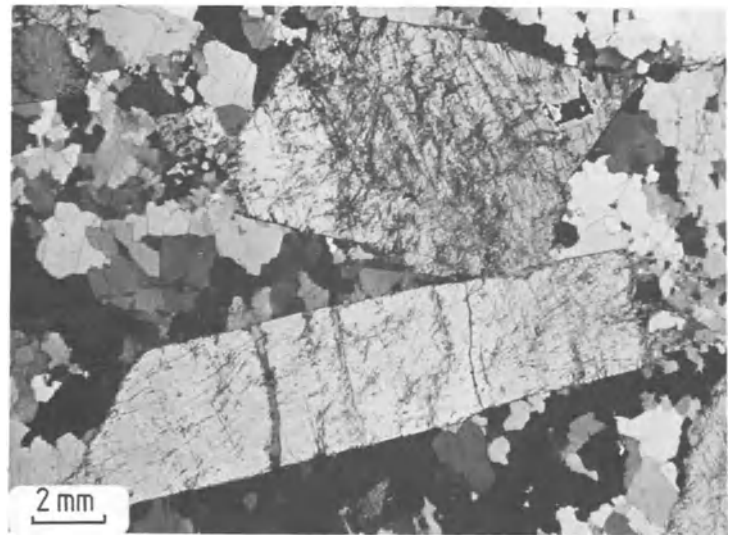

Fig. 110 Idiomorphic scapolite porphyroblast in microcrystalline quartz matrix. Parting on (001). Scapolite hornfels. Wolfsberger Hütte, Saualpe, Carinthia, Austria. Crossed polars.

Character of elongation: (–)

Extinction: in most cases straight.

Special characteristics: inclusions are typical, such as poikiloblastic quartz, calcite and feldspar; fluid inclusions also occur.

Distinguishing features: quartz is optically uniaxial ⊕ and shows no cleavage; nepheline and cancrinite occur in a different paragenesis; cordierite, andalusite and wollastonite are optically biaxial; feldspars tend to be twinned and show oblique extinction.

Alteration: hydrothermal alteration into different zeolites (chabazite, stilbite, analcite, etc.), and also into carbonate. Weathering leads to alteration into kaolinite.

Occurrence: in a CO_2 and SO_2 environment it forms by autopneumatolyses and contact pneumatolyses or by alteration of plagioclase. It occurs in some granites and nepheline syenites and associated pegmatites, rarely in trachytes. As a metamorphic mineral it occurs in some siliceous limestones. In volcanic rocks it occurs as a contact pneumatolytic mineral (Laacher volcanic area, Germany).

Paragenesis: with vesuvianite, diopside, garnet, calcite and wollastonite, and also with cancrinite, melanite and andradite. In metamorphic rocks it tends to occur with pyroxene, amphibole, phlogopite, garnet and sphene; in volcanic rocks with anorthite, nepheline and wollastonite.

3.2.10 Apophyllite

$KCa_4[F|(Si_4O_{10})_2]\cdot 8H_2O$ ditetragonal-dipyramidal

Thin-section characteristics

Form: in thin section it occurs in granular to sheet-like aggregates.

Cleavage: perfect on (001).

Colour: colourless.

Refraction and birefringence:

	most	rare
n_e	= 1.5345	– 1.5445
n_o	= 1.5365	– 1.5439
$\oplus\Delta$	= 0.0020	– 0.0006

Low refraction and very low birefringence, strong dispersion can lead to $\Delta = 0.0000$; occasionally very strong anomalous interference colours. Can be anomalously biaxial.

Character of elongation: (+), rarely (–).

Extinction: tends to be straight.

Optical orientation: $n_\gamma \parallel c$ (rarely $n_\alpha \parallel c$).

Distinguishing features: easily confused with zeolite, which shows lower refraction and tends to be optically biaxial (with the exception of chabazite, which does not show a good cleavage). Nepheline and marialite occur in different parageneses.

Occurrence: hydrothermal; in cavities and fractures in basaltic volcanic rocks. It occurs rarely as a hydrothermal alteration product along fractures in amphibolites; and it is rare in skarns.

Paragenesis: in basaltic rocks with calcite and zeolite. In amphibolite and skarns with prehnite, pectolite and datolite.

3.2.11 Cancrinite

$Na_6Ca_2[(CO_3)_2|(AlSiO_4)_6]$ hexagonal-bipyramidal

General features: uncommon foid, and occurs in alkaline magmatic rocks.

Thin-section characteristics

Form: short columnar (Fig. 111) to needle-shaped, but typically granular (e.g. as interstitial mineral-forming matrix). Tends to be fibrous in veins.

Cleavage: perfect on $\{10\bar{1}0\}$, perpendicular to the long axis (Colour plate 6)

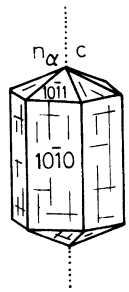

Fig. 111 Crystal form and optical characteristics of cancrinite.

Colour: colourless.

Refraction and birefringence:

n_e	= 1.498 – 1.4885
n_o	= 1.524 – 1.4890
$\ominus\Delta$	= 0.026 – 0.0005

Very low refractive indices and medium high birefringence (ranging from pale-yellow interference colours of the 1st order to medium colours of the 2nd order; Colour plate 6); optically uniaxial $\ominus$, but can be anomalously biaxial with a small axial angle.

Character of elongation: (–).

Extinction: straight.

Distinguishing features: analcite can show anomalous subgrain formation; differs from nepheline by its brighter interference colours; scapolite has higher refractive indices.

Alteration: into calcite and zeolite.

Occurrence: in the presence of high CO_2 partial pressures cancrinite can form pseudomorphs after nepheline in alkaline rocks (e.g. nepheline syenite).

Paragenesis: with nepheline, sodalite group, sanidine, aegirine-augite, melanite and calcite.

4 Biaxial crystals

4.1 Olivine group

$(Mg, Fe)_2[SiO_4]$ orthorhombic–dipyramidal

General features: important dark mineral in ultramafic and basaltic rocks. Minerals of the group show complete diadochy between the endmembers of forsterite $Mg_2[SiO_4]$ and fayalite $Fe_2[SiO_4]$.

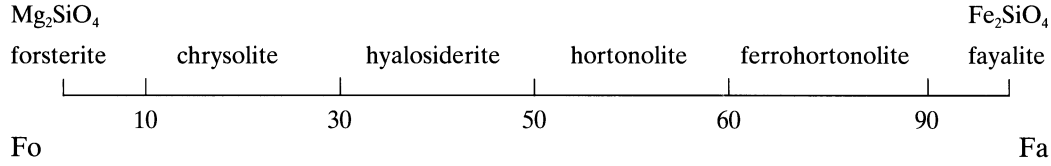

Thin-section characteristics

Optical characteristics strongly depend on the composition.

Form: in volcanic rocks hexagonal and octagonal cross-sections (Fig. 114), which often show corrosion and resorption rims (Fig. 113); in glass-rich volcanic rocks as skeletal crystals (Fig. 112); and in plutonic and metamorphic rocks as granular masses. In basic rocks it can form glomerophyric texture aggregates.

Cleavage: imperfect in Mg-rich members; moderate in Fe-rich members; imperfect on (010) and even less clear on (100). The imperfect cleavage

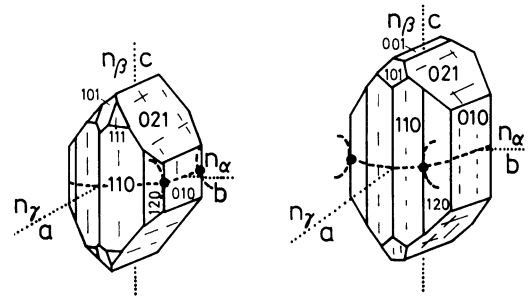

Fig. 112 Crystal form and optical characteristics of fayalite (left) and forsterite (right) (olivine group).

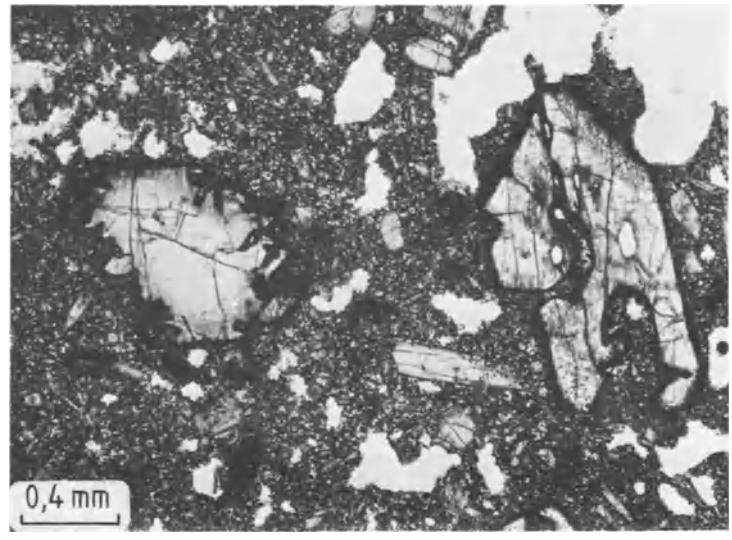

Fig. 113 Idiomorphic, partly corroded olivine phenocrysts with iddingsite rims (black) in microcrystalline matrix, comprised of titanaugite, plagioclase and glass. Alkali olivine basalt. Lanzarote, Canary Islands. Uncrossed polarizers.

Fig. 114 Idiomorphic olivine crystal with spinel inclusions in a tholeiitic basalt of the Vogelsberg, Germany. Characteristic poor cleavage in olivine. Uncrossed polarizers.

is diagnostic and allows olivine to be distinguished from pyroxenes (Fig. 114).

Twinning: on different prism planes, but it is not diagnostic. Twin lamellae on {011}.

Colour: colourless, rare pale yellow or pale green (fayalite), in which case a pale-yellow pleochroism is typical.

Refraction and birefringence:

	Forsterite		Fayalite
n_α	= 1.635	–	1.827
n_β	= 1.651	–	1.869
n_γ	= 1.670	–	1.879
$\oplus\Delta$	= 0.035	–	$\ominus$ 0.052

Medium-high refraction and strong birefringence (bright interference colours of the 2nd order), strongly variable according to orientation and chemistry. In sections parallel to (001) birefringence is twice as high as in sections parallel to (100). Depending on composition, optically biaxial $\oplus$ or $\ominus$ (Fig. 115).

Optic axial angle:
Fa_{00}–Fa_{15}: opt. $\oplus$ with $2V_\gamma$ = 84–90°
Fa_{15}–Fa_{100}: opt. $\ominus$ with $2V_\alpha$ = 90–50°.

Character of elongation: (+) or (–), according to orientation.

Extinction: straight.

Special characteristics: can show twin-like subgrains (similar to undulatory extinction observed in quartz) as an indicator of mechanical deformation of the crystal. In Fe-rich basalts and related rocks, zoning in olivine (best seen under crossed polars) with Mg-rich cores and Fe-rich rims is quite common.

Distinguishing features: pyroxenes can be easily mistaken for olivine because of their similar interference colours; however, pyroxenes show a well-developed cleavage. Also epidote shows good cleavage, is pleochroic and has anomalous interference colours.

Alteration:
a) Serpentinization (Part B, section 4.9) due to hydrothermal alteration, associated with an increase in water content and volume: during low-temperature hydrothermal and very low-grade metamorphism, olivine is replaced by chrysotile, replacing the crystal progressively. Chrysotile nucleates along fractures, with the fibre direction oriented perpendicular to the host-wall rock (Colour plate 9), until the whole olivine is replaced by a mesh texture. In lower greenschist facies olivine is replaced by antigorite, leading to a gridlike texture.

b) In high-temperature geothermal systems olivine changes colour to yellow-brown and reddish-brown along rims and fractures due to oxidation of Fe^{2+} to Fe^{3+} and addition of H_2O: iddingsite (Fig. 113). During this alteration a sub-

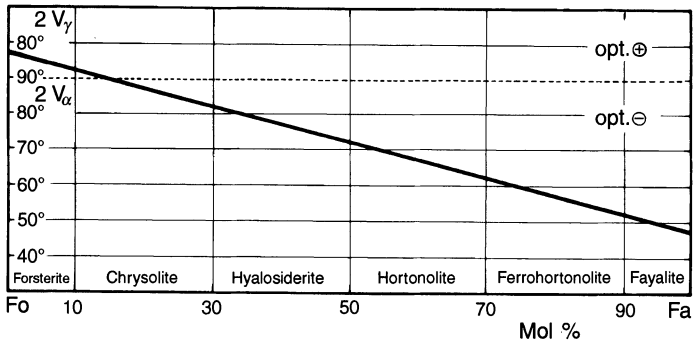

Fig. 115 The optical axial angle (2V) is dependent on the chemical composition of olivine.

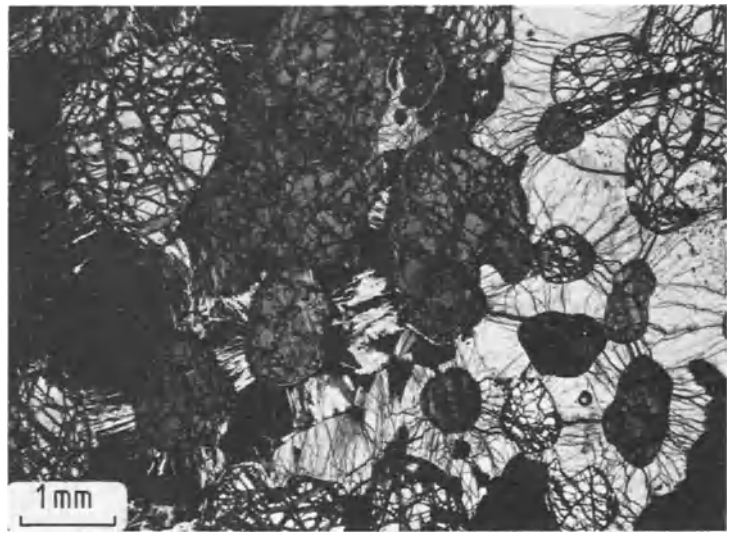

Fig. 116 Olivine crystals forming inclusions in plagioclase. Beginning of kelyphitization. Olivine gabbro. Rhum. Scotland. Crossed polars.

microscopic assemblage forms, consisting of goethite, haematite and clay minerals (smectite), chlorite, etc, replacing olivine. Iddingsite forms pseudomorphs after olivine, shows a weak pleochroism but is not a single mineral. It never occurs in plutonic or metamorphic rocks, only in volcanic rocks and rarely in subsurface volcanic rocks.

Viridite, bowlingite and chlorophaeite are greenish hydrothermal mineral assemblages, which can replace olivine. They form mineral aggregates consisting of chlorite, smectite, serpentine, Fe-talc, mica, goethite and quartz.

c) Reaction rims form where olivine is in contact with anorthite-rich plagioclase in gabbroic rocks (Fig. 116). These kelyphitic textures consist of radiating, fibrous green hornblende, some pyroxene, garnet and spinel.

d) Reaction between olivine with silica-rich melt can lead to a reaction rim of orthopyroxene (commonly bronzite).

Occurrence: characteristic mineral of ultramafic and basic magmatic rocks (e.g. in peridotite, dunite, picrite, gabbro, alkali-olivine basalt, basanite, etc.). Early formed idiomorphic crystals tend to be Mg-rich with increasingly more Fe-rich rims. Zoned crystals are common. In volcanic rocks two olivine generations can be present, as phenocrysts (e.g. core Fa_{10-20}, rim Fa_{40-60}) and as a matrix mineral (Fa_{30-60}; e.g. in alkali-olivine basalt). Olivine which forms early during crystallization from a melt might accumulate at the bottom of the magma body. Pure fayalite commonly occurs in blast-furnace slags. An exception is the fayalite-gabbro of the Radau Valley, Germany. The crystallization of olivine requires a silica-undersaturated magma, otherwise pyroxene would form: $Mg_2SiO_4 + SiO_2 \rightarrow Mg_2Si_2O_6$. With the crystallization of olivine from the magma, the melt can become quartz-normative and hence olivine becomes unstable; however, it does not completely react to pyroxene, but shows resorption rims. Therefore, olivine and quartz may occur together. In metamorphic rocks olivine occurs in serpentinites. Olivine also forms during metamorphism of dolomite (e.g. forsterite marble).

Paragenesis: in ultrabasic rocks with chromite and picotite, ortho- and clinopyroxene. In basic rocks together with titanaugite, ortho- and clinopyroxene, plagioclase, and leucite and clinopyroxene respectively.

4.2 Pyroxene group

4.2.1 Orthopyroxene group: enstatite, bronzite, hypersthene

$(Mg, Fe)_2[Si_2O_6]$ orthorhombic–dipyramidal

General features: there is a nearly complete solid solution between the orthorhombic pyroxenes (opx), but only the first three members occur in nature.

According to the recent nomenclature (Morimoto, 1988) only the names enstatite (Fs_{0-50}) and ferrosilite (Fs_{50-100}) should be used. Here we follow the old tradition and give credit to rock types such as hypersthene-granite, bronzitite, etc.

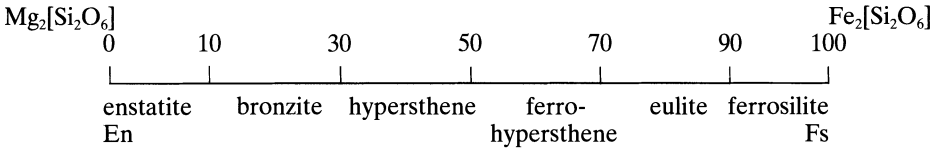

Under higher pressures (e.g. in granulites) orthopyroxene has a higher Al content.

Thin-section characteristics

The optical characteristics vary with increasing Fe-content.

Form: in volcanic rocks columnar, stretched along the c-axis (Fig. 117); in plutonic and metamorphic rocks predominantly as hypidiomorphic to xenomorphic crystals.

Cleavage: excellent parallel to prism planes {210}: in sections perpendicular to the c-axis two cleavage planes can be clearly seen intersecting at angles of 87° and 93° respectively (Fig. 118). In sections parallel to the c-axis only one set of cleavage planes can be seen oriented parallel to the length of the crystal.

Twinning: not very common on (011), (023) and (043): not a diagnostic feature.

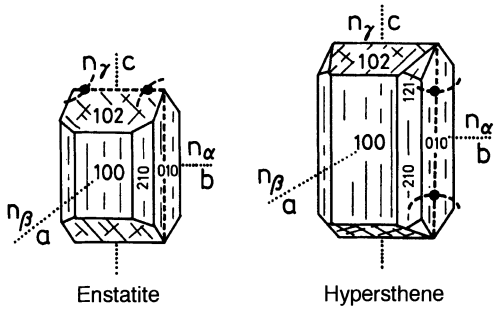

Fig. 117 Crystal form and optical characteristics of the orthopyroxenes enstatite and hypersthene.

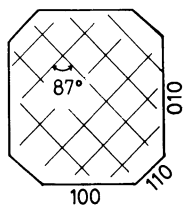

Fig. 118 Basal section of pyroxene showing cleavage planes intersecting at nearly right angles.

Colour: colourless (enstatite), pale light-green (bronzite), pale green to reddish-pale brown with weak pleochroism: α, β, yellowish to reddish; γ, grey-green (hypersthene).

Refraction and birefringence:

	Enstatite	Hypersthene
n_α	= 1.650	– 1.712
n_β	= 1.653	– 1.724
n_γ	= 1.658	– 1.727
⊕Δ	= 0.008	– ⊖ 0.015

High refraction and medium-high birefringence (yellow to orange interference colours of the 1st order), both increasing with increasing Fe-content; zoning in volcanic rocks is common, with Mg-rich cores.

Optic axial angle: systematically varies with increasing Fe-content (Fig. 119).

Enstatite: optically biaxial ⊕ with $2V_\gamma = 54°–83°$.
Bronzite: optically biaxial ⊕ or ⊖ with $2V_\alpha = 97°–63°$.
Hypersthene: optically biaxial ⊖ with $2V_\alpha = 63°–45°$.

Character of elongation: (+).

Extinction: tends to be straight.

Special characteristics: in magmatic rocks orthopyroxene tends to show exsolution lamellae parallel to (100), and can be recognized by a higher birefringence and oblique extinction (Fig. 120). Bronzite and hypersthene quite frequently contain tiny lath-shaped inclusions of ilmenite, which are aligned either parallel (100) or at an angle of 30° to the c-axis. These form by exsolution and give rise to the slight dusting of the crystal when viewed with uncrossed polarizers and they also cause a shimmering effect (Fig. 121).

Distinguishing features: the minerals of the epidote-zoisite group show anomalous interference colours; andalusite has a lower refraction and a negative elongation; kyanite has oblique extinction and a perfect cleavage; the minerals of the melilite and scapolite groups are optically uniaxial; the colourless representatives of the

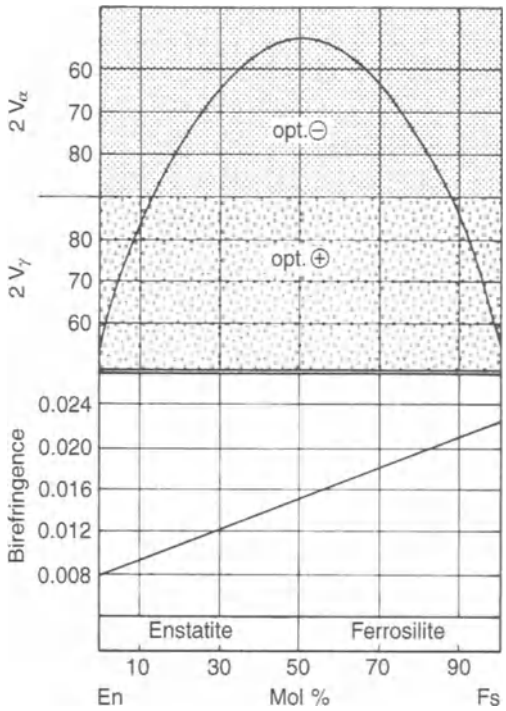

Fig. 119 Optic axial angle (2V) and birefringence of orthopyroxene.

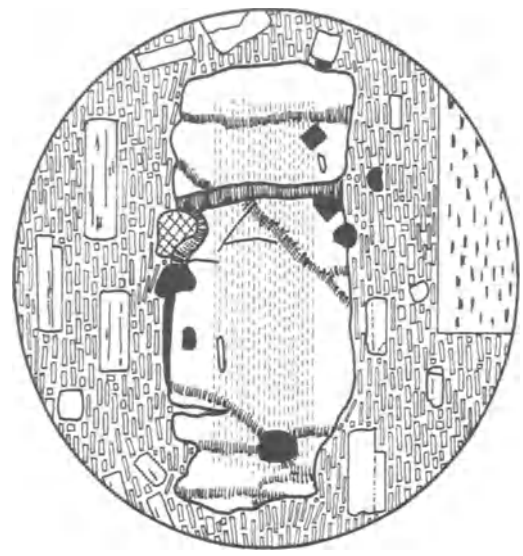

Fig. 120 Exsolution lamellae in orthopyroxene (hypersthene). Quartz andesite. Puracé Volcano, southern Colombia. Uncrossed polarizers.

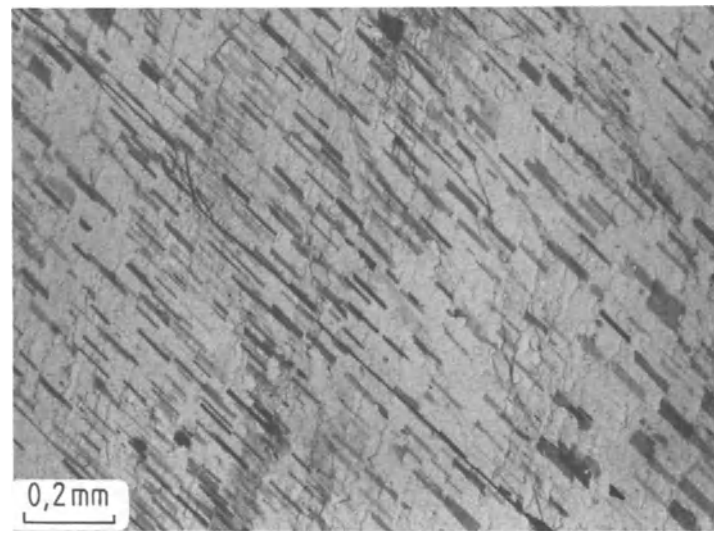

Fig. 121 Bronzite with pervasive fine exsolution lamellae of ilmenite parallel (100). Peridotite. Finero, Ivrea area, northwestern Italy. Uncrossed polarizers.

amphibole group differ because of their oblique extinction and the cleavage intersection angles of 124° and 56° respectively. For differentiating features between amphibole and clinopyroxene see Table 3.

Alteration: quite robust mineral. Can show serpentinization in ultramafic (e.g. harzburgite) and volcanic rocks; commonly as pseudomorphs with oriented growth (bastite; bastitization in harzburgites (Figs 122, 123)) where the cleavage of the newly formed serpentine mineral (lizardite) is parallel to {100} in orthopyroxene. Also chrysotile with mesh texture can form and replace the orthopyroxene. Weathering can lead to the formation of carbonate and Fe-hydroxide or hematite.

Occurrence: very common in plutonic rocks, specially in ultramafic and basaltic rocks. In pyroxenites and peridotites enstatite and bronzite (bronzitite, lherzolite) predominate,

Table 3 Features differentiating orthopyroxene and clinopyroxene

	Orthopyroxene (rhombic)	Clinopyroxene (monoclinic)
Habit	squat columnar, tabular, granular	columnar, stretched parallel to the c-axis; aegirine can be needle-shaped to spherolitic
Colour	tends to be colourless to pale brownish with weak pleochroism	pale green to brownish with weak pleochroism (exception: aegirine-augite with strong green pleochroism)
Extinction	straight	oblique
Birefringence	low (0.005–0.015)	higher (0.023–0.031)
Optic axial angle	enstatite-bronzite: $2V \approx 90°$	$2V\gamma << 90°$ (exception aegirine-augite)

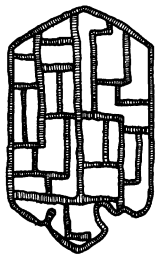

Fig. 122 Bastitization of orthopyroxene. Uncrossed polarizers.

rarely hypersthene (harzburgite). In gabbros and norites (basic rocks with predominantly orthopyroxene (opx) and subordinate clinopyroxene (cpx)) bronzite and hypersthene are common; in diorites and in 'dry' granites (charnockites) only hypersthene is common. There is a clear trend towards more Fe-rich members in more SiO_2-rich magmatic rocks. In volcanic rocks opx occurs as phenocrysts, particularly in andesitic to dacitic rocks; generally opx is represented by hypersthene (Fig. 124). In dark andesites opx occurs as Fe-rich bronzite. Hypersthene is a characteristic phase in the granulite facies in metamorphic rocks.

Paragenesis: in ultrabasic rocks with opx, olivine, cpx and spinel. In basic rocks with opx, cpx, plagioclase and olivine. In volcanic rocks with hypersthene, cpx and plagioclase. In pyroxene-bearing granulites with hypersthene, quartz and garnet. In contact-metamorphic rocks with opx, quartz, plagioclase, biotite, cordierite and diopside.

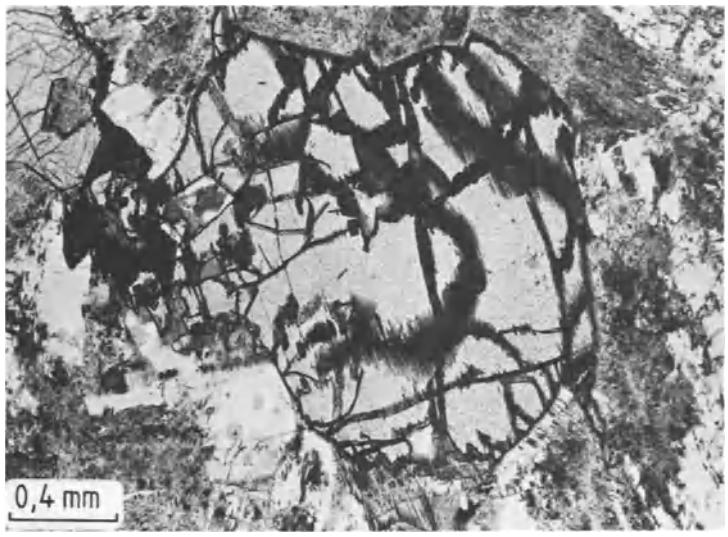

Fig. 123 Hypersthene affected by progressive bastitization advancing from fractures. Also shown are clinopyroxene and sericitized plagioclase. Norite. Bad Harzburg, Harz Mountains, Germany. Uncrossed polarizers.

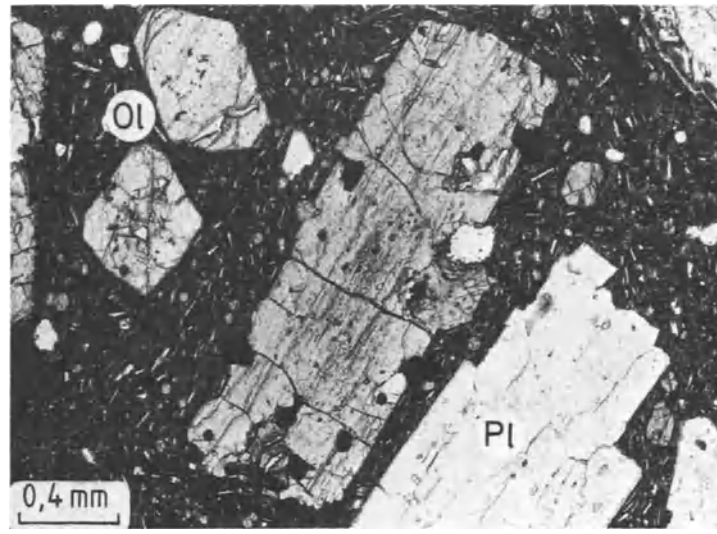

Fig. 124 Idiomorphic hypersthene phenocrysts next to plagioclase and idiomorphic olivine phenocrysts. Quartz andesite. Chiles volcano, northern Ecuador. Uncrossed polarizers.

4.2.2 Clinopyroxenes

$XY[Z_2O_6]$ monoclinic–prismatic

General features: most common mineral group forming dark minerals; X position is generally filled by Ca, and also Na and Li; Y is filled with Mg, Fe^{2+}, Mn and subordinately Fe^{3+}, Al and Ti; the Z position is filled with Si and subordinately Al. The clinopyroxenes (cpx) can be represented in the $Ca_2Si_2O_6$–$Mg_2Si_2O_6$–$Fe_2Si_2O_6$ triangle, with the exception of the alkali pyroxenes and titanaugite (Fig. 125).

Thin-section characteristics

Cleavage: perfect on {110} and (010). In basal sections the two cleavage planes intersect at 87° and 93° respectively (Fig. 118). Less well-developed cleavage on (100), (010) and (001).

Character of elongation: it cannot be determined in clinopyroxenes with the exception of aegirine-augite.

Extinction: oblique; in longitudinal sections perpendicular to [010] it is at an angle of 45° (Fig. 140), which is a diagnostic feature for distinguishing clinopyroxene from clinoamphibole; only in basal sections is extinction symmetric (Fig. 19(d)).

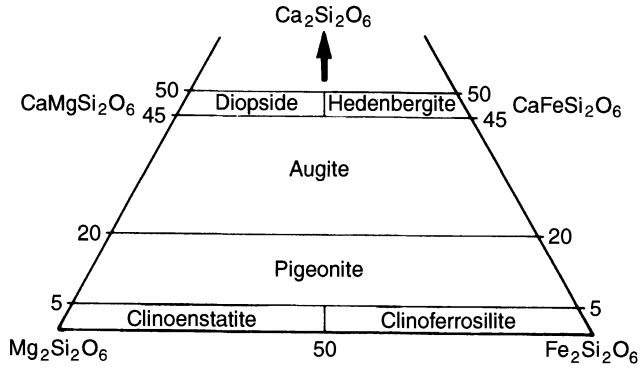

Fig. 125 Nomenclature of clinopyroxenes, excluding the Na-rich representatives.

4.2.2.1 Diopside group

$Ca(Mg, Fe)[Si_2O_6]$

General features: solid solution of the endmembers diopside $CaMg[Si_2O_6]$ and hedenbergite $CaFe[Si_2O_6]$. (Fig. 125).

Thin-section characteristics

Form: short prisms (Figs 126, 127), slender columns, to columnar or granular; in basal sections octagonal (Fig. 118).

Cleavage: perfect on {110}.

Twinning: in volcanic rocks glomerates are typical, variably intergrown. Twinning predominantly on (100), forming pyroxene lamellae, which are oriented obliquely to the cleavage planes.

Colour: colourless to pale green with a very weak, pale-green pleochroism.

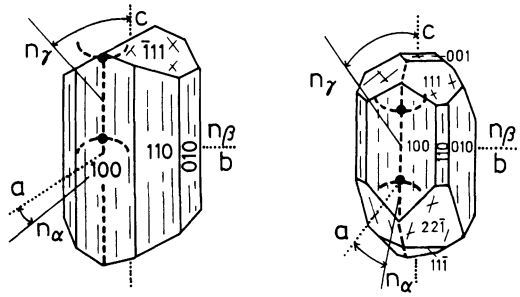

Fig. 126 Crystal form and optical characteristics of clinopyroxenes: augite (left) and diopside (right).

Refraction and birefringence:

	Diopside		Hedenbergite
n_α	= 1.664	–	1.730
n_β	= 1.672	–	1.735
n_γ	= 1.694	–	1.755
$\oplus\Delta$	= 0.030	–	0.025

Medium-high refraction increases with increasing Fe^{2+} content, whereas the medium-high birefringence tends to stay constant (bright interference colours as high as orange of the 2nd order); optically biaxial ⊕.

Optic axial angle: increases with increasing Fe^{2+} content, with $2V_\gamma = 50°–62°$.

Extinction: tends to be oblique, with increasing obliquity with increasing Fe^{2+} content. $\gamma\Lambda c = 38°–48°$ (Fig. 140).

Special characteristics: lamellar exsolutions of orthopyroxenes and bending of crystals.

Distinguishing features: olivine has a higher birefringence and poor cleavage and has straight extinction; omphacite and jadeite occur in different parageneses; amphiboles are more strongly pleochroic, have a different cleavage set and tend to be optically ⊖; orthopyroxenes have a straight extinction. Detailed determinations of the birefringence and axial angle (universal stage) are necessary to differentiate diopside-group pyroxenes from pigeonite and augite-group pyroxenes. Fe-rich members of the epidote group show anomalous interference colours and have a different cleavage.

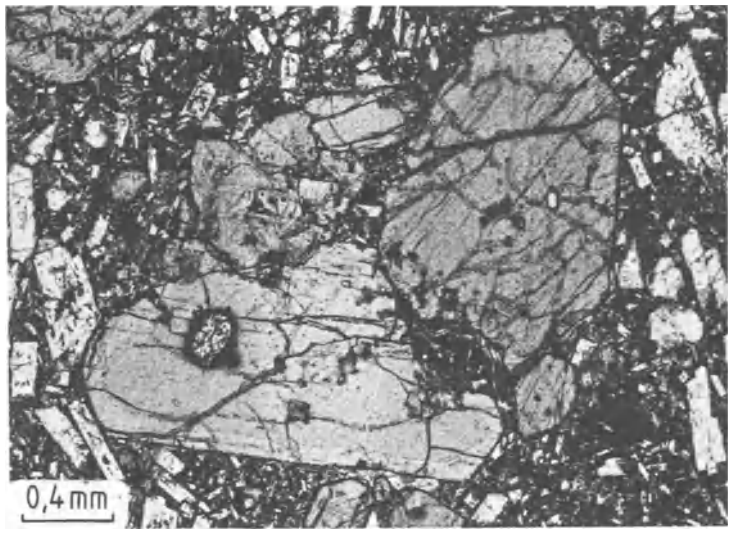

Fig. 127 Idiomorphic, partly corroded diopside phenocrysts in a porphyry surrounded by a matrix consisting predominantly of plagioclase laths and glass. Untypical pleochroic halo in the crystal with the longitudinal section (bottom left). Quartz andesite. Puracé volcano, southern Colombia. Uncrossed polarizers.

Alteration: pneumatolytic to hot-hydrothermal alteration (uralitization, Colour plate 8) into brush-shaped fibrous aggregates of amphibole (tremolite or actinolite). Low-temperature hydrothermal alteration leads to serpentinization. Weathering produces carbonate, hematite and quartz.

Occurrence: diopside-rich pyroxenes are common in Na- and K-rich (alkali) magmatic rocks, also in alkali basalts and alkali gabbros and related rocks (hawaiite, mugearite, latite and monzonite, etc.), but are not so common in tephrites, basanites and phonotephrites, nephelinites, etc. (titanaugite is more typical in these rock types). They occur in certain lamprophyres and ultrabasic rocks, such as dunites and kimberlites (in the latter as chrome-diopside with bright emerald-green colours), and as phenocrysts in tholeiitic basalts and andesites. In contact-metamorphosed rocks diopside is frequently found in siliceous limestones, and hedenbergite tends to occur in skarns (Fe-rich siliceous carbonates) in the amphibolite facies.

Paragenesis: in magmatic rocks together with augite and pigeonite (commonly in the matrix), plagioclase, olivine, with or without foids (nepheline and leucite). In contact-metamorphosed rocks with diopside, grossularite, vesuvianite, forsterite, wollastonite and clinozoisite.

4.2.2.2 Augite group

$(Ca, Mg, Fe^{2+}, Ti, Al)_2[Si_2O_6]$

General features: differs from members of the diopside group (>45 atom-% Ca) in that the solid-solution sequence of the augite-group pyroxenes has by definition a lower Ca-content (<45 atom-%; Fig. 125).

Thin-section characteristics

Form: see diopside (section 4.2.2.1). In volcanic rocks augite occurs as short prismatic crystals (Fig. 126(a)) in special sections; commonly forms glomerophyric intergrowths. In metamorphic rocks it tends to be xenomorphic.

Cleavage: good on {110}.

Twinning: see diopside (Part B, section 4.2.2.1); in volcanic rocks intergrowth twins are common on (101).

Colour: pale grey-green to bright grey-green, rarely brownish; zoning (with Fe-rich rims and brighter colours) and sectional colour change can be common; the very weak pale-greenish to pale-grey pleochroism can be so faint that it is missed.

Refraction and birefringence:

n_α	= 1.671 – 1.735
n_β	= 1.672 – 1.741
n_γ	= 1.703 – 1.774
$\oplus\Delta$	= 0.018 – 0.033

The medium-high refraction and birefringence increase with increasing Fe-content (interference colours of the 2nd order, similar to diopside); optically biaxial ⊕.

Optic axial angle: dependent on chemical composition, $2V_\gamma = 25°–61°$ (Fig. 128).

Extinction: tends to be oblique; dependent on chemical composition $\gamma\Lambda c = 35°–48°$ (Fig. 140).

Special characteristic: common in basaltic and ultramafic plutonic rocks, showing exsolution lamellae of orthopyroxene, with good cleavage on (100). Thin ilmenite exsolution lamellae can occur.

Distinguishing features: see diopside (Part B, section 4.2.2.1); titanaugite shows stronger colours and pleochroism and hourglass texture are typical.

Alteration: during crystallization from a magma augite tends to be altered under wet conditions into green (sometimes also into brown) amphibole (uralitization). This process can also be observed in low- to medium-grade metamorphic rocks and in contact-metamorphosed aureoles. In these cases pseudomorphs of green hornblende to actinolite form after augite. In magmatic rocks chloritization of augite can be observed, and if additional potassium is added, deep-green celadonite pseudomorphs can form (celadonitization). In low-temperature metamorphic environments, chloritization with epidote and talc are typical. Exposed to weathering, carbonate, hematite and quartz form.

Occurrence: augite (augite s.s.) is the most common dark-coloured representative in calc-alkaline and tholeiitic basaltic magmatic rocks

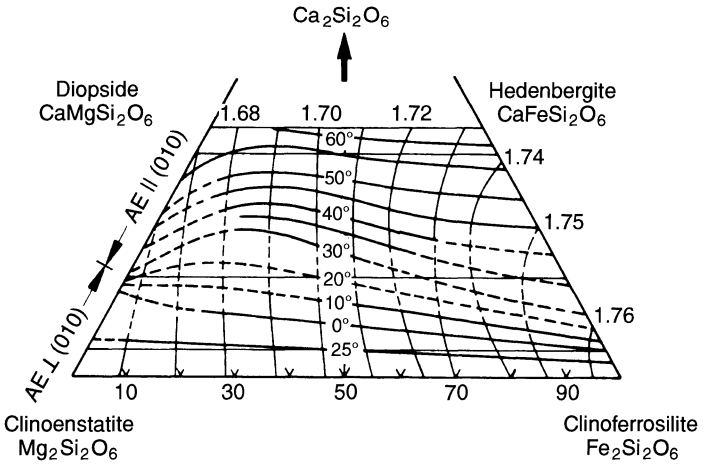

Fig. 128 Position of the axial plane, refraction and axial angle 2V is dependent on the chemical composition of clinopyroxenes.

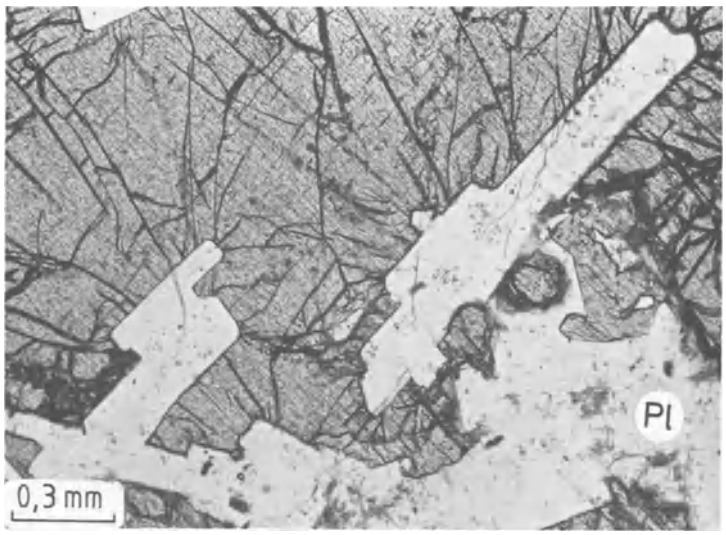

Fig. 129 Augite with subophitic plagioclase inclusions. The excellent cleavage and the high relief are characteristic. Diabase. Överon, north of Göteborg, Sweden. Uncrossed polarizers.

(Fig. 129). Therefore it can be found in gabbroic rocks, granodiorites, andesites and rhyodacites, tholeiitic basalts and related rocks. By contrast, the principal pyroxene in alkaline magmatic rocks is diopside. The Fe-rich endmembers of the augite group occur in very rare rock types. In high-grade metamorphic and contact-metamorphosed siliceous limestones augite forms rather than diopside (e.g. in the pyroxene-hornblende facies or in pyroxene-granulites).

Paragenesis: in calc-alkaline magmatic rocks with augite, hypersthene, plagioclase, hornblende and biotite. In tholeiitic basalts with augite (commonly in the ground matrix), diopside (as phenocryst), plagioclase, pigeonite and olivine.

4.2.2.3 Titanaugite

$Ca(Mg, Fe, Ti)[(Si, Al)_2O_6]$

General features: a pyroxene containing more than 3% weight TiO_2 is called titanaugite. It is easily recognized by its dark colour and occurs in basaltic and ultramafic alkaline magmatic rocks.

Thin-section characteristics

Form: varies, short columnar to thick platy to long columnar phenocrysts (Figs 130, 131).

Cleavage: excellent on {110}.

Twinning: lamellar on (100) and equal-sided twins, intergrown obliquely to the cleavage lamellae.

Colour: brownish-purple to reddish-purple; intensity of colour dependent on Ti^{3+} content; strongly pleochroic; in cases where Fe^{3+} is present, the colour tends to be brownish-yellow, greyish or greenish weakly pleochroic; zonar growth patterns are typical: the core is commonly free of Ti or Ti-poor.
α: pale brownish-yellow.
β: brownish-purple to reddish-purple.
γ: brownish-yellow to violet-brown.

Refraction and birefringence:

n_α	= 1.695 – 1.741
n_β	= 1.700 – 1.746
n_γ	= 1.728 – 1.762
$\oplus\Delta$	= 0.033 – 0.021

Medium-high refraction and birefringence (interference colours of the upper 2nd order and lower 3rd order); because of the strong dispersion of the optic axes anomalous interference colours are typic in the extinction positions (Colour plate 7); instead of black to brown, bluish-grey colours can be observed; optically biaxial ⊕.

Optic axial angle: dependent on the chemical composition, $2V_\gamma = 42°–65°$.

Extinction: oblique, $\gamma \Lambda c = 32°–55°$ (Fig. 140).

Special characteristics: zonar growth patterns, where zoning is parallel to [001] colours are stronger compared to zoning parallel to [$\bar{1}$11], giving rise to hourglass textures (Fig. 131).

Distinguishing features: distinct brownish-purple pleochroism, typical hourglass-growth textures, strong dispersion in the extinction position and anomalous interference colours.

Alteration: in plutonic rocks post-magmatic alteration into titanhornblende.

Occurrence: restricted to Ti-rich volcanic rocks of the alkaline series, common in alkali-olivine basalts, tephrites and basanites, phonotephrites, nephelinites, hyalobasanites (limburgite); alkali-gabbroic rocks, essexite, theralite, camptonite, monchiquite, etc.

Paragenesis: with olivine, plagioclase, nepheline and minerals of the scapolite group, leucite, aegirine-augite and diopsidic pyroxene.

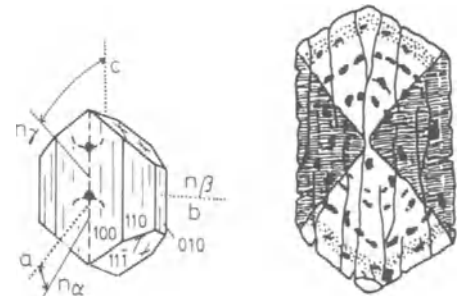

Fig. 131 Titanaugite: optical characteristics and crystal form (left) and hourglass texture (right).

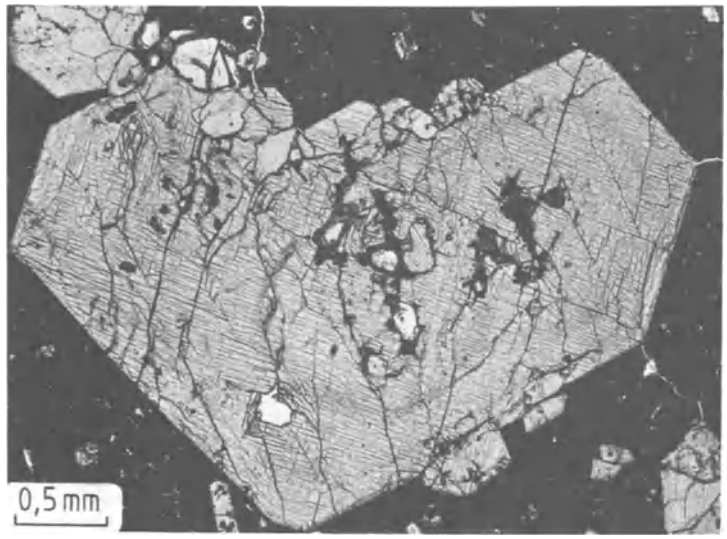

Fig. 130 Basal section of a titanaugite, showing the typical cleavage intersection at nearly right angles. Monchiquite. Rio de Ouro, Serra de Tinguá, Brazil. Uncrossed polarizers.

4.2.2.4 Pigeonite

$(Mg, Fe, Ca)_2[Si_2O_6]$

General features: easily overlooked Ca-poor mineral which is common in tholeiitic basalts.

Thin-section characteristics

Form: typically xenomorphic granular, rarely idiomorphic columnar, with columns longer than in accompaning augite (Fig. 132) (can form rims around augite); typical matrix crystal.

Cleavage: good on {110}.

Twinning: lamellar and polysynthetic on (100).

Colour: colourless; weak pleochroism pale greenish to brownish.

Refraction and birefringence:

n_α	= 1.682 – 1.722
n_β	= 1.684 – 1.722
n_γ	= 1.705 – 1.751
$\oplus\Delta$	= 0.023 – 0.029

The medium-high refraction and birefringence are equivalent to those of the augite and diopside groups (see appropriate sections); optically biaxial ⊕.

Optic axial angle: dependent on chemical composition, $2V_\gamma = 0°–30°$ (tends to be between 10° and 20°).

Extinction: oblique, $\gamma \wedge c = 37°–44°$ (Fig. 140).

Distinguishing features: easily confused with augite and diopside, but they both have a higher axial angle; orthopyroxene has a straight extinction; olivine has a higher birefringence and higher axial angle.

Occurrence: in mafic to intermediate tholeiitic basaltic volcanic and subvolcanic rocks, commonly as matrix mineral next to augite. In diabase, dolerite and also in andesite and dacite. Rare in gabbro and norite (Bushveld, South Africa; Skaergard, Greenland; Harzburg, Harz Mts, Germany).

Paragenesis: with diopside, plagioclase and with or without olivine (as phenocrysts); with pigeonite and augite (as ground matrix). As interstitial mineral between plagioclase lamellae. Not observed together with titanaugite in alkali basalts.

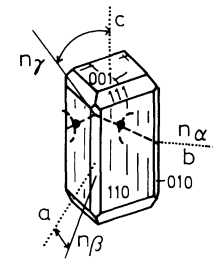

Fig. 132 Crystal form and optical characteristics of pigeonite.

4.2.2.5 Aegirine-augite series

$NaFe^{3+}[Si_2O_6] + Ca(Mg, Fe^{2+})[Si_2O_6]$

General features: mixed crystals of 75–25 mol% aegirine and diopside are classed as aegirine-augites. They form very characteristic dark minerals in alkali basalts of volcanic and plutonic origin; their occurrence is indicative of an excess of alkali elements relative to aluminium.

Thin-section characteristics

Form: short columnar to acicular crystals, elongated along the c-axis (Fig. 133); rarely granular. Octahedral cross-sections are typical; as branching aggregates developed in the ground matrix of phonolitic volcanic rocks.

Cleavage: good on {110}.

Twinning: common on (100).

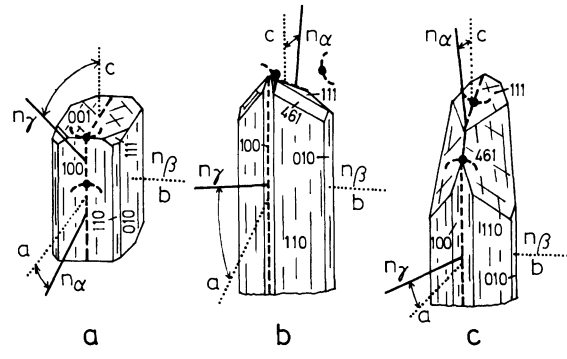

Fig. 133 Crystal form and optical characteristics of aegirine-augite pyroxenes: (a) diopsidic augite, (b) aegirine-augite, (c) aegirine.

Colour: greenish with a strong pleochroism; zoning is common and shows the characteristic hourglass texture.
α: green, olive-green.
β: pale green.
γ: pale green to pale brownish-yellow.

Refraction and birefringence:

n_α	= 1.700 – 1.760
n_β	= 1.710 – 1.780
n_γ	= 1.730 – 1.813
⊕Δ	= 0.030 – 0.053

Medium-high refraction and high birefringence (maximum interference colours of the 3rd and 4th orders), which are higher than those of the diopside and augite series; however, this can be masked by the strong colour; optically biaxial ⊕ or ⊖ (dependent on the chemical composition).

Optic axial angle: dependent on the chemical composition (Fig. 135): $2V_\gamma = 60°–90°$ to $2V_\alpha = 90°–60°$.

Character of elongation: (–).

Extinction: oblique, $\gamma \Lambda c = 55°–85°$ (commonly ≈ 80°; Fig. 140).

Special characteristics: zoning is very distinct with diopside-rich cores, surrounded by aegirine-augite and aegerine-rich rims (Fig. 134); uneven distribution of the aegirine component during growth leads to hourglass textures. Because of a strong dispersion near the extinction position,

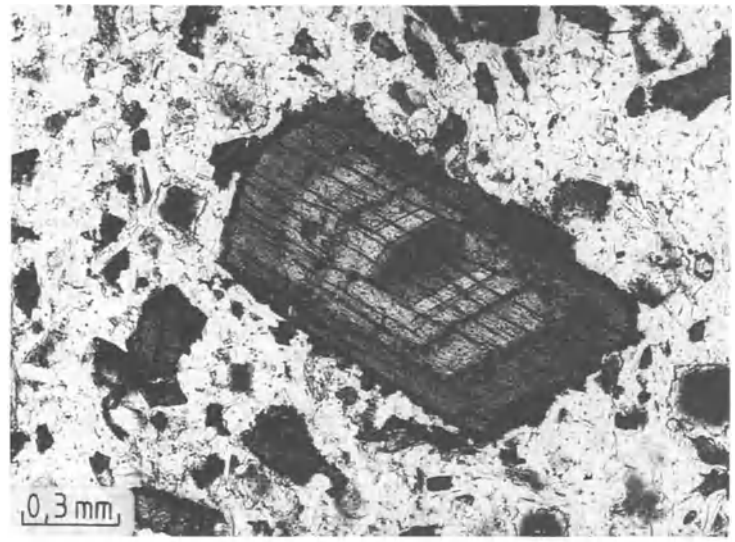

Fig. 134 Zoning in a euhedral aegerine porphyroblast. Nosean leucite rock (selbergite). Rieden, Laacher volcanic area, Germany. Uncrossed polarizers.

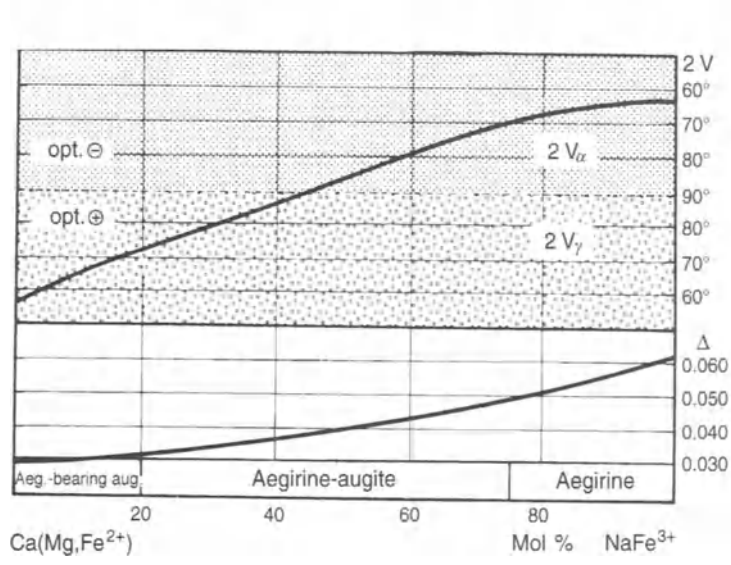

Fig. 135 Optic axial angle (2V) and birefringence of the Na-rich clinopyroxenes.

anomalous brownish to grey-blue interference colours, similar to titanaugite.

Distinguishing features: green hornblende and actinolite show characteristic cleavage intersection at 124° and 56° respectively, and also have a positive elongation and lower refractive indices. Other similar minerals such as pumpellyite and chloromelanite occur in different parageneses.

Alterations: very robust. Pneumatolytic to hydrothermal alteration into sodium-amphibole (arfvedsonite).

Occurrence: aegirine-augite is restricted to strongly differentiated magmatic rocks. Representatives of the alkali series of magmatic rocks: in alkali trachytes, quartz alkali trachytes, pantellerites, phonolites and their equivalent plutonic rocks; also in alkali syenites, alkali granites and foid-syenites and related dykes and sills. In related dark-coloured rocks occurs it in alkali basalts, tephrites and basanites, essexites and theralites, where aegirine-augite occurs only as an alteration product of titanaugite or augite. Also found in contact aureoles of alkali-plutonic rocks.

Paragenesis: with Na-sanidine, nepheline, sodalite group, leucite and melanite; with quartz, albite, zircon and Na-amphibole.

4.2.2.6 Jadeite

$NaAl[Si_2O_6]$

Thin-section characteristics

Form: commonly subhedral to anhedral, granular, platy; also acicular to branching (Figs 136, 137, Colour plate 11).

Cleavage: good on {110}. Lamellae oriented perpendicular to longitudinal axis.

Colour: tends to be colourless, rarely pale green.

Refraction and birefringence:

n_α	= 1.640 – 1.681
n_β	= 1.645 – 1.684
n_γ	= 1.652 – 1.692
$\oplus\Delta$	= 0.006 – 0.021

Medium-high refraction and low birefringence (maximum interference colours of the middle 1st to middle 2nd order); optically biaxial ⊕.

Optic axial angle: varies according to chemical composition, $2V_\gamma$ = 60°–96°.

Extinction: tends to be oblique, $\gamma\Lambda c$ = 32°–55° (Fig. 140).

Special characteristics: stress-induced undulatory extinction and wave-like deformation can be observed.

Distinguishing features: easily differentiated from the other clinopyroxenes because of the low birefringence, the small extinction angle and its typical paragenesis.

Alteration: alteration into albite, or, under retrograde and reduced pressure conditions, into actinolite.

Occurrence: typical mineral in high-pressure and medium-temperature mineral assemblages. In glaucophane schists with basaltic protoliths. Also in quartzites and meta-greywackes.

Paragenesis: in glaucophane-bearing rocks with glaucophane, lawsonite, epidote, Fe-poor pumpellyite, Cr-epidote, albite, with or without quartz, locally also with chlorite, actinolite, calcite and augite-relicts. In jadeite-quartzite with albite, quartz, sericite, chlorite, graphite, calcite and sphene.

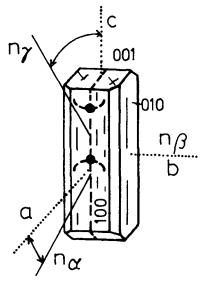

Fig. 136 Crystal form and optical characteristics of jadeite.

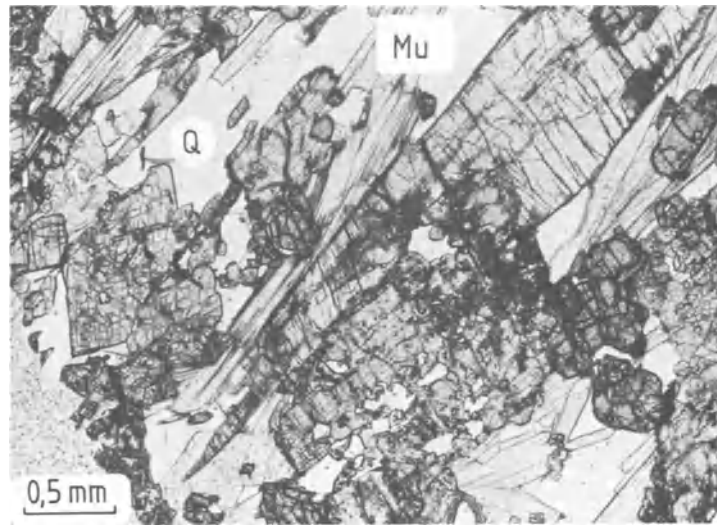

Fig. 137 Poikilitic subhedral jadeite together with glaucophane, quartz and others. Jadeite-schist. Valle d'Aosta, northern Italy. Uncrossed polarizers.

4.2.2.7 Omphacite

$(Ca, Na)(Mg, Fe, Al)[Si_2O_6]$

General features: isomorphs of diopside$_{80-40}$ and jadeite$_{20-60}$, restricted to eclogite facies of metamorphic rocks.

Thin-section characteristics

Form: commonly subhedral to anhedral granoblastic grains, rare columnar (Fig. 138); rutile inclusions are common.

Cleavage: good on {110}.

Colour: colourless to pale green, weakly pleochroic.

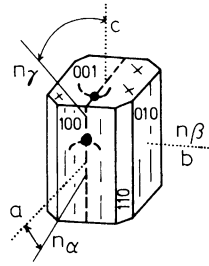

Fig. 138 Crystal form and optical characteristics of omphacite.

Refraction and birefringence:

n_α	= 1.662 – 1.701
n_β	= 1.670 – 1.712
n_γ	= 1.685 – 1.723
$\oplus\Delta$	= 0.012 – 0.028

The medium-high refraction and birefringence are similar to those from diopside and augite; optically biaxial ⊕.

Optic axial angle: $2V_\gamma = 56°–84°$.

Extinction: tends to be oblique, $\gamma \Lambda c = 34°–48°$ (commonly ≈ 40°; Fig. 140). In blueschists undulatory extinction is quite common.

Distinguishing features: it differs from diopside and augite by its characteristic high-pressure paragenesis and can be distinguished from jadeite because of its higher refraction and birefringence.

Alteration: retrograde metamorphism causes alteration at the rims to plagioclase and diopside along grain boundaries (cellular exsolution; Fig. 139).

Occurrence: restricted to eclogites, high-pressure rocks at low fluid partial pressure.

Paragenesis: with pyrope-rich garnet, with or without smaragdite, kyanite, zoisite, quartz, rutile and muscovite (diaphthoritic).

Fig. 139 Omphacite showing partial cellular exsolution during retrograde alteration. Eclogite. Saualpe, Carinthia, Austria. Uncrossed polarizers.

Determination of the maximum extinction angle for pyroxenes and amphiboles

The determination of the extinction angle in monoclinal (triclinal) crystals is an important diagnostic feature, which is easily carried out under the microscope. In suitable sections it is possible not only to distinguish between amphibole and pyroxene (Figs 140, 141) but also between members of the group. In order to determine the exact extinction angle sections parallel to (010) are necessary, which are rarely present. Therefore, only approximate values can be obtained in most cases; e.g. this method does distinguish between diopside and augite, and exact values can be obtained only with a universal stage microscope. Nevertheless, if several individual crystals are measured, a good approximate value can be determined. Measurements of n_γ (or n_β or n_α) from the c-axis (= $n_\gamma \Lambda c$, etc.) with the help of the 360° scale on the circular stage in sections parallel to (010). Only sections with one cleavage set and the highest interference colours are chosen (corresponding to sections parallel to subparallel to the axial plane). The following steps have to be followed when determining the extinction angle:

1. The objective lens, polarizer and analyser all have to be centred.
2. Choose a small aperture (close iris diaphragm as far as possible).
3. Align the cleavage trace parallel to the N–S

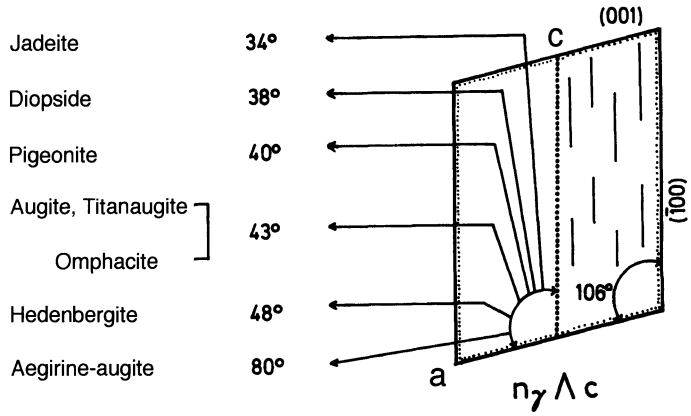

Fig. 140 Extinction angles of the most important clinopyroxenes.

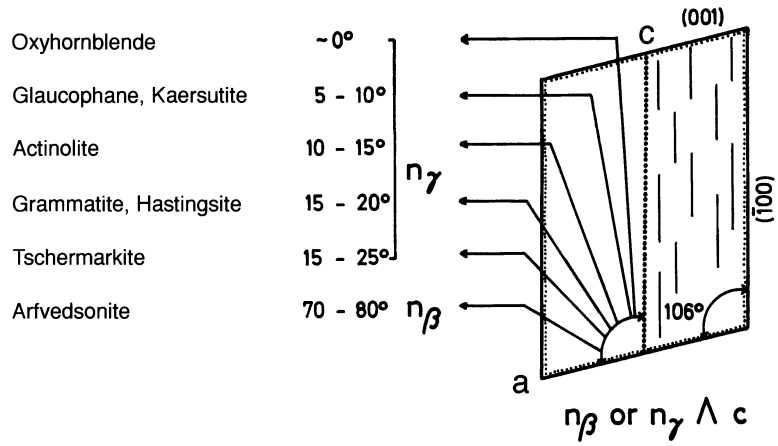

Fig. 141 Extinction angles of the most important representatives of the clinoamphibole group.

cross-hairs and read off the value on the 360° scale on the circular table.

4. Rotate the circular stage until the crystal is extinct under the crossed polars. Read off the angle.
5. Apply this procedure to several individual crystals and use the maximum value.
6. Use the measured values (≈ 0°–20° in amphiboles and ≈ 30°–50° (80°) in clinopyroxenes) for further determinations in respective tables and diagrams (Figs 140, 141).

To achieve maximum extinction the following steps should be carried out (Fig. 142):

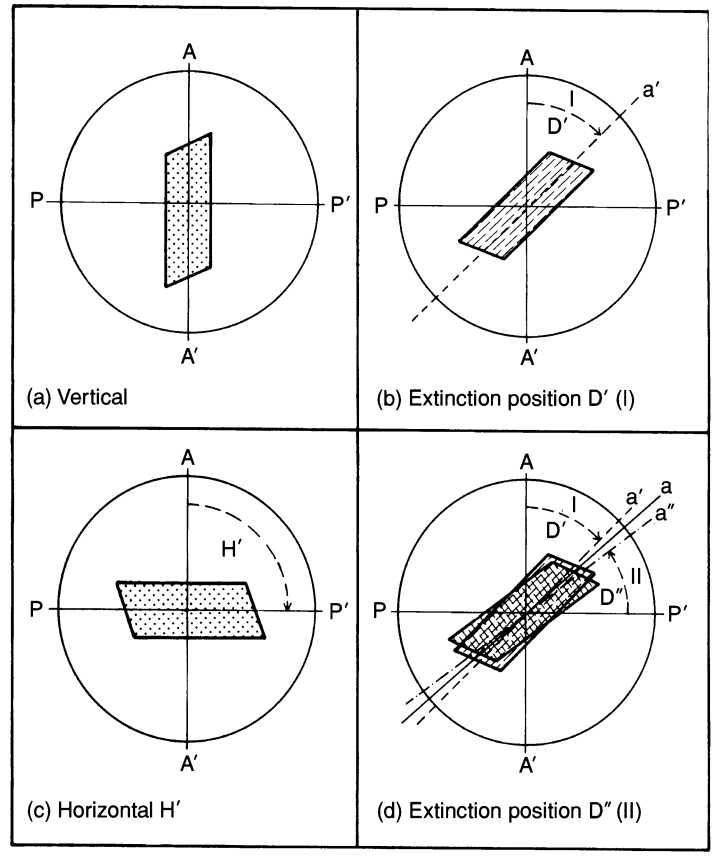

Fig. 142 Determination of the extinction angle in crystals with oblique extinction (example: clinopyroxene):

(a) Orientation of crystal cleavage parallel to the N–S cross-hairs of the ocular.

(b) Rotation to the extinction position (in this case 41°).

(c) Cleavage aligned parallel to the W–E cross-hairs.

(d) Rotation towards the N-direction until the extinction position is reached (in this case 45°).

a) Align the cleavage trace parallel to the N–S cross-hairs and rotate to the extinction position, recording the angle I.
b) Align the cleavage trace parallel to the E–W cross-hairs and rotate towards the N-direction until extinction occurs. Note angle II.
c) The direction which halves the two angles I and II is the direction of maximum extinction.

During determination of the extinction angle, it is important that the measurements are carried out in the correct direction, which is towards n_γ (or in special cases towards n_β or n_α respectively). Rotation of the circular table clockwise or anticlockwise leads in both cases to extinction positions in the crystal. In order to determine in which direction to rotate, the compensator red I is used and the direction of rotation is chosen which produces additive colours ('blue'). In this way n_γ can be determined and the rotation to estimate the extinction angle is carried out clockwise towards n_γ (Z), to get the deviation of $n_\gamma \Lambda c$.

4.3 Amphibole group

General features: amphiboles cannot be clearly differentiated from each other using a polarization microscope or the powder X-ray diffraction method alone. The nomenclature is based on their chemistry. The general formula for amphiboles is:

$A_{0-1}B_2C_5T_8O_{22}(OH, Cl, F)_2$,

with positions occupied by:

A: Na
B: Na, Ca, Mg, Fe^{2+}, ...
C: Mg, Fe^{2+}, Al, Fe^{3+}, ...
T: Si, Al.

Contrary to the pyroxene group, where the rhombic representatives play an important part (orthopyroxenes), the numerous amphiboles are almost exclusively monoclinic. Rhombic amphiboles are restricted to rare paragenesis, and therefore are not dealt with in this book.

The only colourless monoclinic amphibole is the Fe-poor tremolite. The presence of Fe^{2+}, Fe^{3+} and Ti gives rise to the diagnostic pleochroism. Fe^{2+} causes the greenish to yellow-greenish colour of the common hornblende and of actinolite. Oxidation of Fe^{2+} to Fe^{3+} and the high Ti-content give rise to the brown to red-brown colours in hornblende. Higher contents of alkalis, specially Na and K, are responsible for the lilac and purple-blue colours of the alkali amphiboles (glaucophane, arfvedsonite, etc.).

All amphiboles are prismatic [001], where the short columnar habit predominates in magmatic and high-grade metamorphic rocks, whereas the fibrous habit is common in low-grade metamorphic rocks. Characteristic for all amphiboles is their good cleavage on {110}, with intersection angles in basal sections of 124° and 56° respectively (Figs 143, 144). Amphiboles also differ from pyroxenes in their optical characteristics, being optically negative (with some rare exceptions), with extinction angles between 0° and 25° (Fig. 141). The optical character of the main optical zone in longitudinal sections, which in most cases is positive, is also a diagnostic feature of amphiboles.

A clear, unambiguous differentiation between the various amphiboles is possible only by chemical methods. Therefore, we treat only the most important representatives in this book. Leake (1978) deals extensively with the nomenclature and classification of amphiboles.

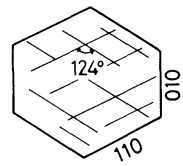

Fig. 143 Basal section of clinoamphibole showing clear cleavage and cleavage intersection at 124° and 56° respectively.

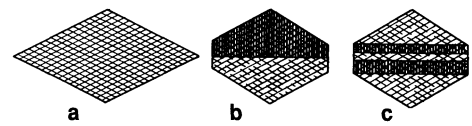

Fig. 144 Basal sections of clinoamphiboles:
(a) Untwinned.
(b) Single twinning.
(c) Multiple twinning in the form of lamellae.

4.3.1 Actinolite group

$Ca_2(Mg, Fe)_5[(OH)_2|Si_8O_{22}]$ monoclinic–prismatic

General features: restricted to low-grade metamorphic rocks. Solid-solution series between the Fe-free tremolite, Fe > Mg-bearing actinolite, Fe-bearing actinolite and Fe-endmember ferroactinolite.

Thin-section characteristics

Form: subhedral columnar, acicular to fibrous, rare aggregates of asbestos-like parallel (amianthus) or randomly (nephrite) oriented fibres. Porphyroblastic blade-shaped actinolite- or garbenschiefer-schist shows preferred growth of [001] within the schistosity plane (Fig. 146).

Cleavage: perfect on {110} with cleavage intersection angles of 124° and 56° respectively (Fig. 145). Deformation-induced parting perpendicular to the long axis.

Twinning: common on (100), also multiple twinning (Fig. 144), rare polysynthetic twinning on (001).

Colour: colourless (tremolite) to pale green (Mg-rich actinolite), with increasing Fe^{2+} content; pale greyish-green, accompanied by a weak pleochroism:
α: light yellowish-green
β: pale greenish-yellow
γ: pale bluish green.
An emerald-green variety can occur in eclogites (**smaragdite**), which shows the same characteristics in regard to refraction, birefringence and extinction angles as tremolite. Pleochroism varies between pale yellowish-green to pale green.

Birefringence and refraction:

	Tremolite		Actinolite
n_α	= 1.608	–	1.647
n_β	= 1.618	–	1.659
n_γ	= 1.630	–	1.667
$\ominus\Delta$	= 0.022	–	0.020

Refraction is medium-high and increases with increasing Fe^{2+} content, whereas the birefringence is medium-high and decreases with increasing Fe^{2+} content (interference colours of the lower to medium 2nd order); optically biaxial ⊖.

Optic axial angle: dependent on chemical composition, decreasing with increasing Fe^{2+} content. Tremolite: $2V_\alpha = 85°$; actinolite: $2V_\alpha = 80°$.

Character of elongation: (+), of diagnostic importance.

Extinction: oblique $\gamma \wedge c = 10°–15°$ (Fig. 141); in basal sections symmetric extinction (Fig. 151).

Distinguishing features: green hornblende is clearly coloured; aegirine-augite has a greater extinction angle; negative main optical zone and cleavage are distinctive in pyroxenes. Wollastonite, which can be easily mistaken for tremolite, shows nearly straight extinction and has a smaller axial angle; cummingtonite tends to be optically ⊕ and has a higher refractive index;

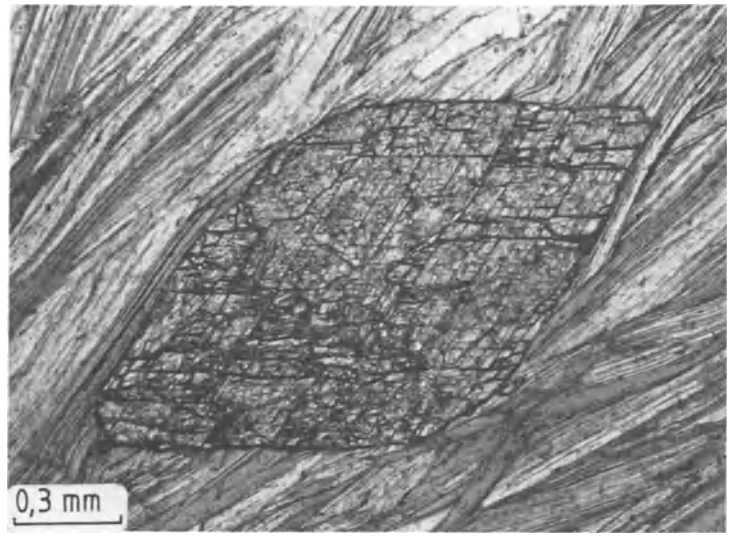

Fig. 145 Basal section of a nematoblastic actinolite crystal. Actinolite-albite-chlorite schist. Talgenköpfe, Zillertal Alps, Austria. Uncrossed polarizers.

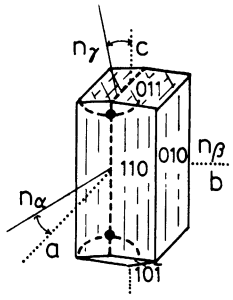

Fig. 146 Crystal form and optical characteristics of actinolite.

the rhombic amphiboles generally show straight extinction.

Alteration: restricted to greenschist facies; with increasing metamorphic grade replaced by hornblende.

Occurrence: tremolite occurs in low- to high-grade metamorphic dolomite-bearing siliceous carbonates. Actinolite forms in basaltic volcanic rocks and in CaMgFe-rich sediments. It is stable only under low-grade metamorphic conditions, in greenschists, talcschists, serpentinite and in actinolite or garbenschiefer. It occurs as a retrograde mineral in blueschists. In diaphthoritic eclogite it forms pseudomorphs of fibrous crystals after omphacite (Part B, section 4.2.2.7); this variety is Cr-rich (smaragdite) and is also found in gabbros which have been uralitized or saussuritized.

Paragenesis: tremolite occurs in greenschist facies together with quartz, chlorite, epidote, calcite antigorite and talc. In amphibolitic facies rocks it occurs together with diopside and cummingtonite (Mg-Fe amphibole). Locally, actinolite occurs in greenschist-facies metamorphic mineral assemblages together with quartz, albite, epidote, biotite, calcite, pumpellyite, chlorite and sphene. With increasing temperature it is replaced by hornblende (recognized by the bluish-green absorption colours in the direction of the long crystallographic axis).

Actinolite also can form during late magmatic autohydrothermal alteration of augite and salite. By contrast, diopside is replaced by tremolite. These alterations tend to be fibrous to acicular and are referred to as uralite. Occasionally green hornblende can form during uralitization.

4.3.2 Green ('common') hornblende

Hastingsite series	$NaCa_2(Mg, Fe^{2+})_4Fe^{3+}[(OH)_2\|Al_2Si_6O_{22}]$	monoclinic–prismatic
Tschermakite series	$Ca_2(Mg, Fe)_3(Al, Fe^{3+})_2[(OH)_2\|Al_2Si_6O_{22}]$	
Barroisite series	$CaNa(Fe^{2+}, Mg)_3(Al, Fe^{3+})_2[(OH)_2\|AlSi_7O_{22}]$	

General features: the chemistry of the 'green' hornblende is complex. It forms the most important and common dark-coloured amphibole in magmatic rocks (e.g. in tonalite) and in metamorphic rocks (e.g. amphibolite). In the former case it is part of the hastingsite series and in the latter case it is part of the tschermakite series.

Thin-section characteristics

Form: tends to be subhedral to anhedral, short to long prismatic (Figs 147–150) or acicular to fibrous, rarely idiomorphic (specially in volcanic rocks); basal sections are hexagonal.

Cleavage: perfect on {110} with cleavage intersection angles of 124° and 56°. Sections subparallel to the c-axis show one parallel cleavage set (Fig. 151), which marks the main optical zone.

Twinning: single twins are common with twin lamellae on (100) (Fig. 144).

Colour: always strong green, varying between greenish-yellow and bluish-green. Strongly pleochroic, with the stronger colours appearing in orientations parallel to γ and the weaker ones

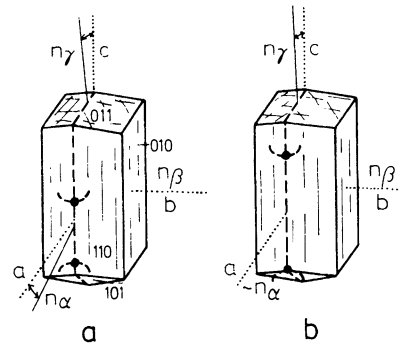

Fig. 147 Crystal form and optical characteristics of (a) hastingsite and (b) tschermakite.

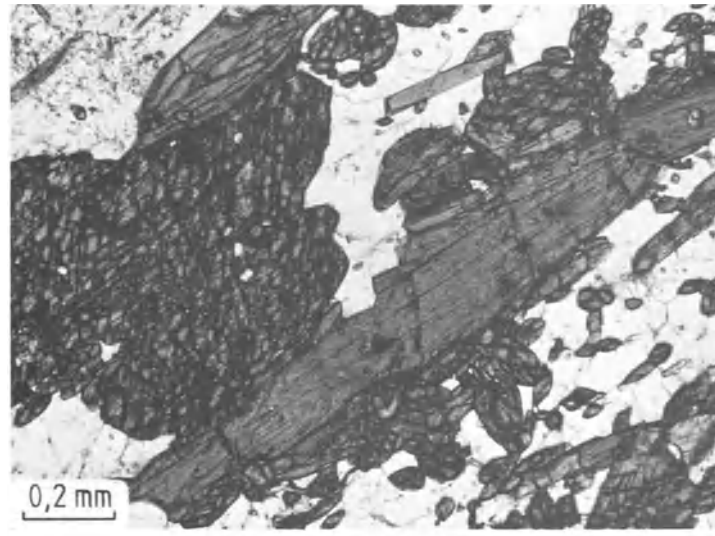

Fig. 148 Tschermakitic hornblende in basal and longitudinal sections. High relief and strong colour are characteristic. Amphibolite. Boulder from the Rhine near Kehl, Germany. Uncrossed polarizers.

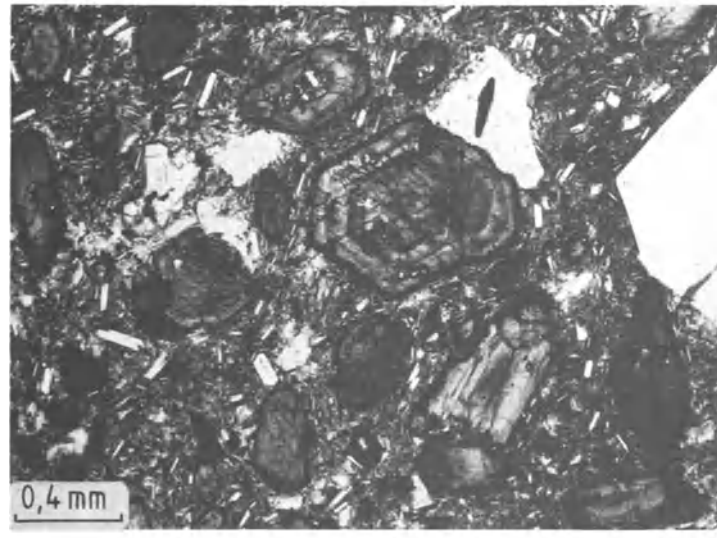

Fig. 149 Ti-rich hastingsitic hornblende with clear growth zoning and opacite alteration around the rims. Quartz andesite. Pitayó, east of Popayán, southern Colombia. Uncrossed polarizers.

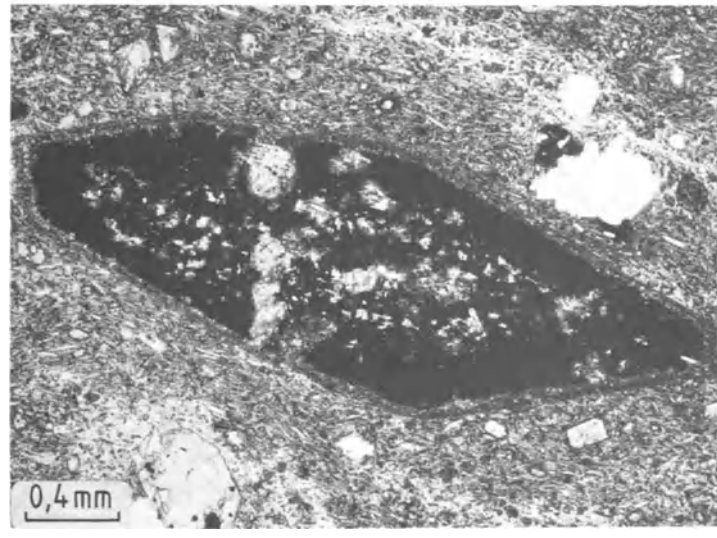

Fig. 150 Oxyhornblende replaced by opacite. Hexagonal outline of the original hornblende still clearly visible. Quartz andesite. Doña Juana volcanic complex, southern Colombia. Uncrossed polarizers.

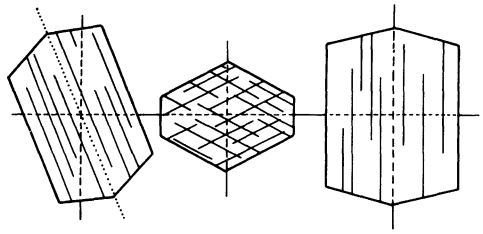

Fig. 151 Extinction in clinoamphiboles:
(a) Oblique extinction in the a–c plane.
(b) Symmetric extinction.
(c) Straight extinction in the b–c plane.

parallel to α; barroisite shows bluish-green colours.

Pleochroism
Hastingsite and tschermakite:
α: pale yellowish-green, pale bluish, yellow
β: greenish to olive-green, deep green, greenish-yellow
γ: olive-green to bluish-green, brownish-green.
Barroisite:
α: pale yellowish, pale greenish
β: yellowish-green to grey-green
γ: deep bluish-green, indigo blue, greenish-blue.

Refraction and birefringence:

	Hastingsite	Tschermakite and barroisite
n_α	= 1.646 – 1.700	1.640 – 1.673
n_β	= 1.658 – 1.719	1.659 – 1.690
n_γ	= 1.662 – 1.722	1.658 – 1.696
⊖Δ	= 0.016 – 0.022	0.018 – 0.023

In both hastingsite and tschermakite the medium-high refraction and birefringence (interference colours of the upper 1st and lower 2nd order) increase with increasing Fe-content; all these amphiboles are optically biaxial ⊖.

Optic axial angle: dependent on chemical composition; increasing axial angle with increasing Mg-content:
Hastingsite: $2V_\alpha = 34°–90°$
Tschermakite: $2V_\alpha = 65°–90°$
Barroisite: $2V_\alpha = 65°–90°$.

Character of elongation: (+), important diagnostic feature.

Extinction: oblique; basal sections show symmetric extinction.
Hastingsite: $\gamma \Lambda c = 14°–20°$ (Fig. 141)
Tschermakite: $\gamma \Lambda c = 15°–22°$ (Fig. 141)
Barroisite: $\gamma \Lambda c = 15°–22°$.

Special characteristics: pleochroic halos around radioactive inclusions.

Distinguishing features: in order to differentiate it from other members of the amphibole group, paragenesis is important; actinolite shows significantly paler absorption colours; clinopyroxene generally exhibits only weak pleochroism (exceptions: aegirine-augite, titanaugite), greater extinction angle and different cleavage characteristics; tourmaline has a columnar habit and straight extinction; and epidote is characterized by bright anomalous interference colours.

Alteration: rare in volcanic rocks, where green hornblende can be replaced by brown hornblende, due to oxidation of Fe^{2+} to Fe^{3+} (→ oxyhornblende). This process can be accompanied by a partial or complete opacitization (Part B, section 4.3.3). The onset of alteration into oxyhornblende is marked by a colour change from green to green-brown, which affects the crystal initially along fracture and cleavage surfaces. In plutonic rocks green hornblende can be replaced around the rim by biotite. Retrograde metamorphism in low-grade metamorphic rocks can lead to replacement of green hornblende by actinolite and finally into chlorite (next to epidote, quartz and calcite) or antigorite. During weathering green hornblende alters into an aggregate comprised of carbonate, limonite and quartz.

Occurrence: hastingsite occurs in magmatic rocks, particularly in intermediate plutonic rocks and dykes of granodiorite, tonalite, monzonite, quartz-diorite and diorite. It also can be present in gabbros (hornblende-gabbro) and granites. Green hornblende is uncommon in volcanic rocks (Fig. 149), where the 'brown' hornblende/oxyhornblende, which is rare in dyke rocks and siliceous plutonic rocks, predominates. The green tschermakite hornblende is very characteristic in amphibolite facies, found in amphibolite schists and amphibolites (Fig. 148). In high-grade metamorphic rocks (e.g. marbles, siliceous carbonates, etc.) green hornblende is rare and belongs to the pargasite series rather than the tschermakite group. The bluish barroisite is restricted to the lower grade metamorphic rocks (greenschist facies). In contact-metamorphosed rocks green tschermakite hornblende is typical in the hornblende-hornfels facies (e.g. amphibole-fels).

Paragenesis: in intermediate plutonic rocks together with oligoclase to andesine, microcline or orthoclase, quartz, biotite, sphene and pyroxene (early formed minerals during crystallization, often rimmed by hornblende which can be uralitized). In granites it occurs in the same

paragenesis as listed above with the addition of orthoclase. In regionally metamorphosed rocks it appears first in the upper greenschist facies, together with albite, epidote and almandine. In medium-grade rocks it appears together with oligoclase or andesine to labradorite, garnet and rutile. In high-grade rocks together with diopside, phlogopite and scapolite. In contact-metamorphic rocks green hornblende occurs together with plagioclase, diopside, biotite and quartz.

4.3.3 Brown hornblende

Oxyhornblende $NaCa_2Mg_2Fe^{3+}_3[O_2|Al_2Si_6O_{22}]$ monoclinic–prismatic
Kaersutite $NaCa_2(Mg, Fe^{2+})_4(Ti, Fe^{3+})[(OH)_2|Al_2Si_6O_{22}]$
Katophorite $Na_2Ca(Mg, Fe^{2+})_4(Fe^{3+}, Al)[(OH)_2|AlSi_7O_{22}]$

General features: oxyhornblende found in volcanic rocks is to a large extent former green oxidized hastingsite, with greatly changed optical characteristics due to heating to a minimum temperature of 800 °C. Apart from oxidation of Fe^{2+} to Fe^{3+}, $(OH)^-$ changes into O^{2-}. Titan-hornblende with >5% weight TiO_2 is referred to as kaersutite. Ti-poorer representatives are called katophorites.

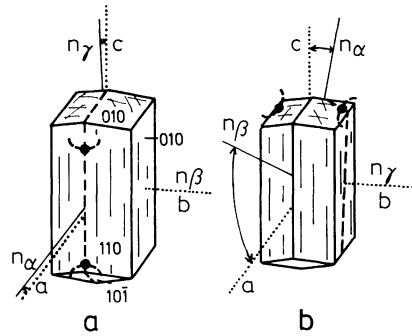

Fig. 152 Crystal form and optical characteristics of (a) kaersutite and (b) katophorite.

Thin-section characteristics

Form: euhedral to subhedral crystals with short to long prismatic habit, often with corroded margins (Fig. 152).

Cleavage: perfect on {110}.

Twinning: lamellar twinning is common on (100).

Colour: strong brown to reddish-brown and strongly pleochroic, with partly patchy colour distribution, due to uneven distribution of oxidization within one crystal. Kaersutite and katophorite have brownish colours, similar to biotite, showing strong pleochroism, often clearly zoned or with patchy or hourglass-like colour distribution. In katophorite γ the direction of maximum absorption is parallel to the b-axis (important diagnostic feature).

	Oxyhornblende	Kaersutite	Katophorite
α:	pale yellow, pale brown, yellowish-brown	pale yellowish-brown	pale yellowish-red, yellow-orange
β:	dark brown, red-brown	green-brown, red-brown	dark brown, red-brown, black
γ:	black-brown, dark brown, dark red-brown.	deep green-brown, chestnut-brown.	green-brown, deep red-brown.
Refraction and birefringence:			
n_α	= 1.650 – 1.702	1.669 – 1.696	1.639 – 1.681
n_β	= 1.683 – 1.769	1.683 – 1.725	1.658 – 1.688
n_γ	= 1.689 – 1.796	1.695 – 1.743	1.660 – 1.690
$\ominus\Delta$	= 0.039 – 0.094	0.026 – 0.047	0.021 – 0.009

The medium refraction and very high birefringence (interference colours of the medium 2nd order) vary, depending on the degree of oxidation. The interference colours tend to be masked by the strong crystal colours; optically biaxial ⊖.

Refraction and birefringence of kaersutite is similar to those of the 'common' hornblende; birefringence of kaersutite is low to medium high (interference colours of the 1st and 2nd order); optically biaxial ⊖.

Oxyhornblende	Kaersutite	Katophorite
Optic axial angle:		
$2V_\alpha = 56°–88°$ ($\approx 60°$)	$2V_\alpha = 74°–82°$ (commonly $\approx 80°$)	$2V_\alpha = 0°–57°$ (commonly $\approx 35°$)
Character of elongation:		
(+)	(+)	(–)

In dark-coloured crystals it is difficult to determine.

Extinction:
Extinction angle increases with increasing oxidation.

$\gamma \Lambda c = 0°–12°$	$\gamma \Lambda c = 3°–19°$	$\alpha \Lambda c = -8°–16°$

Special characteristics: zoning with brighter core and darker rim, or isomorphic multilayered colour change.

Distinguishing features: very high birefringence colours and the small extinction angle are diagnostic. Oxyhornblende has a much higher birefringence; the common green hornblende has a lower birefringence and shows brown-green to greenish absorption colours; aenigmatite has a larger extinction angle; katophorite shows the strongest absorption parallel to the b-axis which is at right angles to its crystal elongation direction (diagnostic feature to distinguish it from kaersutite.).

Alteration: pressure decrease in ascending magma leads to disequilibrium between the earlier formed oxyhornblende with the magma. The crystal is replaced by an aggregate of magnetite, hematite, Fe-poor clinopyroxene, etc. This process is called opacitization (Fig. 150) and it can also affect biotite, first around the margin and then progressively the whole crystal is replaced. Pressure decrease also leads to corroded crystal margins. Only in rapidly cooled lava flows and in ignimbrites opacitzation is absent or minimal. Weathering leads to formation of carbonate, limonite and quartz.

Occurrence: oxyhornblende predominantly occurs in intermediate to acidic volcanic rocks, such as biotite-hornblende dacites, quartz-latite andesites, ignimbrites and other pyroclastics.

Kaersutite occurs in basic plutonic and volcanic to subvolcanic rocks and dykes rich in sodium (alkali series) (e.g. essexite, theralite, tephrite, basanite, camptonite, monchiquite, etc.). It is very rare in alkali basalts, and therefore the term basaltic hornblende, summarizing Ti-poor amphiboles with 3–5% TiO_2, is considered here to be superfluous.

Katophorite can occur in Na-rich magmatic rocks (e.g. in nepheline syenite and in subvolcanic Na-shonkinites, such as phononephelinites of the Tertiary Katzenbuckel volcanic province in the southern Odenwald, Germany).

Paragenesis: oxyhornblende occurs with plagioclase, biotite, ortho- and clinopyroxene, magnetite and rock-glass.
Kaersutite occurs next to titanaugite, olivine, plagioclase and apatite. Katophorite occurs together with nepheline, sodium sanidine, aegirine-augite, Ti-biotite, arfvedsonite, olivine and apatite.

4.3.4 Glaucophane and crossite

$Na_2(Mg, Fe^{2+})_3(Al, Fe^{3+})_2[(OH)_2|Si_8O_{22}]$ monoclinic–prismatic

General features: characteristic alkali amphiboles of high-pressure metamorphic rocks.

Colour: blue to purple absorption colours, strongly pleochroic (Colour plate 10), zoned with colours increasing towards the rim:

Thin-section characteristics

Form: long prismatic to acicular along [001], bladed, rare needle-like to fibrous.

Glaucophane	Crossite
α: colourless to pale yellow-green	colourless to pale green
β: lilac to bluish-purple	deep blue
γ: ultramarine to sky-blue.	lilac to greyish-purple.

Refraction and birefringence:

n_α = 1.595 – 1.630	n_α = 1.630 – 1.665
n_β = 1.614 – 1.650	n_β = 1.650 – 1.670
n_γ = 1.620 – 1.652	n_γ = 1.652 – 1.680
$\ominus\Delta$ = 0.025 – 0.022	$\ominus\Delta$ = 0.020 – 0.008

The medium-high birefringence increases with increasing Fe^{3+} content, whereas the relatively low birefringence (interference colours of the 1st and 2nd orders) decreases; optically biaxial ⊖.

Optic axial angle: varies with chemical composition.
Glaucophane: $2V_\alpha = 0°–50°$
Crossite: $2V_\alpha = 0°–90°$.

Character of elongation: glaucophane (+); crossite (+) or (–).

Extinction angle: oblique.
Glaucophane: $\gamma \Lambda c = 5°–7°$ (Fig. 153)
Crossite: $\beta \Lambda c = 5°–9°$.

Distinguishing features: the strong absorption colours are diagnostic. Arfvedsonite occurs in different parageneses, has different bluish-green to grey-green or grey-blue colours and a negative elongation (can also be optically biaxial ⊕); dumortierite has straight extinction and a higher birefringence; tourmaline always has straight extinction parallel to its long axis and is optically ⊖ (if anomalously biaxial it has a small axial angle) and has a negative elongation.

Alteration: retrograde alteration into barroisite, actinolite or chlorite.

Occurrence: glaucophane and crossite occur in glaucophane schists, which tend to originate from Na-rich volcanic rocks. Also present in eclogites.

Paragenesis: with clinozoisite, zoisite, lawsonite, jadeite-rich pyroxenes, muscovite, almandine, pumpellyite, carbonate, rutile, retrograde epidote, actinolite, albite and chlorite (penninite). In eclogites together with garnet, omphacite, rutile and epidote.

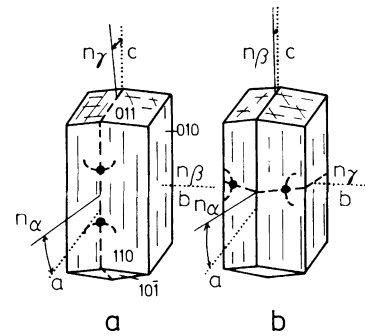

Fig. 153 Crystal form and optical characteristics of (a) glaucophane and (b) crossite.

4.3.5 Arfvedsonite and riebeckite

$Na_3(Mg, Fe^{2+})_4(Fe^{3+}, Al)[(OH)_2|Si_8O_{22}]$ monoclinic–prismatic

General features: characteristic Fe-rich alkali amphiboles of rare alkali-magmatic rocks.

Thin-section characteristics

Form: thick prismatic parallel to the c-axis, acicular, granular or bladed parallel to {010}; also poikilitic (sieve texture) (Fig. 154).

Cleavage: perfect amphibole cleavage on {110}.

Twinning: simple on (100).

Colour: blue to brownish-green and grey-blue absorption colours, showing strong pleochroism:

Arfvedsonite
α: blue-green, dark blue-green
β: pale bluish-green, grey-blue
γ: pale yellowish-green, dark green, greenish blue-grey.

Riebeckite
dark blue to green-blue
yellow-brown to pale yellow-green, dark blue.

Refraction and birefringence:

n_α	= 1.623 – 1.700
n_β	= 1.631 – 1.706
n_γ	= 1.635 – 1.710
⊕Δ	= 0.010 – 0.012

n_α	= 1.650 – 1.701
n_β	= 1.655 – 1.711
n_γ	= 1.670 – 1.717
⊕Δ	= 0.006 – 0.016

The medium-high refraction increases with increasing Fe^{2+}, whereas the relatively low birefringence (interference colours of the 1st order) decrease; optically biaxial ⊖ to ⊕.

Optic axial angle: dependent on the chemical composition.
$2V_\alpha$ = commonly 70°–80° (0°–100°)

$2V_\alpha$ = 40°–100°

Character of elongation:
(–)

(–)

Extinction: angle tends to be oblique
$\alpha \wedge c$ = –10° to –25°
$\beta \wedge c$ = 65°–80°

$\alpha \wedge c$ = 0°–30°

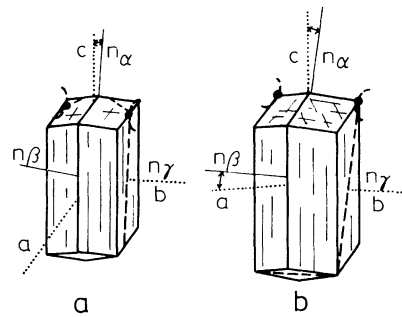

Fig. 154 Crystal form and optical characteristics of (a) arfvedsonite and (b) riebeckite.

Special characteristics: strongly anomalous interference colours are often masked by the strong colour of the crystal.

Distinguishing features: glaucophane occurs in different parageneses and is characterized by purple to violet absorption colours; tourmaline is characterized by minimum absorption colours parallel to the c-axis, whereas arfvedsonite shows a maximum in this orientation.

Alteration: none.

Occurrence: arfvedsonite occurs in nepheline-syenite, Na-syenite and related pegmatites; in volcanic pantellerite and comendite. Riebeckite occurs in Na-rich magmatic rocks, particularly in acidic plutonic rocks, less frequently in Na- and nepheline-syenite and related pegmatites; in volcanic pantellerite and comendite (alkali rhyolite to alkali trachyte).

Paragenesis: arfvedsonite occurs with riebeckite, aegirine, aegirine-augite, hastingsite, katophorite, alkali feldspar, respectively and anorthoclase (in volcanic rocks) and nepheline. Riebeckite occurs with arfvedsonite, aegirine, alkali feldspar and anorthoclase, respectively (in volcanic rocks), and quartz or nepheline.

4.4 Mica group

General features: this is a very important, widely distributed mineral group of monoclinic-prismatic (pseudo-hexagonal) flaky phyllosilicates. The white micas are comprised of muscovite, phengite, paragonite and glauconite and they belong to the dioctahedral representatives of the phyllosilicates (two of the three octahedral lattice spaces are occupied with trivalent cations). All other (dark) micas are trioctahedral (where all three octahedral positions are occupied by bivalent cations).

Thin-section characteristics

Form: flakes, plates (Fig. 155) on {001}, fine scales (sericite), prismatic parallel to the c-axis (in pegmatites), spherolitic (lepidolite) or fan-shaped (zinnwaldite).

Cleavage: perfect on (001). Sections perpendicular to {001} show parallel sets of cleavage (Fig. 155). Elastic bending due to mechanical stress, increasing stress and strain leads to plastic deformation and formation of kink bands (Fig. 158).

Twinning: twinning with [310] as twin axis, but not recognizable under the microscope.

Character of elongation: always (+).

Extinction: parallel to cleavage, almost straight $\beta\Lambda a$ and $\gamma\Lambda a$ respectively = 0.5°–2°. In the extinction position interference colours of the 1st order are visible, whereas with the vibration direction perpendicular to the c-axis n_β does not vary much (n_γ–n_β maximum 0.005).

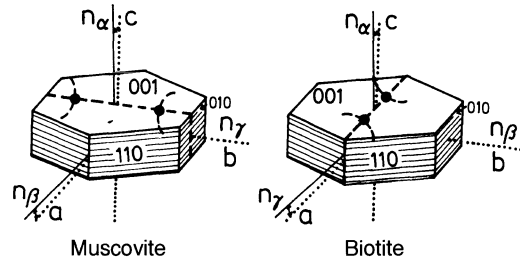

Fig. 155 Crystal form and optical characteristics of the phyllosilicates (e.g. mica).

4.4.1 Muscovite

$KAl_2[(OH, F)_2|AlSi_3O_{10}]$ monoclinic–prismatic

General features: this white mica occurs in acidic plutonic rocks and is absent in fresh volcanic rocks. A fine-grained scaly variety is common in low-grade metamorphic rocks (**sericite**). Phengite is also described as sericite and is very difficult to distinguish optically from muscovite.

Thin-section characteristics

Colour: colourless, rarely pale yellow, pale green or pale brown. Cr-rich muscovite is called fuchsite, which is rare and pleochroic: α pale greenish-blue, β yellowish, γ pale bluish-green.

Refraction and birefringence:

	Muscovite	Fuchsite
n_α	= 1.552 – 1.570	1.559 – 1.571
n_β	= 1.582 – 1.619	1.593 – 1.604
n_γ	= 1.588 – 1.624	1.595 – 1.612
$\ominus\Delta$	= 0.036 – 0.054	0.036 – 0.041

Medium-high refraction and high birefringence (bright, strong interference colours of the upper 2nd to lower 3rd orders) (Colour plate 11); sections parallel to the cleavage show very low interference colours of the 1st order, where there is little difference between rays vibrating perpendicular to the c-axis and n_β (n_γ–n_β maximum 0.005).

Optic axial angle: $2V_\alpha$ = 28°–47° (Fig. 156); can be measured in sections perpendicular to the c-axis (Part A, section 3.3.4).

Extinction: in sections perpendicular to the cleavage the extinction is straight or nearly straight: $\alpha\Lambda c$ = 0°–5°, $\beta\Lambda c$ = 1°–3°.

Special characteristics: occurs also as fine-grained scaly aggregates of sericite. Parallel intergrowth between biotite and muscovite can occur. Pale-yellow pleochroic haloes around zircon inclusions are rare occurrences.

Distinguishing features: sericite is distinguishable from other phyllosilicates only by X-ray

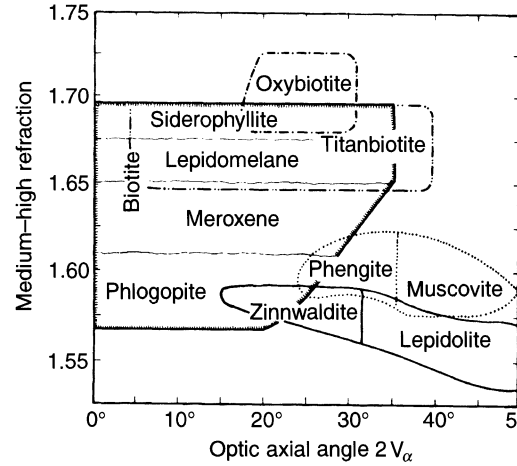

Fig. 156 Optic axial angle (2V) and medium-high refraction in the mica group.

methods; phengite is similar but has a smaller axial angle; chlorite and kaolinite have a much lower birefringence; lepidolite, talc, pyrophyllite and paragonite are difficult to distinguish from muscovite under the microscope.

Alteration: in higher-grade metamorphic rocks muscovite becomes unstable and is replaced by alkali feldspar-bearing assemblages. It is a fairly robust mineral when exposed to weathering; fine-grained aggregates can be altered to hydromuscovite and illite.

Occurrence: not too common in granites to granodiorites, never in volcanic rocks. Very common in pegmatites and pneumatolytically formed rocks. As sericite it occurs in numerous plutonic rocks and palaeovolcanic rocks (quartz-porphyry to porphyrite). In these rocks sericite formed as a hydric or pneumatolytic alteration mineral from feldspar (sericitization). In a similar way foids undergo alteration (leucite, nepheline). In sediments and sedimentary rocks muscovite occurs in many clastic rocks such as arkoses and greywackes. White micas weather into clay minerals which, with the addition of potassium during diagenesis, react to sericite and/or phengite. In low-grade metamorphic conditions sericite can become rock-forming (e.g. sericite phyllites, greenschist and quartzite). At medium-grade metamorphism sericite aggregates recrystallize and form mesoscopic muscovite flakes. Muscovite makes a major chemical contribution to the chemistry of mica schists and muscovite gneisses (Fig. 157). The sequence from phyllite → mica schist → muscovite gneiss marks progressive metamorphism. In eclogites and granulites muscovite occurs only as diaphthoritic newly formed mineral. In contact-metamorphosed rocks sericite occurs in the outer zones of the contact aureole in knotenschiefer; nearer to the contact white mica appears in the form of muscovite. The rare Cr-rich variety, fuchsite, is found in low-grade metamorphic schists (e.g. in the Zillertal Alps).

Paragenesis: in plutonic rocks together with quartz, microcline, orthoclase, plagioclase and biotite. In pegmatites it can appear together with phlogopite, lepidolite, tourmaline and topaz. In low-grade rocks sericite occurs together with albite, chlorite and quartz, and also paragonite; with increasing metamorphic-grade biotite, chloritoid and microcline join the assemblage. In medium-grade metamorphic-rocks muscovite is accompanied by biotite, albite, almandine, staurolite, kyanite, and also sillimanite. In contact aureoles sericite occurs next to quartz, albite and andalusite- or cordierite-blasts; muscovite is stable in the lower hornfels facies next to quartz, plagioclase, biotite and/or hornblende. Fuchsite occurs together with quartz, albite, chlorite, biotite and actinolite.

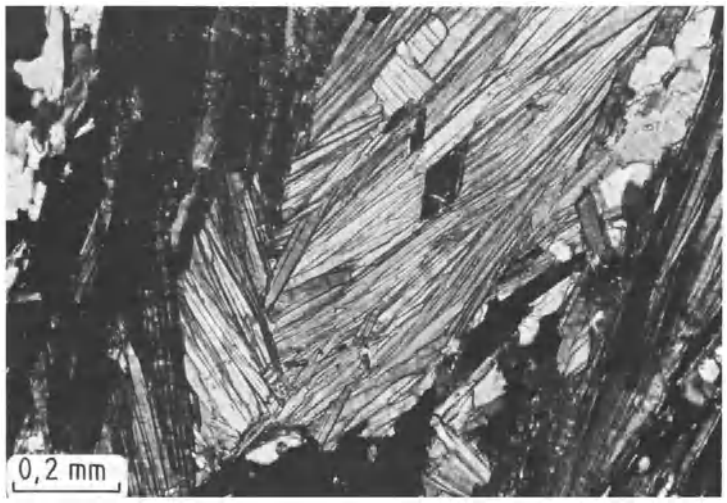

Fig. 157 Lepidoblastic muscovite in a mica schist. Muscovite schist. Gallivaggio, Splügen, southern rump, northern Italy. Crossed polars.

4.4.2 Phengite

$K(Mg, Fe)_{0.5}Al_{1.5}[(OH)_2|Al_{0.5}Si_{3.5}O_{10}]$ monoclinic–prismatic

General features: fine- to coarse-grained white mica in medium- to high-grade metamorphic rocks.

Thin-section characteristics

Colour: colourless, rarely pale green (Fe^{3+}-rich).

Refraction and birefringence:

	Fe-free	Fe-rich
n_α	= 1.547	– 1.571
n_β	= 1.584	– 1.610
n_γ	= 1.587	– 1.612
$\ominus\Delta$	= 0.040	– 0.041

Medium-high refraction and high birefringence (interference colours of the 2nd and 3rd orders); optically biaxial ⊖.

Optic axial angle: optically it cannot be differentiated from sericite muscovite (chemical diagnosis necessary). Chlorite and kaolinite both have lower refractive indices.

Occurrence: in glaucophane schists, eclogites, gneisses and phyllites.

Paragenesis: glaucophane, clinopyroxene, lawsonite, paragonite as well as the parageneses listed under muscovites (Part B, section 4.4.1).

4.4.3 Lithionite series

4.4.3.1 Lepidolite

$KLi_{1.5}Al_{1.5}[(F, OH)_2|AlSi_3O_{10}]$ monoclinic–prismatic

General features: rare mica, which occurs in Li-rich pegmatites.

Thin-section characteristics

Colour: colourless; in slightly thick thin sections a weak pleochroism can be observed with pale-pink to pale-purple colours.

Refraction and birefringence:

n_α	= 1.524 – 1.548
n_β	= 1.543 – 1.587
n_γ	= 1.545 – 1.588
$\ominus\Delta$	= 0.018 – 0.038

Low refraction and medium-high birefringence (bright interference colours of the 2nd order), optically biaxial ⊖.

Optic axial angle: $2V_\alpha = 23°–58°$ (Fig. 156), rarely 0°.

Special characteristics: commonly intergrown with muscovite.

Distinguishing features: muscovite has a higher refraction and birefringence.

Occurrence: in Li-rich granitic pegmatites (e.g. Erzgebirge, Germany); in greisen.

Paragenesis: with quartz, topaz, tourmaline, spodumene, amblygonite, beryl and cassiterite.

4.4.3.2 Zinnwaldite

$KLiFe^{2+}Al[(F, OH)_2|AlSi_3O_{10}]$ monoclinic–prismatic

General features: rare mica, occurs in fluorine-bearing pneumatolytic rocks.

Thin-section characteristics

Colour: colourless, can be pale-coloured with a weak pleochroism (brownish-grey).

Refraction and birefringence:

n_α	= 1.535 – 1.558
n_β	= 1.570 – 1.589
n_γ	= 1.572 – 1.590
$\ominus\Delta$	= ~0.035

Low refraction and medium-high birefringence (bright interference colours of the 2nd order); optically biaxial ⊖ (Fig. 155).

Optic axial angle: $2V_\alpha = 15°–32°$ (Fig. 156).

Special characteristics: commonly an oriented intergrowth with muscovite or lepidolite.

Distinguishing features: lepidolite has a lower refraction and muscovite a higher refraction and birefringence.

Alteration: none.

Occurrence: as newly formed crystals replacing pneumatolytically affected biotite and muscovite in greisen and granite pegmatites.

Paragenesis: with muscovite, lepidolite, quartz, topaz, cassiterite and wolframite.

4.4.4 Biotite series

Phlogopite $KMg_3[(OH)_2|AlSi_3O_{10}]$ monoclinic–prismatic
Biotite s.s. $K(Mg, Fe^{2+})_3[(OH)_2|AlSi_3O_{10}]$

General features: the biotite series is comprised of the following dark mica representatives, which have a diadochic exchange between Mg and Fe^{2+}:

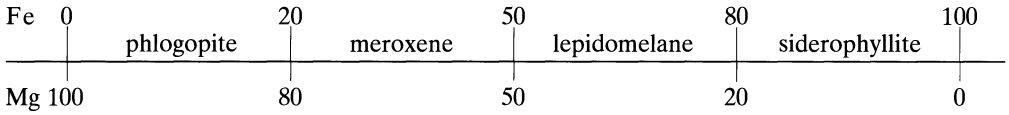

The term **biotite s.s.** is used for the meroxene to siderophyllite members.

4.4.4.1 Phlogopite

Thin-section characteristics

Colour: dependent on the Fe-content, colourless to yellowish, greenish to pale brown, rarely pink; in sections parallel to (001) almost no pleochroism; in sections oriented oblique or perpendicular to (001) absorption is very strong: α, colourless, pale yellow, pale orange, pale pink; β ≈ γ, brownish-yellow, leather-brown, reddish-orange, reddish-brown, pale red-brown.

Refraction and birefringence:

n_α	= 1.522 – 1.568
n_β	= 1.548 – 1.609
n_γ	= 1.549 – 1.613
⊖Δ	= 0.027 – 0.045

Relatively low refraction and high birefringence (bright interference colours of the 2nd and 3rd orders; basal sections show a very low birefringence: blackish-grey interference colours of the 1st order); optically biaxial ⊖.

Optic axial angle: $2V_\alpha = 2°–8°$ (rarely up to 15°; Fig. 156); in very thin sections nearly optically uniaxial ⊖.

Special characteristics: zoning is rare with a greenish core and paler or darker coloured edges; pleochroic haloes around radioactive inclusions, similar to biotite (Fig. 159).

Distinguishing features: it differs from biotite by its paler colour; and from muscovite by its smaller axial angle.

Alteration: none.

Occurrence: in mafic and ultramafic plutonic rocks (e.g. mica-peridotite; Fig. 158), kimberlites, carbonatites and foids. In contact-metamorphosed siliceous carbonates and marbles.

Paragenesis: with olivine, diopside, calcite, pyrope (in kimberlite) or olivine, melilite, leucite, nepheline (in silica-undersaturated volcanic rocks) or calcite, tremolite, diopside, forsterite (in siliceous carbonates) or calcite, apatite, coppite (in carbonatites).

Fig. 158 Tectonically deformed phlogopite with clearly developed kink bands and undulatory extinction, next to deformed olivine. Phlogopite peridotite. Finero, Ivrea area, northern Italy. Crossed polars.

Fig. 159 Intensively brown-coloured pleochroic biotite with good basal cleavage and pleochroic haloes surrounding zircon inclusions. Cordierite sillimanite gneiss. Erratic boulder, Baltic Sea coastline, near Kiel. Uncrossed polarizers.

4.4.4.2 Biotite s.s.

Thin-section characteristics

Colour: strong brown, yellow-brown, red-brown, olive-green or green (in low-grade metamorphic rocks); strongly pleochroic, which is particularly well developed in sections perpendicular or oblique to (001) (Colour plate 12); parallel to (001) there is hardly any absorption.

α: yellow, leather-coloured, pale brown, pale greenish.

β: reddish-brown, greenish-brown, bluish-green, dark brown, black.

γ: reddish-brown, yellow-brown, dark brown, green, black.

Refraction and birefringence:

	Meroxene		Lepidomelane		Siderophyllite
n_α =	1.571	–	1.598	–	1.616
n_β =	1.609	–	1.651	–	1.696
n_γ =	1.610	–	1.652	–	1.697
$\ominus\Delta$ =	0.039	–	0.054	–	0.081

Medium-high refraction and high birefringence. Bright interference colours of the 3rd and 4th order are generally not recognizable, because of the strong mineral colour; optically biaxial ⊖, sometimes nearly uniaxial ⊖.

Optic axial angle: $2V_\alpha$ = 0°–35° (Fig. 156) dependent on the Fe-content; the axial angle can be small, so that in basal sections the isogyre cross suggests uniaxial optical behaviour.

Special characteristics: in volcanic rocks resorbed margins are common or opacitic rims (black, opaque rim). Often rich in inclusions (apatite, quartz, rutile, hematite, tourmaline, etc.). In plutonic rocks it can occur intergrown with muscovite; pleochroic haloes around radioactive inclusions are common (zircon, monacite, sphene, etc.). Tectonically strained crystals can be bent or kinked (kink-bands).

Distinguishing features: brown hornblende in longitudinal sections shows oblique extinction (oxyhornblende ≈ 0°); brown tourmaline shows the maximum absorption colours perpendicular to the elongation direction, whereas biotite has them parallel; phlogopite is less strongly coloured; green biotite has higher birefringence than chlorite. Can be confused with stilpnomelane, which, however, has a golden-coloured pleochroism.

Alteration: in volcanic rocks biotite can be affected by oxidation (→ oxybiotite) and water loss; rapidly decreasing vapour pressure leads to opacitization: biotite (and also syngenetic hornblende) is replaced by a fine-grained aggregate of magnetite, haematite, spinel and pyroxene during this process. The biotite is first affected around its edges (black opaque rims), and eventually the whole crystal is replaced. Exsolution of titanium in biotite leads to inclusions of fine needles of rutile (sagenite, Fig. 71). Diaphthoritic alteration of biotite into chlorite (Fig. 160), also epidote, carbonate and quartz, etc. During weathering biotite is bleached (hydrobiotite) and weathers into an aggregate of carbonate, limonite and quartz.

Occurrence: biotite occurs in plutonic rocks, dykes and in volcanic rocks. Meroxene is found in basaltic rocks (e.g. gabbro, norite and lamprophyre). Lepidomelane is the most common biotite found in intermediate and acidic magmatic rocks. The dark-green siderophyllite occurs in nepheline syenite and related pegmatites. In regionally metamorphosed areas biotite (lepidomelane) occurs in medium greenschist-facies to upper amphibolite-facies grade metapelitic rocks. In contact aureoles of up to hornfels-facies grade.

Paragenesis: in magmatic rocks with brown hornblende, plagioclase, orthoclase, quartz, augitic pyroxene and hypersthene (intermediate to acidic volcanic rocks); plagioclase, quartz, green hornblende, sphene, with or without muscovite (granite). In metamorphic rocks with quartz, albite, epidote and chlorite (epidote-chlorite schist); quartz, muscovite, almandine, staurolite and kyanite (mica schist); plagioclase, quartz and muscovite (gneiss).

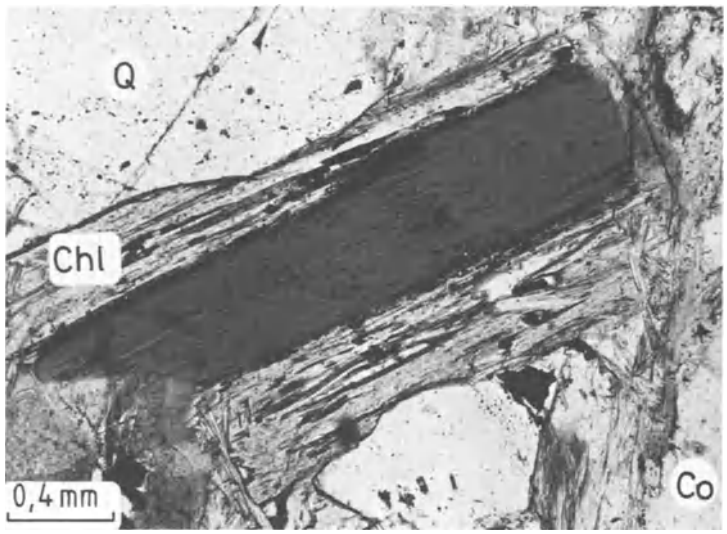

Fig. 160 Chloritized biotite, together with quartz and others. Cordierite sillimanite gneiss. Erratic boulder, Baltic Sea coastline, near Kiel. Uncrossed polarizers.

4.4.5 Oxybiotite

$KMgFe^{3+}_2[O_2|AlSi_3O_{10}]$ monoclinic–prismatic

General features: oxybiotite is formed from biotite by oxidation of Fe^{2+} to Fe^{3+}, which is common in volcanic rocks. As in oxyhornblende, the OH group is replaced by oxygen.

Thin-section characteristics

Colour: intensive brown to red-brown, strongly pleochroic; in sections parallel to (001) almost no pleochroism:
α: yellow-brown to reddish-brown
β ≈ γ: brown-red to dark brown-red.

Refraction and birefringence:

n_α	= 1.600 – 1.610
n_β	= 1.677 – 1.722
n_γ	= 1.680 – 1.730
$\ominus\Delta$	= 0.080 – 0.120

Medium-high refraction and very high birefringence. The very strong interference colours of the 4th and 5th orders can be masked by the strong colour; optically biaxial ⊖.

Optic axial angle: $2V_\alpha = 20°–30°$ (Fig. 156), which is much larger than in biotite.

Special characteristics: opacite rims; pleochroic haloes around radioactive inclusions.

Distinguishing features: distinguished from biotite by its higher refraction, birefringence, a larger axial angle and strong colour; it differs from titanbiotite by its higher birefringence.

Alteration: replaced by opacite, which is a fine-grained aggregate of magnetite, hematite, spinel and pyroxene. Weathering leads to alteration of the iron component into hematite and/or limonite.

Occurrence: as intratelluric blasts in intermediary volcanic rocks, rich in Fe-rich biotite.

Paragenesis: with oxyhornblende, clino- and orthopyroxene, plagioclase, sanidine and sodium-sanidine respectively (in old rocks, orthoclase), and quartz.

4.4.6 Titanbiotite

$K(Mg, Fe^{2+}, Ti)_3[(O, OH, F)_2|AlSi_3O_{10}]$ monoclinic–prismatic

General features: rare biotite with a high TiO_2 content (7–12.5%), which has more or less the same optical characteristics as biotite.

Thin-section characteristics

Colour: differs from biotite by its reddish colour and strong pleochroism; in sections parallel to (001) the pleochroism is very weak.
α: yellow-orange to pale yellow
β: orange to brown-orange
γ: brown-red to deep red-brown.

Refraction and birefringence:

n_α	= 1.599 – 1.655
n_β	= 1.642 – 1.692
n_γ	= 1.643 – 1.695
$\ominus\Delta$	= 0.044 – 0.040

Medium-high refraction and high birefringence; strong interference colours of the 2nd and 3rd orders are masked by its strong colour; optically biaxial ⊖.

Optic axial angle: $2V_\alpha = 5°–38°$ (Fig. 156).

Special characteristics: radioactive inclusions surrounded by haloes.

Distinguishing features: biotite is not as red-coloured as oxybiotite and has a higher refraction and birefringence.

Alteration: none.

Occurrence: in Na-rich (alkaline) magmatic rocks with a high TiO_2 content (e.g. subvolcanic Na-shonkinite of the Katzenbuckel/Odenwald, Germany; Fig. 161).

Paragenesis: with nepheline, Na-sanidine, kaersutite (titanhornblende), nosean, aegirine-augite and apatite.

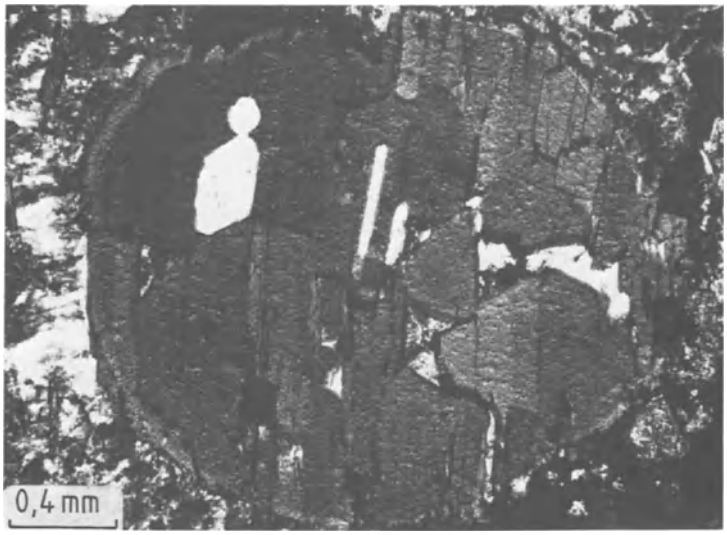

Fig. 161 Titanbiotite with a clear 'bird's-eye' structure and strong red-brown colour. Intratelluric blasts in Nashonkinite. Katzenbuckel/Odenwald, Germany. Uncrossed polarizers.

4.5 Stilpnomelane

Complex H_2O-bearing phyllosilicate monoclinic and triclinic

Thin-section characteristics

Form: flaky, radiating and brush-like acicular.

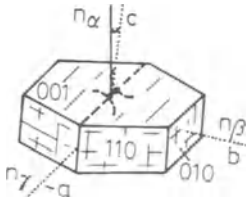

Fig. 162 Crystal form and optical characteristics of stilpnomelane.

Cleavage: perfect on (001), sometimes parting on (010) (Fig. 162).

Colour: yellowish, greenish and brownish with a strong pleochroism:

α: pale yellow, gold-yellow, pale brown

β ≈ γ: deep brown, deep red-brown, black-brown, chestnut brown, deep yellow-brown and dark green respectively (ferro-stilpnomelane).

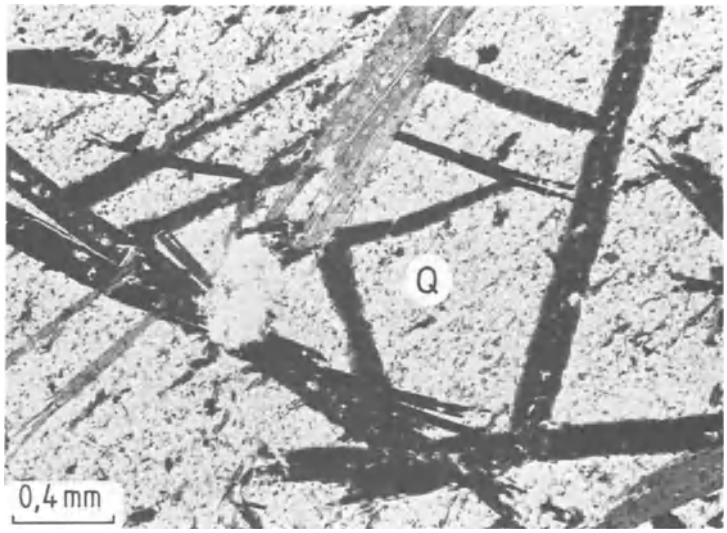

Fig. 163 Lath-shaped stilpnomelane with a strong biotite-like pleochroism. Stilpnomelane quartzite. Gössl, eastern Tirol, Austria. Uncrossed polarizers.

Refraction and birefringence:

n_α	= 1.543 – 1.634
n_β	= 1.576 – 1.745
n_γ	= 1.576 – 1.745
$\ominus\Delta$	= 0.033 – 0.111

Medium-high refraction and birefringence. Interference colours vary between the 2nd-order white of higher orders. In basal sections isotropic (Δ = 0.000); optically biaxial $\ominus$. Varying optical characteristics dependent on different degrees of oxidation of iron: two major varieties are distinguished, ferro- and ferri-stilpnomelane.

Optic axial angle: $2V_\alpha = 0°$, pseudo-uniaxial.

Character of elongation: (+).

Extinction: tends to be straight $\gamma\Lambda a = 0°$.

Distinguishing features: intergrown with biotite. Biotite has a rougher surface with a mottled texture ('bird's-eye' structure), has a different colour and a much better cleavage on (001) (Fig. 163).

Alteration: none.

Occurrence: very common and often confused with biotite; in low-grade metamorphic rocks (stilpnomelane-schist, phyllites, calc-phyllite and quartzite). Also in blueschist-facies metamorphic rocks and in silicate-rich iron-ore deposits.

Paragenesis: with quartz, sericite, chlorite and calcite. In blueschists next to glaucophane, garnet and sphene. Together with talc, phengite or chloritoid in high-pressure parageneses in metapelites.

4.6 Glauconite and celadonite

$(K, Ca, Na)_{0.8}(Fe^{3+}, Al, Mg, Fe^{2+})_2[(OH)_2|Si_{3.7}Al_{0.3}O_{10}]$ monoclinic–prismatic

General features: mica-like dioctahedral phyllosilicate. Glauconite is a synsedimentary to diagenetic mineral in marine sediments; celadonite is a Fe^{3+}-rich glauconite, restricted to basaltic volcanics.

Thin-section characteristics

Form: rounded to elliptically shaped aggregates (Colour plate 13), fine-grained to fine-grained sheaths and fibrous radiating aggregates. Forms pseudomorphs after olivine or pyroxene (celadonite) with preferred orientation.

Cleavage: good on (001), but difficult to recognize (Fig. 164).

Colour: green, yellow-green, olive-green and bluish-green with a clear pleochroism.

α: dark blue-green, pale yellow-green, greenish-yellow

$\beta \approx \gamma$: brownish-yellow, dark olive-green, blue-green.

Refraction and birefringence:

n_α	= 1.592 – 1.612
n_β	= 1.613 – 1.643
n_γ	= 1.614 – 1.644
$\oplus\Delta$	= 0.022 – 0.032

Medium-high refraction and birefringence (increases with increasing Fe^{3+} content); bright interference colours of the 2nd order are masked by the strong crystal colours; optically biaxial $\ominus$.

Optic axial angle: $2V_\alpha = 0°–20°$ (to 30°).

Character of elongation: (+).

Extinction: oblique, $\gamma\Lambda a = 2°–3°$.

Special characteristics: in very fine-grained aggregates pleochroism is not visible.

Distinguishing features: ortho- and leptochlorite have a lower birefringence, and green biotite a much higher birefringence.

Alteration: prone to weathering with new formation of limonite.

Occurrence: glauconite occurs in green sands and sandstones, also in carbonates and marls. Celadonite can fill cavities and fractures in basaltic volcanic rocks (basalt, diabases, spilite) as well as forming pseudomorphs after olivine and pyroxene. Celadonite is also present in zeolite-facies rocks.

Paragenesis: glauconite with quartz, calcite and pyrite. Celadonite with chlorite, chrysotile, saponite, carbonate and heulandite, laumontite, prehnite and montmorillonite respectively (zeolite facies).

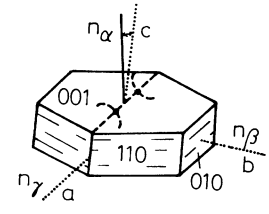

Fig. 164 Crystal form and optical characteristics of glauconite.

4.7 Talc

$Mg_3[(OH)_2|Si_4O_{10}]$ monoclinic-prismatic or triclinic

General features: layer-silicate; not very common forms in Mg-rich rocks.

Thin-section characteristics

Form: fibrous, scaly or dense, randomly oriented or subparallel to radiating aggregates (Fig. 166).

Cleavage: perfect on (001), nonelastic bending (Fig. 165).

Colour: colourless.

Refraction and birefringence:

n_α	= 1.539 – 1.550
n_β	= 1.589 – 1.594
n_γ	= 1.589 – 1.596
$\ominus\Delta$	= 0.050 – 0.046

Relatively low refraction and medium-high birefringence (strong interference colours of the upper 3rd order, similar to muscovite; basal section shows grey-white interference colours of the 1st order); optically biaxial ⊖.

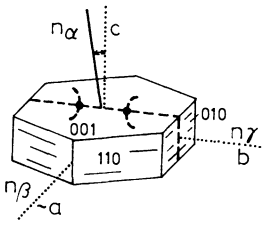

Fig. 165 Crystal form and optical characteristics of talc.

Optical axial angle: $2V_\alpha = 0°–30°$.

Character of elongation: (+).

Extinction: straight.

Distinguishing features: from pyrophyllite and sericite by chemical or X-ray analyses; muscovite has a higher axial angle; brucite is optically ⊕ with anomalous interference colours; gibbsite is optically biaxial ⊕ and has oblique extinction.

Alteration: none.

Occurrence: in low-grade metamorphic rocks, found in talcschists often together with serpentine. Pure talc rock is referred to as talcfels, formed by hydrothermal interaction with dolomite or mafic rocks, particularly those rich in olivine and enstatite. In metapelites the presence of talc is an indicator of high-pressure conditions.

Paragenesis: in greenschist facies with tremolite, clinochlore, quartz or antigorite, tremolite or magnesite to dolomite or actinolite, clinochlore, quartz or antigorite and actinolite. In metapelitic high-pressure assemblages with phengite, kyanite, chloritoid, garnet, chlorite and stilpnomelane.

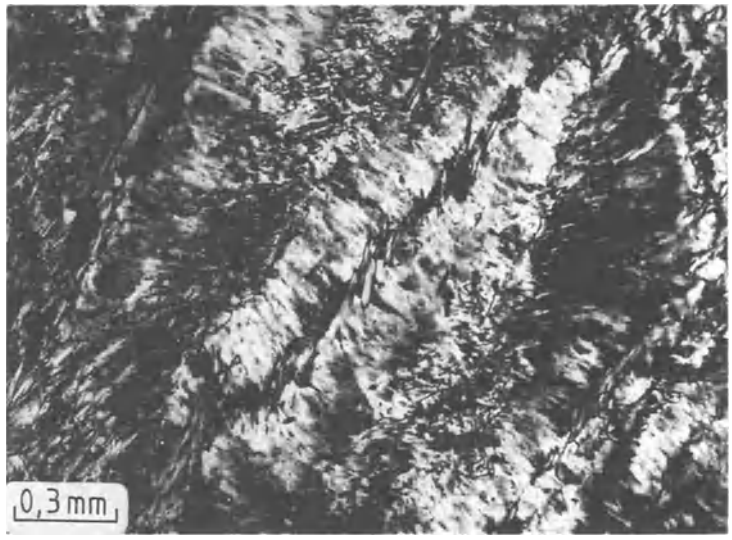

Fig. 166 Talc in talcfels. Göpfersgrün, Fichtelgebirge, Germany. Crossed polars.

4.8 Chlorite group

General features: very important rock-forming minerals; subdivision according to the old convention into $MgFe^{2+}$-chlorites (orthochlorite) and $MgFe^{2+}$ Fe^{3+}-chlorites (leptochlorite). The polarizing microscope cannot differentiate between these two groups.

4.8.1 Orthochlorite

$(Mg, Fe^{2+}, Al)_6[(OH)_8|AlSi_3O_{10}]$ monoclinic–prismatic

General features: in this general group the following trioctahedral Fe-free 14 Å-normal chlorites are summarized and can be distinguished under a polarization microscope (Fig. 167):
Mg-chlorite (0–20 mol% Fe; equivalent to the penninite-clinochlore-grochauite series).
Mg Fe^{2+}-chlorite (20–40 mol% Fe; equivalent to Mg-diabantite–Mg-pycnochlorite–Mg-rhipidolite series).
Fe^{2+}Mg-chlorite (40–60% Fe; equivalent to Fe-diabantite–Fe-pycnochlorite–Fe-rhipidolite series).

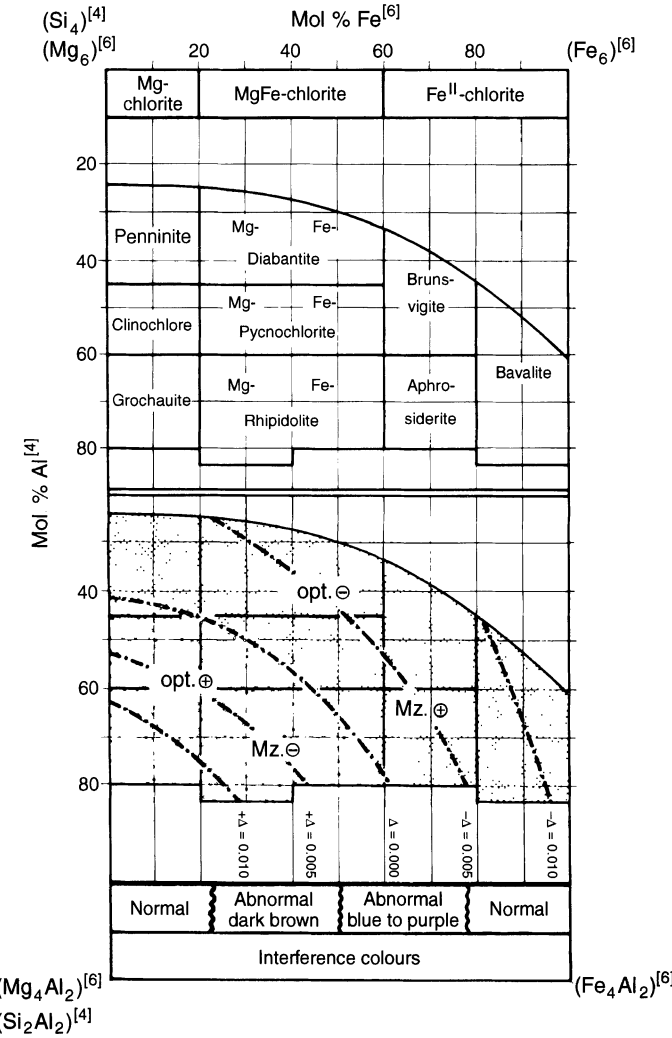

Fig. 167 Nomenclature and optical characteristics of orthochlorites.

Fe^{2+}-chlorite (60–100 mol% Fe; equivalent to brunsvigite–aphrosiderite–bavalite series).

Thin-section characteristics

Form: thin to thick {001} plates, flaky, radiating, scaly to fibrous, dense to randomly oriented, rare tubular rosettes ($MgFe^{2+}$-chlorite) or layered (Fe^{2+}-chlorite) aggregates; generally anhedral, forming secondary alterations, particularly after biotite; thin platy to fibrous, fine-grained with inclusions of opaque minerals. Can be deformed and kinked.

Cleavage: perfect on (001).

Twinning: lamellar after the penninite-twinning law (001) and after the mica-law [310], rarely developed in penninite and clinochlore.

Colour: colourless to pale green with a weak pleochroism; colour intensity increases with increasing Fe^{2+} content:
Mg-chlorite: colourless to pale yellowish-green or blue-green.
$MgFe^{2+}$- and $Fe^{2+}Mg$-chlorite: pale blue-green.
Fe^{2+}-chlorite: dark olive-green or dark brown-green to pale yellow or pale brown.
Pleochroism in general is weaker than in biotite and hornblende.

Refraction and birefringence:

Mg-chlorite	$MgFe^{2+}$- and $Fe^{2+}Mg$-chlorite
n_α = 1.562 – 1.594	n_α = 1.589 – 1.605
n_β = 1.565 – 1.594	n_β = 1.595 – 1.608
n_γ = 1.565 – 1.606	n_γ = 1.595 – 1.615
$\oplus\ominus\Delta$ = 0.003 – 0.012	$\oplus\ominus\Delta$ = 0.002 – 0.010

Fe^{2+}-chlorite
n_α = 1.632 – 1.665
n_β = 1.638 – 1.676
n_γ = 1.638 – 1.675
$\ominus\Delta$ = 0.004 – 0.010

Medium-high refraction; noticeably lower birefringence with anomalous interference colours (aspecial feature); optically biaxial ⊕ or ⊖.

Optic axial angle: not a very good diagnostic feature; can appear pseudo-uniaxial, dependent on chemical composition (Fig. 168).

Mg-chlorite	$2V_\alpha$ = 0° – 5° (penninite)
	$2V_\gamma$ = 0° – 30° (clinochlore)
$MgFe^{2+}$- and $Fe^{2+}Mg$-chlorite	$2V_\alpha$ = 0° – 10°
	$2V_\gamma$ = 0° – 40°
Fe^{2+}-chlorite	$2V_\alpha$ = 0° – 30°

Character of elongation: (+) or (–), always opposite to the optical sign, which is very helpful for determining the optical character of very small crystals.

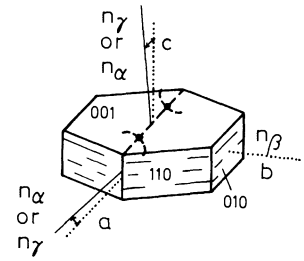

Fig. 168 Crystal form and optical characteristics of chlorite.

Extinction: nearly straight (γ or $\alpha \wedge a \approx 0°$); the extinction angle viewed perpendicular to the cleavage plane (001) is always 0° (rarely 3°–7° in clinochlore).

Special characteristics: parallel intergrowth with biotite or phlogopite is common; pleochroic haloes around radioactive minerals; in Fe-rich Mg-chlorites strong colour zonation and isomorphic layering is typical. The anomalous interference colours characteristic for various chlorites are:

Mg-chlorite:	optically ⊖, anomalous interference colours (penninite, as well as diabantite and Al-poor pycnochlorite); optically ⊕, normal interference colours (grochauite; 20 mol% Fe^{2+}).
$MgFe^{2+}$-chlorite:	optically ⊕, anomalous leather-brown interference colours (clinochlore and Al-rich pycnochlorite as well as rhipidolite with <50% Fe^{2+}; 20–50 mol% Fe^{2+}).
$Fe^{2+}Mg$-chlorite:	optically ⊖, anomalous blue interference colours (rhipidolite > 50 mol% Fe^{2+} and aphrosiderite; 50–80 mol% Fe^{2+}).
Fe^{2+}-chlorite:	optically ⊖, normal, rare abnormal blue-grey interference colours (bavalite; 80–100 mol% Fe^{2+}).

Bent, tubular chlorite aggregates are called 'helminth'.

Distinguishing features: all other similar phyllosilicates have a higher birefringence and normal interference colours; antigorite has a similar pale colour and weak pleochroism as Mg-chlorite, but it has a lower birefringence; green biotite, glauconite and celadonite, which can be

similar to each other in colour and pleochroism, all have a higher birefringence. The leptochlorites can be distinguished clearly from the orthochlorites only by X-ray techniques.

Alteration: fairly robust to weathering; alteration into clay minerals, Mg-Fe-carbonate, limonite and SiO_2. During progressive metamorphism and addition of potassium, alteration to biotite and/or hornblende and in blueschist facies into glaucophane and epidote respectively.

Occurrence: orthochlorite is an important rock-forming mineral in regional greenschist-facies metamorphosed rocks (Figs 169, 170), e.g. in chlorite schist, phyllite, chlorite-actinolite schist, quartzite and also in rocks of lower contact metamorphism (albite-epidote-hornfels facies). In higher-grade metamorphic rocks it appears only as a diaphthoritic secondary mineral, altering biotite, green hornblende, garnet, cordierite and forms pseudomorphs (chloritization). Occurs as an autohydrothermal mineral in different magmatic rocks in cavities and fissures; as an alteration mineral of mafic minerals (chloritization), e.g. in gabbro, diabase, spilite; and also as a fine-grained aggregate in fractures together with clinozoisite and epidote, actinolitic hornblende, quartz and carbonate (pycnochlorite to rhipidolite). Mg-rich chlorite (penninite) is rare and can form pseudomorphs after biotite in acidic palaeorhyolites (quartz-porphyry) and in granitic to granodioritic rocks. The Cr-bearing, slightly pink chlorite can form as primary chlorite in ultrabasic (peridotite, lherzolite) rocks.

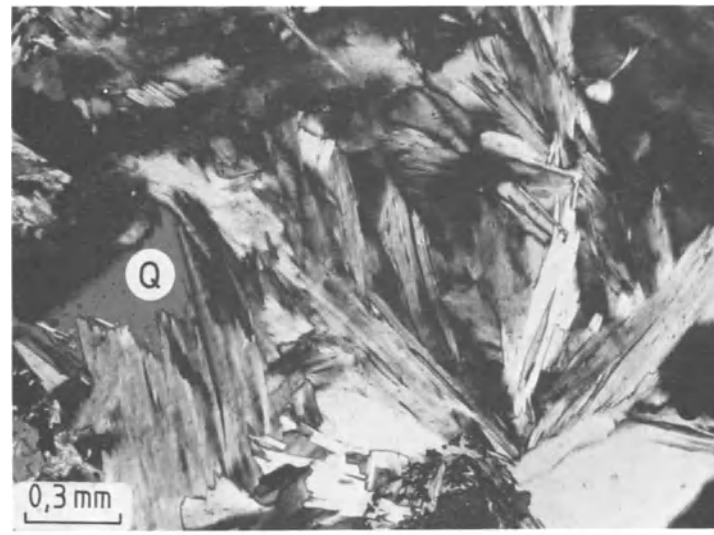

Fig. 169 Scaly orthochlorite. Quartz-albite-chlorite schist. Zöptau, Moravia, CR. Crossed polars.

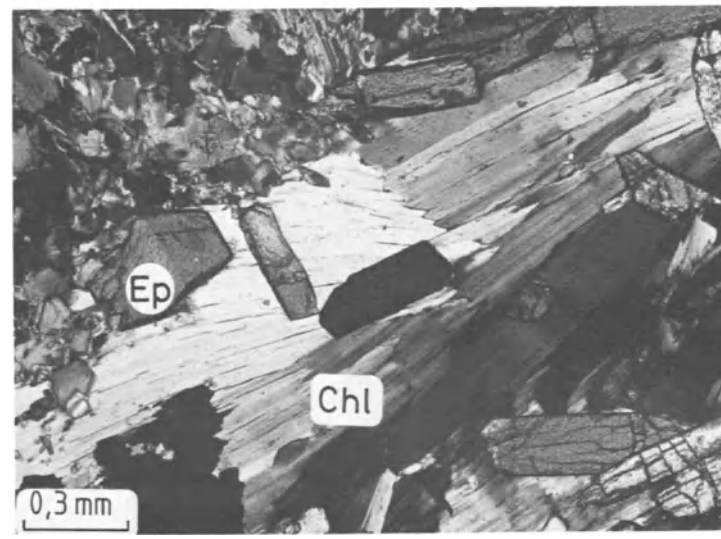

Fig. 170 Sheath-like orthochlorite with perfect cleavage on (001), together with epidote and others. Greenschist. Jambalo, north of Popayán, central Cordillera, southern Colombia. Crossed polars.

Chlorite in cavities in basalts tends to be $MgFe^{2+}$-chlorite of the diabantite-pycnochlorite series. Chlorites which form part of the groundmass in diabase and spilites also belong to this series.

Paragenesis: with albite, sericite, biotite, quartz and epidote (in phyllites) or albite, epidote, zoisite, actinolite, stilpnomelane, quartz, talc, tremolite and magnesite (in chloriteschist). In blueschists together with actinolite, albite, glaucophane, epidote, with or without lawsonite and pumpellyite. $MgFe^{2+}$-chlorite (diabantite) forms as an alteration mineral in basic volcanic rocks which contain biotite, pyroxene, amphibole as well as delessite (leptochlorite).

4.8.2 Leptochlorite

$(Mg, Fe^{2+})_{5-4}(Al, Fe^{3+})_{1-2}[(OH)_8|AlSi_3O_{10}]$ monoclinic–prismatic

General features: trioctahedral 14Å normal chlorite (oxidized chlorite) characterized by high Fe-content: $Fe^{3+} > 4\%$ weight.

Thin-section characteristics

Chlorites of the orthochlorite series cannot be distinguished from those of the leptochlorites with a polarization microscope. Therefore they are not described here in any detail. They are very similar to the Fe^{2+}-rich orthochlorites (Part B, section 4.8.1).

Occurrence: generally they occur together with the $MgFe^{2+}$-orthochlorites. Delessite is a $MgFe^{2+}$ Fe^{3+}-leptochlorite occurring predominantly in cavities and fractures and in the matrix of intermediate and basic volcanic rocks e.g. in palaeobasalt, diabase, spilite and also in gabbro.

Paragenesis: with orthochlorite (diabantite, pycnochlorite), calcite, zeolite and quartz.

4.9 Serpentine group

$(Mg_6[(OH)_8|Si_4O_{10}]$ monoclinic–prismatic

General features: during alteration of Mg-rich mafic rocks, rock-forming trioctahedral phyllosilicates can form. Three main groups can be distinguished: antigorite, chrysotile and lizardite.

4.9.1 Antigorite

Thin-section characteristics

Form: flaky after {001}, lath-shaped, parallel or felted fibrous masses, also dense (Fig. 171(a)).

Cleavage: perfect on (001).

Colour: colourless; Fe-bearing varieties have a weak pleochroism from pale greenish-yellow to pale green.

Refraction and birefringence:

	Fe-free	Fe-rich
n_α	= 1.546	– 1.595
n_β	= 1.551	– 1.603
n_γ	= 1.552	– 1.604
$\ominus\Delta$	= 0.006	– 0.009

Low refraction and birefringence (grey-white interference colours of the 1st order); optically biaxial ⊖.

Optic axial angle: $2V_\alpha = 27°–60°$.

Character of elongation: (+).

Extinction: tends to be straight with $\alpha\Lambda c \approx 0°$.

Special characteristics: multiple twinning with the same orientation forming a fan in the [010] direction with undulatory extinction. In ultrabasic rocks, antigorite has a gridlike texture, where the fibres grow in two preferred orientations forming a grid.

Distinguishing features: chrysotile is also fine-grained and fibrous; Mg-chlorite has anomalous interference colours, lower birefringence and is optically biaxial ⊕; talc and pale-green micas show a significantly higher birefringence. Can be differentiated from the extremely fine-grained lizardite only by X-ray analysis.

Alteration: hydrothermally with the addition of SiO_2 into talc.

Occurrence: as low-grade metamorphic serpentinization of olivine-rich rocks (peridotite and other ultrabasic rocks, gabbros, lamprophyres, etc.); a major component in serpentinite. Also forms from Mg-rich orthopyroxenes. Can be accompanied by lizardite which can form the major component in pseudomorphs after orthopyroxene (bastite; Part B, section 4.2.1; Figs 122, 123).

Paragenesis: with olivine and/or enstatite or bronzite, diallage, chrysotile and magnetite; chrysotile, talc, magnesite to breunerite.

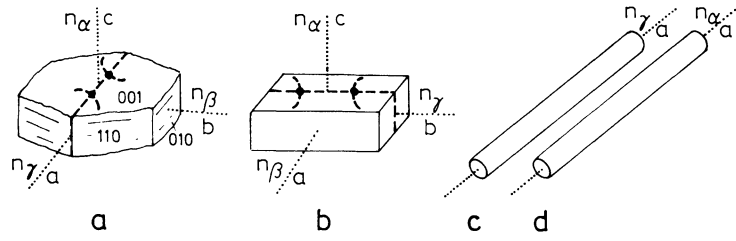

Fig. 171 Crystal form and optical characteristics of serpentine minerals: (a) antigorite in monoclinic form; (b) lizardite in orthorhombic form; (c) chrysotile γ and (d) chrysotile α, both in trigonal form.

4.9.2 Chrysotile

Form: fibrous, parallel growth, brush-shaped or irregular (Fig. 171(c),(d)).

Cleavage: none.

Colour: commonly colourless, rarely greenish (Fe^{2+}-bearing varieties) with a weak pleochroism from greenish-yellow to pale green to pale yellow.

	Chrysotile γ	Chrysotile α
n_α	= 1.532 – 1.552	1.538 – 1.560
n_β	= 1.545 – 1.561	1.546 – 1.567
n_γ	= 1.545 – 1.561	1.546 – 1.567
⊕Δ	= 0.013 – 0.009	⊖ 0.008 – 0.007

Low refraction and birefringence (grey-white to straw-yellow interference colours of the 1st order). Chrysotile γ: optically biaxial ⊕; chrysotile α: optically ⊖.

Optic axial angle: chrysotile γ: $2V_\gamma$ = 10°–90°; chrysotile α: $2V_\alpha$ = 30°–35°.

Character of elongation: chrysotile γ: (+); chrysotile α: (–).

Extinction: tends to be straight.

Special characteristics: chrysotile pseudomorphs after olivine can appear in two forms: mesh texture (Fig. 172), where the margin is comprised of chrysotile γ, and the centre of α chrysotile; antigorite: fibrous masses, where the opposite is the case.

Distinguishing features: in larger crystals it can be differentiated from antigorite; in small fibres it can be identified by X-ray analysis; fibrous amphiboles such as grammatite, actinolite, etc., have a higher refraction and birefringence. It is distinguished from fibrous lizardite only by X-ray analysis.

Alteration: under low-grade metamorphic conditions it reacts to antigorite. Low-temperature hydrothermal interaction with ultrabasites can lead to serpentinization of olivine and pyroxene, which are altered into chrysotile.

Occurrence: can occur together with lizardite, which can form oriented pseudomorphs after orthopyroxene (bastite; Part B, section 4.2.1; Figs 122, 123).

Paragenesis: with olivine, enstatite or bronzite, diallage and magnetite; also garnet (garnet-serpentinites).

Fig. 172 Fibrous serpentine (chrysotile), formed from serpentinization of olivine. Serpentinite. Finero, Ivrea area, northwestern Italy. Crossed polars.

4.10 Feldspar family

General features: the feldspars take up 60–65% weight of the earth's crust and are therefore the most important rock-forming mineral group. They predominate in magmatic rocks, where their chemical composition and abundance determine their systematics and nomenclature (Figs 255, 256).

Natural feldspar is comprised of three principal components:

$K[AlSiO_8]$	K-feldspar	or (orthoclase)
$Na[AlSi_3O_8]$	Na-feldspar	ab (albite)
$Ca[Al_2Si_2O_8]$	Ca-feldspar	an (anorthite).

At high temperatures there is complete solid solution and Al, Si-disorder among the alkali feldspars (or–ab; Fig. 173) and among the plagioclase feldspars (ab–an; Fig. 173). At reduced temperatures and increasing Al, there is Si-disorder exsolution (Fig. 174). This occurs in the solid state leading to exsolution lamellae in the host feldspar (perthite and antiperthite respectively; Part B, section 4.10.1).

Among the feldspars a high- and low-temperature modification can be distinguished (Fig. 175). At high temperatures Si and Al are statistically in disorder and feldspars are of a

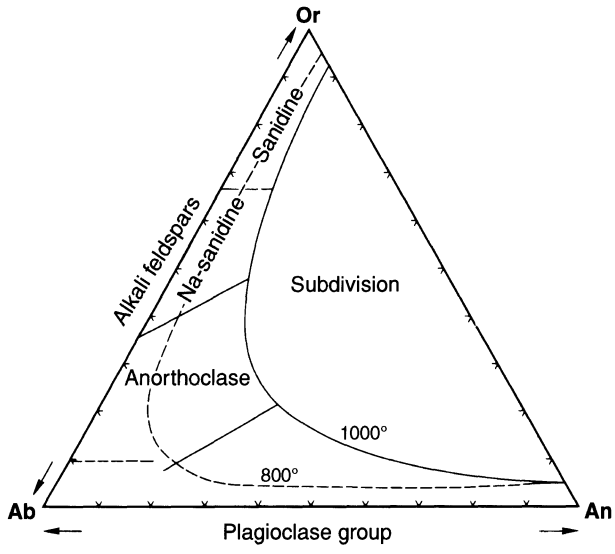

Fig. 173 Subdivision of high-temperature feldspars.

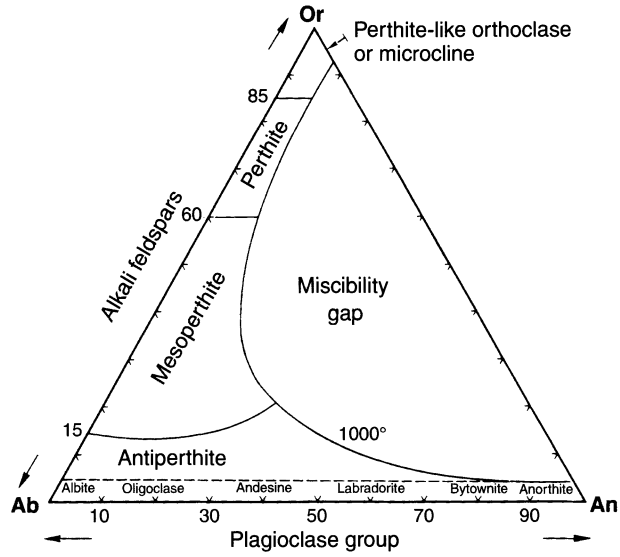

Fig. 174 Miscibility gap in the feldspar system in the 'plutonic facies'.

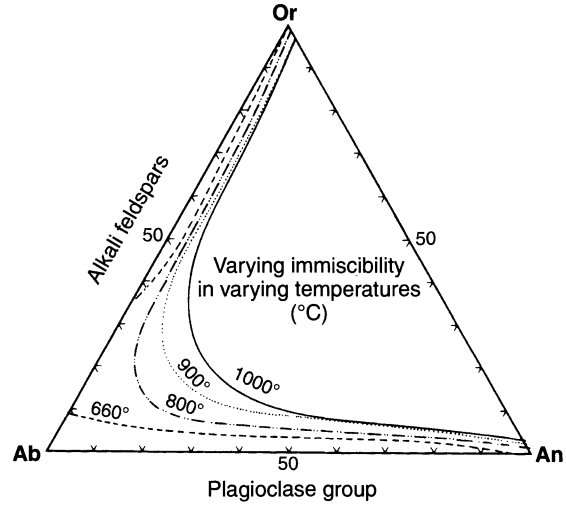

Fig. 175 Varying immiscibility with varying temperatures in the feldspar system.

monoclinic symmetry. If a magma, which contains such feldspars, is rapidly cooled (volcanic facies), then the high-temperature modification remains metastable in sanidine and/or high-temperature plagioclase. If the cooling path is slow (plutonic facies), then there is much more order among Si and Al and feldspars tend to be of triclinic symmetry. Because kinetics in alkali feldspars are very slow, disequilibrium is very common. High-temperature and low-temperature modifications express themselves in the form of different optical orientations (high-temperature and low-temperature optics). Between the two endmembers an infinite number of intermediate structures are possible.

4.10.1 Alkali feldspars

Thin-section characteristics

Form: thick to thin plates or laths stretched, particularly in the case of sanidine, along {010} and commonly forming Carlsbad twins (Figs 177, 179(a)). Untwinned feldspars, or those which form the rare Baveno or Manebach twins, tend to be elongated in the [100] direction. Subhedral to anhedral grains can occur as interstitial mineral in volcanic rocks. Two generations of alkali-feldspars can be common in volcanic rocks: one developed as phenocrysts and the other as microliths in the matrix; spherolitic growth and fine crystalline intergrowth with quartz in volcanic acidic glass-rich rocks can occur (Fig. 65).

Cleavage: perfect on (001), good on (010) and bad on {110}. The crystals show two sets of cleavage planes which intersect at right angles with the intersection direction parallel to the a-axis [100] (Fig. 176(a)–(d)).

Twinning: very common and characteristic. Simple, polysynthetic and complex twinning are equally frequently observed in feldspars. Common are plate-like twin pairs after the Carlsbad law (Figs 177, 178). Polysynthetic twinning is restricted to triclinic feldspars (e.g. microcline). Growth twins are distinguished from each other by the length of the twin axis:

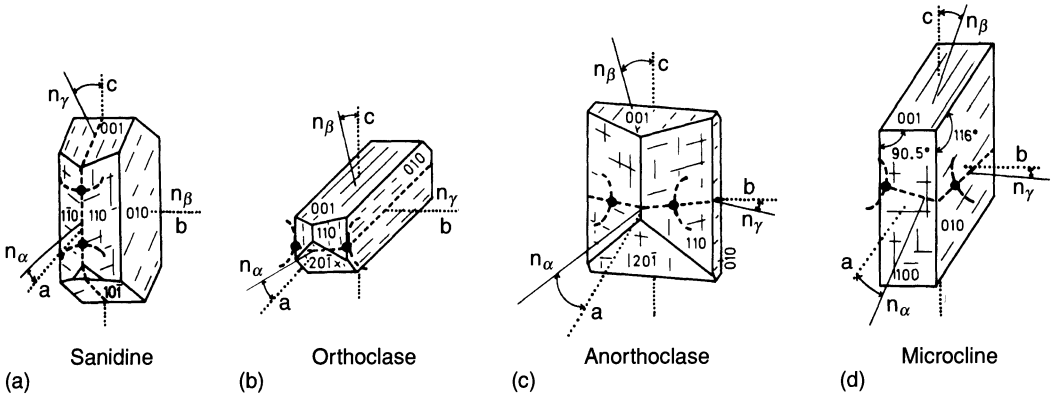

Fig. 176 Crystal form and optical characteristics of alkali feldspars: (a) sanidine, (b) orthoclase, (c) anorthoclase and (d) microcline.

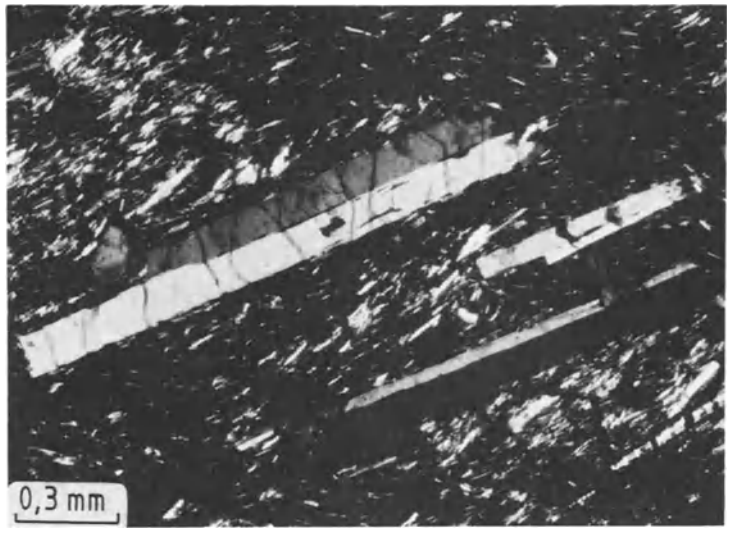

Fig. 177 Idiomorphic sanidine phenocrysts with typical Carlsbad twins, embedded in a matrix comprised of predominantly sanidine and aegirine-augite. Phonolite with a trachytic texture. Monte Rojo, Gran Canaria. Crossed polars.

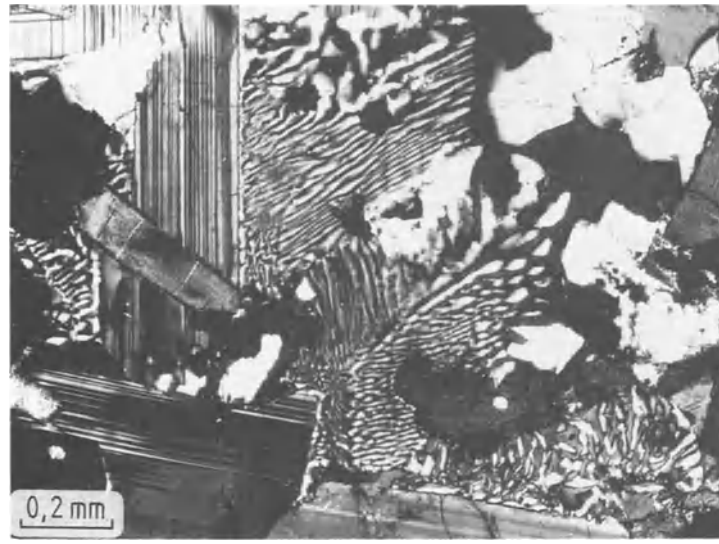

Fig. 178 Perthite exsolution in K-feldspar (centre) with transition into graphic quartz-feldspar intergrowth (top and bottom). Plagioclase (left) and quartz (right). Granite. Halmstad, Sweden. Crossed polars.

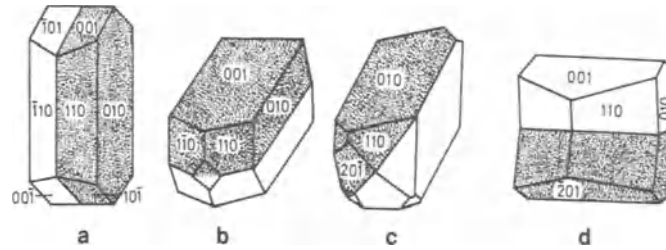

Fig. 179 Typical twinning laws in feldspars:

(a) Carlsbad twin.

(b) Manebach twin.

(c) Baveno twin.

(d) Pericline twin.

a) In monoclinic and triclinic symmetry (possible in all feldspars):

Twinning law	*Axis*	*Twin plane*
Carlsbad law	parallel [001]	(010) (Fig. 179(a))
Manebach law	perpendicular (001)	(001) (Fig. 179(b))
Baveno law	perpendicular (021)	(021) (Fig. 179(c)).

b) In triclinic symmetry (with the exception of sanidine, orthoclase and monalbite):

Albite law	perpendicular (010)	(010) (Fig. 188)
Pericline law	parallel [010]	(h01) (Fig. 179(d)).

In low-temperature K-feldspars of triclinic symmetry the complex microcline twinning is common; it forms by a combination of the albite and pericline laws (Fig. 180).

Colour: colourless (fresh) to milky (old).

Refraction and birefringence:

	Sanidine	Orthoclase	Anorthoclase	Microcline
n_α	= 1.518 – 1.525	1.518 – 1.523	1.527 – 1.522	1.518 – 1.520
n_β	= 1.522 – 1.530	1.522 – 1.528	1.533 – 1.528	1.522 – 1.524
n_γ	= 1.523 – 1.532	1.523 – 1.530	1.535 – 1.529	1.524 – 1.526
$\ominus\Delta$	= 0.005 – 0.007	0.005 – 0.007	0.008 – 0.007	0.006 – 0.006

Low refraction and birefringence (grey interference colours of the 1st order); optically biaxial $\ominus$.

Optic axial angle: 2V varies enormously: 60°–65° to 85° and 20°–110° respectively (anorthoclase). In high-temperature feldspars the axial plane is oriented parallel (010) with $2V_\alpha$ = 60°–65° (Fig. 176(a)). With decreasing temperature at formation and increasing order $2V_\alpha$ = 0°; at higher temperatures, K-feldspar falls into the transition zone to the orthoclase optical field with $2V_\alpha$ = 60°–80° and the axial plane oriented perpendicular to (010) (Fig. 176(b)).

Special characteristics: very fine-grained inclusions of sericite, chlorite, opaque minerals, etc.,

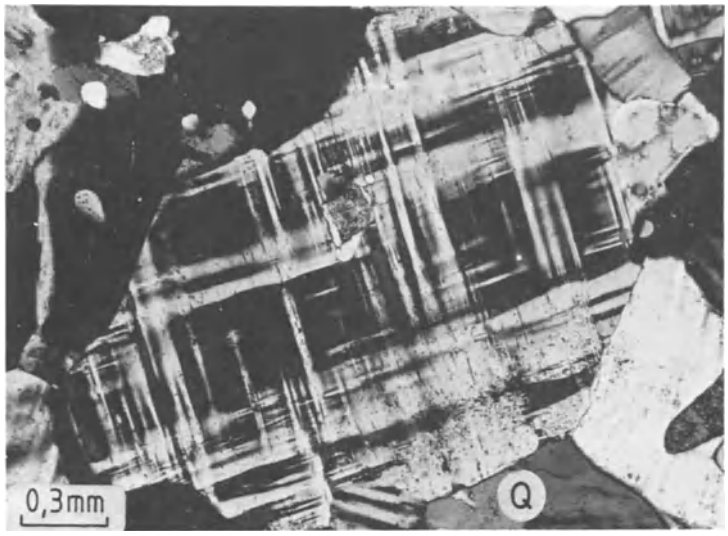

Fig. 180 Cross-hatched twinning in microcline next to quartz and others. Orthogneiss. Gallivaggio, Splügen, southern rump, northern Italy. Crossed polars.

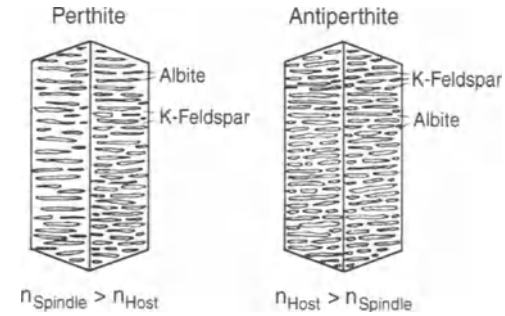

Fig. 181 Exsolution in alkali feldspars.

which can be aligned parallel to the two cleavage planes, can produce cloudy grey to brownish colours. Oriented intergrowths of chemically homogeneous crystal domains are common. Exsolutions are:

a) Perthite: K-feldspar is the host mineral, and it shows oriented intergrowth with Na-feldspar (Figs 181, 182).

According to the size of the host component, perthites are subdivided into:

1. Macroperthite: the Na-feldspar intergrowth is recognizable with the naked eye.
2. Microperthite: the Na-feldspar intergrowth is recognizable only with the aid of a microscope (filmperthite and stringperthite).
3. Cryptoperthite: the Na-feldspar intergrowth is recognizable only by X-ray analysis (e.g. lunar rock).

b) Antiperthite: Na-feldspar is the host and is intergrown in a systematic fashion by K-feldspar (Fig. 181). A similar subdivision, based on the size of the host component, is made as for perthite. In order to differentiate perthite and antiperthite the higher refraction characteristics of Na-feldspar are made use of, by carrying out the Becke line test: in the case of perthite the Becke line moves into the albite spindle stage and in the case of antiperthite it moves out of the spindle stage into the host albite.

Characteristic features (Table 4)

Sanidine: clear, tabular, colourless, often elongated lath-shaped crystals which can be Carlsbad twinned.

Orthoclase: perthite exsolution lamellae with simple growth twins are common. In comparison to sanidine orthoclase has a higher axial angle ($2V_\alpha > 60°$).

Anorthoclase: fine-grained cross-hatched twinning similar to the microcline law (Fig. 184). Rhomb-shaped cross-sections are common.

Microcline: typical twinning after the microcline law (Fig. 180).

Distinguishing features: generally feldspars are easily identified because of their characteristic twinning: monoclinal alkali feldspars always show simple twinning, whereas in triclinic feldspars complex lattice twins are more common, with or without simple twinning. Lamellar twinning is typical in plagioclase (with the exception of microcline and anorthoclase). Plagioclase, with the exception of albite, has a higher refraction compared to alkali feldspars. If no characteristic twinning is developed, then clouding, good cleavage and the biaxial character are important differentiating features, particularly from quartz. Nepheline is optically uniaxial, and shows straight extinction, is not well developed and is untwinned.

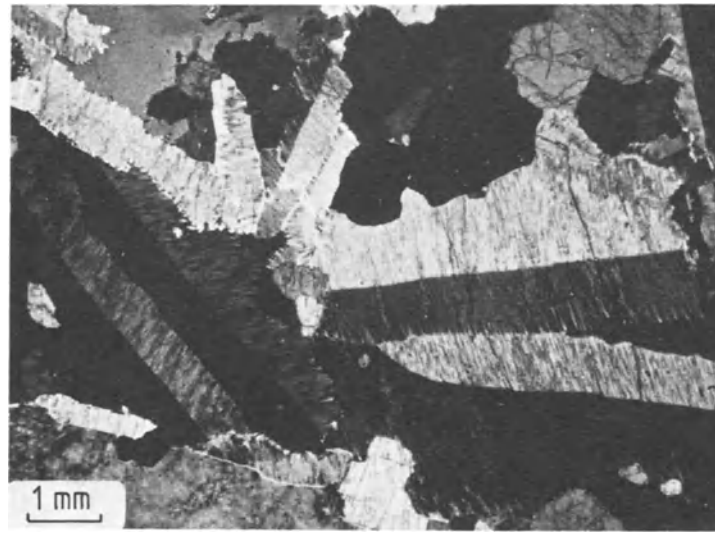

Fig. 182 Orthoclase showing perthite exsolution and characteristic Carlsbad twins. Sodalite syenite. Ditro, Transylvania, Romania. Crossed polars.

Table 4 Features differentiating alkali feldspars

	Sanidine	Anorthoclase	Orthoclase	Microcline
n	1.518–1.532	1.522–1.535	1.518–1.530	1.518–1.526
$2V_\alpha$	0–65° ⊖	20–110° ⊖	>60° ⊖	(>60° ⊖)
Twinning	Carlsbad twin	lattice	Carlsbad twin	lattice
Δ	0.005–0.007	0.007–0.008	0.005–0.007	0.006
Staining	–	some	+	+
Exsolution	–	+	+	+

4.10.1.1 Sanidine

$(K, Na)[AlSi_3O_8]$ monoclinic–prismatic

General features: high-temperature form of alkali feldspars (Fig. 176(a)) with the composition range of Or_{100-65} Ab_{0-35} An_{0-10} (Fig. 173). Alkali feldspars with $<Or_{65}$ are called Na-sanidine.

Special characteristics: fresh and young sanidine shows poor or no cleavage.

Alteration: sericite alteration or replacement by kaolinite leads to clouding. Through geological time the crystals develop exsolution compounds and transition into orthoclase. K-feldspars in older volcanic rocks generally occur as orthoclase.

Occurrence: major phase in young and fresh intermediate to acidic volcanic rocks. As phenocrysts (in e.g. trachytes; Drachenfels, near Bonn) as well as in the matrix (e.g. trachyte, phonolite, etc.; Fig. 177). Na-sanidine can occasionally be found as a rim around plagioclase.

Paragenesis: in silica-saturated volcanic rocks with quartz, plagioclase, biotite, hornblende, ortho- and clinopyroxene, and rock-glass. In trachytes with plagioclase, biotite or aegirine-augite. In phonolites with nepheline, aegirine-augite and minerals of the sodalite group.

4.10.1.2 Orthoclase

$K[AlSi_3O_8]$ monoclinic–prismatic

General features: always cloudy, morphologically monoclinic, forming the transition between sanidine and microcline with metastable intermediate Al, Si ordering (Figs 176(b), 182, 183). The term orthoclase is also used for diagrams and petrological quantifications for the $KAlSi_3O_8$ component.

Alteration: orthoclase crystallizes towards the end of the crystallization sequence in magmatic rocks (autometasomatism) and is often accompanied by sericitization and kaolinization, which results in clouding due to the fine distribution of inclusions. Hydrothermal alteration leads to kaolinization.

Occurrence: as an exsolution and transition mineral between sanidine and microcline, orthoclase tends to occur in older volcanic/magmatic rocks, e.g. palaeorhyolites (quartz porphyry) to palaeoandesites (porphyrites) (Fig. 182).

Paragenesis: with albite to andesine, biotite, hornblende and pyroxene. In plutonic rocks with microcline, quartz, albite-rich plagioclase, biotite, muscovite and sphene.

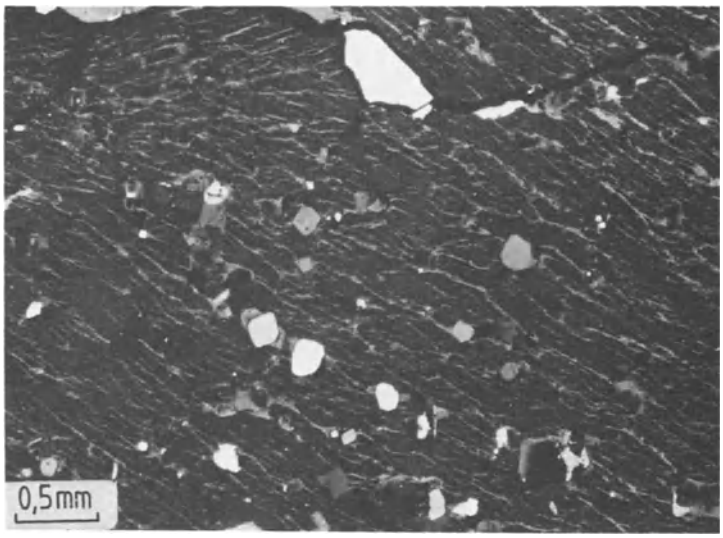

Fig. 183 Orthoclase with perthite exsolution (vein perthite) and numerous nepheline and apatite inclusions. Elaeolite syenite. Salt Range, Pakistan. Crossed polars.

4.10.1.3 Anorthoclase

$(Na, K)[AlSi_3O_8]$ monoclinic–prismatic

General features: morphologically monoclinic (Fig. 176(c)). A decay product of K-rich monalbite as a consequence of exsolution and transformation. The chemical range of Na-rich alkali feldspar is $Ab_{77-62}Or_{12-35}An_{2-20}$.

Special characteristics: polysynthetic twinning (Fig. 184) similar to microcline and/or antiperthite exsolution is common (Fig. 185). Zoning is common! Rhombic-shaped sections are typical.

Distinguishing features: can be confused with other feldspars. Paragenesis is important!

Alteration: see sanidine.

Occurrence: as phenocrysts and also in the matrix of Na-rich volcanic and shallow plutonic (subvolcanic) rocks, e.g. alkali rhyolites (pantellerite), alkali trachyte to latite, mugearite (matrix) and phonolite. Also in older volcanic rocks (e.g. palaeolatite/rhombic-porphyry) and in some plutonic rocks.

Paragenesis: with quartz, aegirine-augite, aenigmatite, arfvedsonite, glass or nepheline and aegirine-augite (in phonolites).

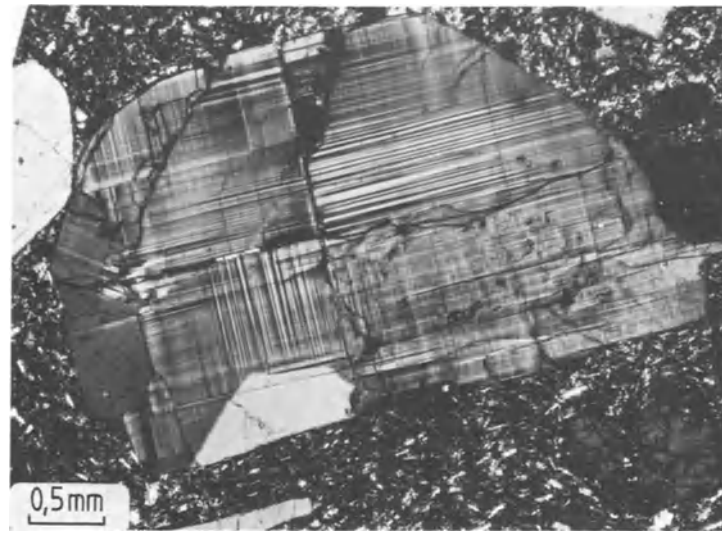

Fig. 184 Anorthoclase phenocryst with characteristic fine lamellae forming a cross-hatched twinning similar to microcline in a hemi-crystalline matrix of alkali feldspar and glass. Trachyte. Fontanafredda, Colli Euganei, northern Italy. Crossed polars.

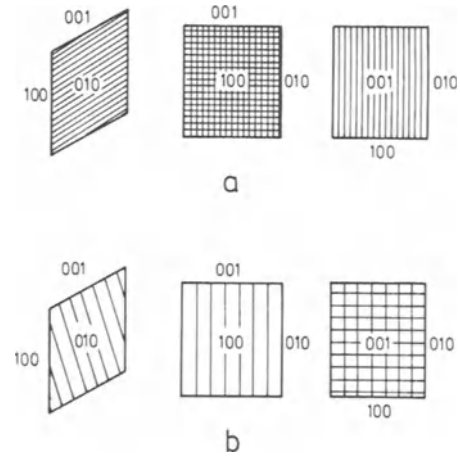

Fig. 185 Twinning according to the albite and pericline laws in (a) anorthoclase, (b) microcline.

4.10.1.4 Microcline

$K[AlSi_3O_8]$ triclinic–pinacoidal

General features: the term microcline applies to all triclinic low-temperature K-feldspars (Fig. 176(d)) with or without perthite exsolution textures. The fine polysynthetic cross-hatched twinning (albite and pericline twinning law; Fig. 180) is characteristic. However, is some sections microcline may not be so easily identified (Fig. 186).

Alteration

a) In slowly cooling plutonic rocks microcline perthite can form with albite string, veins and spindles.

b) Hydrothermal interaction, which can occur during the late stages of crystallization (auto-metasomatism), can cause sericitization (the second most important alteration.).

c) Replacement of K-feldspar by albite to form chessboard albite.

d) Progressive replacement of K-feldspar by plagioclase forming myrmekite. This results in patches of plagioclase intergrown with vermicular quartz. The intergrowth is often wart-like in shape and is commonly found at the margins of feldspar and plagioclase crystals penetrating an alkali feldspar crystal.

e) If fluor is added at a late stage (fluor pneumatolysis) reaction into topaz and tourmaline occurs.

f) Hydrothermal interaction can lead to kaolinization.

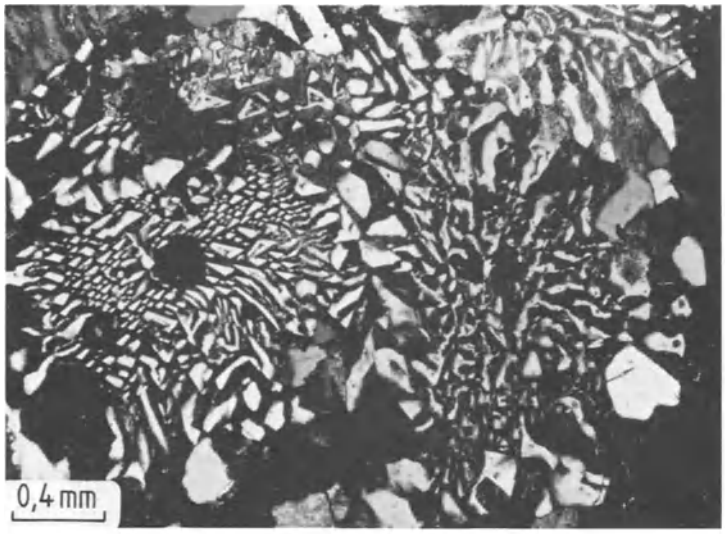

Fig. 186 Granophyric intergrowth of alkali feldspar with quartz. Granophyric palaeorhyolite (quartz porphyry). Rosskopf near Barr, Alsace, France. Crossed polars.

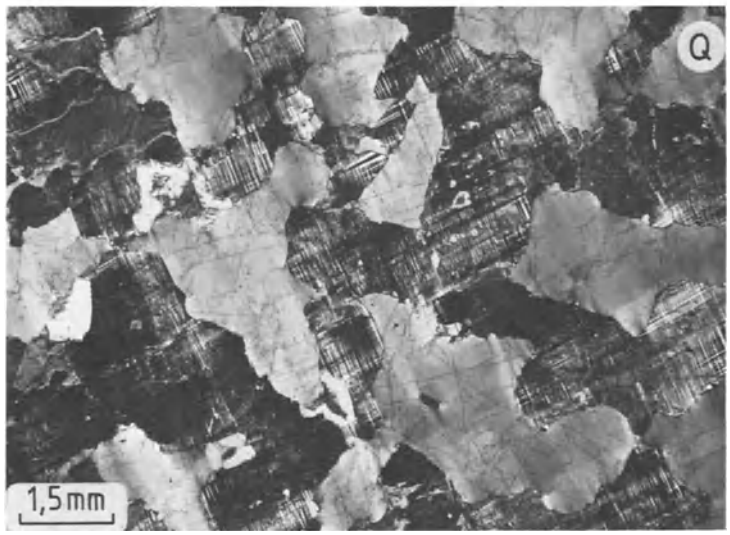

Fig. 187 Graphic intergrowth of quartz showing undulatory extinction with microcline with typical cross-hatched twinning. Granophyric granite. Erratic boulder, Baltic Sea coastline, near Kiel. Crossed polars.

Distinguishing features: sections of two plagioclase twins which grow at right angles to each other are free of spindles, but show sharply defined plates, which abruptly stop at a crossing lamella. Microcline lacking the characteristic cross-hatched texture can be distinguished from orthoclase by its extinction angle in sections perpendicular to (010): maximum of 19° in microcline, 0° in orthoclase (Fig. 187).

Occurrence and paragenesis: the same as plagioclase (Part B, section 4.10.2).

4.10.2 Plagioclase series

$Na[AlSi_3O_8] \leftrightarrow Ca[Al_2Si_2O_8]$ triclinic–pinacoidal (monalbite = monoclinic)

General features: dependent on the anorthite content six plagioclase minerals are distinguished (Fig. 174) which can crystallize either in a high- or a low-temperature form (high- or low anorthite and high- and low-albite). High-plagioclase is restricted to volcanic rocks whereas low-plagioclase is found in plutonic and metamorphic rocks.

Thin-section characteristics

The optical characteristics are dependent on the chemical composition and also the degree of Al/Si ordering and hence the condition of formation (Fig. 189).

Form: thin to thick plates, isometric to stretched along [100] or [001], as a matrix mineral in volcanic rocks; phenocrysts, often corroded and zoned with glass inclusions aligned within the growth zones. Two generations of plagioclase crystals are common in volcanic rocks: phenocrysts and matrix microliths. Strong zoning in volcanic but also in plutonic rocks with corroded cores and rims can be observed.

Cleavage: perfect on (001), good on (010) and not so good on (110) and $(1\bar{1}0)$ respectively. Crystals show two cleavage intersection planes at an angle of 86°. In young volcanic rocks this cleavage can hardly be seen under the microscope.

Twinning: several twinning laws can occur simultaneously in plagioclase. In the case of albite, pericline twinning produces, polysynthetic lamellae (Figs 188, 190). Albite-law twins are very common and typical. In oligoclase albite-law twinning tends to produce very thin lamellae. Increasing Ca-content leads to increasing width in the albite-twin lamellae (Fig. 191); simple twinning tends to occur in the pure endmembers, albite and anorthite. Often one twin lamella (e.g. albite law) is abruptly transected by another one (pericline law).

Most important twin laws are:

Twinning law	Twin axis	Intergrowth plane
a) Albite law	perpendicular [010]	(010) (Fig. 188)
b) Pericline law	parallel [010]	(001) (Fig. 179(d))
c) Carlsbad law	parallel [001]	(010) (Fig. 179(a))

In volcanic rocks Banat intergrowth can occur, where several plagioclase crystals are intergrown in a cross or T-shaped fashion. Translation and pressure twins are not uncommon (Fig. 192).

Remarks: albite twins generally form sharply defined lamellae parallel to (010). The width of the lamellae can vary within one thin section and within a twinned crystal. Twinning lamellae can also pinch out (Fig. 190). In the case of pericline twinning the lamellae are oriented perpendicular to (010) and if albite twinning is also developed, then the two sets of lamellae intersect at right angles. This can give rise to microcline-like textures, but the grid is coarser and the lamellae are better defined. If no twinning lamellae are developed, as is common in albite (e.g. schists), then its identification is very difficult.

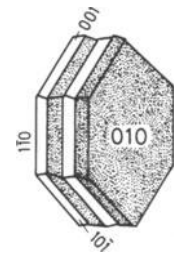

Fig. 188 Typical twinning in plagioclase after the albite law (polysynthetic twinning).

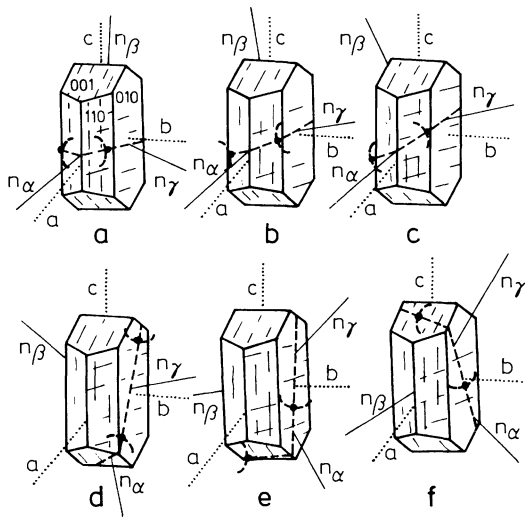

Fig. 189 Crystal form and optical characteristics of low-temperature plagioclase: (a) albite, (b) oligoclase, (c) andesine, (d) labradorite, (e) bytownite and (f) anorthite.

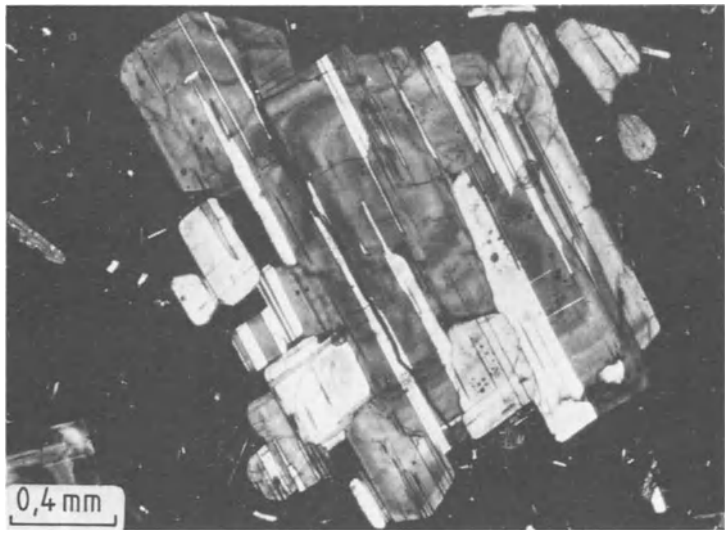

Fig. 190 Idiomorphic plagioclase showing twinning after the albite and pericline laws and zoning, surrounded by a hyaline matrix. Dacitic pumice. Mojanda volcano, northern Ecuador. Crossed polars.

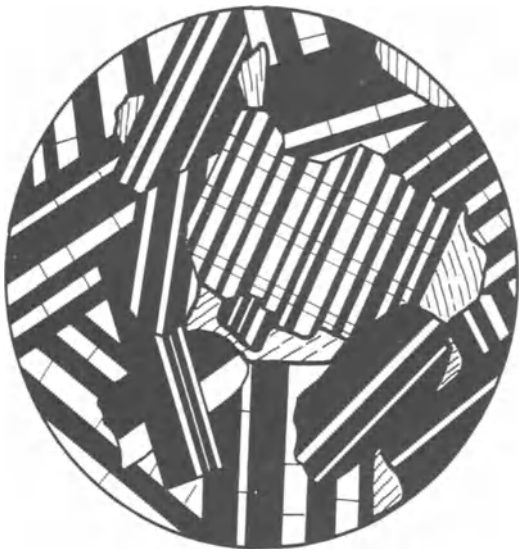

Fig. 191 Polysynthetic twinning plagioclase in anorthosite. The high anorthite content is visible by the broad twin lamellae. Crossed polars.

Fig. 192 Hypidiomorphic plagioclase crystal with clearly visible glide-twins next to augite. Tectonized gabbro. Northern Italy. Crossed polars.

Colour: colourless (fresh). Inclusions (sericite, chlorite, opaque minerals) can lead to crowding in the crystal.

Refraction and birefringence:

	High-albite	Low-albite	Anorthite
n_α	= 1.527	1.527	1.575
n_β	= 1.532	1.533	1.583
n_γ	= 1.534	1.539	1.588
$\oplus\Delta$	= 0.007	0.007	0.013

The corresponding values for the various intermediate plagioclase crystals fall in between the endmembers.

Low refraction and birefringence (grey, white-grey to yellowish interference colours of the 1st order); optically biaxial ⊕ or ⊖ (Fig. 193).

Optic axial angle: $2V_\alpha$ varies between 50° and 105°; in the plutonic facies it passes through the 90° (optically neutral) position three times, whereas in the volcanic facies this occurs only once (Fig. 193). The size of the axial angle and the orientation of the axial plane are dependent on the anorthite content and condition of crystallization. The dispersion of the optical axes can vary causing anomalous (low anomalous interference colours: grey-blue to grey-brown) interference colours.

Remarks: the exact anorthite content can be determined only by universal stage microscopy or a geochemical method (e.g. use of an electron microprobe analyser). However, an estimate is possible in sections perpendicular to the albite twinning plane, by measuring the extinction angle (see later in this section).

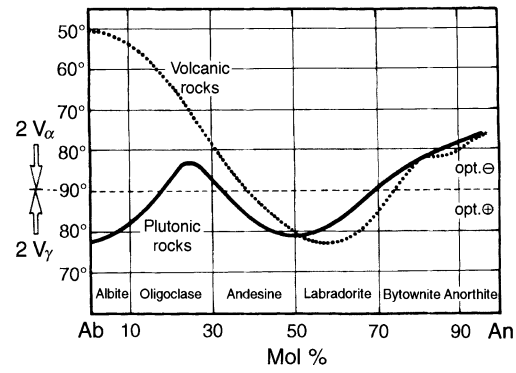

Fig. 193 Change of the optic axial angle as a function of temperature of crystallization.

Opt. ⊕ plutonic: Ar_{0-17}, Ar_{32-70}

Opt. ⊖ plutonic: Ar_{17-32}, Ar_{70-100}

Opt. ⊖ volcanic: Ar_{0-38}, $Ar_{\approx 75-100}$

Opt. ⊕ volcanic: $Ar_{38-\approx 75}$

Special characteristics: plagioclase in magmatic and metamorphic rocks (specially in volcanic rocks) commonly shows zoning (Figs 194, 195). Twinning can transect twinning lamellae. Extinction can vary within the growth zones, if there is a slight chemical variation. The following types of zoning can be differentiated:

1. Normal zoning: decreasing anorthite content from core to rim (Fig. 195(a)) as a consequence of chemical disequilibrium in the melt during crystallization. This is also common in metamorphic rocks.

2. Oscillatory zoning: irregular, partly reversed changes in the anorthite content within the zones (Fig. 195(b)), probably as a conse-

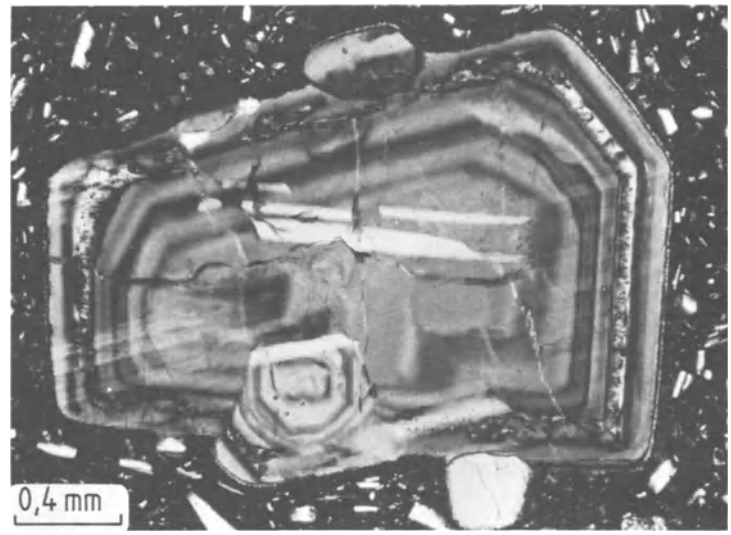

Fig. 194 Idiomorphic, strongly zoned phenocryst of plagioclase (core: bytownite, rim: andesine) in a microcrystalline-hemicrystalline matrix. Quartz andesite. Galeras volcano, southern Colombia. Crossed polars.

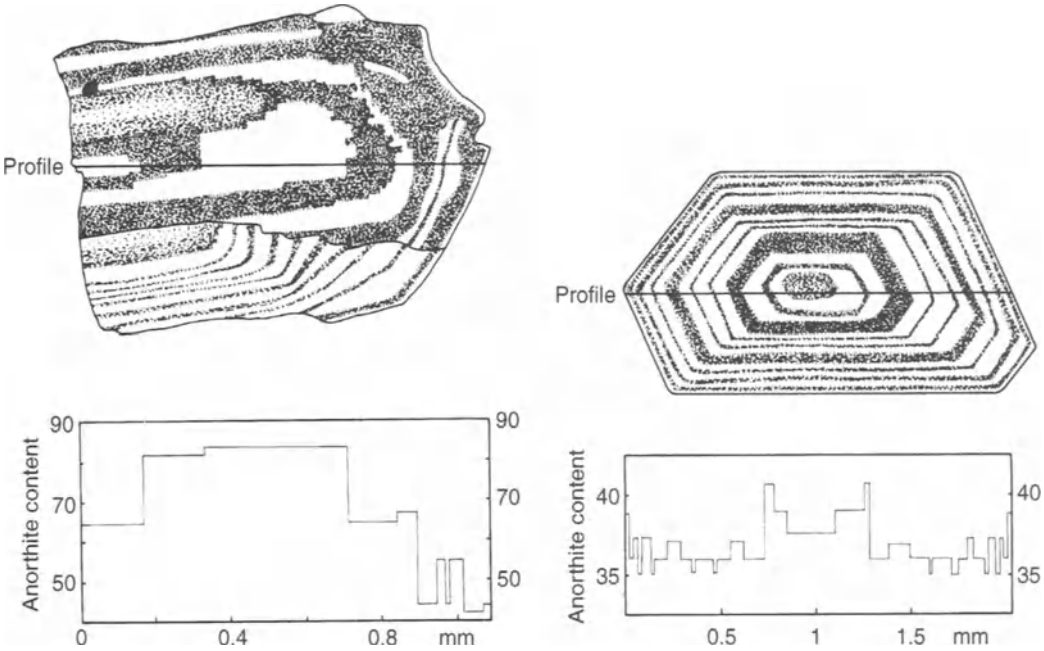

Fig. 195 Zoning in plagioclase: normal zoning (left) and oscillatory zoning (right).

quence of pH_2O variations in the melt phase (volcanic rocks).

3. Inverse zoning: increasing anorthite content from core to rim as a consequence of progressive metamorphism.

Distinguishing features: non-twinned granoblastic albite is common in schists. Plagioclase is easily differentiated from other minerals by the characteristic polysynthetic twinning. In the absence of twins, identification is difficult and plagioclase can be confused with orthoclase and zeolite; however, plagioclase has a higher refractive index and zonar growth is common. It differs from quartz by its good cleavage, it is often clouded, is twinned and is optically biaxial with a large axial angle. Non-twinned plagioclase can also be confused with cordierite. Alkali feldspars show characteristic perthitic internal textures, which are absent in plagioclase. Characteristic twinning in microcline can be distinguished from albite and pericline twins by the former being irregular, discontinuous and bleb-like.

Alteration

a) Under hydrothermal conditions there is alteration into sericite, which starts with a clouding of the crystal (Fig. 196).

b) During the albitization of basaltic volcanic rocks the anorthite-rich plagioclase is replaced by albite + calcite (spilitization). This is common in spilite and diabase.

c) Under retrograde metamorphic conditions the anorthite component becomes unstable, and is replaced by a fine-grained aggregate of clinozoisite, zoisite, albite, actinolite and sericite; a greenish colour (saussuritization) results.

d) Fluor-pneumatolysis results in the crystallization of topaz, tourmaline and Li-mica at the expense of plagioclase.

e) Hydrothermal alteration can also lead to propylitization (greenish coloration), alteration into aggregates of albite, calcite, chlorite, sericite, quartz, etc.

f) Zeolitization can occur during hydrothermal alteration (natrolite, thomsonite, scolecite, heulandite).

g) Weathering causes kaolinization and calcite formation. Albite is more stable than anorthite-rich plagioclase. The anorthite component, commonly in the core, can be 'filled' whereas the albite rim remains unclouded.

Occurrence

1. Present in almost all magmatic rocks. The anorthite content decreases progressively from basic to acidic rocks:

gabbro → diorite → granite → aplite, pegmatite
An > 50 <50 <30 <10

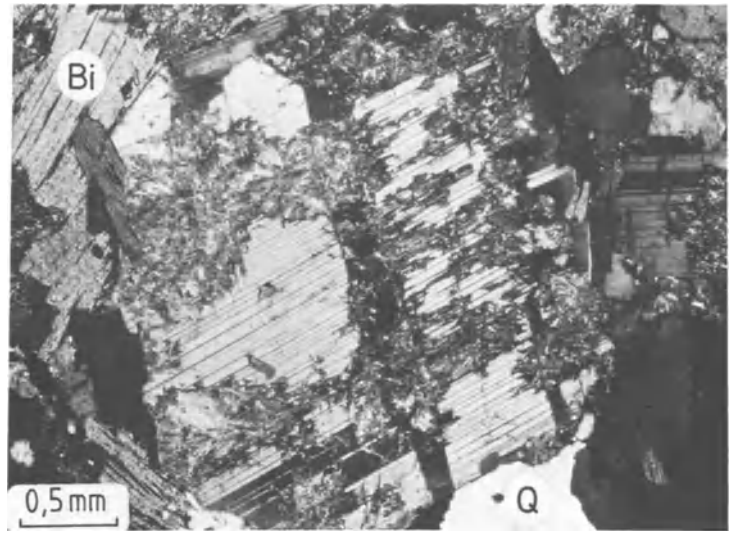

Fig. 196 Sericitization in albite-rich plagioclase. The thin lamellae indicate a very low anorthite content. Twinning after the albite and pericline laws. Granodiorite. Hochstädten, east of Auerbach, Odenwald, Germany. Crossed polars.

In pegmatites albite is typical, and it can be antiperthitic (Fig. 181). Hydrothermal paragenesis always contains pure albite. Decreasing anorthite content with increasing acidity can be observed in volcanic rocks:

basalt → andesite → dacite → rhyolite
An 70–50 60–40 50–30 40–20

Plagioclase phenocrysts in volcanic rocks tend to be more anorthite-rich than those in the groundmatrix (exceptions are rare). Hydrothermally altered plagioclase in spilites are pure albite.

2. In metamorphic rocks the albite-rich members are important. In low-grade metamorphic and diaphthoritic rocks only albite and oligoclase are representative for the plagioclase group. In greenschist-facies rocks non-twinned or simply twinned albite is most common. In mid- to high-grade metamorphic rocks (e.g. in gneisses) oligoclase and andesine are the most common plagioclase representatives.
3. In arkoses and greywackes (albite).

Paragenesis: in magmatic rocks with orthoclase, microcline, quartz, biotite, hornblende, clino- and orthopyroxene or titanaugite, olivine, rockglass (alkali basalt) or diopside-rich augite, and olivine (gabbro). In low-grade metamorphic rocks with chlorite, sericite, epidote, actinolite, calcite and quartz. In medium grade metamorphone rocks with hornblende and pyroxene.

Determination of the anorthite content using the extinction angle in suitable sections: in order to determine the anorthite content with the microscope the universal stage is necessary. However, an approximate value can be obtained much more easily. The most common methods applied are the zoning method by Rittmann and the microlith method for matrix plagioclase in volcanic rocks. The zoning method is based on the fact that the extinction angle measured relative to cleavage or the prevailing twinning system is dependent on composition and therefore related to the anorthite content. Plagioclase tends to be twinned according to the albite law (010) and shows polysynthetic twin lamellae. In sections which are approximately perpendicular to the twinning plane the extinction is symmetric. These sections are referred to as symmetric zones and, since Schuster (1881), they are the preferred sections to be used to determine the extinction angle. When choosing these sections the following must be observed:

1. The lamellae of the twinned crystal should not be too small.
2. Sections which are perpendicular to (010), or nearly so, show very sharp cleavage or twin planes along (010) which do not move sideways during focusing and unfocusing of the microscope (best viewed with ×25 or ×40 objective lens).
3. Albite twins can be identified when the lamellae planes are oriented N–S and the lamellae show equal brightness.
4. This is followed by measuring the extinction angle, by rotating to the right and to the left. The following should be observed:
   a) In both directions the extinction angle should be nearly the same or very similar, and should not differ by more than 5°. The higher value is used.
   b) Several crystals are measured and the highest value is taken.
5. A compensator quartz red I (551 nm) is used to determine the optical sign.

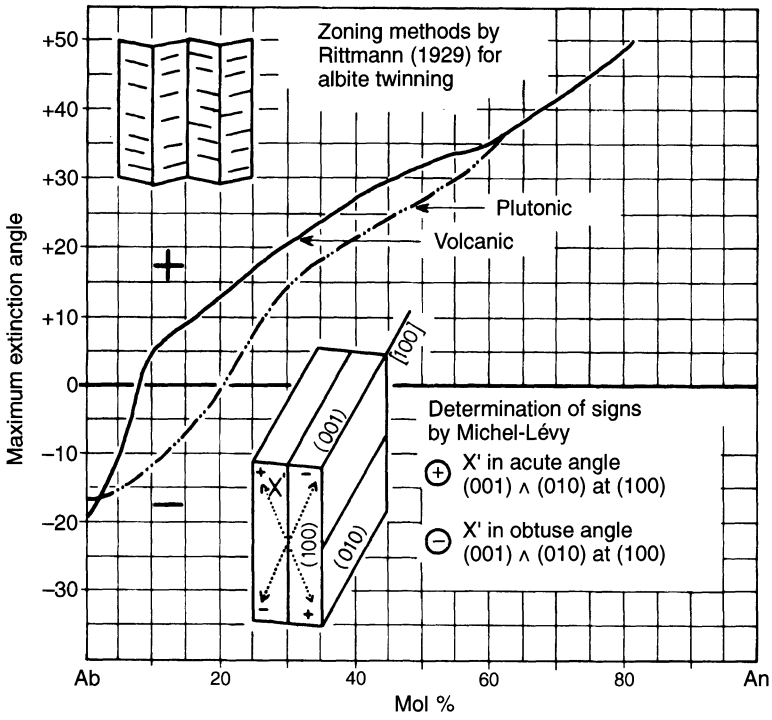

Fig. 197 Determination of the anorthite content of plagioclase, simplified after the zoning method of Rittmann (1929).

6. In the diagram above (Fig. 197) one reads off the anorthite content against the extinction angle. Volcanic and plutonic facies are distinguished by the rock textures first and then the appropriate curve is chosen in the diagram.

The **microlite method** makes use of the observation that plagioclase-microlites tend to be stretched along the a-axis. Sections parallel to the a-axis have the (010) cleavage trace and albite twins aligned parallel to it. If one measures the maximum extinction angle relative to the long axis of the microlite, then the anorthite content can be estimated by reading off diagram Fig. 198. If the maximum extinction is between 0° and 20°, then an estimate of the refractive index relative to the mounting material must be carried out. If canada balsam or caedax has been used, then it is enough to observe the Becker line. If the latter moves into the balsam, then the anorthite content is <30 and vice versa (e.g. the axial angle = 10° and n < caedax = anorthite 16).

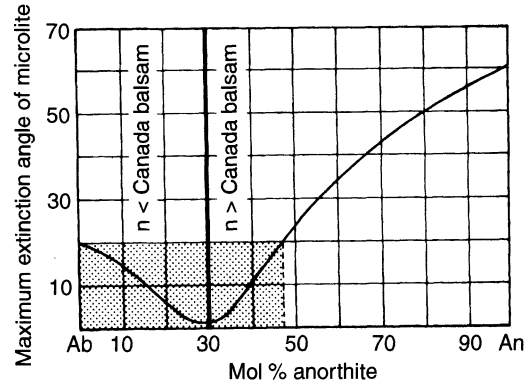

Fig. 198 Determination of the anorthite-content in plagioclase after the microlite method.

4.11 Zeolite family

General features: zeolites are chemically and structurally similar to the feldspars. They are water-bearing tectosilicates, which according to modern nomenclature can be subdivided into seven different groups. Since they cannot be differentiated by microscopic methods alone the old procedure based on shape is used here and can be applied to thin sections viewed under a microscope:

Plates

1 Spheroidal hematite, coloured red-brown, filling cavities in a microcrystalline matrix comprised of plagioclase, pyroxene and rock-glass. Pyroxene andesite. Mojanda volcano, northern Ecuador. Uncrossed polarizers, 1.4 × 2.0 mm.

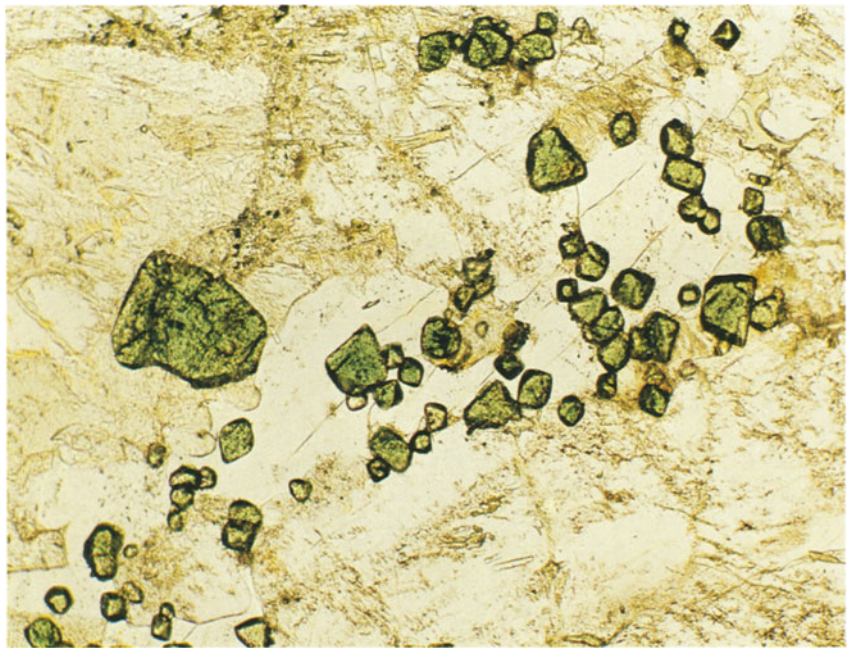

2 Bright-green hercynite developed as octahedral and as rounded grains, showing a strong positive relief relative to quartz (bright, unaltered, xenomorphic grains) and cordierite, which is pale yellow to pale light-brown, originating from a slight pinitization. Small-grained sillimanite needles are recognizable because of their high relief. Spinel-sillimanite-cordierite-gneiss. Bodenmais, Bavaria, Germany. Uncrossed polarizers, 1.3 × 1.8 mm.

3 Zircon forming an idiomorphic crystal which has crystallized early from the magma. It shows bright-yellow to blue interference colours of the 2nd order, weak cleavage and sharply defined fractures. It is surrounded by microcline-perthite (grey to white interference colours of the 1st order), spindles are mostly sericitized (brown); nepheline shows grey-black to grey interference colours of the 1st order, and apatite (inclusion in microcline-perthite; section is nearly perpendicular to the optic axis, therefore almost isotropic). Nepheline syenite. Laugen valley in southern Norway. Crossed polars, 2.2 × 3.1 mm.

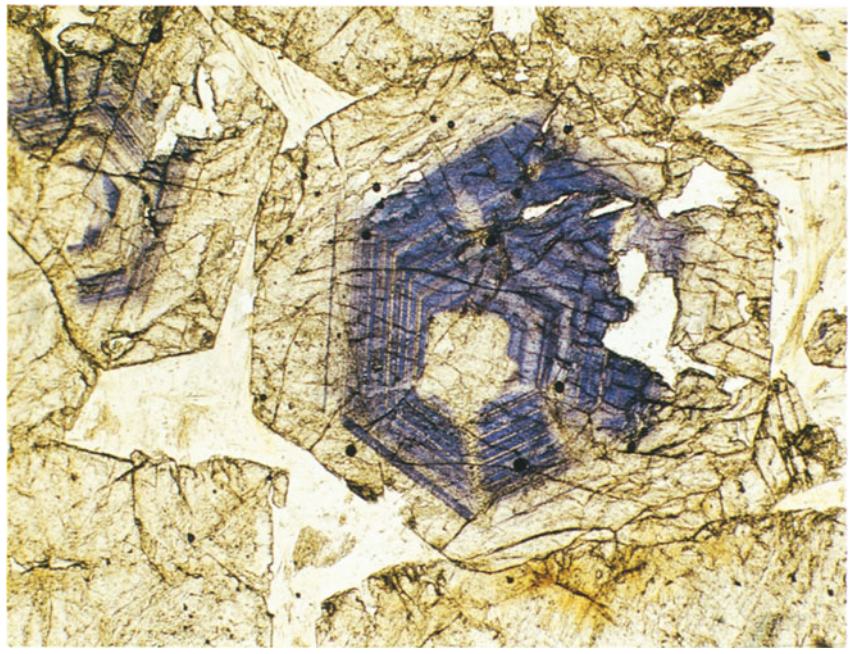

4 Idiomorphic, zoned corundum crystals with patchy blue pleochroism and strong relief relative to acicular, colourless sillimanite (top right). Sillimanite-corundum gneiss. Urals. Uncrossed polarizers, 2.2 × 3.1 mm.

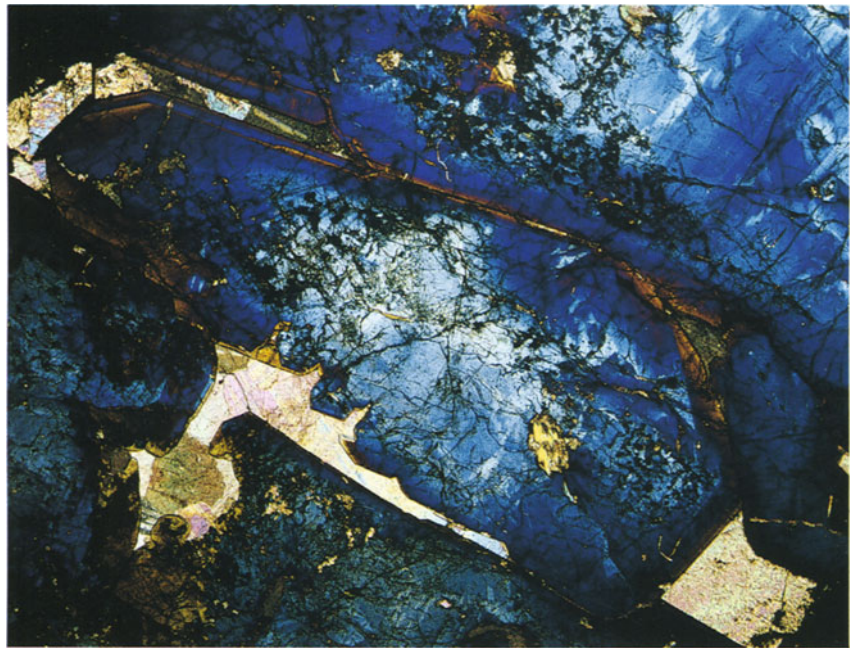

5 Hypidiomorphic vesuvianite crystals with strong anomalous interference colours (lavender-blue to leather-brown), also showing weak cleavage. Accompanying minerals are calcite with greenish to reddish-white interference colours of the higher orders. Contact-metamorphic siliceous carbonate. Predazzo, Dolomites, northern Italy. Crossed polarizers, 8.0 × 11.0 mm.

6 Short to long prisms of cancrinite phenocrysts, showing well-developed cleavage and interference colours of the 1st order (straw-yellow) and 2nd order (blue). Accompanied by alkali feldspar, apatite and ore. Foyaite-syenite ejecta. Laacher volcanic area, Germany. Crossed polars, 2.4 × 3.2 mm.

7 Simple twinning in titanaugite with clear zonal growth pattern and typical anomalous interference colours of the 1st order (grey-blue to dark brown). Clearly developed pyroxene cleavage and crystal outlines. Hyalobasanite. Sasbach, Kaiserstuhl volcano, Germany. Crossed polars, 4.0 × 5.5 mm.

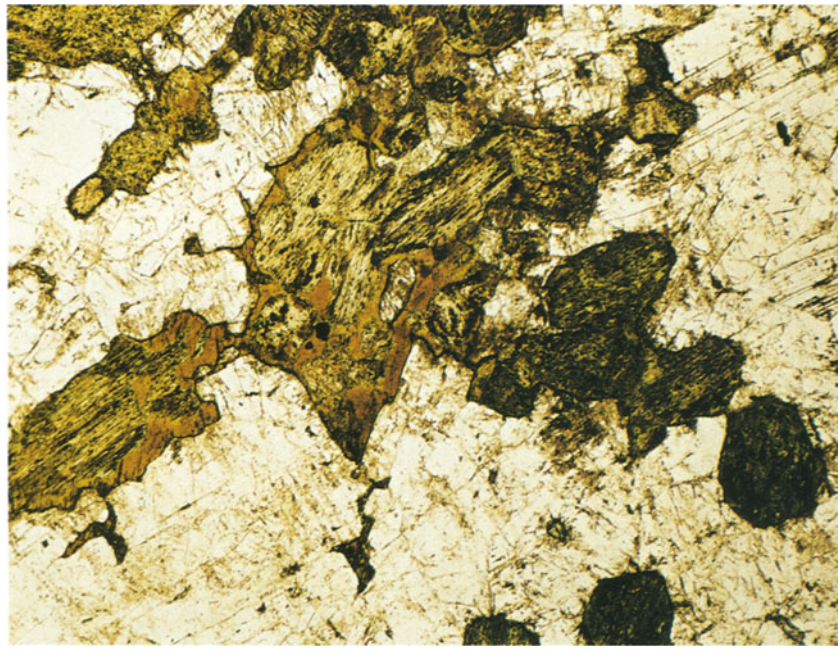

8 Hypidiomorphic augite in a 'wet' environment altered to pale green to brown amphibole (uralitization). Augite is partly intergrown with colourless, partly sericitized plagioclase (weak brownish, milky). Gabbro. Nieder-Beerbach, Odenwald, Germany. Uncrossed polarizers, 3.3 × 4.6 mm.

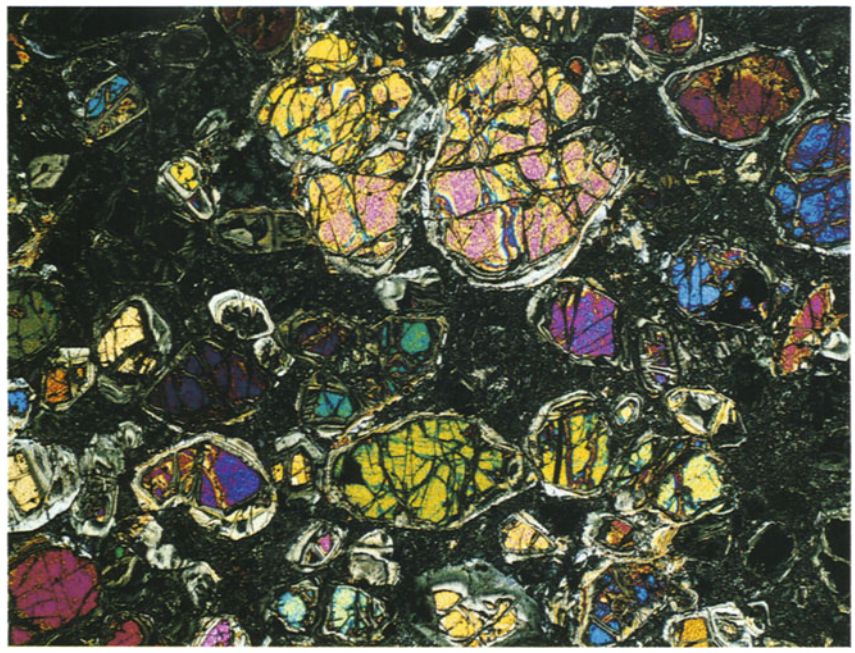

9 Serpentinization of olivine. Fibrous chrysotile aggregates with low birefringence replacing olivine along its rims and fractures. Olivine phenocrysts show bright interference colours of the 2nd order embedded in fibrous antigorite. Serpentinized peridotite. Northeast of Dillenburg, Hessen, Germany. Crossed polars, 3.6 × 5.5 mm.

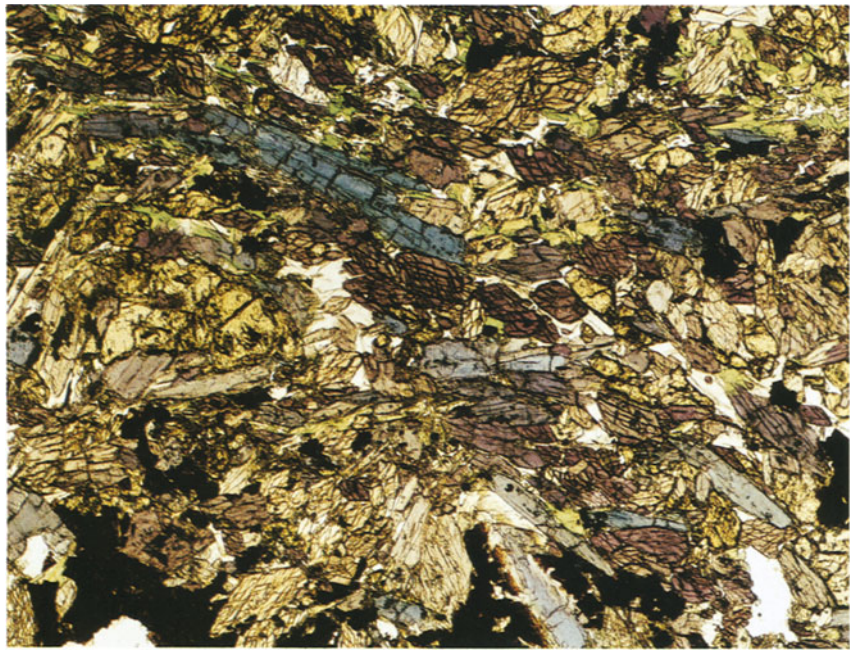

10 Lepidoblastic glaucophane with brownish to purple-blue pleochroism, showing cleavage characteristic for amphiboles. Other minerals present are epidote (yellow to yellow-green pleochroism), chlorite (deep green), albite (colourless) and opaque minerals. Epidote-glaucophane schist. Island of Syros, Cyclades, Greece. Uncrossed polarizers, 2.5 × 3.4 mm.

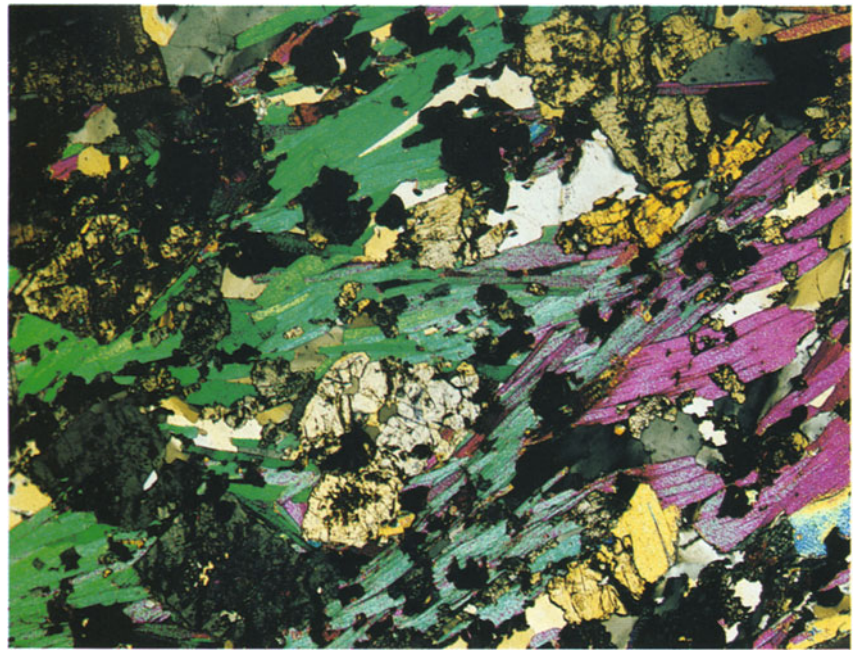

11 Lepidoblastic muscovite with bright interference colours of the 2nd and 3rd orders, next to poikiloblastic jadeite (white-grey to straw-yellow interference colours of the 1st order), almandine (isotropic) and quartz (grey-white interference colours of the 1st order; undulatory extinction). Almandine-glaucophane-jadeite-muscovite schist. Valle d'Aosta, northern Italy. Crossed polars, 4.0 × 5.5 mm.

12 Biotite showing strong pleochroism ranging from pale to strong brown. Well-developed basal cleavage traces are recognizable. Accompanying minerals are bronzite (weak brown) and pale-greenish pleonaste with strong relief. Mica-bearing peridotite. Kaltes Tal near Bad Harzburg, Harz, Germany. Uncrossed polarizers, 4.0 × 5.5 mm.

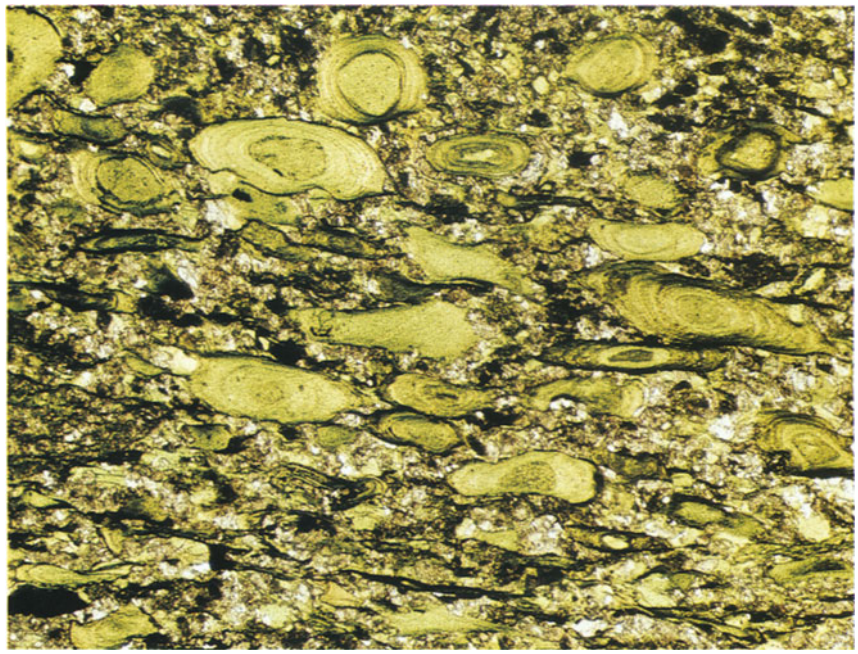

13 Rounded to elliptical stretched glauconite aggregates, showing concentric growth rings. Glauconite with characteristic bright-green pleochroism. The matrix consists of colourless to red-brown Fe-hydroxide bearing calcite. Canaglia, Sardinia. Uncrossed polarizers, 2.4 × 3.2 mm.

14 Idiomorphic sphene crystal showing strong pleochroic colours which mask the higher-order interference colours. Accompaning minerals are microcline-perthite, which locally is altered into sericite, nepheline and apatite. Nepheline syenite. Gjone near Larvik, southern Norway. Crossed polarizers, 2.4 × 3.2 mm.

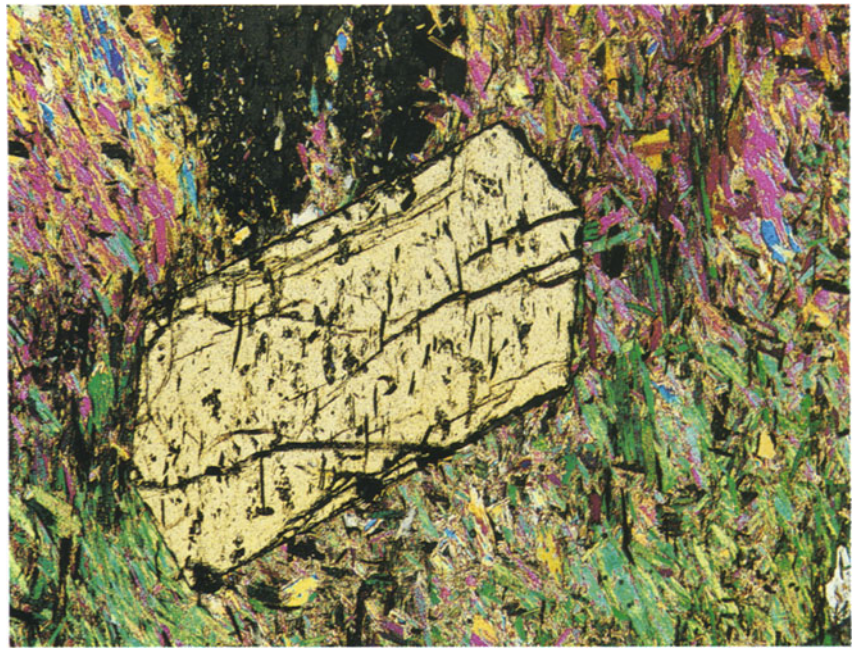

15 Idiomorphic, weakly pleochroic staurolite phenocryst with straw-yellow interference colours of the 1st order, next to almandine (isotropic) and lepidoblastic muscovite, which shows bright interference colours of the 2nd order. Garnet-staurolite-mica schist. Alpe Sponda, southern side of Lukmanier Pass, Canton Ticino, Switzerland. Crossed polars, 3.6 × 5.0 mm.

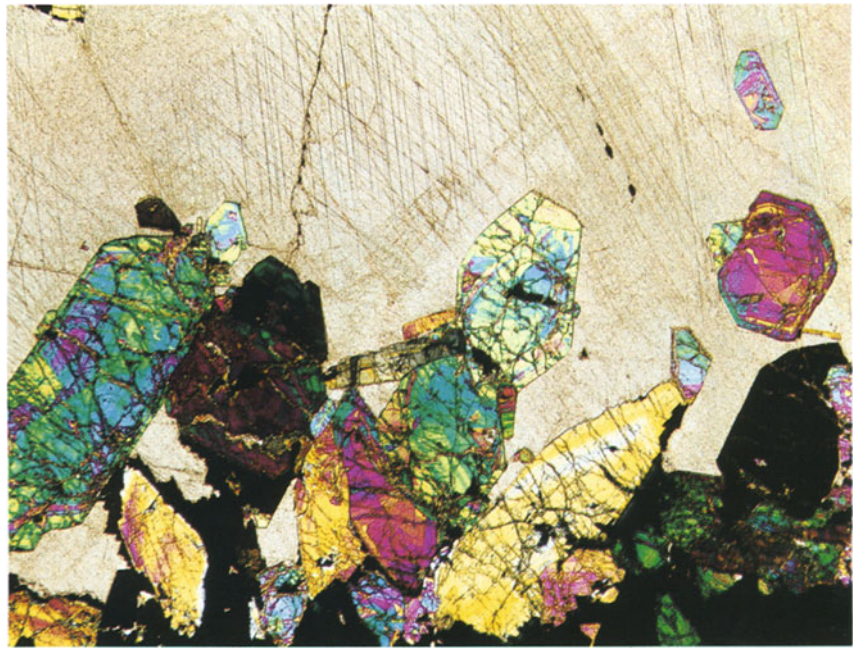

16 Idiomorphic, zoned epidote crystal with strong anomalous interference colours of the 2nd order (orange, yellow, red, green, blue), together with calcite, which clearly shows rhombic cleavage and mother-of-pearl interference colours of the higher orders. Epidote-marble. Lukmanier Pass, Canton Graubünden, Switzerland. Crossed polars, 5.0 × 6.9 mm.

a) Fibrous- or needle-shaped zeolites (natrolite, mesolite, thomsonite, scolecite, mordenite and laumontite).
b) Flaky zeolites (heulandite, stilbite and epistilbite).
c) Cube-shaped zeolites (chabazite, phillipsite and harmotome).

Trigonal chabazite (Part B, section 3.1.7) and the cubic analcite (Part B, section 2.7) and other minerals belong to the zeolite family.

Zeolite has the lowest refractive index of all minerals; zeolites are important minerals which form during the hydrothermal-magmatic stage, filling cavities and veins. They also play an important role in the classification of low-grade metamorphic (zeolite facies) rocks. In sedimentary rocks, particularly in pyroclastics and greywackes, analcite, clinoptilolite, heulandite, laumontite, mordenite and phillipsite are common. Phillipsite and clinoptilolite are important minerals in deep-sea sediments.

4.11.1 Fibrous zeolites

4.11.1.1 Natrolite

$Na_2[Al_2Si_3O_{10}] \cdot 2H_2O$ rhombic–pyramidal (pseudotetragonal)

Thin-section characteristics

Form: acicular to stalk-like parallel to the c-axis, fibrous to radiating and kidney-shaped (Figs 199, 200); rectangular cross-sections are typical.

Cleavage: good on {110}.

Twinning: rare on {110}.

Colour: colourless, older crystals can be clouded.

Refraction and birefringence:

n_α	= 1.473 – 1.489
n_β	= 1.476 – 1.491
n_γ	= 1.485 – 1.501
$\oplus\Delta$	= 0.012 – 0.012

Very low refraction with a negative relief and very low birefringence (white to straw-yellow in-

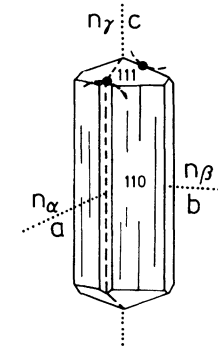

Fig. 199 Crystal form and optical characteristics of natrolite.

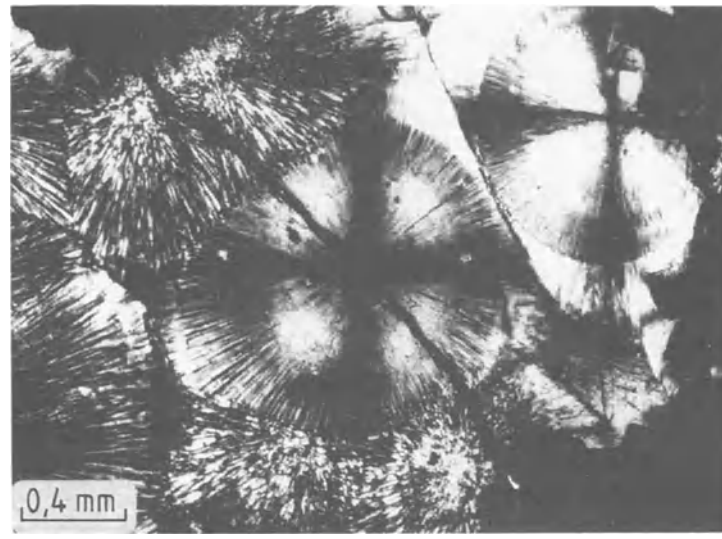

Fig. 200 Fibrous zeolite (mesolite) with very low refraction and birefringence forming the 'Brewster's Cross'. Tertiary tholeiitic basalt. Faeroe Islands. Crossed polars.

terference colours of the 1st order); optically biaxial ⊕.

Optic axial angle: $2V_\gamma = 58°–64°$.

Character of elongation: (+).

Extinction: in longitudinal sections straight, in basal section symmetric.

Special characteristics: pseudomorphs after plagioclase, nepheline and the minerals of the sodalite group are common.

Distinguishing features: thomsonite has a higher refraction and the other fibrous zeolites tend to have oblique extinction; chabazite is optically uniaxial; scolecite shows negative character of elongation.

Occurrence: in cavities and fractures in intermediate and basic magmatic rocks, particularly in volcanic rocks (e.g. in fractures in nephelinephonolites of the Hohentwiel/Hegau, Germany). As an autometasomatic alteration product of feldspars and foids (e.g. in the form of natrolite), together with the mineral hydronephelite, which typically replaces nepheline; common in nepheline syenites.

Paragenesis: with nepheline, Na-sanidine, scolecite, mesolite, heulandite, stilbite, laumontite, analcite, thomsonite, calcite and chalcedony.

4.11.1.2 Mesolite

$Na_2Ca_2[Al_2Si_3O_{10}]_3 \cdot 8H_2O$ monoclinic–sphenoidic

Thin-section characteristics

Form: fibrous aggregates.

Cleavage: perfect on (110) and on $(1\bar{1}0)$ (Fig. 201).

Twinning: simple twins on {100}, almost always twinned.

Colour: colourless.

Refraction and birefringence:

n_α	= 1.505
n_β	= 1.505
n_γ	= 1.506
⊕Δ	= 0.001

Low refraction and extremely low birefringence (maximum grey interference colours of the 1st order); optically biaxial ⊕.

Optic axial angle: $2V_\gamma = 80°$.

Character of elongation: alternating: (+) or (–).

Extinction: in most cases oblique.

Distinguishing features: all other fibrous zeolites show a much higher birefringence and tend to have a smaller axial angle.

Occurrence: in cavities in basaltic flows, particularly in basalts and phonolites.

Paragenesis: in basalts with zeolite and chalcedony. In phonolites with zeolite and calcite.

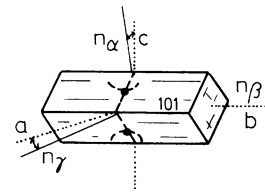

Fig. 201 Crystal form and optical characteristics of mesolite.

4.11.1.3 Thomsonite

$NaCa_2[Al_5Si_5O_{20}] \cdot 6H_2O$ rhombic–dipyramidal

Thin-section characteristics

Form: fibrous to radial or irregular arrangements, columnar stretched parallel to the c-axis or flaky parallel to {010}, rarely idiomorphic (Fig. 202).

Cleavage: perfect on (010) and good on (100).

Twinning: sometimes developed on {110}.

Colour: colourless.

Refraction and birefringence:

n_α	= 1.497 – 1.530
n_β	= 1.513 – 1.532
n_γ	= 1.518 – 1.545
$\oplus\Delta$	= 0.020 – 0.015

Low refraction and relatively low birefringence, which is nevertheless unusually high for zeolites (white interference colours of the 1st order to blue colours of the 2nd order); optically biaxial ⊕.

Optic axial angle: $2V_\gamma = 44°–75°$.

Character of elongation: alternates between (+) or (–).

Extinction: tends to be straight.

Distinguishing features: natrolite has a lower refraction and birefringence; all the other fibrous zeolites show oblique extinction; chabazite and analcite are optically uniaxial.

Occurrence: particularly common in amygdales in basic to ultramafic magmas (e.g. alkali basalt, phonolite, theralite, etc.). It can replace laumontite in the zeolite facies.

Paragenesis: with natrolite, chabazite, scolecite, analcite, calcite, albite, chalcedony, chlorite and clay minerals.

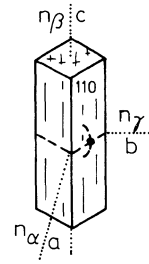

Fig. 202 Crystal form and optical characteristics of thomsonite.

4.11.1.4 Scolecite

$Ca[Al_2Si_3O_{10}]\cdot 3H_2O$ monoclinic–domatic (pseudorhombic)

Thin-section characteristics

Form: tends to be fibrous or radially arranged, rarely prismatic, growing parallel to the c-axis (Fig. 203).

Cleavage: good on {110}.

Twinning: almost always on (100).

Colour: colourless to cloudy.

Refraction and birefringence:

n_α	= 1.509 – 1.514
n_β	= 1.516 – 1.520
n_γ	= 1.521 – 1.525
$\ominus\Delta$	= 0.012 – 0.011

Low refraction and birefringence (grey to white interference colours of the 1st order), optically biaxial ⊖.

Optic axial angle: $2V_\gamma = 36°$ (–58°).

Character of elongation: (–) (distinguishes scolecite from natrolite and thomsonite).

Extinction: tends to be oblique, $\alpha\Lambda c = 15°–18°$.

Distinguishing features: natrolite and thomsonite tend to show oblique extinction; laumontite has a (+) elongation. Other fibrous minerals are characterized by a much higher refractive index.

Occurrence: as a hydrothermal mineral, similar to natrolite and thomsonite, in amygdales and fractures in basic rocks; also in cavities in metamorphic rocks. Tends to form pseudomorphs.

Paragenesis: with natrolite, thomsonite, stilbite, heulandite, calcite, chlorite, adularia and chalcedony.

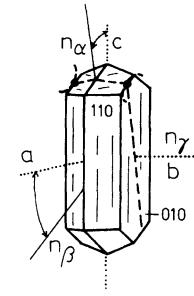

Fig. 203 Crystal form and optical characteristics of scolecite.

4.11.1.5 Mordenite

$(Ca, K_2, Na_2)[AlSi_5O_{12}]_2 \cdot 6H_2O$ rhombic–pyramidal

Thin-section characteristics

Form: tends to be fibrous, radiating aggregates, dense in pore-space in sediments and sedimentary rocks.

Cleavage: good on (100), not so good on (010).

Colour: colourless, can be coloured red by haematite inclusions.

Refraction and birefringence:

n_α	= 1.472 – 1.483
n_β	= 1.475 – 1.485
n_γ	= 1.477 – 1.487
$\oplus\Delta$	= 0.005 – 0.004

Extremely low refraction and birefringence (black-grey interference colours of the 1st order); optically biaxial ⊕ or ⊖.

Optic axial angle: $2V_{\alpha,\gamma} = 76°–90°$.

Character of elongation: can be (+) or (–).

Extinction: tends to be straight.

Distinguishing features: natrolite and thomsonite have a smaller axial angle and a higher birefringence; phillipsite tends to be twinned; other zeolites show oblique extinction and a higher refraction.

Occurrence: in amygdales and fractures in basic to acidic volcanic rocks. It also occurs as a hydrothermal alteration product of volcanic glasses, and as a mineral of the zeolite facies.

Paragenesis: in intermediary to basic volcanic rocks with heulandite, laumontite and stilbite. In sandstones with quartz and analcite. In limestones with carbonate, glauconite, kaolinite and hydromica.

4.11.1.6 Laumontite

$Ca[Al_2Si_4O_{12}] \cdot 4H_2O$ monoclinic–sphenoidic

Thin-section characteristics

Form: tends to form radiating and spherolitic aggregates; also as idiomorphic prismatic crystals parallel to the c-axis (Figs 204, 205).

Cleavage: perfect on (010) and {110}, good on (100); in the [001] zone, laumontite shows three very distinctive cleavage sets.

Twinning: sometimes after (100).

Colour: colourless.

Refraction and birefringence:

n_α	= 1.502 – 1.513
n_β	= 1.512 – 1.524
n_γ	= 1.514 – 1.525
$\ominus\Delta$	= 0.012 – 0.012

Low refraction and birefringence (white to straw-yellow of the 1st order); optically biaxial ⊖.

Optic axial angle: $2V_\alpha = 22°–47°$.

Character of elongation: (+).

Extinction: tends to be oblique, $\gamma \Lambda c = 8°–11°$ (dependent on the degree of water loss.).

Distinguishing features: natrolite and thomsonite have a straight extinction; scolecite has a (–) elongation; heulandite has a lower birefringence. Other similar fibrous minerals all show a much higher birefringence.

Occurrence: in cavities and fractures in basic and acidic magmatic rocks; in basalt, gabbro to rhyolite and granite. In regionally metamorphosed areas it occurs in the zeolite facies in metagreywackes and metatuffs; with increasing metamorphism it is replaced by heulandite.

Paragenesis: with heulandite, thomsonite, stilbite, apophyllite, analcite, epidote, datolite, albite, quartz, calcite, prehnite and chlorite.

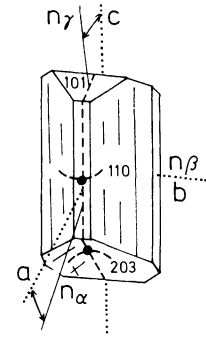

Fig. 204 Crystal form and optical characteristics of laumontite.

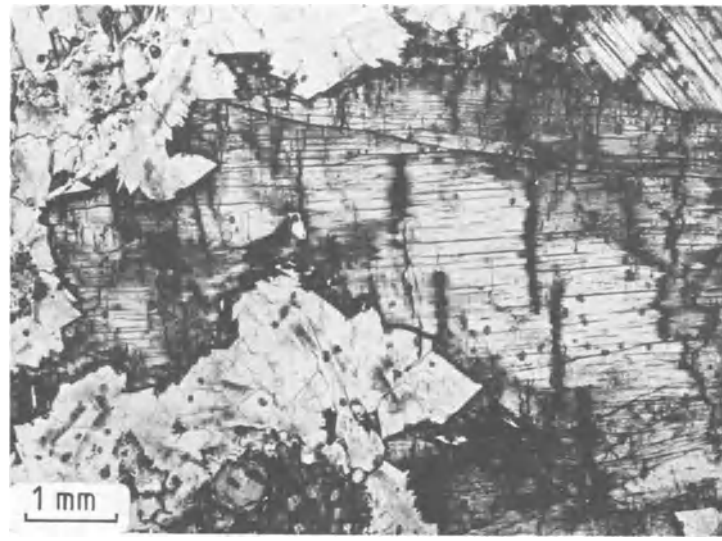

Fig. 205 Laumontite showing red coloration along its rims and fractures; characteristic cleavage. Cavity in leucite tephrite. Vesuvius volcano, Italy. Uncrossed polarizers.

4.11.2 Flaky zeolites

4.11.2.1 Heulandite

$Ca[Al_2Si_7O_{18}]\cdot 6H_2O$ monoclinic–prismatic (pseudorhombic)

Thin-section characteristics

Form: tabular, flaky {010}; subparallel aggregates, rare in rosettes (Figs 206, 207).

Cleavage: perfect on (010).

Twinning: simple on (001).

Colour: colourless, often coloured red by Fe-oxides.

Refraction and birefringence:

n_α	= 1.496 – 1.499
n_β	= 1.497 – 1.500
n_γ	= 1.501 – 1.505
$\oplus\Delta$	= 0.005 – 0.006

Very low refraction and birefringence (grey interference colours of the 1st order); sections parallel (010) with grey-black interference colours of the 1st order ($\Delta = 0.001$); optically biaxial $\oplus$.

Optic axial angle: $2V_\gamma$ = 0°–50° (tends to be 34°).

Character of elongation: (–).

Extinction: oblique, $\beta \Lambda c$ = 0°–32°.

Special characteristics: conoscopic axial images show crossed dispersion in sections parallel to (010).

Distinguishing features: natrolite and thomsonite show straight extinction; scolecite and laumontite are optically biaxial $\ominus$; stilbite tends to occur in branching aggregates and intercrossing twins are typical.

Occurrence: in amygdales and cracks of basic and acidic rocks. It is an important alteration product in volcanic glass. Heulandite also occurs in the zeolite facies in regionally metamorphosed rocks, and as a diagenetic matrix mineral in sandstones.

Paragenesis: commonly together with analcite and laumontite, quartz, stilbite and clay minerals. In sedimentary rocks with stilbite, analcite, laumontite and clay minerals.

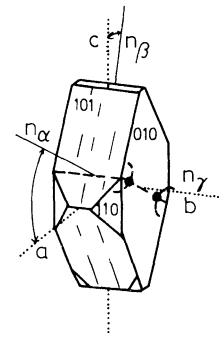

Fig. 206 Crystal form and optical characteristics of heulandite.

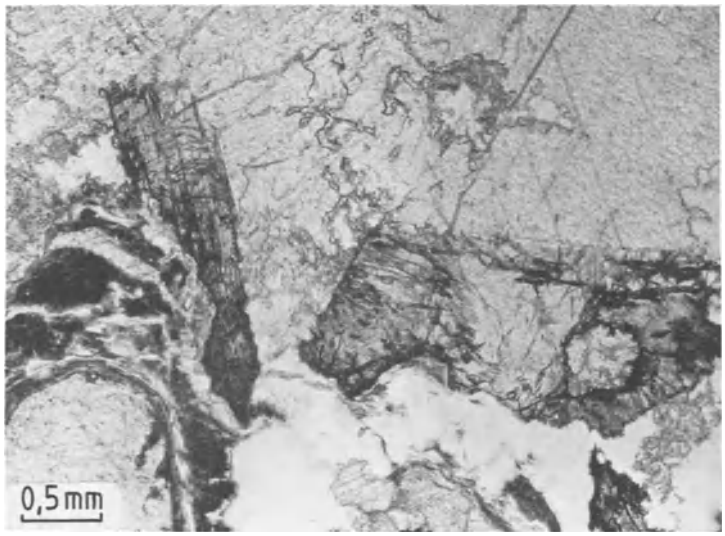

Fig. 207 Pale-red heulandite next to dolomite with typical rhombohedral cleavage. Cavity filling in a porphyry. Lasfreide Cave, Seiser Alm, South Tyrol, Italy. Uncrossed polarizers.

4.11.2.2 Stilbite

$Ca[Al_2Si_7O_{18}]\cdot 7H_2O$ monoclinic–prismatic

Thin-section characteristics

Form: commonly in branching aggregates, rare in spherolites and also as idiomorphic tabular crystals parallel to {010} and elongated in the direction of the c-axis (Figs 208, 209).

Cleavage: perfect on (010), poor on $\{10\bar{1}\}$.

Twinning: interpenetrating twins on (100).

Colour: colourless.

Refraction and birefringence:

n_α	= 1.486 – 1.498
n_β	= 1.494 – 1.507
n_γ	= 1.496 – 1.509
$\ominus\Delta$	= 0.010 – 0.011

Very low refraction and low birefringence (grey to white interference colours of the 1st order); optically biaxial ⊖.

Optic axial angle: $2V_\alpha = 30°–49°$.

Character of elongation: alternating (+) or (–).

Extinction: tends to be oblique, $\alpha\Lambda c = 3°–12°$.

Distinguishing features: heulandite, harmotome and phillipsite are optically biaxial ⊕.

Occurrence: same as all other zeolites, in amygdales and fractures in basic and acidic magmatic rocks.

Paragenesis: commonly together with heulandite, laumontite, calcite, quartz and clay minerals.

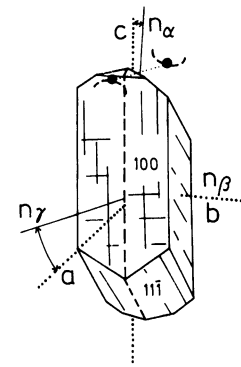

Fig. 208 Crystal form and optical characteristics of stilbite.

Fig. 209 Stilbite with branching, flaky crystal aggregates. Cavity in Tertiary tholeiitic basalt. Teigarhorn, eastern Iceland. Crossed polars.

4.11.2.3 Epistilbite

$Ca[Al_2Si_6O_{16}] \cdot 5H_2O$ monoclinic–prismatic

Thin-section characteristics

Form: tends to occur in radiating branching crystal, rarely acicular and prismatic, stretched along the c-axis or blade-shaped (Fig. 210).

Cleavage: perfect on (010).

Twinning: simple on {110} and {102}; intergrowth twins on (100) and {110}.

Colour: colourless.

Refraction and birefringence:

n_α	= 1.502 – 1.505
n_β	= 1.510 – 1.515
n_γ	= 1.512 – 1.519
$\ominus\Delta$	= 0.010 – 0.014

Low refraction and low birefringence, the latter being relatively high compared with other zeolites (grey-white to straw-yellow interference colours of the 1st order); optically biaxial $\ominus$.

Optic axial angle: $2V_\alpha = 44°$.

Character of elongation: (+).

Extinction: generally oblique $\gamma \wedge c = 10°$.

Distinguishing features: compared with other zeolites, the relatively high birefringence is distinctive; thomsonite has straight extinction; stilbite has a lower refraction and two cleavage sets; phillipsite is optically biaxial $\oplus$ and has straight extinction.

Occurrence: in hydrothermal amygdales in basalt and andesite.

Paragenesis: tends to occur together with stilbite, mordenite, heulandite, chabazite, laumontite and scolecite.

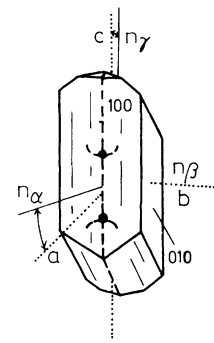

Fig. 210 Crystal form and optical characteristics of epistilbite.

4.11.3 Cubic zeolites

Chabazite (section 3.1.7)

4.11.3.1 Phillipsite

$(Ca_{0.5}, K, Na)_5[Al_5Si_{11}O_{32}] \cdot 10H_2O$ monoclinic–prismatic (pseudorhombic)

Thin-section characteristics

Form: thick columns parallel to the c-axis (Figs 211, 212) and flattened parallel {010}, idiomorphic intercrossed twins. Fine-grained it can fill pore spaces in sediments and sedimentary rocks.

Cleavage: clear on (010) and (100).

Twinning: interpenetrating twins on (100) and {110}.

Colour: colourless, also pale white and pale yellow.

Refraction and birefringence:

n_α	= 1.483 – 1.504
n_β	= 1.484 – 1.509
n_γ	= 1.486 – 1.514
$\oplus\Delta$	= 0.003 – 0.010

Very low refraction and birefringence (grey to straw-yellow interference colours of the 1st order); optically biaxial ⊕.

Optic axial angle: $2V_\gamma = 60°–80°$.

Character of elongation: (+).

Extinction: tends to be oblique $\gamma \Lambda c = 11°–30°$.

Special characteristics: twinning can produce pseudorhombic, pseudotetragonal or pseudocubic symmetry.

Distinguishing features: stilbite is optically biaxial ⊖; harmotome has a different optical orientation.

Occurrence: in miarolitic basic volcanic rocks and in cracks (e.g. in alkali basalt, tephrite, phonolite and also nepheline syenite). Fills cavities together with calcite in the hyalobasanite (limburgite) of the Kaiserstuhl, Germany. It is an important mineral in ocean-floor sediments; here, it also occurs as a secondary mineral, formed by alteration of volcanic glass, in hyaloclastites.

Paragenesis: with analcite, natrolite, mesolite, thomsonite, chabazite, calcite, chalcedony and clay minerals.

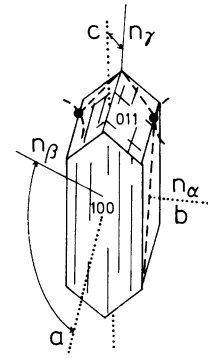

Fig. 211 Crystal form and optical characteristics of phillipsite.

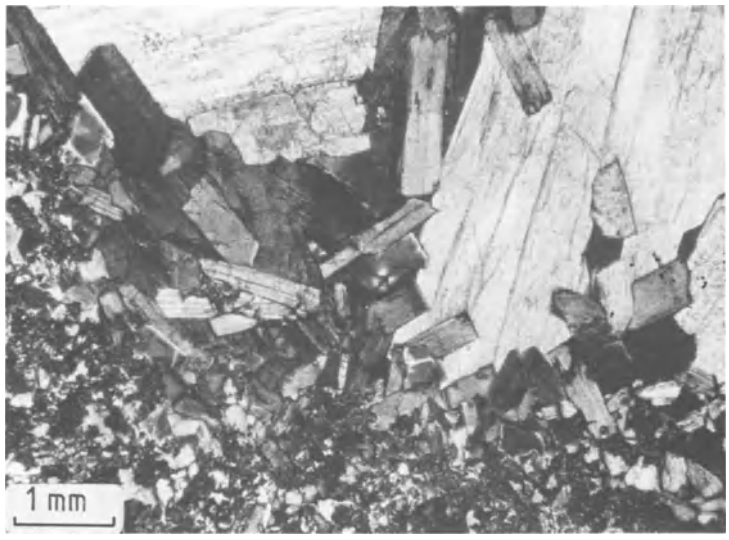

Fig. 212 Columnar to acicular zeolite crystal (phillipsite) filling a cavity. Tertiary zeolite-rich tholeiitic basalt. Teigarhorn, eastern Iceland. Crossed polars.

4.11.3.2 Harmotome

$Ba[Al_2Si_6O_{16}] \cdot 6H_2O$ monoclinic–sphenoidic

Thin-section characteristics

Form: tends to occur as interpenetrating twins of pseudorhombic symmetry, rare in thick columnar form (Fig. 213).

Cleavage: good on (010), poor on (100).

Twinning: interpenetrating twins on (100) (= 'morvenite') or intergrowth of four crystals, along {110}.

Colour: colourless.

Refraction and birefringence:

n_α	= 1.503 – 1.506
n_β	= 1.506 – 1.509
n_γ	= 1.508 – 1.514
$\oplus\Delta$	= 0.005 – 0.008

Low refraction and birefringence (grey to white interference colours of the 1st order), optically biaxial ⊕.

Optic axial angle: $2V_\gamma = 79°$ (during heating when mounting a section it can increase to 32°).

Character of elongation: can be either (+) or (–).

Extinction: oblique, $\beta \Lambda c = 28°–32°$ (during heating when mounting a section it can increase to 82°).

Distinguishing features: stilbite is optically biaxial ⊖; phillipsite is very similar, but it has a different optical orientation.

Occurrence: in miarolitic basic rocks, and in fractures in gabbros.

Paragenesis: with hyalophane (barium feldspar), laumontite, natrolite and calcite.

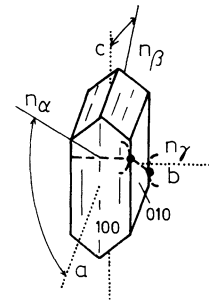

Fig. 213 Crystal form and optical characteristics of harmotome.

4.12 Aenigmatite (cossyrite)

$Na_4Fe^{2+}_{10}Ti_2[O_4|(Si_2O_6)_6]$ triclinic

General features: rare mineral, related to amphiboles, restricted to Na-rich magmatic rocks.

Thin-section characteristics

Form: columnar to acicular (Fig. 214). Similar form and habit to amphibole.

Cleavage: good on {100} and $\{1\bar{1}0\}$, with a cleavage intersection angle of approximately 66° (this feature distinguishes aenigmatite from amphibole). The twin plane halves the obtuse angle of the cleavage set.

Twinning: polysynthetic twins on $(0\bar{1}1)$ are common.

Colour: almost opaque (= black, Fig. 215); thin flakes red-brown to reddish-black translucent and pleochroic.
α: pale red-brown
β: dark chestnut-brown
γ: deep dark brown.

Refraction and birefringence:

n_α	= 1.81
n_β	= 1.82
n_γ	= 1.88
$\oplus\Delta$	= 0.07

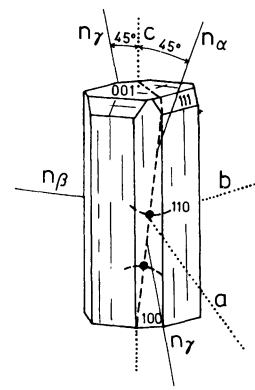

Fig. 214 Crystal form and optical characteristics of aenigmatite.

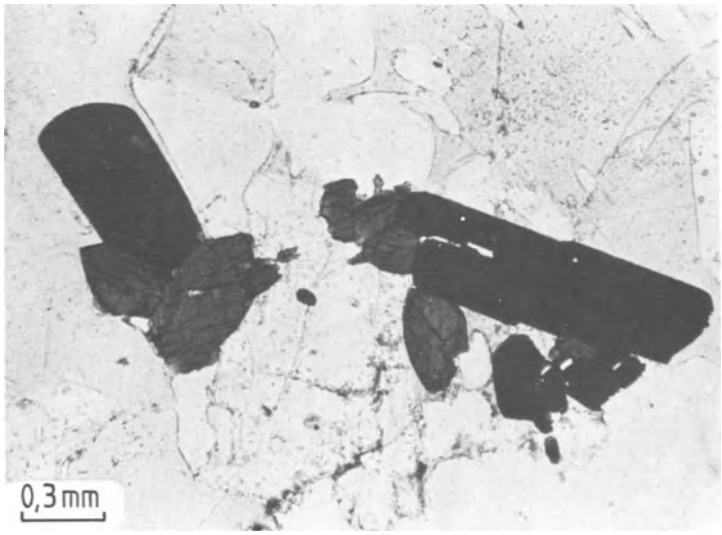

Fig. 215 Hypidiomorphic aenigmatite showing bright colours and strong relief in a glass-rich sodium-trachyte ('pantellerite'). Mt. Gelkhamar, Pantelleria island, Italy. Uncrossed polarizers.

High refraction and very high birefringence. The interference colours are of the upper orders and are very pale, masked by the dark crystal absorption colours; optically biaxial ⊕.

Optic axial angle: $2V_\gamma = 27°–55°$.

Extinction: always oblique, $\gamma\Lambda c$ 40°–45° parallel (010) and $\gamma\Lambda c \approx 4°$ (100).

Special characteristics: homoaxial intergrowth with arfvedsonite is common; orthite inclusions are surrounded by a black to smoky-brown halo.

Distinguishing features: rhönite occurs with a different paragenesis; in the case of kaersutite and arfvedsonite the twinning plane halves the angle of the cleavage planes.

Occurrence: in light-coloured Na-rich (alkaline) magmatic rocks, such as sodium syenite and sodium trachyte, pantellerite, comendite, nepheline syenite (foyaites), phonolite and nepheline-syenite pegmatites.

Paragenesis: with aegirine-augite, arfvedsonite or riebeckite, anorthoclase and nepheline.

4.13 Sphene (titanite)

$CaTi[O|SiO_4]$ monoclinic–prismatic

Thin-section characteristics

Form: tends to form idiomorphic, rhombic cross-sections, euhedra are common (in magmatic rocks, Fig. 216), rarely spindle-shaped or in clusters as thin granules (in metamorphic and sedimentary rocks).

Cleavage: good on {110}, generally not parallel to the crystal outlines.

Twinning: simple, along (100).

Colour: colourless, tends to be pale brown due to Fe-content, yellow to greenish with noticeable pleochroism; can show patchy colour distribution.
α: nearly colourless
β: pale yellow to pale greenish
γ: yellow to red-brown.

Refraction and birefringence:

n_α	= 1.843 – 1.950
n_β	= 1.870 – 2.034
n_γ	= 1.943 – 2.110
⊕Δ	= 0.100 – 0.192

High refraction and birefringence. White interference colours of the upper orders tend to be masked by the crystal colour and total reflection (Colour plate 14); optically biaxial ⊕. The high refraction causes a strong relief and an irregular surface.

Optic axial angle: $2V_\gamma = 20°–56°$.

Extinction: rhombic sections show symmetric extinction; because of the strong dispersion the extinction can be incomplete. Extinction tends to be oblique: $\gamma\Lambda c = 36°–51°$.

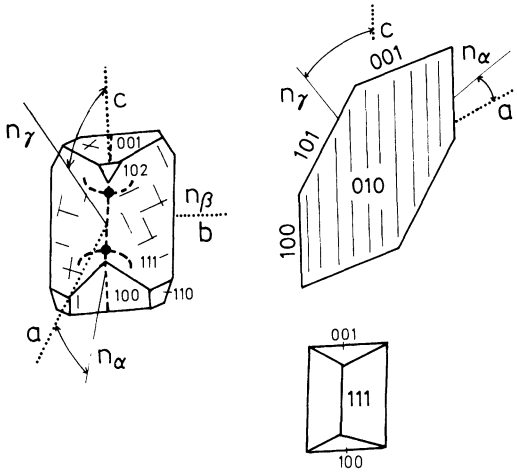

Fig. 216 Crystal form and optical characteristics and typical cross-sections of sphene.

Special characteristics: thorium content can cause pleochroic haloes; zoned crystals have a higher refractive index along their margins; in metamorphic rocks they tend to form clusters of small rounded pellets.

Distinguishing features: rutile, zircon and cassiterite are optically uniaxial ⊕; anatase and members of the carbonate group are optically uniaxial ⊖. If fine grained, sphene could be confused with epidote and orthite.

Alteration: under hydrothermal conditions it decays into pale-yellow leucoxene (ilmenite; Part B, section 1.2).

Occurrence: as a late magmatic phase in acidic and intermediate plutonic rocks (granite, granodiorite and tonalite, in particular in syenite to nepheline syenite), commonly together with greenish amphibole. It is rare in respective volcanic rocks, and absent in gabbro and basalt because there the Ti-content tends to pass into pyroxene (titanaugite) and ilmenite respectively. Sphene is a hydrothermal mineral in pegmatites and in alpine fractures. It also occurs in low- to medium-grade metamorphic rocks in amphibolite, marble and siliceous carbonates.

Paragenesis: with green hornblende, plagioclase, K-feldspar, quartz, apatite or nepheline, aegirine-augite, sanidine and apatite.

4.14 Topaz

$Al_2[(F, OH)_2|SiO_4]$ rhombic–dipyramidal

General features: fluor-bearing mineral, which forms in greisen (e.g. in cassiterite granite).

Thin-section characteristics

Form: short columns (Fig. 217), acicular parallel to the c-axis or brush-like (pycnite); typical as single granules.

Cleavage: very good on (001).

Colour: colourless.

Refraction and birefringence:

	(F)	(F, OH)
n_α	= 1.606 –	1.634
n_β	= 1.609 –	1.637
n_γ	= 1.616 –	1.644
⊕Δ	= 0.011 –	0.008

Medium-high refraction and low birefringence (grey-white to straw-yellow interference colours of the 1st order); optically biaxial ⊕. With increasing F-content the refraction decreases and the axial angle increases.

Optic axial angle: $2V_\gamma = 48°$ (F, OH); up to 68° (F).

Character of elongation: (+).

Extinction: in longitudinal sections the extinction is straight and in basal sections it is symmetric.

Special characteristics: tends to be rich in fluid inclusions.

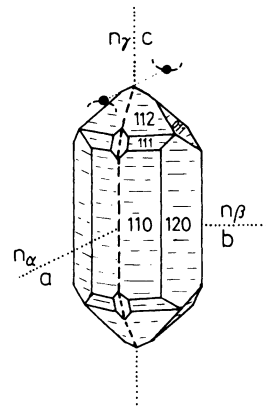

Fig. 217 Crystal form and optical characteristics of topaz.

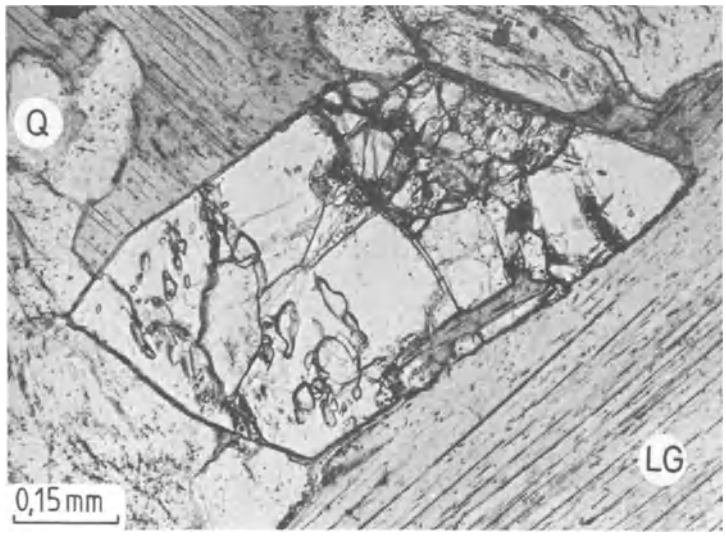

Fig. 218 Poikilitic topaz showing strong relief compared with quartz. Accompanying minerals are lithium-mica and quartz. Greisen. Zinnwald, Erzgebirge, Germany. Uncrossed polarizers.

Distinguishing features: quartz has a much lower refraction, tends to be optically uniaxial ⊕ and has no cleavage; barite and coelestine occur in different parageneses; beryl is optically uniaxial ⊖; andalusite has a patchy pinkish colour and is optically biaxial ⊖.

Alteration: into kaolinite is possible.

Occurrence: tends to occur at the margin of granite bodies (Fig. 218) and in contact aureoles as deuteric mineral which formed late during crystallization. Addition of fluor partly or completely alters feldspars and micas. It is also in topaz rhyolites.

4.15 Cordierite

$(Mg, Fe)_2Al_3[AlSi_5O_{18}]$ rhombic–dipyramidal (pseudo-hexagonal).

General features: cordierite (dichroite) is an important mineral in Al-rich metamorphic rocks.

Thin-section characteristics

Form: short prismatic parallel to the c-axis (Fig. 219), very rare as idiomorphic crystals in volcanic rocks or as porphyroblasts in hornfels; in metamorphic rocks it occurs as xenomorphic, irregular-shaped grains.

Cleavage: poor on (100), not visible under the microscope, often irregular fractures.

Twinning: in {110} and {310}; polysynthetic and pseudohexagonal parallel and interpenetrating trillings are common (Fig. 220). These are easily identified under crossed polars. Of the six sectors revealed, two tend to show extinction and the same interference colours at any one time, belonging to one crystal. Interpenetrating trillings are common in hornfels schist.

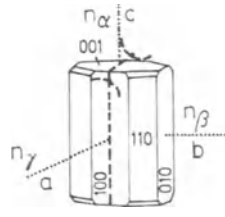

Fig. 219 Crystal form and optical characteristics of cordierite.

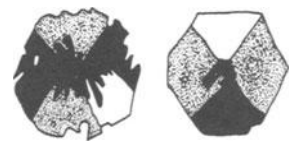

Fig. 220 Pseudohexagonal interpenetrating triplets of cordierite. Crossed polars.

Colour: colourless, if the thin section is of standard thickness; in 'thick' thin sections yellowish to pale-blue to pale-purple pleochroism; in volcanic rocks occasionally bright-blue and pale-purple pleochroism.

Refraction and birefringence:

n_α	= 1.527 – 1.560
n_β	= 1.532 – 1.574
n_γ	= 1.537 – 1.578
$\oplus\Delta$	= 0.008 – 0.018

Low refraction and birefringence (grey to straw-yellow interference colours of the 1st order); optically biaxial ⊖ or ⊕.

Optic axial angle: $2V_\alpha = 35°–106°$.

Character of elongation: (–), in most cases it cannot be determined.

Extinction: tends to be straight.

Special characteristics: radioactive inclusions, such as zircon, cause pleochroic haloes in cordierite; in metamorphic rocks poikiloblastic textures are typical, with quartz, biotite and/or graphite intergrowth. In volcanic rocks glass inclusions are common; in paragneisses fibrolitic sillimanite inclusions can be observed. Polysynthetic twinning is common.

Distinguishing features: can be mistaken for quartz, which, however, is uniaxial (rarely biaxial ⊕) and always fresh. Plagioclase tends to be zoned and has better cleavage (Table 5).

Alteration: subjected to weathering and diaphthoritic alteration, cordierite is progressively replaced, starting from the edges and along fractures by a dense aggregate of sericite and/or chlorite and also biotite. Cordierite pseudomorphs comprised of sericite and other phyllosilicates are referred to as pinite, and the process is called pinitization (Figs 221, 222). The break-down reaction consumes water, and hence is an indicator of hydrothermal interaction.

Table 5 Features distinguishing cordierite from quartz and feldspar

Cordierite	Quartz	Feldspar
biaxial (large 2V)	uniaxial, also anomalously biaxial (small 2V)	biaxial
poor cleavage	no cleavage	good cleavage
yellow pleochroic haloes	inclusion-free	
irregular fractures with clouding and pinitization	no alteration minerals	sericitization, saussuritization

Occurrence: in small quantities in magmatic rocks, as well as in granite and gabbro, rhyolite and andesite. Cordierite is an index mineral for the anatectic origin of the rock, or contamination by Al-rich contact rocks (e.g. clay-rich sediments). It is very common in contact-metamorphic rocks. In the outer contact aureole cordierite porphyroblasts are nobbly schists and it occurs in cordierite-hornfels. Cordierite is also present in regional-metamorphosed metapelites of high grade (e.g. cordierite gneiss). It is also

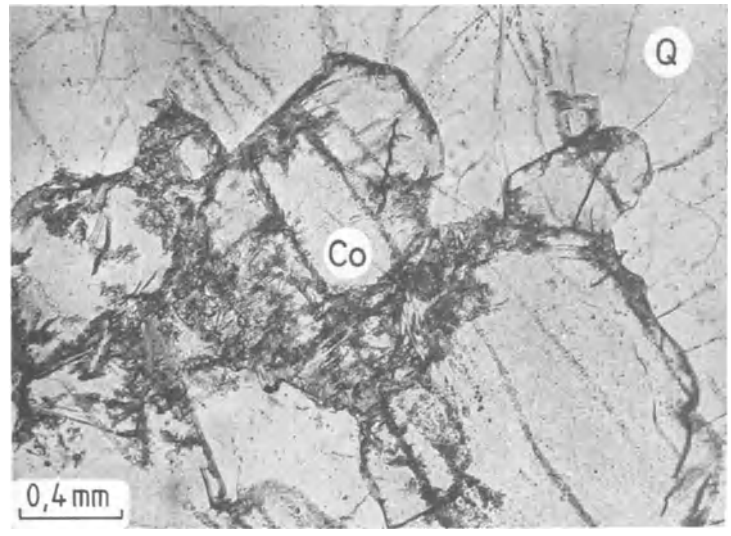

Fig. 221 Cordierite with pinitized margins next to quartz. Cordierite gneiss. Erratic boulder, Baltic Sea coastline, near Kiel, Germany. Uncrossed polarizers.

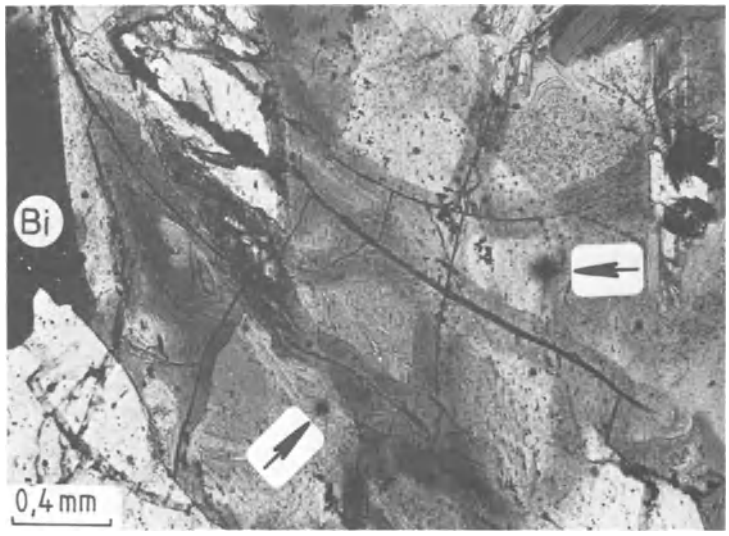

Fig. 222 Cordierite showing the typical yellowish pinitization along fractures and along the grain margins, affecting the whole crystal. Pleochroic haloes around zircon inclusions can be seen (arrows). Cordierite gneiss. Bodenmais, Bavarian Forest, Germany. Uncrossed polarizers.

common in granulites and charnockites, and can be found in pegmatitic metatectites.

Paragenesis: in magmatic and metatectites with quartz, K-feldspar, plagioclase, andalusite, sillimanite, biotite, garnet and hypersthene. In knobbly schist as newly formed blasts in a matrix of quartz, biotite, sericite, chlorite and graphite. In hornfels together with biotite, muscovite, quartz, plagioclase, andalusite, hypersthene and garnet. In silica-undersaturated rocks together with corundum and spinel. In regionally metamorphosed rocks together with sillimanite (as fibrolitic inclusions in cordierite), garnet, biotite, ilmenite and hercynite.

4.16 Al_2SiO_5 group

Andalusite	rhombic–dipyramidal
Sillimanite	rhombic–dipyramidal
Kyanite	triclinic–pinacoidal

General features: these three aluminum silicates are almost exclusively restricted to metamorphosed clay-rich sediments (metapelites). They are important metamorphic index minerals: kyanite is indicative of higher pressures, andalusite is stable at lower pressures but higher temperatures and sillimanite occurs at higher pressures and temperatures.

4.16.1 Andalusite

Thin-section characteristics

Form: columnar parallel to the c-axis (Fig. 223), nearly rectangular and square to longitudinal and basal sections; acicular to fibrous, brush-like, parallel fibrous, granular to skeletal, common in aggregates; porphyroblasts can be densely packed with quartz inclusions (sieve texture); individual crystals can form divergent, finger-like arrangements.

Cleavage: good on {110}, with the intersecting angle at 89°, only visible in coarse crystals.

Twinning: rare along {101}.

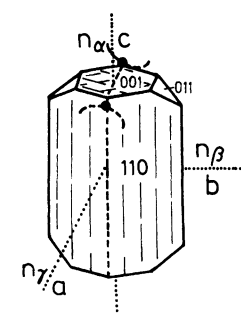

Fig. 223 Crystal form and optical characteristics of andalusite.

Colour: colourless (as **chiastolite**), otherwise pinkish colours with a patchy colour distribution are common (Fe-content) or greenish (Mn-content); pleochroism is weak:
α: pink, bright red, yellow
β: colourless, pale yellow, greenish
γ: colourless, pale yellow, greenish-yellow.

Refraction and birefringence:

n_α	= 1.633 – 1.642
n_β	= 1.639 – 1.644
n_γ	= 1.644 – 1.650
$\ominus\Delta$	= 0.009 – 0.012

Medium-high refraction (similar to apatite) and low birefringence (grey to straw-yellow interference colours of the 1st order); optically biaxial ⊖. The greenish Mn-rich variety is called **viridine**; it shows clear pleochroism and is optically biaxial ⊕.

Optic axial angle: $2V_\alpha = 73°–86°$ (~84°).

Character of elongation: in longitudinal sections (–).

Extinction: tends to be straight parallel to the prism sides and parallel to the {110} cleavage. Basal sections show symmetric extinction.

Special characteristics: can have yellowish pleochroic haloes around radioactive minerals (zircon); commonly contains graphite inclusions which can be symmetrically arranged forming a weak cross (chiastolite variety; Figs 224, 225).

Distinguishing features: sillimanite has a (+) elongation; kyanite shows oblique extinction and has higher birefringence and also shows a patchy blue coloration; the orthopyroxenes have a (+) elongation.

Alteration: replaced by sericite if subjected to hydrothermal and diaphthoritic alteration (very common in most crystals). With increasing pressure it is replaced by kyanite.

Occurrence: most common in metapelites in contact aureoles (e.g. knobbly schist of the outer zone of contact aureoles) where it forms porphyroblasts; chiastolite can be common. In the inner contact aureole it can occur together with cordierite in the hornfels facies. In regional low-pressure metamorphosed areas (Abukuma-type), andalusite can occur as porphyroblasts in medium-grade andalusite mica schists; also in pegmatites.

Paragenesis: in knobbly schists as porphyroblasts in a matrix of sericite and quartz. In hornfels facies together with biotite, cordierite, quartz, and occasionally pyroxene. In regionally metamorphosed rocks together with muscovite, biotite, almandine, also sillimanite and kyanite or staurolite and cordierite.

Fig. 224 Different chiastolite forms (symmetric arrangement of graphite).

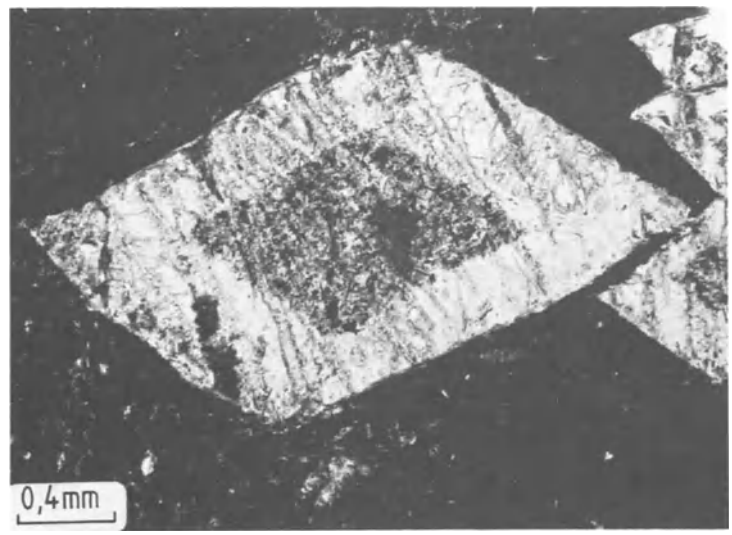

Fig. 225 Andalusite with graphite inclusions (chiastolite). Schist from Fichtelgebirge, Germany. Uncrossed polarizers.

4.16.2 Sillimanite

Thin-section characteristics

Form: acicular, fibrous parallel to the c-axis (Figs 226, 227), branching, hair-like, rarely columnar parallel to the c-axis; common as subparallel whirlpool-like fibrous swarms and strings in quartz or cordierite (Fig. 228). Brush-like aggregates of fibrous sillimanite are called **fibrolite** (Fig. 229). Fibrolite can be kinked or bent.

Cleavage: perfect on (010), only visible in larger crystals; cleavage traces run diagonally across the pseudotetragonal cross-section.

Colour: colourless, in 'thick' thin sections it can be pale-brownish to pale-brown pleochroic; fibrolite can be dirty yellow-brown.

Refraction and birefringence:

n_α	= 1.653 – 1.661
n_β	= 1.657 – 1.662
n_γ	= 1.672 – 1.683
$\oplus\Delta$	= 0.018 – 0.022

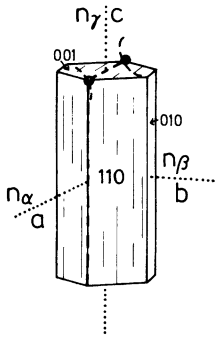

Fig. 226 Crystal form and optical characteristics of sillimanite.

Medium-high refraction and birefringence (interference colours of the upper 1st order to blue of the 2nd order; not recognizable in needles; basal sections show grey to white interference colours of the 1st order); optically biaxial ⊕.

Optic axial angle: $2V_\gamma = 21°–30°$ (in most cases it cannot be measured).

Character of elongation: (+).

Extinction: straight parallel to the trace of the cleavage, basal sections show symmetric extinction.

Distinguishing features: apatite and andalusite have (–) elongation; kyanite is optically biaxial ⊖ and also has two perfect cleavage sets; zoisite has a lower birefringence and tremolite has oblique extinction.

Alteration: sericitization.

Occurrence: high-grade metamorphism in metapelites (e.g. cordierite sillimanite gneiss). As contact-metamorphic mineral only in the sanidinite facies.

Paragenesis: with andalusite, cordierite (often with whirl-pool like fibrolite inclusions), quartz, K-feldspar, plagioclase, biotite, muscovite, almandine and spinel. Sillimanite and kyanite often occur together; 'sillimanitization' (Fig. 230) is characteristic for progressive metamorphic conditions.

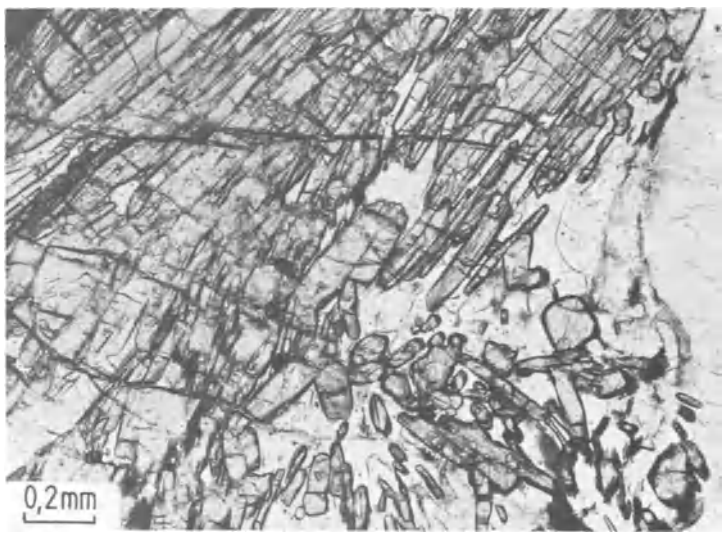

Fig. 227 Idiomorphic sillimanite laths showing perfect cleavage and strong relief relative to quartz. Sillimanite gneiss. Erratic boulder, Baltic Sea coastline, near Kiel, Germany. Uncrossed polarizers.

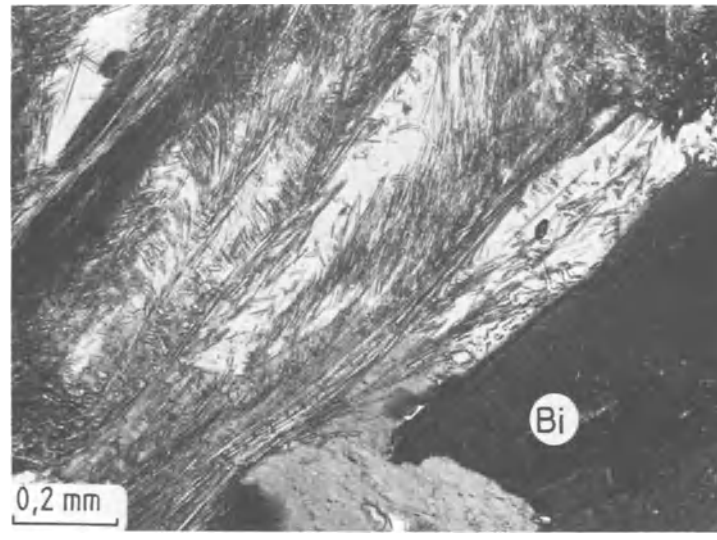

Fig. 228 Fibrolite in quartz next to biotite. Sillimanite gneiss. Erratic boulder, Baltic Sea coastline, near Kiel, Germany. Uncrossed polarizers.

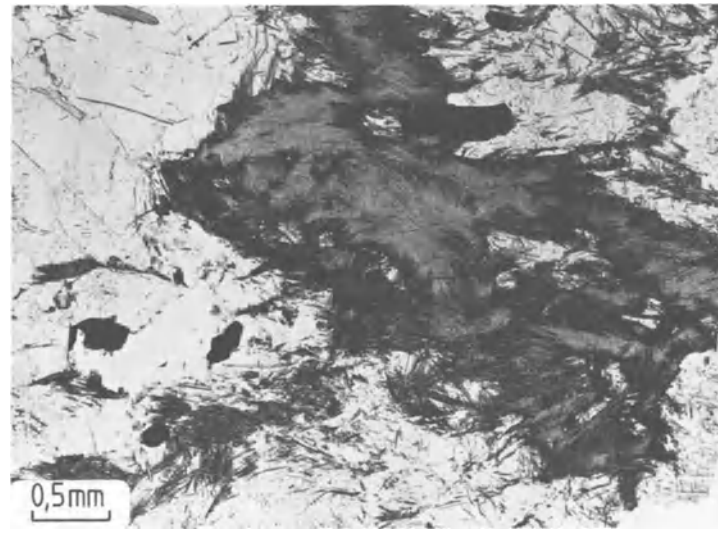

Fig. 229 Sillimanite fibrolite forming dark fibrolitic aggregates. Erratic boulder, Baltic Sea coastline, near Kiel, Germany. Uncrossed polarizers.

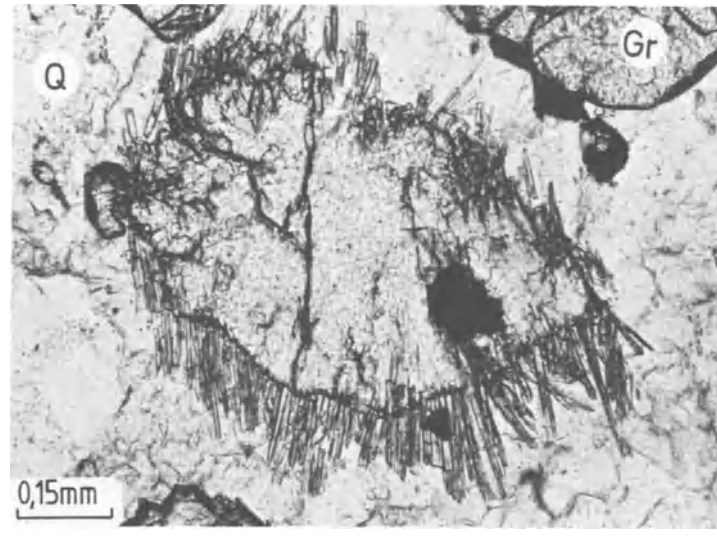

Fig. 230 Kyanite replaced by sillimanite along its margins. Kyanite granulite. Harlanden/ Danube, Austria. Uncrossed polarizers.

4.16.3 Kyanite

Thin-section characteristics

Form: tabular, broad lath-shaped, stretched along the c-axis (Fig. 231); in schists as broad prisms, rarely in radial arrangements. Kyanite rich in fine dusty graphite inclusions is called **rhaeticite**. Can be crystallographically intergrown with staurolite; deformation-induced bent crystals have been observed.

Cleavage: perfect on (100) and excellent on (010) (Fig. 232); along (001) characteristically frayed parting.

Twinning: simple on (100) and lamellar with [100] as twinning axis and nearly equal extinction angle in both twin halves.

Colour: colourless to pale blue, sometimes with patchy blue weak pleochroism:
α: colourless
β: pale purple-blue
γ: pale cobalt-blue.

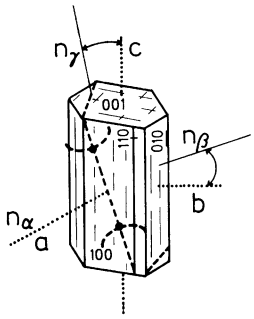

Fig. 231 Crystal form and optical characteristics of kyanite.

Refraction and birefringence:

n_α	= 1.710 – 1.718
n_β	= 1.719 – 1.724
n_γ	= 1.724 – 1.734
$\ominus\Delta$	= 0.012 – 0.016

High refraction and relatively low birefringence (orange-yellow interference colours of the 1st order); optically biaxial ⊖.

Optic axial angle: $2V_\alpha$ = 78°–83°.

Character of elongation: (+).

Extinction: always oblique: $\gamma' \Lambda_c$ = 27°–32° on (100) and $\gamma' \Lambda c$ = 5°–8° (010); $\alpha' \Lambda a$ = 0°–3° on (001).

Special characteristics: patchy blue, pleochroic colour distribution. Porphyroblasts tend to contain numerous inclusions of quartz and mica (sieve texture). Crystallographic intergrowth with staurolite is possible (Part B, section 4.17).

Distinguishing features: hypersthene shows straight extinction in longitudinal sections; clinozoisite has anomalous interference colours; sillimanite has a higher birefringence, but a lower refraction and is optically ⊕; andalusite has a similar birefringence, but a much lower refraction and is distinct because of its patchy pink colour distribution.

Alteration: under progressive metamorphic conditions it is replaced by sillimanite; diaphthoritic alteration leads to sericitization.

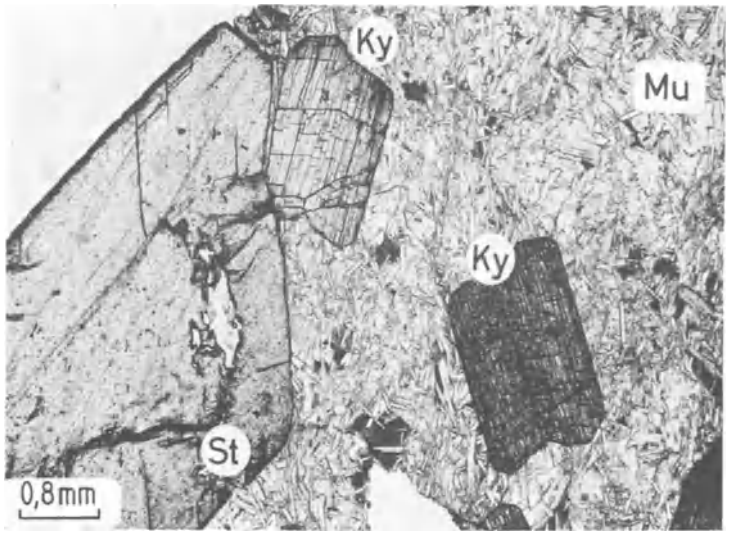

Fig. 232 Twinned kyanite porphyroblast with perfect cleavage in two directions and a strong relief adjacant to a large staurolite porphyroblast. Staurolite-kyanite-muscovite-mica schist. Alp Sponda, Canton Ticino, Switzerland. Uncrossed polarizers.

Occurrence: characteristic for medium- and high-pressure mineral assemblages; porphyroblastic (e.g. in kyanite-staurolite-mica schist, kyanite gneiss and kyanite quartzite as well as in granulite and eclogite).

Paragenesis: with staurolite, almandine, green hornblende, biotite, muscovite, quartz and rutile.

4.17 Staurolite

$Al_4Fe^{2+}[O|OH|SiO_4]_2$ monoclinic–prismatic (pseudo-rhombic)

General features: index mineral in medium-grade Al-rich rocks, often together with kyanite.

Thin-section characteristics

Form: idiomorphic with short prismatic habit, stretched parallel to the c-axis with hexagonal cross-section; common as interpenetrating twins (Fig. 233). Smaller crystals can form glomerophyric-textured aggregates.

Cleavage: good on (010); in a thin section, specially in small crystals, difficult to recognize.

Twinning: interpenetrating twins on {023} or {232}; under the microscope not readily recognizable (Fig. 233).

Colour: bright orange-yellow (Colour plate 15) with clear pleochroism in longitudinal sections. In basal sections weak or non-pleochroic:
α: colourless
β: colourless, pale yellow, yellowish-brown
γ: light yellow, orange-yellow, reddish-brown.

Refraction and birefringence:

n_α	= 1.736 – 1.747
n_β	= 1.742 – 1.753
n_γ	= 1.748 – 1.761
$\oplus\Delta$	= 0.011 – 0.014

High refraction and relatively low birefringence (orange-yellow interference colours of the 1st order); optically biaxial ⊖.

Optic axial angle: $2V_\gamma = 80°–90°$.

Character of elongation: (+).

Extinction: occurs mostly in bases and cuts which are symmetrical.

Special features: can show oriented intergrowth with kyanite, rarely muscovite; poikiloblastic intergrowth with quartz is common (sieve texture; Fig. 234); rare inclusion of other minerals (rutile, tourmaline, garnet).

Distinguishing features: orange-yellow pleochroism and sieve texture are distinctive. Brown tourmaline is optically uniaxial ⊖ and has a negative elongation; epidote is greenish-yellow and has a higher birefringence with anomalous interference colours and is optically biaxial ⊖; the same applies to orthite.

Alteration: with increasing metamorphic grade it is replaced by almandine and kyanite or almandine and sillimanite respectively. During retrograde alteration staurolite tends to be replaced by chlorite and sericite.

Occurrence: restricted to medium-grade metapelites, such as staurolite micaschists, garnet micaschist, quartzite and metabauxite.

Paragenesis: with biotite, muscovite, kyanite, next to quartz, albite, rutile, andalusite and almandine or sillimanite or tourmaline.

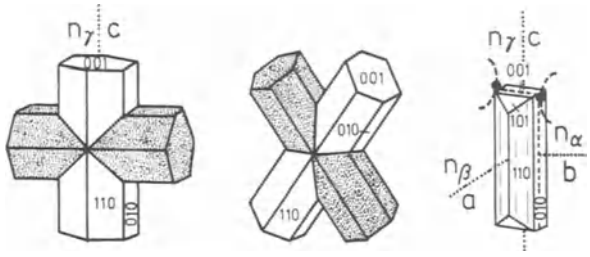

Fig. 233 Crystal form and optical characteristics and twinning in staurolite.

Fig. 234 Poikiloblastic (sieve texture) in twinned staurolite crystal.

4.18 Wollastonite

$Ca_3[Si_3O_9]$ triclinic–pinacoidal (pseudo-monoclinic), monoclinic–prismatic (para-wollastonite)

Thin-section characteristics

Form: columnar to acicular parallel to the b-axis (Fig. 235), subparallel or diverging or brush-like aggregates are common, also platy on {100} with almost rectangular cross-sections, poikiloblastic.

Cleavage: perfect on (100), good on ($\bar{1}02$) and (001) (Fig. 236).

Twinning: lamellar on (100).

Colour: colourless.

Refraction and birefringence:

n_α	= 1.616 – 1.640
n_β	= 1.628 – 1.650
n_γ	= 1.631 – 1.653
$\ominus\Delta$	= 0.013 – 0.014

Medium-high refraction and relatively low birefringence (maximum orange-yellow interference colours of the 1st order, in longitudinal sections grey to white interference colours of the 1st order); optically biaxial $\ominus$.

Optic axial angle: $2V_\alpha = 36°–60°$.

Character of elongation: can be (+) or (–).

Extinction: always oblique; in longitudinal sections almost straight: $\beta \Lambda b = 0°–5°$; $\alpha \Lambda c = 30°–44°$.

Special characteristics: none.

Distinguishing features: tremolite has a characteristic amphibole cleavage and a much larger axial angle and higher birefringence; zoisite has a higher refraction and lavender-blue interference colours.

Alteration: into quartz, chalcedony or opal.

Occurrences: in contact-metamorphosed zones in the hornfels facies in lime silicate rocks and siliceous marbles. In the same rocks it is also found in regionally metamorphosed areas in low- to medium-grade facies (e.g. lime silicate rocks Auerbach/Bergstrasse, Germany). It is rare in phonolites (e.g. wollastonite phonolite from Kaiserstuhl, Germany), in nepheline syenite and nephelinite.

Paragenesis: with diopside, fassaite, vesuvianite, epidote, grossularite, calcite, quartz and microcline. Monticellite together with wollastonite are index minerals of the onset of the sanidine facies.

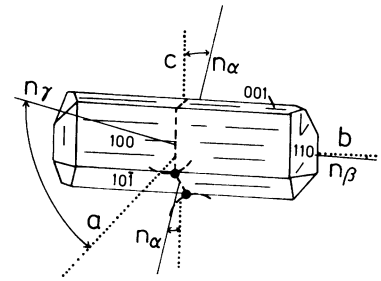

Fig. 235 Crystal form and optical characteristics of wollastonite.

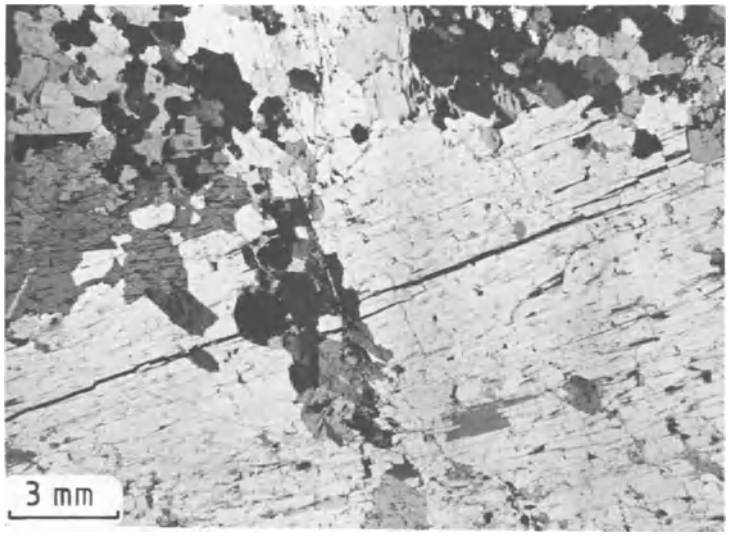

Fig. 236 Coarse prismatic wollastonite with well-developed cleavage. Siliceous metacarbonate. Sala, central Sweden. Crossed polars.

4.19 Chloritoid

$(Fe^{2+}, Mg, Mn)_2(Al, Fe^{3+})Al_3[(OH)_4|O_2|(SiO_4)_2]$ triclinic–pinacoidal (twinning can produce pseudo-hexagonal symmetry)

General features: chemically very similar to staurolite; it occurs exclusively in regionally metamorphosed areas in the greenschist facies.

Thin-section characteristics

Form: idiomorphic, porphyroblastic, platy on {001}; longitudinal or flaky, radial and plate-like aggregates, often in glomerates (Figs 237, 238). Habit similar to mica.

Cleavage: perfect on (001), good on (110).

Twinning: twins, trillings or polysynthetic twins on (001).

Colour: colourless, tends to be green or grey-green with a very strong pleochroism:
α: greenish, olive-green, colourless, greenish-blue
β: slate-blue, indigo blue, blue-green
γ: colourless, yellow-green, yellow pale greenish-brown.

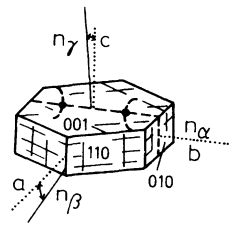

Fig. 237 Crystal form and optical characteristics of chloritoid in monoclinic form.

Refraction and birefringence:

n_α	= 1.705 – 1.730
n_β	= 1.708 – 1.734
n_γ	= 1.712 – 1.740
⊕Δ	= 0.005 – 0.022

High refraction and relatively low birefringence (grey-white to straw-yellow interference colours of the 1st order; basal sections are approximately isotropic); optically biaxial ⊕. Low anomalous interference colours are common (r > v).

Optic axial angle: $2V_\gamma$ = 36°–70°, in rare cases optically ⊖ with $2V_\gamma \approx 124°$.

Character of elongation: (–).

Extinction: tends to be oblique, $\beta \wedge b = 20°$ (in the triclinic form); straight in the direction of the b-axis: $\alpha \wedge b = 0°$ (in the monoclinic form).

Special characteristics: hourglass textures are common; zonal growth with darker cores and brighter rims; inclusions (in particular of quartz) are typical; four-fold partitioning.

Distinguishing features: chlorite has a much lower refraction, absorption colours and commonly anomalous interference colours; biotite has a smaller axial angle and is optically biaxial ⊖; all other micas show higher birefringence colours.

Alteration: by progressive regional metamorphism it is replaced by staurolite, almandine and

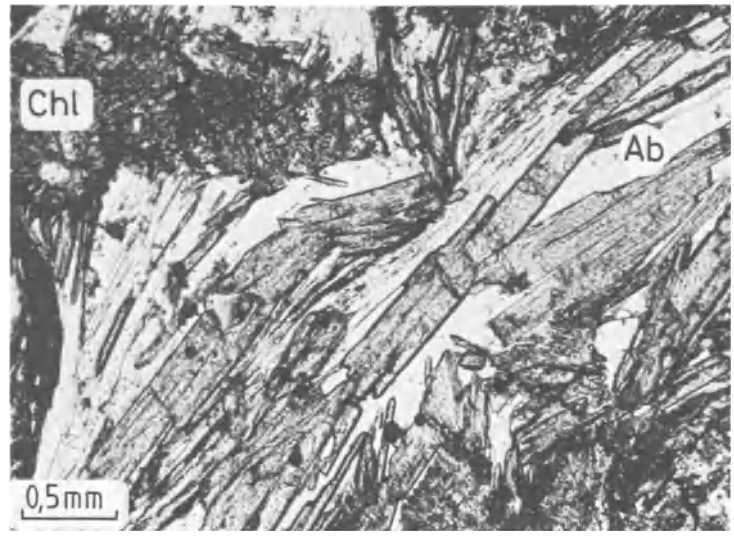

Fig. 238 Columnar chloritoid together with albite and chlorite. Albite-chlorite-chloritoid schists. Baños, eastern Cordillera, Ecuador. Uncrossed polarizers.

hercynite. Retrograde chloritization and/or weathering into kaolinite/limonite.

Occurrence: typical mineral in Fe-Al-rich metapelites of the greenschist facies (e.g. chloritoid phyllites) and also in glaucophane schists.

Paragenesis: with quartz, albite, sericite, chlorite, biotite, almandine, rutile and also glaucophane, never together with stilpnomelane. Can occur with staurolite, kyanite and almandine.

4.20 Epidote zoisite group

General features: zoisite replaces the albite component in plagioclase in low- to high-grade metamorphic rocks. Both the endmembers, epidote and clinozoisite, form the epidote sequence, in which part of the aluminium is progressively replaced by Fe^{3+}; epidote is a typical mineral of the greenschist facies. Orthite differs from epidote by its high content of rare earth elements, particularly cerium and lanthanum.

Special characteristics: members of the epidote–zoisite group show concentric zonal patterns, with Fe-poor cores and Fe-rich rims (interference colours); rims can alter to hornblende or pyroxene. A characteristic section from a metamorphic rock is illustrated in Fig. 239.

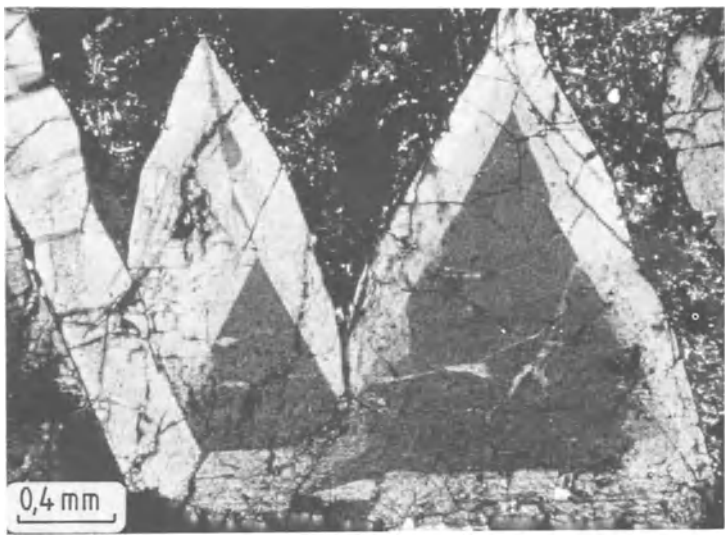

Fig. 239 Zoisite with three-sided section and zonar growth. Anomalous interference colours (deep blue to brown) are typical. Zoisite schist. Scotland. Crossed polars.

4.20.1 Zoisite

$Ca_2(Al, Fe^{3+})Al_2[O|OH|SiO_4|Si_2O_7|$ rhombic–bipyramidal

Thin-section characteristics

Form: short prisms parallel to the b-axis (Fig. 240), in longitudinal sections commonly rhombic-shaped or hexagonal cross-sections; granular and divergent radiating prisms.

Cleavage: perfect on (100) and poor on (001) (Fig. 240).

Colour: nearly colourless; the Mn-rich variety is called **thulite** and shows purple-pink to yellowish pelochroism:
α: pale greenish-yellow
β: purple-pink
γ: yellow.

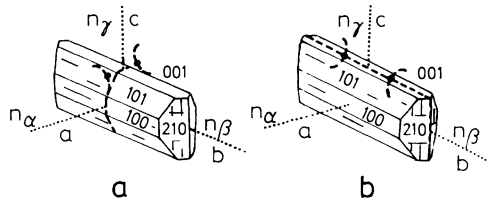

Fig. 240 Crystal form and optical characteristics of (a) Fe-poor and (b) Fe-rich zoisite.

Refraction and birefringence:

n_α	= 1.685 – 1.705
n_β	= 1.688 – 1.701
n_γ	= 1.697 – 1.725
$\oplus\Delta$	= 0.003 – 0.008

Medium-high refraction and relatively low birefringence with anomalous interference colours in sections approximately perpendicular to the optic axis (deep blue-grey to brown interference colours); in different sections normal interference colours of the 1st order (grey to orange-yellow); optically biaxial ⊕.

Optic axial angle: $2V_\gamma = 0°–69°$.

Character of elongation: in longitudinal sections always (–).

Extinction: tends to be straight.

Special characteristics: anomalous interference colours; intergrowth with epidote and clinozoisite is common. Orientation of the axial plane is dependent on the Fe-content (Fig. 240).

Distinguishing features: clinozoisite is optically very similar, but differs by its extreme anomalous interference colours (bright prussian blue); apatite is optically uniaxial ⊖, and so is vesuvianite, which can be anomalously biaxial, with anomalous interference colours and hence could be confused with zoisite. Hypersthene is optically biaxial ⊖.

Alteration: none.

Occurrence: zoisite without exception occurs in regionally metamorphosed rocks (e.g. in greenschist, actinolite and glaucophane rocks). At low-metamorphic grade it forms from the anorthite component of plagioclase (saussuritization). During this process anorthite is replaced by a very fine-grained aggregate of zoisite, epidote-clinozoisite, sericite and calcite which is poikilitically intergrown with the stable albite component (albite to oligoclase) in plagioclase. In medium-grade rocks zoisite is common in the zoisite-amphibolite facies. At high grade it occurs in calc-silicate rock, gneiss, granulite and eclogite.

Paragenesis: in medium-grade rocks, together with chlorite, sericite, actinolite, epidote, clinozoisite, albite and prehnite. In the zoisite-amphibolite facies it occurs next to hornblende and plagioclase. In calc-silicate rock it forms a stable paragenesis with diopside, and in eclogite it occurs together with omphacite, garnet, kyanite and quartz.

4.20.2 Epidote

$Ca_2Fe^{3+}Al_2[O|OH|SiO_4|Si_2O_7]$ monoclinic–prismatic

Thin-section characteristics

Form: columnar acicular parallel to the b-axis (Fig. 241) or xenomorphic granular, also divergent radiating crystals; in longitudinal sections lath-shaped. Cross-sections are hexagonal or rhombic.

Cleavage: perfect on (001) and clear on (100) with an intersection angle of ≈115°.

Twinning: sometimes on (100) with heart-shaped cross-sections.

Colour: pale greenish-yellow with pleochroism; the Mn-rich variety is called **piemontite** with a noticeable pink to purple pleochroism.

	Epidote	Piemontite
α:	colourless, light lemon-yellow	lemon-yellow to orange
β:	greenish, green-brown	amethyst colour to pinkish
γ:	pale green, yellow-green.	brick-red to purple.

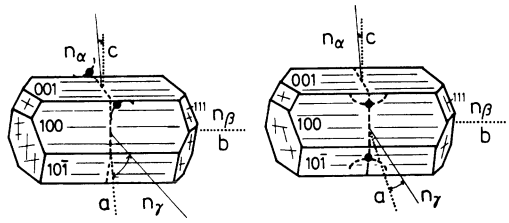

Fig. 241 Crystal form and optical characteristics of epidote (left) and clinozoisite (right).

Refraction and birefringence:

n_α	= 1.715 – 1.751	n_α	= 1.730 – 1.794
n_β	= 1.725 – 1.784	n_β	= 1.740 – 1.807
n_γ	= 1.734 – 1.797	n_γ	= 1.762 – 1.829
$\ominus\Delta$	= 0.015 – 0.051	$\oplus\Delta$	= 0.025 – 0.073

High refraction and highly variable medium-high birefringence (similar to the pyroxene group), epidote has bright intensive anomalous interference colours (bright blue, orange, red, green turquoise of the 2nd order; Colour plate 16). In piemontite the interference colours of the higher orders are masked by its particular colour. Epidote is optically biaxial ⊖, piemontite is optically biaxial ⊕ or ⊖.

Optic axial angle: epidote: $2V_\alpha$ = 64°–90°; piemontite: $2V_\gamma$ = 64°–106°.

Character of elongation: not characteristic, changing (+) or (–).

Extinction: in direction of the b-axis (perpendicular to cleavage) always straight, otherwise oblique ≈ 30°.

Special characteristics: often patchy colour distribution, anomalous (higher than normal) interference colours due to strong dispersion of the birefringence; characteristic concentric pattern with Fe-poor cores and Fe-rich rims.

Distinguishing features: because of its intensive and anomalous interference colours epidote is easily differentiated from other similar minerals. Olivine tends to be colourless with a bad cleavage; pyroxenes are optically biaxial ⊕ and show characteristic pyroxene cleavage with intersection angles of 87°.

Alteration: robust. Can be chloritized.

Occurrence: epidote and clinozoisite are most commonly found in low-grade metamorphic rocks, where they occur in greenschists, calcareous phyllites and blueschists; also in medium-grade rocks where both minerals occur (e.g. in certain mica schists and gneisses). During retrograde metamorphism epidote and zoisite form as part of the saussuritization, e.g. decay of the anorthite component of plagioclase (saussuritization by feldspar). Epidote is widely distributed also in contact-metamorphic rocks (e.g. knobbly schist, biotite hornfels, calc-silicate rock and skarns). Marly to calcareous clay-rich original rocks are chemically suitable for epidote growth. Epidote can also form hydrothermally, occurring in fractures and cavities in magmatites which rocks are rich in pyroxene and amphibole where they replace the anorthite component in plagioclase. Piemontite occurs in Mn-rich schists, and also in hydrothermally altered volcanic rocks.

Paragenesis: epidote and clinozoisite in low-grade rocks occur together with actinolite, microcline, albite, calcite and quartz, or with chlorite, albite, vesuvianite, tremolite; with increasing metamorphic grade together with albite/oligoclase, hornblende and almandine. In the blueschist facies with epidote, glaucophane, lawsonite, pumpellyite, clinozoisite, chlorite, muscovite, quartz, albite, calcite and sphene. In contact-metamorphosed rocks with vesuvianite, fassaite, andradite or grossularite, actinolite, hornblende, biotite and albite.

4.20.3 Clinozoisite

$Ca_2AlAl_2[O|OH|SiO_4|Si_2O_7]$ monoclinic–prismatic

Thin-section characteristics

Form: prismatic parallel to the b-axis (Fig. 241) or xenomorphic granular with hexagonal cross-sections and lath-shaped longitudinal sections.

Cleavage: perfect on (001).

Twinning: tends to be lamellar on (100).

Colour: colourless.

Refraction and birefringence:

n_α	= 1.670 – 1.718
n_β	= 1.672 – 1.725
n_γ	= 1.690 – 1.734
$\oplus\Delta$	= 0.004 – 0.015

High refraction and birefringence (anomalous bright prussian-blue interference colours); optically biaxial ⊕.

Optic axial angle: $2V_\gamma = 40°–90°$.

Character of elongation: changes between (+) and (–).

Extinction: in longitudinal sections parallel to the b-axis (also parallel and perpendicular to the cleavage traces) always straight, otherwise oblique (≈30°).

Special characteristics: anomalous (blue) interference colours.

Distinguishing features: zoisite is similar, rhombic and has straight extinction; vesuvianite is optically uniaxial ⊖; kyanite shows patchy bluish pleochroism, normal interference colours and is optically ⊖; anomalously biaxial grossularite has lower birefringence colours; lawsonite and pumpellyite have higher birefringence colours; where pumpellyite does not show any bluish-green colour, it can be differentiated from clinozoisite only by X-ray analysis.

Alteration: none.

Occurrence and paragenesis: see epidote (Part B, section 4.20.2).

4.20.4 Orthite (allanite)

$(Ca, Mn, Ce, La, Y, Th)_2(Fe^{2+}, Fe^{3+}, Ti)\ (Al, Fe^{3+})_2[O|OH|SiO_4|Si_2O_7]$ monoclinic–prismatic

Thin-section characteristics

Form: tends to be in the form of rounded to irregular-shaped grains, rarely acicular parallel to the b-axis.

Cleavage: good on (001) and poor on (100).

Twinning: tends to be on (100).

Colour: in a fresh stage pale grey-yellow to orange-brown, with red-brown pleochroism, also partly with greenish colours:
α: grey-yellow, colourless
β: yellow-brown, brown
γ: dark brown, greenish.

Refraction and birefringence:

n_α	= 1.690 – 1.813
n_β	= 1.700 – 1.857
n_γ	= 1.706 – 1.891
⊕Δ	= 0.013 – 0.036

High refraction and medium-high birefringence (interference colours are masked by the crystal colour; in case of complete metamictization isotropic with n = 1.54); commonly optically biaxial ⊖, rarely biaxial ⊕.

Optic axial angle: varies with $2V_\alpha = 40°–123°$.

Character of elongation: cannot be identified because of the strong colour.

Extinction: in longitudinal sections parallel to the b-axis, otherwise oblique.

Special characteristics: almost always zoned and rimmed by epidote and clinozoisite; occasionally it is metamictic–isotropic, radioactivity causing damage to the crystal lattice; as inclusions in other minerals such as biotite, pleochroic haloes and extension fractures.

Distinguishing features: brown hornblende shows characteristic 124° cleavage intersection and occurs in different parageneses.

Alteration: can alter into epidote; during weathering it is replaced by carbonate and limonite.

Occurrence: in granitic to dioritic plutonic rocks as a rare pneumatolytic mineral; rare in low- to high-grade metamorphic rocks, but more common in contact-metamorphic rocks.

Paragenesis: in magmatic rocks and pegmatites together with epidote, sphene, tourmaline and also with fluorite and monazite.

4.21 Pumpellyite

$Ca_2(Al, Fe^{3+}, Fe^{2+}, Mg)Al_2[(OH)_2|SiO_4|Si_2O_7]\cdot H_2O$ monoclinic–prismatic

General features: characteristic mineral of low-grade metamorphic rocks of basic volcanic origin.

Thin-section characteristics

Form: lath-shaped parallel to the b-axis (Fig. 242), acicular or fibrous; generally in radiating, divergent aggregates, rosettes or spherolites, also in parallel or subparallel bundles.

Cleavage: similar to zoisite, perfect on (100) and good on (001).

Twinning: common on (001) and (100).

Colour: colourless to blue-green, pleochroic; colour intensity and pleochroism depend on Fe^{3+} content; colour zonation is common:
α and γ: colourless to pale yellowish
β: light green to blue-green.

Refraction and birefringence:

$n_\alpha = 1.665 - 1.710$
$n_\beta = 1.670 - 1.720$
$n_\gamma = 1.683 - 1.726$
$\oplus\Delta = 0.010 - 0.020.$

Medium-high refraction and relatively low birefringence; anomalous blue and leather-brown interference colours are common, normal interference colours are rare (straw-yellow of the 1st order to blue of the 2nd order); optically biaxial ⊕.

Optic axial angle: varies strongly $2V_\gamma = 7°–110°$.
$2V_\gamma$ { Fe-poor variety = 10°. / Fe-rich variety = 85°.

Character of elongation: not characteristic, either (+) or (–).

Extinction: oblique, depending on Fe^{3+} content:
$\gamma \wedge c$ { in Fe-poor members = 4°. / in Fe-rich members = 22°.

Special characteristics: zonal growth; anomalous interference colours are common; oak-leaf-shaped intergrowth between pumpellyite and lawsonite on (010) together with epidote.

Distinguishing features: similar to clinozoisite and epidote. Clinozoisite has a higher refraction and a lower birefringence; Fe-rich epidote is optically biaxial ⊖; zoisite generally has a straight extinction, and so has lawsonite; the latter has normal interference colours.

Alteration: none.

Occurrence: in metamorphic rocks of the greenschist facies, derived from basalts, diabase, spilite and their pyroclastic equivalents. Also stable at higher pressures, and stable in metamorphic rocks of the blueschist facies. Also fills amygdaloidal basalt.

Paragenesis: in the pumpellyite-prehnite zone with prehnite, chlorite, albite, quartz, calcite and sphene. In the pumpellyite-chlorite zone with albite, chlorite, stilpnomelane, sericite, quartz, calcite, sphene with/without actinolite. In the blueschist facies with lawsonite, glaucophane, crossite and epidote.

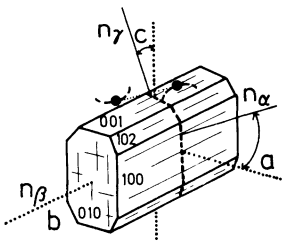

Fig. 242 Crystal form and optical characteristics of pumpellyite.

4.22 Lawsonite

$CaAl_2[(OH)_2|Si_2O_7|\cdot H_2O$ rhombic–dipyramidal

General features: index mineral in metamorphic rocks of the blueschist facies.

Thin-section characteristics

Form: commonly idiomorphic crystals, with a platy habit, stretched along the c-axis (Fig. 243), commonly in lath-shaped sections.

Cleavage: very good on (010), good on (100), not perfect on {101}: cleavage trace intersection of 67°.

Twinning: polysynthetic on {101}; parquet-floor-like patterns are possible with undulatory extinction.

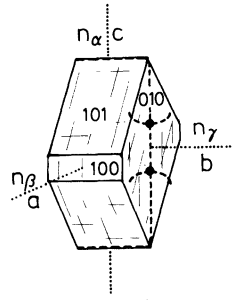

Fig. 243 Crystal form and optical characteristics of lawsonite.

Colour: colourless, in 'thick' thin sections pleochroic (α: blue, β: yellow, γ: colourless).

Refraction and birefringence:

n_α	= 1.663 – 1.665
n_β	= 1.672 – 1.675
n_γ	= 1.682 – 1.686
⊕Δ	= 0.019 – 0.021

Medium-high refraction and relatively low birefringence (orange interference colours of the 1st order to maximum blue of the 2nd order); optically biaxial ⊕.

Optic axial angle: $2V_\gamma = 76°–87°$ (tends to ≈ 84°).

Character of elongation: (–).

Extinction: straight in longitudinal sections, symmetric in basal sections.

Special characteristics: commonly intergrown with pumpellyite, typical undulatory extinction, parquet-floor-like textures.

Distinguishing features: clinozoisite and zoisite tend to have anomalous interference colours; epidote is yellow-green; pumpellyite is very similar and has oblique extinction; and prehnite has a higher birefringence. Tremolite has a cleavage-trace intersection angle of 124° or 56° respectively.

Alteration: sericitization and chloritization can occur. There is replacement by epidote or pumpellyite at the transition into the greenschist facies.

Occurrence: in lawsonite-glaucophane schists; it is rare in greenschists and amphibolites.

Paragenesis: with glaucophane, albite, jadeite, with/without pumpellyite, sericite, sphene, epidote and clinozoisite.

4.23 Anhydrite

$CaSO_4$ rhombic–dipyramidal

Thin-section characteristics

Form: fine- to medium-grained sugar-like aggregates (Fig. 245); commonly columnar to acicular, rarely fibrous.

Cleavage: perfect on (001), very good on (010) and good on (100) (Fig. 244(a)).

Twinning: tends to be polysynthetic on {101} in response to deformation.

Colour: colourless.

Refraction and birefringence:

n_α	= 1.570
n_β	= 1.575
n_γ	= 1.613
⊕Δ	= 0.044

Relatively low refraction and high birefringence (interference colours up to green of the 3rd order); optically biaxial ⊕.

Optic axial angle: $2V_\gamma = 42°$.

Character of elongation: untypical, (+) or (–).

Extinction: straight, parallel to the cleavage traces.

Special characteristics: can show deformation-induced bent cleavage traces.

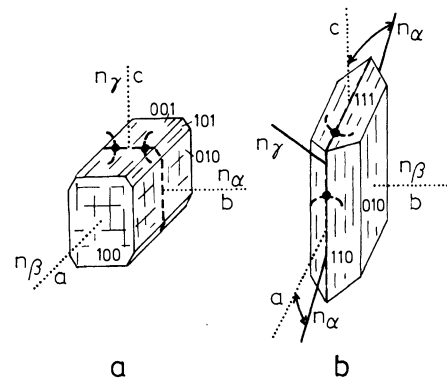

Fig. 244 Crystal form and optical characteristics of (a) anhydrite and (b) gypsum.

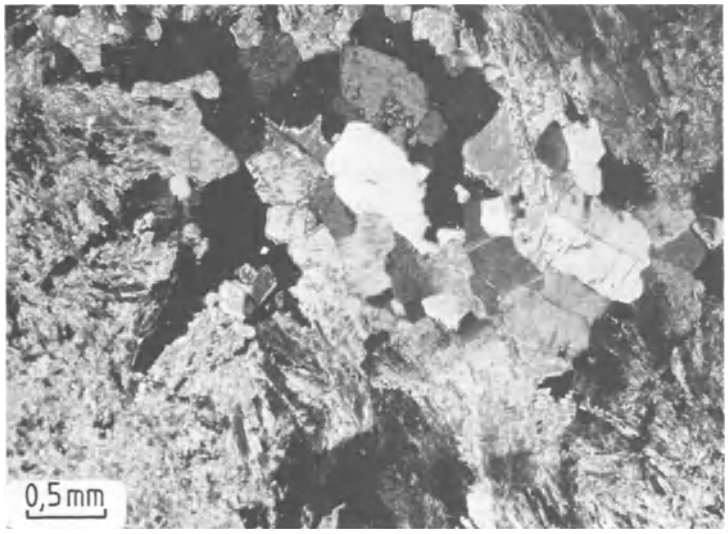

Fig. 245 Short to long prismatic anhydrite crystals. Anhydrite. Mühlberg near Ilfeld, Harz Mts, Germany. Crossed polars.

Distinguishing features: gypsum does not have such good cleavage and has low refraction and birefringence.

Alteration: with the addition of water, there is a volume increase of up to 60% and progressive replacement by gypsum, starting from the cleavage planes.

Occurrence: rock-forming in NaCl accumulations; accompanying mineral in chloritic evaporites, diagenetically formed from gypsum. Rare in amygdales in volcanic basalts together with quartz, chlorite, prehenite and zeolite.

Paragenesis: with gypsum, rock-salt, illite, talc, quartz and calcite.

4.24 Gypsum

$CaSO_4 \cdot 2H_2O$ monoclinic–prismatic

Form: platy on {010} (Fig. 244(b)) to coarse prismatic or acicular along the c-axis (Fig. 246); also as fine scaly aggregates, fine grains, dense or sphaerolitic.

Cleavage: very good on (010), good on (100) and {011}.

Twinning: swallow-tail twins on (100) are common, twins on (001) are rare.

Colour: colourless.

Refraction and birefringence:

n_α = 1.519 – 1.521
n_β = 1.523 – 1.526
n_γ = 1.529 – 1.531
$\oplus\Delta$ = 0.010

Low refraction and birefringence (grey to white interference colours of the 1st order, similar to K-feldspar); optically biaxial ⊕.

Optic axial angle: $2V_\gamma = 58°$ (at 19°C), temperature sensitive, decreasing with increasing temperature.

Character of elongation: untypical, (+) or (–).

Extinction: tends to be oblique, $\alpha \wedge a = 15°$; there is marked dispersion of the extinction on (010); in sections parallel to the b-axis straight extinction occurs.

Special characteristics: during the preparation of thin sections, involving heating of the rock chip, polysynthetic twins can form on (100), which can be bent.

Distinguishing features: anhydrite has pseudocubic cleavage and straight extinction, higher refraction and birefringence; with fine-grained aggregates gypsum can be mistaken for chalcedony, but the latter is optically uniaxial ⊕.

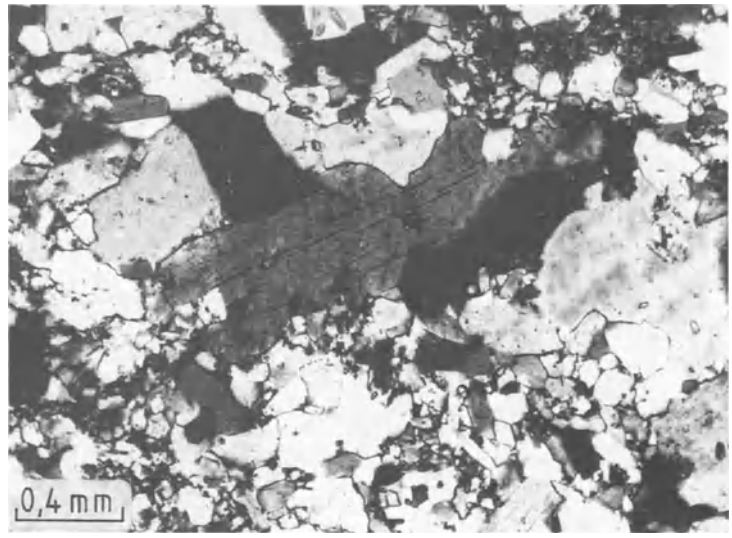

Fig. 246 Fine-grained, commonly hypidiomorphic to xenomorphic gypsum crystals. Monomineralic gypsum. Osterode, Harz Mts, Germany. Crossed polars.

Alteration: diagenetic alteration into anhydrite; during heating (e.g. during thin-section preparation) there is water loss and transition into bassanite ($CaSO_4 \cdot \frac{1}{2}H_2O$).

Occurrence: rock-forming in rock-salt sequences. Gypsum also occurs in sedimentary rocks, as concretions in clay-rich rocks, and in areas of interaction between fumeroles and basic volcanic rocks.

Paragenesis: with anhydrite, halite, clay minerals, calcite and other carbonate minerals, and quartz.

4.25 Aragonite

$CaCO_3$ rhombic–dipyramidal

Thin-section characteristics

Form: tends to occur in radiating acicular aggregates (Fig. 247), rarely in short to long prisms, stretched along the c-axis with hexagonal cross-sections (Fig. 248).

Cleavage: poor, not visible.

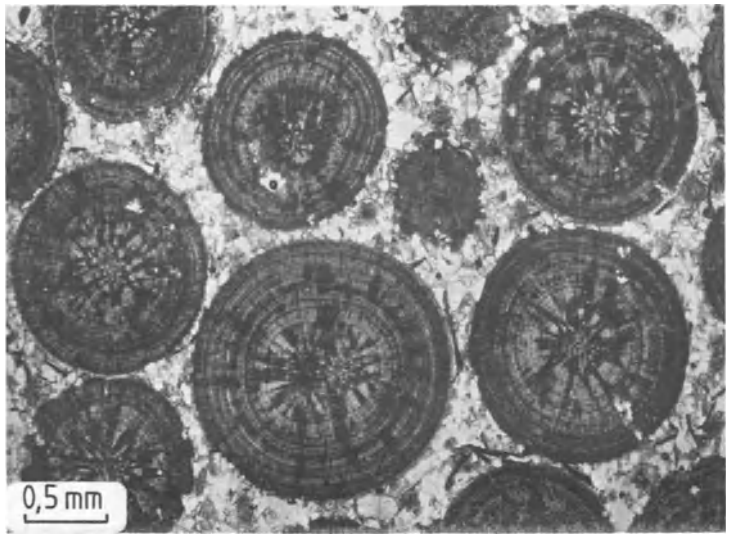

Fig. 247 Aragonite spherolite (peastone) in a fine-grained carbonaceous sinter deposit (pisolite). Carlsbad, Germany. Uncrossed polarizers.

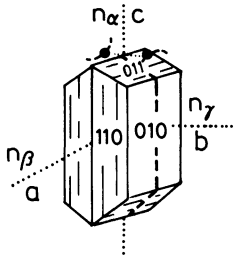

Fig. 248 Hexagonal cross-sections in aragonite.

Twinning: tends to be lamellar on {110}, also contact and interpenetrating twins.

Colour: colourless.

Refraction and birefringence:

n_α	= 1.530 – 1.531
n_β	= 1.680 – 1.681
n_γ	= 1.685 – 1.686
$\ominus\Delta$	= 0.155 – 0.156

Medium refraction index and high birefringence similar to calcite (white interference colours of the 9th order); optically biaxial ⊖.

Optic axial angle: $2V_\alpha = 18°$.

Character of elongation: (–).

Extinction: straight in longitudinal sections, symmetrical in basal sections.

Special characteristics: the relief varies depending on the orientation of the section.

Distinguishing features: calcite is not always optically uniaxial ⊖, but it shows the characteristic rhombohedric cleavage.

Alteration: into calcite.

Occurrence: in cavities and fissures in basic rocks; as a precipitate in geothermal areas ('Carlsbad sinter'), including geysers; as stalactites in geodes; as a component of organic shell material; and as a high-pressure mineral in aragonitic marble (Crete).

Paragenesis: with zeolite, calcite and other carbonates.

4.26 Barite

$BaSO_4$ rhombic-dipyramidal

Thin-section characteristics

Form: tends to occur in flaky or radiating aggregates; granular, dense, fibrous, and also idiomorphic in long prisms or in plates (Fig. 249).

Cleavage: perfect on (001), good on (110) and (010).

Twinning: polysynthetic interpenetrating on {110}.

Colour: colourless.

Refraction and birefringence:

n_α	= 1.636 – 1.637
n_β	= 1.637 – 1.639
n_γ	= 1.647 – 1.649
$\oplus\Delta$	= 0.011 – 0.012

Medium refraction and relatively low birefringence (orange-yellow interference colours of the 1st order); optically biaxial ⊕.

Optic axial angle: $2V_\gamma = 36°–38°$.

Character of elongation: (+).

Extinction: straight in the direction of the (001) cleavage trace, symmetrical in basal sections.

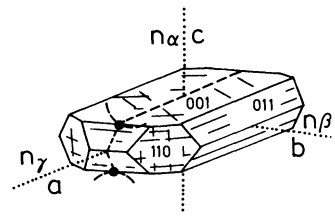

Fig. 249 Crystal form and optical characteristics of barite.

Special characteristics: in flaky aggregates they can be kinked and crenulated.

Distinguishing features: replaced by SiO_2 and carbonate; chalcedony forms pseudomorphs after it.

Occurrence: forms veins in many hydrothermal deposits together with or without sulphides, and also forms concretions in sandstones (e.g. as desert roses).

Paragenesis: with different sulphides, quartz and celestite.

4.27 Goethite

FeOOH rhombic–dipyramidal

General features: crystalline hydroxide iron minerals are called goethite and lepidocrocite; the cryptocrystalline form is **limonite** (Part B, section 2.10.1).

Thin-section characteristics

Form: acicular parallel to the c-axis; radiating fibres, divergent acicular, flaky, oolitic, earthy (Fig. 251).

Cleavage: good on (010).

Colour: bright yellow, brown and brownish-orange, not strongly pleochroic:
α: bright yellow or brown
β: yellow-brown
γ: orange or olive-coloured.

Refraction and birefringence:

	Pure	H_2O-rich
n_α	= 2.275	– 2.15
n_β	= 2.409	– 2.22
n_γ	= 2.415	– 2.23
$\ominus\Delta$	= 0.140	– 0.08

Very high refraction and birefringence, depending on the H_2O content. The interference colours are not identifiable due to the strong crystal colour; optically biaxial ⊖.

Optic axial angle: strong dispersion of the optic axis, $2V_\alpha$ = 0°–27° (according to the wavelength of light).

Extinction: in longitudinal sections, straight.

Special characteristics: because of its strong dispersion, goethite is optically uniaxial ⊖, when λ = 605–620 nm.

Distinguishing features: haematite is optically uniaxial ⊖ and has predominantly red-brown absorption colours; lepidocrocite, which is very similar to haematite, is more platy in habit and together with goethite it tends to be idiomorphic. Similar to brookite.

Alteration: none.

Occurrence: a weathering product of Fe-rich minerals and rocks; a component of soils. Forms concentric aggregates filling cavities and veins. Occurs in fossilized marine iron ore deposits (minette, residual ore) as iron oolites. Dense masses of goethite and lepidocrocite are called limonite.

Paragenesis: with lepidocrocite and hematite.

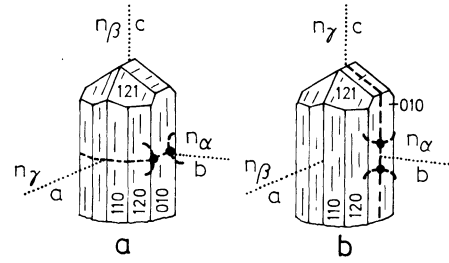

Fig. 250 Crystal form and optical characteristics of goethite: (a) for yellow light; (b) for red light.

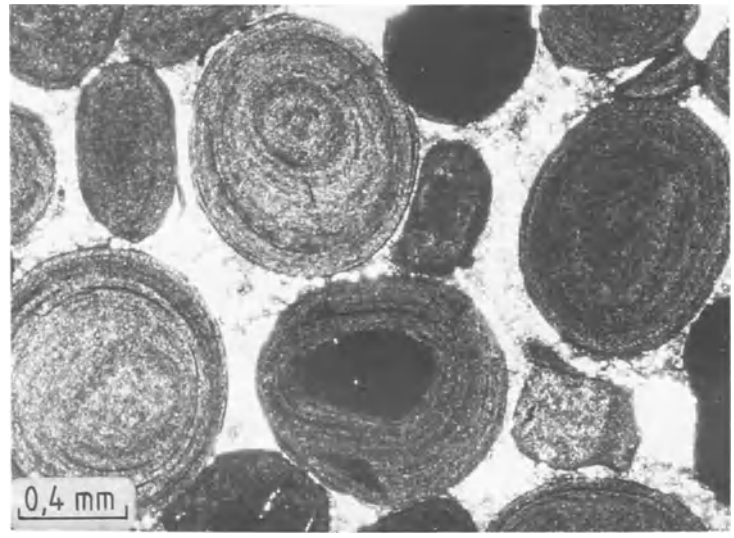

Fig. 251 Ooid comprised of goethite in an iron oolite, middle Jurassic ε. Fricktal, Switzerland. Uncrossed polarizers.

4.28 Prehnite

$Ca_2(Al, Fe^{3+})[(OH)_2|AlSi_3O_{10}]$ rhombic–pyramidal

General features: alteration product of the anorthite component in plagioclase in magmatic and metamorphic rocks.

Thin-section characteristics

Form: platy on {001}, mosaic-like intergrowth (parquet-floor), in fan-shaped, radial configurations or dendritic arrangements (Figs 252, 253(a),(b)).

Cleavage: good on (001).

Twinning: rare in fine lamellae on (110) and (001).

Colour: colourless.

Refraction and birefringence:

n_α	= 1.611 – 1.630
n_β	= 1.617 – 1.641
n_γ	= 1.632 – 1.669
$\oplus\Delta$	= 0.021 – 0.039

Medium-high refraction and birefringence (interference colours of the 2nd order, often anomalous deep blue to leather-brown), increasing with increasing Fe content; optically biaxial ⊕.

Optic axial angle: $2V_\gamma = 64°–71°$ (to $2V_\gamma = 0°$ in mosaic form).

Character of elongation: untypical, (+) or (–).

Fig. 252 Prehnite as hydrothermal formation in diabase-amygdale. Upper mid-Devonian. Helgebachtal west of Leun/Lahn, Germany. Crossed polars.

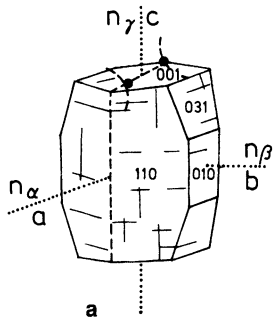

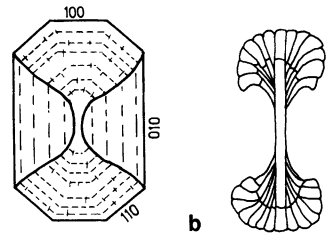

Fig. 253 (a) Crystal form and optical characteristics of prehnite. (b) Typical forms of prehnite.

Extinction and special characteristics: straight parquet-floor pattern; microcline-like with anomalous interference colours and incomplete extinction.

Distinguishing features: lawsonite has a lower birefringence, higher axial angle and normal interference colours; thomsonite and other zeolites have a lower refraction and birefringence; chondrodite shows a pale gold-yellow pleochroism and lamellar twinning.

Alteration: none.

Occurrence: hydrothermal replacement of plagioclase, in particular in spilites, diabase and their pyroclastic derivatives; can also occur in certain gabbroic rocks, granodiorite, and in amygdales. In basic and basalt-derived rocks in the greenschist and zeolite facies as low-temperature replacement of anorthite in plagioclase (e.g. in actinolite schist, prasinite, metabasalt, etc.). During high-pressure metamorphism prehnite reacts to lawsonite. Prehnite also occurs in certain calc-silicate rocks.

Paragenesis: in magmatites together with epidote, albite, quartz and calcite. In regionally metamorphosed rocks together with zoisite, clinozoisite, pumpellyite, albite and actinolite; and in contact-metamorphic rocks together with zoisite, grossularite, axinite and albite.

Part C Appendices

Appendix 1 Tables for the microscopic identification of rock-forming minerals

Table 6 Refraction plotted against birefringence of rock-forming minerals

Birefringence		Up to 0.005	Up to 0.010	Up to 0.015	Up to 0.020	Up to 0.025
Refraction <1.55	Optical character +	Apophyllite Chabazite Mesolite Mordenite Tridymite	Gypsum Harmotome Heulandite Phillipsite	Plagioclase Natrolite	Thomsonite	
	−	Analcite Apophyllite Chabazite Cristobalite Mordenite Nepheline Marialite	Alkali feldspar Laumontite	Epistilbite Plagioclase Scolecite Stilbite		
1.55 to 1.60	+		Chalcedony Lizardite Quartz	Chrysotile Clinochlore Plagioclase	Cordierite	
	−		Antigorite Chrysotile Beryl	Penninite Plagioclase	Cordierite	
1.60 to 1.65	+		MgFe-chlorite Topaz	Barite		
	−		Fe(II)-chlorite FeMg-chlorite	Andalusite Wollastonite		
1.65 to 1.70	+	Åkermanite	Arfvedsonite Bronzite Enstatite		Jadeite	Lawsonite Omphacite Sillimanite
	−	Apatite	Arfvedsonite Magnesio-riebeckite	Crossite Gehlenite	Barkevikite Katophorite	Actinolite Glaucophane Tremolite Tschermakite
1.70 to 1.80	+		Zoisite	Chloritoid Staurolite Clinozoisite	Pumpellyite Thulite	
	−		Corundum Vesuvianite	Chloritoid Hypersthene	Kyanite (disthene)	Hastingsite
>1.80	+					
	−					

Up to 0.030	Up to 0.050	Up to 0.075	Up to 0.100	>0.100	Birefringence	
					Optical character	Refraction
					+	<1.55
Cancrinite					–	
	Anhydrite				+	1.55 to 1.60
Lepidolite	Mejonite Talc Zinnwaldite				–	
	Anhydrite				+	1.60 to 1.65
Glauconite Celadonite	Glauconite Phengite Phlogopite Celadonite	Muscovite			–	
	Forsterite Prehnite				+	1.65 to 1.70
	Titanbiotite Tourmaline		Biotite s.s.	Aragonite Calcite Dolomite	–	
Augite Diopside Pigeonite	Diopside Piemontite Stilpnomelane Titanaugite			Xenotime	+	1.70 to 1.80
Kaersutite	Epidote Piemontite		Oxyhornblende	Magnesite Oxybiotite	–	
	Orthite	Aegirine-augite Aenigmatite Fayalite Zircon	Cassiterite	Rutile Siderite Sphene (titanite)	+	>1.80
	Orthite	Aegirine-augite Anatase		Goethite	–	

Table 7(a) Opaque and nearly opaque minerals (important minerals are shown in bold)

No./ *Page*	Mineral	Form and habit	Cleavage	Twinning	Colour	Refraction (n)
1.1 *30*	**Magnetite** cub.	octahedral, granular, skeletal			iron-black	2.42
1.2 *31*	Ilmenite trig.	laminar, rhombohedral, skeletal, granular, flaky			black, very thin; dark brown	2.33–2.51
1.3 *31*	Hematite trig.	tabular, foliated, fibrous, oolitic, granular		simple lamellar	black, very thin; blood-red–yellowish red	2.87–3.22
1.4 *32*	Pyrite cub.	octahedral, cubic, granular		interpenetrating twins (110)	black	
1.5 *33*	Pyrrhotite hex.	granular, rarely tabular, massive			black	
1.6 *33*	**Graphite** hex.	flakes, grains	perfect (0001)		black, very thin; green-grey	1.5–2.0
1.7 *34*	Carbon. substances amorph.	dust particles			black, very thin; brownish to grey	1.5–1.9
2.2 *36*	**Chromite** cub.	octahedral, granular			deep-brown, almost opaque	2.05–2.16
4.12 *143*	Aenigmatite tricl.	columnar to acicular	good, cleavage intersection angle 66°	polysynthetic twinning	dark brown to almost opaque	1.81–1.88

Special diagnostic features	Occurrence; paragenesis
magnetite → martitization titanomagnetite → leucoxene	in almost all magmatic rocks, in many low- to high-grade metamorphic rocks, in sediments and sedimentary rocks; ilmenite.
skeletal leucoxene-forming; anisotropic effect → optically uniaxial ⊖	in almost all magmatic rocks, in high-grade metamorphic rocks, in sediments and sedimentary rocks; magnetite
pseudomorphs after magnetite are common; red coloration in different rock types, optically uniaxial ⊖	postmagmatic in igneous rocks, in low- to medium-grade metamorphic rocks, in sedimentary rocks
weathers easily; in transmitted light difficult to identify	postmagmatic in igneous rocks, in metamorphic schists, in bituminous limestones and in black shales
in transmitted light difficult to identify	in mafic to ultramafic plutonic rocks, rarely in equivalent volcanic rocks; magnetite, ilmenite, olivine, ortho- and clinopyroxene, plagioclase
smeared margins	in graphitic phyllites and graphitic gneisses; quartz, K-feldspar, albite, mica, chlorite, rutile
black pigment in many sedimentary rocks	in coals, sediments with organic components and low-grade metamorphic rocks; quartz, calcite, clay minerals
small grains appear almost opaque	in mafic and ultramafic magmatic rocks; olivine, serpentine, titanaugite
for optical data and characteristics see Table 7(d)	in felsic, Na-rich magmatic rocks; aegirine-augite, arfvedsonite or riebeckite, anorthoclase, nepheline

Table 7(b) Isotropic minerals with higher refraction (n > 1.7) (important minerals are shown in bold)

No./ *Page*	Mineral		Form and habit	Cleavage	Twinning	Colour	Refraction (n)
2.1 *35*	Perovskite ps.-cub.		octahedral, cubic, skeletal	good on {100}, rarely recognizable	simple and lamellar, rarely recognizable	violet-grey, dark brown, yellowish, greenish, colourless	2.30–2.38
2.2 *36*	**Spinel group** cub.	Spinel	octahedral		simple, rarely recognizable	colourless, pink, pale bluish	1.72–1.74
		Pleonaste				greenish grey	1.77
		Hercynite				deep green, emerald green	1.78–1.80
		Picotite	granular			yellowish, brownish	2.00
		Chromite				deep brown, almost opaque	2.05–2.16
2.3	Pyrochlore cub.		octahedral, granular		simple	reddish-to-black brown	1.96–2.02
37	Koppite cub.		dodecahedral			colourless, red, brown	2.12–2.18
2.4	**Garnet group** cub.	**Pyrope**	rhombic-dodecahedral, deltoid-icositetrahedron, rounded-granular	not good on {110}, mainly subparallel, irregular fractures		pale red	1.72–1.76
		Almandine				colourless, reddish	1.77–1.82
		Spessartine				pale yellow	1.79–1.81
		Grossularite				colourless, greenish, yellowish	1.735–1.77
		Andradite				greenish, brownish	1.85–1.89
		Uvarovite				pale emerald-green	1.84–1.87
38		**Melanite**				brown	1.86–2.00

Special diagnostic features	Occurrence; paragenesis
can show zonal colour distribution; paramorphic with anomalous birefringence; very small grains appear opaque	in silica-undersaturated Ca-rich magmatic rocks, predominantly in melilite-bearing volcanic rocks, alnoites and kimberlites; melilite, nepheline, sodalite group, also leucite, magnetite but never ilmenite
no anomalies	in granulites and contact-metamorphic rocks; cordierite, corundum, almandine
	in mafic plutonic rocks and dolomitic marble; carbonates, serpentine
hercynite can be zoned (dark core)	in ultramafic Ti-rich plutonic rocks and cordierite-sillimanite gneisses
minute inclusions in olivine or serpentine	in olivine aggregates and in serpentinite, alkali basalts; olivine, serpentine
small grains appear opaque	in mafic to ultramafic magmatic rocks; olivine, serpentine, titanaugite
under the microscope differentiation from perovskite, picotite, chromite and melanite is not possible	in foyaitic pegmatites and ejected volcanic blocks
	in carbonatites; calcite, apatite, phlogopite
celyphytic rims are common	in peridotites, kimberlites, serpentinites and eclogites; olivine, serpentine, pyroxene, phlogopite
sieve texture and heliocentric inclusion spirals	in low- to high-grade metamorphic rocks, rare in magmatites; biotite, muscovite, quartz, chlorite, hornblende
component with almandine	in certain hornfels rocks and in sediments
anomalous birefringence is common; zonal growth patterns or patchy colour distribution	in siliceous limestones, garnetiferous rocks and siliceous marbles; diopside, vesuvianite, calcite, wollastonite
	in Fe-metasomatosed skarn
	in chromite-rich rocks
clear zonal texture	in silica-undersaturated, alkali-rich, Na-rich magmatic rocks; nepheline, leucite, sodalite group, aegirine-augite, sanidine

Table 7(b) Optically isotropic minerals, rock-glass and cryptocrystalline phases with generally low refraction (n < 1.51)

No./ *Page*	Mineral		Form and habit	Cleavage	Twinning	Colour	Refraction (n)
2.5 *42*	**Leucite** tetr. ps.-cub.		deltoid-icositetrahedron		fine lamellar, polysynthetic	colourless	1.508–1.509
2.6.1 *43*	**Sodalite group**	**Sodalite** cub.	square, hexagonal and ten-sided shape, rounded edges, corroded crystals, xenomorphic only in plutonic rocks	poor on {110}	on {111}; not easily visible under the microscope	colourless, rarely pale grey	1.483–1.490
2.6.2 *43*		**Nosean** cub.				colourless, grey, rarely blueish	1.488–1.495
2.6.3 *43*		**Hauyne** cub.				light blue, purple-blue, blue-green	1.496–1.508
2.7 *46*	Analcite cub.		typically xenomorphic, rarely idiomorphic	poor on (001), difficult to see	polysynthetic, similar to leucite	colourless	1.486–1.487
2.8 *47*	Cristobalite tetr. ps.-cub.		tabular, 'balls', fibrous, chalcedony-like		complex lamellar, not clearly visible under the microscope	colourless	1.484–1.487
2.9 *48*	Fluorite cub.		cubic, typically massive	perfect on {111}, 2 to 3 cleavage traces are common	not recognizable under the microscope	colourless, bluish, purple	1.434
2.10.1 *48*	Amorphous substances	Limonite	oolitic, crust- and soil-like, radiating			ochre-yellow to reddish-brown	2.0–2.1
2.10.2 *49*		Opal	amorphous, colloidal forms	irregular fractures		colourless, yellowish, reddish	1.44–1.46
2.10.3 *50*		**Rock-glass**	amorphous	conchoidal fractures		colourless, yellowish, brownish	1.48–1.61

Special diagnostic features	Occurrence; paragenesis
typically shows anomalous birefringence (paramorphous with lamellae twinning)	in silica-undersaturated Na-rich volcanic rocks; nepheline, sodalite group, aegirine-augite, olivine, clinopyroxene, melanite, glass. Never together with quartz.
weakly birefringent around inclusions	in Na-rich silica-undersaturated volcanic and plutonic rocks; nepheline, leucite, aegirine-augite, melanite, olivine, titanaugite, glass. Never together with quartz.
almost always dark rims, opaque streaks and clusters, zonar and irregular colour distribution; locally as fine-grained inclusions	predominantly in volcanic rocks, such as phonolites, tephrites, foids, rarely plutonic rocks; nepheline, leucite, sanidine, plagioclase, aegirine-augite, melanite, olivine, titanaugite, rock-glass
weak anomalous birefringence (similar to leucite); optically uniaxial ⊖	as interstitial mineral in cavities in basalts and other basic volcanic rocks, in zeolite facies; nepheline, leucite, olivine, titanaugite and heulandite, desmine, laumontite
very low birefringence, 'ball-structure'; optically uniaxial ⊕, also optically biaxial ⊖ with $2V_\alpha = 25°$ and $\Delta = 0.003$	in cavities in silica-oversaturated volcanic rocks, devitrification product, in rocks of sanidine-facies; glass, tridymite, alkali feldspar, zeolite
zonar and patchy colour distribution	in hydrothermal veins, in sandstone and biogenic dolomite, rare in Li-granite, greisen, pegmatites; topaz, tourmaline, quartz, hematite
rarely weak birefringence; when dendritic → opaque	in almost all weathered and altered rocks found as pigment
commonly altered into low-cristobalite or chalcedony (shrinkage cracks and anomalous birefringence)	in volcanic rocks forming crusts, in pores and cavities in acidic to basic volcanic rocks; tridymite, zeolite
inclusions surrounded by anomalous birefringence colours; fluidal texture, contraction fractures (ball to onion-shaped), radial devitrification textures	in volcanic rocks and in subsurface parts of dykes and sills; parageneses are diverse (see Part B, section 2.10.3)

Table 7(c) Optically uniaxial minerals (important minerals are printed in bold)

No./ *Page*	Mineral		Form and habit	Cleavage	Twinning	Colour	Pleochroism	Opt. ch.
3.1.1 *54*	**Rutile** tetr.		idiomorphic, columnar, acicular, granular	perfect on (110) and good on (100)	'knee' twins	yellowish to red-brown	generally not recognizable	⊕
3.1.2 *55*	Cassiterite tetr.		granular, columnar, acicular, idiomorphic	good on (100)	cyclically repeated 'knee' twins	grey, yellowish, reddish, brownish	very weak	⊕
3.1.3 *56*	**Zircon** tetr.		rounded grains; short- to long-prismatic	poor on (110)	not recognizable	colourless, pale brownish, greenish, pink	rare, very weak	⊕
3.1.4 *57*	Xenotime tetr.		short columns, granular	good on (110)	rare	colourless, yellowish, greenish, reddish	rare, very weak	⊕
3.1.5 *57*	Melilite group	**Åkermanite** tetr.	platy	weak on (001) and on (110)	interpenetrating twins	colourless	rare and extremely weak	⊕
		Gehlenite tetr.	short prisms, thick tabular			colourless, yellowish		⊖
3.1.6.1 *59*	SiO_2 group	**Quartz** trig.	hypidiomorphic–xenomorphic, granular, typically corroded	irregular fractures	not recognizable	colourless		⊕
3.1.6.2 *63*		Chalcedony trig.	acicular, radiating, dense					
3.1.6.3 *63*		Tridmyite ps.-hex.	platy to flaky, branching aggregates	weak, difficult to see	interpenetrating twins or drillings			
2.8 *47*		Cristobalite ps.-cub	platy, spherical, acicular, chalcedony-like		complex lamellar, rarely visible			⊖
3.1.7 *64*	Chabazite trig.		idiomorphic, pseudocubic	clear, rhombohedric on $(10\bar{1}1)$	simple on (0001)	colourless		⊕ ⊖

Main zone	Refraction (n)	Max. Δ	Special diagnostic features	Occurrence; paragenesis
(+)	2.605–2.901	0.296	needle-like crystals appear black; grid-like network (sagenite); can cause radioactive haloes; also anomalously biaxial ⊕	accessory in many metamorphic rocks (e.g. amphibolite), rare in magmatic rocks, secondary in biotite; in metamorphic rocks: kyanite, cordierite, corundum, spinel, biotite, quartz
(+)	1.990–2.100	0.098	zonar to patchy or stripy colour distribution, causes pleochroic haloes; also anomalously biaxial ⊕	in greisen and contact skarn, rare in granites, in pegmatitic-pneumatolytic ore deposits; quartz, Li-mica, K-feldspar, tourmaline, topaz, fluorite, rutile
(+)	1.922–2.015	0.065	black rim caused by refraction; zonar and rich in inclusions; causes radioactive haloes, sometimes anomalously biaxial, metamict → isotropic malacon	common in acidic, rare in basaltic rocks, frequently found in nepheline syenites and related pegmatites, in sedimentary rocks and granular in metamorphic rocks; quartz, K-feldspar, biotite, hornblende or nepheline, apatite, biotite, K-feldspar
(+)	1.720–1.827	0.107	extremely high birefringence (typically masked by its own colour); causes pleochroic haloes	in felsic plutonic rocks, orthogneisses, sands and sandstones; brown zircon, ilmenite, rutile, cassiterite
(–)	1.631–1.639	0.008	anomalous interference colours (lavender-blue or leather colours) are common	in extreme strongly silica-undersaturated volcanic rocks, very rare in plutonic and contact metamorphic rocks (e.g. gehlenite), in slags of blast furnaces; nepheline, leucite, perovskite, pyroxene, olivine, never together with quartz. For other parageneses see Part B, section 3.1.5
(+)	1.658–1.669	0.011	central dividing line with rod-like structure	
(+)	1.5442–1.5533	0.0091	always fresh and unaltered, often anomalously biaxial ⊕ with undulatory extinction, often corroded (with 'bays' and 'hollows')	in acidic to intermediate magmatic rocks, in sedimentary and metamorphic rocks, never together with foid minerals; microcline, albite, biotite, green hornblende, sphene or K-feldspar, plagioclase, hornblende and rock-glass.
(–) (+)	1.530–1.543	0.010	commonly anomalously biaxial ⊕, quartzine with Mz (+)	in fractures and amygdules of volcanic rocks, as a mineral of pseudomorphosis and silification; opal, zeolites
(–)	1.477–1.481	0.004	almost exclusively optically biaxial ⊕; branching triplets with 'roof-tile texture'	in fractures and voids of acidic to intermediate volcanics, in contact metamorphic rocks of the sanidinite facies; rock glass, cristobalite, tridymite
(+) (–)	1.484–1.487	0.003	ps.cub.→ Table 7b; 'ball' shaped texture; lussatite has Mz (+), lussatine has Mz (–)	
	1.478–1.490	0.005	cubed zeolite mostly showing subgrains; often anomalously biaxial ⊕	in fractures and cavities of mafic volcanic and also plutonic rocks; other zeolites, calcite, analcite

Table 7c *Continued*

No./ *Page*	Mineral		Form and habit	Cleavage	Twinning	Colour	Pleochroism	Opt. ch.
3.2.1 *65*	Anatase tetr.		detrital, granular, bladed	perfect on (001) and {111}	simple, rarely visible	yellowish, brownish, bluish, black		⊖
3.2.2.1 *66*		**Calcite** trig.	interlocked granular, fibrous, oolitic		lamellar twinning, very thin lamellae	colourless	pseudo-dichroism	⊖
3.2.2.2 *68*	**Carbonate group**	Dolomite trig.	granular	perfect after rhombohedral faces {10$\bar{1}$1}	lamellar	colourless, grey-brownish		⊖
3.2.2.3 *69*		Magnesite trig.	granular, fibrous, dense, gel-like		rare lamellar pressure-twins	colourless, grey-brownish		
3.2.2.4 *70*		Siderite trig.	granular, oolitic, bladed, dendritic aggregates		simple, very rarely lamellar	colourless, pale yellow-brown		
3.2.3 *70*	Corundum trig.		platy, hexagonal outlines, acicular, columnar, detrital	splits along {10$\bar{1}$1} and {0001}: 94°	lamellar	colourless, reddish, bluish	clear in coloured crystals	⊖
3.2.4 *71*	Vesuvianite tetr.		short columnar, granular, acicular, spherulitic	not good on (100)		colourless, yellowish, greenish, brownish	very rare weak	⊖ ⊕
3.2.5 *71*	**Tourmaline** trig.		columnar, acicular, spherulitic, rarely granular	irregular fractures		grey, brownish, greenish, yellowish, reddish, bluish	strong; in basal sections no pleochroism	⊖
3.2.6 *73*	**Apatite** hex.		idiomorphic, short to long columnar, granular; also oolitic, radiating branching	poor on (0001) and {10$\bar{1}$0}		colourless, pale red, grey, brownish	microscopic ore inclusions → weak dichroism	⊖

Main zone	Refraction (n)	Max. Δ	Special diagnostic features	Occurrence; paragenesis
(–)	2.488–2.561	0.073	sometimes zoned or patchy colour distribution; rarely anomalously biaxial ⊖	in sediments and sedimentary rocks, in many weathered rocks
	1.486–1.658	0.172	chagrin changes according to orientation of section; in metamorphic rocks tends to be anomalously biaxial ⊖	in sedimentary rocks (specially in carbonates), in metamorphic rocks, in cavities in volcanic rocks, in ore deposits
	1.500–1.703	0.185	always idiomorphic, coarser lamellae than in calcite	same as for calcite and as porphyroblasts in talc and chlorite schist
(–)	1.509–1.782	0.219		in talc and chlorite schist, as gel-magnesite in serpentinites, as ore deposit in metasomatic zones
	1.633–1.875	0.242	highest relief and birefringence in carbonates; strongly developed 'pseudo-dichroism'	as gangue in ore body, as ore in metasomatic and hydrothermal deposits
(–)	1.760–1.772	0.009	zonar or patchy colour distribution with pleochroism, occasionally anomalously biaxial ⊖	in Al-rich and silica-poor contact-metamorphic rocks; in regional metamorphic schist; in emery; as xenolithic inclusions in magmatic rocks; for paragenesis see Part B, section 3.2.3
(+) (–)	1.701–1.738	0.006	zonar or patchy colour distribution, anomalous lavender-blue or leather-brown interference colours; hour-glass texture; often anomalously biaxial ⊖	in contact-metamorphic and in impure regional metamorphic marbles; fassaite, calcite, grossularite, wollastonite, epidote, sphene, spinel
(–)	1.635–1.671	0.035	frequently zonar colour change; radioactive haloes around zircon; rarely anomalously biaxial	in pegmatites and metamorphic rocks, as pneumatolytic formation in tourmaline granite; topaz, beryl, Li-mica, cassiterite, fluorite, spodumene, apatite
(–)	1.631–1.667	0.005	mostly idiomorphic; zonar colours change due to oriented inclusions; sometimes anomalously biaxial ⊖	accessory mineral in almost all magmatic rocks, in pegmatites, sedimentary rocks, phosphorites and metamorphic rocks

Table 7c *Continued*

No./ *Page*	Mineral	Form and habit	Cleavage	Twinning	Colour	Pleochroism	Opt. ch.
3.2.7 *74*	Beryl hex.	short to long columnar, granular	not good, often not visible		colourless, pale blue, pale green	rare, weak	⊖
3.2.8 *75*	**Nepheline** hex.	xenomorphic granular, rarely short columnar	mostly not visible		colourless, cloudy		⊖
3.2.9 *76*	Scapolite group tetr.	granular, short columnar	good on (100) and {110}		colourless, yellow, cloudy		⊖
3.2.10 *78*	Apophyllite tetr.	platy, granular, tabular	very good on (001)	very good	colourless		⊕ ⊖
3.2.11 *78*	Cancrinite hex.	short columnar to fibrous	clear along $\{10\bar{1}0\}$		colourless, pale yellow		⊖

Main zone	Refraction (n)	Max. Δ	Special diagnostic features	Occurrence; paragenesis
(–)	1.565–1.610	0.009	commonly anomalously biaxial ⊖	in granite pegmatites, very rare in regional metamorphic schists; quartz, tourmaline, topaz, Li-mica, cassiterite
(–)	1.526–1.546	0.005	cloudy appearance; can show subgrains; can be anomalously biaxial ⊖; in cross-section rectangular cleavage	in silica-undersaturated alkali magmatic rocks; leucite, sodalite group, aegirine-augite, melanite, melilite, olivine, titanaugite, titanbiotite, apatite. Never together with quartz.
(–)	1.531–1.600 Marialite Mejonite	 0.005 0.038	fluid and mineral inclusions are common	in some granites, nepheline-syenites and associated pegmatites, in trachytes, contact metamorphic siliceous limestones and ejected volcanic blocks; for parageneses see Part B, section 3.2.9
(+) (–)	1.5345–1.5445	0.002	often anomalously biaxial ⊕; anomalous subgrain formation	in fractures and amygdules in basic volcanic rocks; calcite, zeolite
(–)	1.4885–1.524	0.026	sometimes anomalously biaxial	very rare in nepheline syenites instead of nepheline; nepheline, sodalite group, sanidine, aegirine-augite, melanite, calcite

Table 7d Optic biaxial minerals (important minerals are shown in bold)

No./ *Page*			Mineral	Form and habit	Cleavage	Twinning	Colour	Pleochroism	Opt ch.	Main zone
4.1 *79*	**Olivine group**		**Forsterite** to **fayalite** rhomb.	hexagonal to octahedral crystal outlines, granular, skeletal corroded margins	not good ('curved' cleavage: distinctive mark to pyroxenes)	rare simple twins; also as broad twin lamellae	colourless, rare pale yellow or greenish	very weak (fayalite)	⊕ ⊖	(+) (–)
4.2.1 *81*	**Pyroxene family**	**Orthopyroxene**	**Enstatite** rhomb.	short columns, hypidiomorphic to xenomorphic, granular	very good along {210}, less good along (100)	rare, knee-shaped and star-shaped columnar twins	colourless	very weak to weak	⊕	(+) (–)
			Bronzite rhomb.				pale green		⊕ ⊖	
			Hypersthene rhomb.				pale green, reddish, pale brown		⊖	
4.2.2.1 *86*		**Clinopyroxene**	**Diopside group** monocl.	short columns, lath-shaped, granular	good along {110} and (010); cleavage angle of 87°	rare, simple or lamellar	colourless to pale green	weak, hardly noticeable	⊕	
4.2.2.2 *87*			**Augite group** monocl.			often lamellar, interpenetrating twins or star twins	pale grey green, pale brown			
4.2.2.3 *88*			**Titanaugite** monocl.	short to long columns, platy		simple or lamellar	brownish, purple, brownish-yellow	clearly visible		
4.2.2.4 *90*			Pigeonite monocl.	xenomorphic granular, rarely long columns		often lamellar	colourless, pale pink, greenish, brownish	very weak		
4.2.2.5 *90*			**Aegirine-augite** monocl.	short columns, granular, acicular		common	strong green, brown-green	clearly visible to strong	⊕ ⊖	(–)
4.2.2.6 *92*			Jadeite monocl.	granular, platy, acicular, matted		rare as fine lamellae	colourless, pale green	very weak	⊕	
4.2.2.7 *93*			Omphacite monocl.	granular, rarely columnar		rare lamellar	colourless, pale green	very weak		

Refraction (n)	Max. Δ	Extinction angle	Axial angle 2V	Special diagnostic features	Occurrence; paragenesis
1.635–1.670 ⋮ 1.827–1.879	0.035 ⋮ 0.052	0°	84°–90° 90°–50°	corrosion and alteration are common; zonar growth mostly invisible picotite and chromite inclusions occur	in basic to ultrabasic magmatic rocks, also in quartz-bearing magmatites, in serpentinites and in forsterite-marble; titanaugite, plagioclase, foids or chromite, picotite, opx, cpx, serpentine
1.650–1.658 ⋮ 1.712–1.727	0.008 ⋮ 0.015	0°	54°–83° 97°–63°	zoning in volcanic rocks with Mg-rich core; in plutonic rocks often with exsolution lamellae; alteration into serpentine	in basic to ultrabasic rocks, rare in acidic plutonic rocks; cpx, olivine, spinel or cpx, olivine, plagioclase
			63°–45°		in intermediate to acidic volcanic rocks, in contact metamorphic rocks, in pyroxene-granulites; cpx, plagioclase, hornblende, biotite, rock-glass
1.664–1.755	0.030	38°–48° γ Λ c	50°–62°	exsolution lamellae of opx. (diallage) are common; alteration into uralite and serpentine	in alkali basalts, tholeiitic basalts, dunites and kimberlites, siliceous limestones and skarns; augite, pigeonite, plagioclase, olivine, foids, etc. (see Part B, section 4.2.2.1)
1.671–1.774	0.033	35°–48° γ Λ c	25°–61°	zonar or sectional colour change; partly irregular extinction; alteration into uralite (amphibole), chlorite, seladonite, epidote, talc	in calcalkaline and tholeiitic magmatites, in siliceous limestones instead of diopside; olivine, hypersthene, diopside, plagioclase, hornblende, biotite
1.695–1.762	0.033	32°–55° γ Λ c	42°–65°	well-developed zonar or hourglass texture; in extinction position anomalous brown to blue-grey interference colours	only in Ti-rich magmatic rocks of the alkali series; olivine, cpx, plagioclase, nepheline, sodalite group, leucite, aegirine-augite
1.682–1.751	0.029	37°–44° γ Λ c	0°–30°	matrix pyroxene, often difficult to recognize	in basic to intermediate volcanic rocks; cpx, plagioclase, olivine
1.700–1.813	0.050	55°–85° γ Λ c	60°–90° 90°–60°	often strong zonar growth; hourglass texture; in extinction position anomalous brown to grey-blue interference colours	in alkali rocks; nepheline, sodalite group, leucite, sanidine, melanite
1.640–1.692	0.021	32°–55° γ Λ c	60°–96°	shear-induced undulatory extinction	in glaucophane rocks and jadeite-quartzites; glaucophane, lawsonite, epidote, pumpellyite, etc. (see also Part B, section 4.2.2.6)
1.662–1.723	0.028	34°–48° γ Λ c	56°–84°	cellular exsolution during diaphthoritic alteration; continuously together with rutile	only in eclogites; garnet, smaragdite, kyanite, zoisite, rutile

Table 7d *Continued*

No./ *Page*	Mineral			Form and habit	Cleavage	Twinning	Colour	Pleochroism	Opt ch.	Main zone
4.3.1	monocl.	Actinolite series	**Tremolite** ⋮ **Actinolite**	long columnar, lath-shaped, acicular, fibrous, asbestos-like	perfect along {110}; characteristic cleavage intersection of 124°	common, sometimes lamellar	colourless pale-green	very weak	⊖	(+)
97			smaragdite				pale green to yellow-green	noticeable		
4.3.2		Green hornblende	**Hastingsite group**	short to long columnar, acicular to needle-shaped		simple or twin lamellae	bright green to yellow-green	strong		
			Tschermakite group							
98			**Barrosite group**				blue-green	noticeable		
4.3.3	Amphibole group	Brown hornblende	**Oxyhornblende**	short to long columnar		lamellae are common	strong red-brown to dark brown	strong		
			Kaersutite	short columnar (phenocrysts), rarely fibrous (matrix)			reddish-brown			
101			Katophorite				greenish-brown			
4.3.4		Alkali amphibole	Glaucophane	long columnar, rarely acicular, fibrous or platy		very rare	blue to purple	strong	⊖	(+)
102			Crossite						⊖	(+) (−)
4.3.5			Arfvedsonite	thick columnar, acicular, granular, flaky		sometimes simple	blue to brownish-green	strong	⊜	(−)
103			Riebeckite						⊕	(−)

Refraction (n)	Max. Δ	Extinction angle	Axial angle 2V	Special diagnostic features	Occurrence; paragenesis
1.608–1.630 ⋮ 1.647–1.667	0.022 ⋮ 0.020	10°–15° γ Λ c	85° ⋮ 80°	sometimes pleochroic haloes, untypically weak pleochroism (stronger in all other amphiboles), no pleochroism in tremolite; colour and pleochroism increases with increasing Fe-content	in green-, talc and blueschists, serpentinite, prasinite and hornblendegarben schists, and product of uralitization; chlorite, quartz, albite, sericite, calcite, also epidote, biotite and sphene; in dolomitic marble and siliceous limestone: talc, chlorite, quartz, epidote, calcite
1.608–1.630	0.022	15° γ Λ c	≈85°		in diaphthoritic eclogites and in uralite in saussuritized gabbros; garnet, omphacite, kyanite, muscovite
1.646–1.722	0.022	14°–20° γ Λ c	34°–90°	sometimes pleochroic haloes; use paragenesis to distinguish green hornblende from other amphiboles; diaphthoritic alteration into actinolite, chlorite, antigorite	in intermediary to acidic plutonic rocks and lamprophyrs, rare in volcanic rocks, abundant in amphibolite, amphibole-schists; microcline and/or orthoclase, plagioclase, quartz, biotite, pyroxene, sphene, also plagioclase, garnet, sphene (in amphibolites)
1.640–1.696	0.023	15°–22° γ Λ c	65°–90°		
1.640–1.696	0.022	15°–22° γ Λ c	65°–90°		in low-grade metamorphic rocks; albite, epidote, almandine
1.650–1.796	0.094	0°–12° γ Λ c	56°–88°	tends to be opacitized; variable refraction and birefringence in a single crystal; radioactive haloes; opacitization, corrosion	in acidic to intermediary volcanic rocks; plagioclase, biotite, orthopyroxene, clinopyroxene, rock-glass
1.669–1.743	0.047	3°–19° γ Λ c	74°–82°	zonar and patchy colour distribution; hourglass structure; isomorphic; resorption, corrosion and opacitization common	in Na-rich basic magmatic rocks; titanaugite, olivine, plagioclase
1.639–1.690	0.021	−8°–16° γ Λ c	0°–57°		in Na-rich magmatites (Na-shonkinites); nepheline Na-sanidine, aegirine-augite, titanbiotite, arfvedsonite, olivine, apatite
1.595–1.652	0.025	5°–7° γ Λ c	0°–50°	zonar; strong absorption colours and strong pleochroism ranging from blue to purple are very characteristic	in glaucophane-schist and eclogite; jadeite, lawsonite, zoisite, clinozoisite, rutile, pumpellyite, almandine, also garnet, omphacite, rutile, epidote
1.630–1.680	0.020	5°–9° β Λ c	0°–90°		
1.623–1.710	0.012	65°–80° β Λ c	0°–100°	poikilitic throughgrowth (sieve texture); strong anomalous interference colours	in Na-syenite and associated pegmatites; nepheline syenite, pantellerite and comendite; aegirine-augite, alkali feldspar, also anorthoclase, nepheline, sodalite, katophorite, riebeckite
1.650–1.717	0.016	3°–15° α Λ c	40°–100°	strong anomalous interference colours	same as arfvedsonite; also in Na-rich acidic magmatic rocks

Table 7d *Continued*

No./ *Page*	Mineral		Form and habit	Cleavage	Twinning	Colour	Pleochroism	Opt ch.	Main zone
4.4.1 *105*	monocl. Mica group	**Muscovite**	platy, flaky, scaly, columnar	perfect on (001), kinking due to deformation	not visible under the microscope	colourless, rarely pale yellow or greenish		⊖	(+)
4.4.2 *107*	monocl. Mica group	Phengite				colourless, rarely pale green			
4.4.3.1 *107*	monocl. Mica group Lithionite series	Lepidolite				colourless, rarely pale pink	very weak		
4.4.3.2 *107*	monocl. Mica group Lithionite series	Zinnwaldite				colourless to brown-grey	weak		
4.4.4.1 *108*	monocl. Mica group Biotite series	Phlogopite				colourless, yellow, greenish, brownish	clear		
4.4.4.2 *109*	monocl. Mica group Biotite series	**Biotite**				strong brown or green	very strong		
4.4.5 *111*	monocl. Mica group	Oxybiotite				red-brown to dark brown			
4.4.6 *111*	monocl. Mica group	Titanbiotite				orange to red-brown			
4.5 *112*	Stilpnomelane monocl. and tricl.		acicular, flaky, radial, dendritic, platy	good		yellowish, greenish, brown	strong	⊖	(+)
4.6 *113*	Glauconite and celadonite monocl.		rounded, elliptic, scaly, radial, fine-grained	clear		green	good to absent	⊖	(+)
4.7 *114*	**Talc** monocl.		fibrous, dense, scaly, subparallel aggregates	perfect	cannot be seen	colourless		⊖	(+)

Refraction (n)	Max. Δ	Extinction angle	Axial angle 2V	Special diagnostic features		Occurrence; paragenesis
1.552–1.624	0.054	parallel to cleavage ≈ 0° (0.5°–2°) β Λ a	28°–47°	typically fine-speckled in extinction orientation (bird's eye structure)	fine-scaled aggregates (= sericite); pleochroic haloes around zircon inclusions; greenish Cr-muscovite pleochroic (variety: fuchsite)	in acidic plutonic rocks and pegmatites, sericite also very common in palaeovolcanics (sericitized feldspars), in sedimentary rocks and phyllites, abundant in metamorphic rocks; quartz, microcline, orthoclase, plag., biotite or albite, chlorite, quartz, biotite or quartz, albite, biotite, staurolite, kyanite, almandine (metamorphic)
1.547–1.612	0.041		24°–36° (0°)		almost exclusively in fine-scaled aggregates (= sericite); optically it cannot be distinguished from muscovite	in glaucophane schist, eclogites, gneiss and phyllites; paragenesis as for muscovite or glaucophane, clinozoisite, lawsonite, paragonite
1.524–1.588	0.038		23°–58° (0°)		pleochroic haloes around zircon; also spherolitic	in Li-bearing granite pegmatites and in greisen; quartz, topaz, tourmaline, beryl, spodumene, cassiterite
1.535–1.590	0.035		15°–32°		blue-grey pleochroism; also fan-shaped	in granite pegmatites and in greisen; lapidolite, quartz, topaz, cassiterite, wolframite
1.522–1.613	0.045		2°–8° (15°)		rarely zonar; pleochroic haloes around inclusions; with increasing Fe-content intensive absorption colours	in basic to ultrabasic plutonic rocks, in kimberlites, marbles and siliceous limestones; olivine, diopside, calcite, pyrope (in kimberlites) or olivine, melilite, leucite, nepheline
1.571–1.697	0.081		0°–35°		in volcanic rocks opacitized and corroded; pleochroic haloes; often mistaken for optically ⊖	in acidic to basic magmatic rocks, in metamorphic rocks; brown hbl, plagioclase, orthoclase, quartz, cpx, opx, glass (magmatic) or quartz, albite, muscovite, chlorite or almandine, staurolite, kyanite (metamorphic)
1.600–1.730	0.120		20°–30°		margins tend to be opacitized; pleochroic haloes around zircon	only as intratelluric phenocrysts esp. in intermediary volcanic rocks; oxyhornblende, quartz, plagioclase, sanidine, clino- and orthopyroxenes, rock-glass
1.599–1.695	0.044		5°–38°		weathered grains are bleached; pleochroic haloes around zircon	in Na-rich, Ti-rich magmatic rocks; nepheline, nosean, Na-sanidine, kaersutite, aegirine-augite, apatite
1.543–1.745	0.111	0°	0°	pseudo-uniaxial, similar to biotite, (but no bird's eye structure) kinked grains possible		in phyllites, schist, quartzites and blueschist; quartz, sericite, chlorite, calcite or glaucophane, sphene, garnet
1.592–1.644	0.032	2°–3° γ Λ a	0°–20°	never as oolite (contrary to chamosite)		in green sands and green sandstones, sometimes in limestones and marbles; quartz, calcite, pyrite
				pseudomorphs after olivine		filling cavities in basalts, also zeolite facies; olivine, pyroxene, zeolite, calcite, chlorite, chrysotile
1.539–1.596	0.050	0°	0°–30°	can be distinguished from sericite only by X-ray analysis		in talcschist and talc-rich mafic rocks; tremolite, clinochlore, quartz, antigorite or actinolite, clinochore, quartz, antigorite

Table 7d *Continued*

No./ *Page*	Mineral			Form and habit	Cleavage	Twinning	Colour	Pleochroism	Opt. ch.	Main zone
4.8.1 *115*	Chlorite group, monocl.	Orthochlorite	**Mg-chlorite**	thin to thick plates, flaky, scaly, fibrous, dense, matted	very good along (001)	lamellar, only sometimes visible in Mg-chlorite	colourless, greenish	very weak	⊖ ⊕	(+) (–)
			$MgFe^{2+}$-Fe^{2+}Mg-chlorite				pale green	weak	⊕ ⊖	(–) (+)
			Fe^{2+}-chlorite				dark olive to brown-green	good	⊖	(+)
4.8.2 *118*		Leptochlorite	Delessite Chamosite Thuringite	oolitic	cannot be distinguished from orthochlorites by polarizing microscopy alone. (see Fe^{2+} chlorite (orthochlorite))					
4.9.1 *118*	Serpentine group, monocl.		**Antigorite**	flaky, lath-shaped, scaly, dense	perfect on (001)	simple, not visible	colourless to pale green	very weak	⊖	(+)
4.9.2 *119*			**Chrysotile**	fibrous, brush-shaped					⊕ ⊖	(+) (–)
			Lizardite	fine-scaly fibrous	perfect on (001)				⊖	(+)
4.10.1.1 *125*	Feldspar group	Alkali feldspars	**Sanidine** monocl.	thin to thick plates, lath-shaped, hypidiomorphic to xenomorphic, granular	very good on (001), good on (010), cleavage angle approx. 90°	simple twin pairs	colourless			
4.10.1.2 *126*			**Orthoclase** monocl.						⊖	
4.10.1.3 *126*			**Anorthoclase** monocl.			microscopic to submicroscopic twins			⊕	
4.10.1.4 *127*			**Microcline** tricl.			grid-twinning			⊖	
4.10.2 *129*		Plagioclase	**Albite Oligoclase Andesine Labradorite Bytownite Anorthite** tricl.	thin to thick platy, lath-shaped, granular	very good on (001), good on (010), angle of cleavage sets approx. 86°	commonly as polysynthetic twins			⊕ or ⊖	

Refraction (n)	Max. Δ	Extinction angle	Axial angle 2V	Special diagnostic features	Occurrence; paragenesis
1.562–1.606	0.012	parallel to cleavage ≈ 0°	0°–5° 0°–30°	anomalous blue interference colours (pennine); normal interference colours (clinochlore)	in ultrabasic rocks, palaeo-rhyolites and acidic plutonic rocks; olivine, serpentine, pyroxene or quartz, orthoclase, microcline, biotite, brown or green hornblende
1.589–1.615	0.010		0°–10° 0°–40°	anomalous brown interference colours (MgFe-chlorite); anomalous blue interference colours (FeMg-chlorite)	in amygdules in magmatic rocks, alteration products of mafic minerals; biotite, pyroxene, amphibole, delessite
1.632–1.675	0.010		0°–30°	commonly normal interference colours; rare anomalous blue-grey interference colours	in low-grade metamorphic rocks, in blueschists and as diaphthoritic mineral formed from biotite or garnet; albite, sericite, biotite, quartz, epidote or albite, epidote, zoisite, actinolite, quartz or actinolite, albite, glaucophane, epidote, pumpellyite, lawsonite
					delessite in amygdules, in fractures and in the matrix of intermediary to basic volcanic rocks, otherwise similar to MgFe-chlorite; orthochlorite, calcite, zeolite, quartz
1.546–1.604	0.009	0°	27°–60°	fan-shaped multiple twins with undulatory extinction; grid texture in ultrabasic rocks	in low-grade metamorphic serpentinized rocks, in serpentinites (stress-induced); olivine, diallagite, chrysotile, orthopyroxene or talc, magnesite
1.532–1.561 1.538–1.567	0.013 0.008		10°–90° 30°–35°	forms from olivine in mesh texture; asbestos-forming in fractures	in hydrothermally altered ultrabasic and basic rocks; in greenschist facies (stress-free diaphthoresis); for paragenesis see antigorite
1.538–1.560	0.010		0°	main phase in bastite (pseudomorphous after opx)	in massive serpentinites or in opx-rich bastitized magmatic rocks; bronzite, chrysotile, antigorite
1.518–1.532	0.007		60°–65° (0°)	platy laths with twinning after Carlsbad law	in young volcanic rocks; quartz, plag., biotite, hbl, opx, cpx, rock-glass or nepheline, sodalite group, aegirine-augite, titanbiotite
1.518–1.530	0.007		60°–80°	commonly perthitic exsolution and Carlsbad twins; sericite common	in acidic to intermediary plutonic rocks, in older volcanic and subvolcanic rocks, in orthogneisses and arkoses; microcline, quartz, plag., biotite, hbl, sphene, sericite
1.522–1.535	0.008		110°–90° 60°–84°	microcline-like twinning; rare zonar growth (similar to plagioclase)	in Na-rich volcanic and subvolcanic rocks; aegirine-augite, aenigmatite, arfvedsonite, rock-glass, foids or quartz
1.518–1.526	0.006		60°–80°	microcline twinning law; commonly sericitized	in acidic to intermediary plutonic rocks, in pegmatites, in medium- to high-grade metamorphic rocks, in arkoses; orthoclase, quartz, plagioclase, biotite, hornblende, muscovite
1.527–1.539 ⋮ 1.575–1.588	0.007 ⋮ 0.013		50°–105°	size of axial angle and anorthite content dependent on conditions of formation: zonar growth is typically resorbed and corroded, commonly altered	in almost all magmatic and metamorphic rocks, in arkoses and greywacke; orthoclase, microcline, quartz, biotite, hornblende, orthopyroxene, clinopyroxene or olivine, titanaugite, glass, foids

Table 7d *Continued*

No./ *Page*	Mineral			Form and habit	Cleavage	Twinning	Colour	Pleochroism	Opt ch.	Main zone
2.7 *46*		Analcite cub.		rare rounded, commonly xenomorphic, octagonal	bad on (001)	polysynthetic, similar to leucite			⊖	
4.11.1.1 *135*	Fibrous zeolites	Natrolite group	Natrolite rhomb.	acicular, lath-shaped, fibrous, radiating aggregates	good	rare			⊕	(+)
4.11.1.2 *136*			Mesolite monocl.	fibrous		not distinct	colourless		⊕	
4.11.1.3 *136*			Thomsonite rhomb.	radially or randomly oriented fibres, columnar, flaky	perfect	sometimes simple			⊕	(±)
4.11.1.4 *137*			Scolecite monocl.	fibrous, radial	good	simple, very common			⊖	(–)
4.11.1.5 *138*		Mordenite group	Mordenite rhomb.	fibrous, dense, radial, fine-grained	good		colourless, rare reddish		⊕	(±)
4.11.1.6 *138*			Laumontite monocl.	radial, columnar, spherolitic	perfect	sometimes simple	colourless		⊖	(+)
4.11.2.1 *139*	Flaky zeolites	Heulandite–stilbite group	Heulandite monocl.	platy, flaky, in rosettes or subparallel aggregates		simple			⊕	(–)
4.11.2.2 *140*			Stilbite (desmine) monocl.	radial, fibrous to bundled aggregates, rare platy		interpentrating twins are common			⊖	(±)
4.11.2.3 *141*			Epistilbite monocl.	radial, fibrous aggregates, lath-shaped		simple and interpenetrating twins			⊖	(+)
4.11.3.1 *142*	Cubic zeolites	Phillipsite group	Phillipsite monocl.	thick columnar, mostly as interpenetrating twins	clear	interpenetrating twins or interpenetrating quadruplets	colourless		⊕	(+)
4.11.3.2 *143*			Harmotome monocl.						⊕	(±)
3.1.7 *64*		Chabazite trig.		idiomorphic, rhombohedral, rare xenomorphic	perfect on the rhombohedral planes ($10\bar{1}1$)	simple on (0001)			⊕ ⊖	

Refraction	Max. Δ	Extinction angle	Axial angle 2V	Special diagnostic features	Occurrence; paragenesis
1.486–1.487	0.001		very small	weakly birefringent subgrains; pseudocubic habit (see Part B, section 2.7)	in cavities and as interstitial material in volcanic rocks; heulandite, stilbite, laumontite
1.473–1.501	0.012	0°	58°–64°	pseudomorphs after plagioclase and foids are common; sometimes in the form of 'ice flowers'	in cavities and fractures in basic to intermediary magmatic rocks; nepheline, Na-sanidine, heulandite, stilbite, analcite, calcite, laumontite, scolecite, thomsonite
1.505–1.506	0.001	2°–5° β Λ c	80°	isotypic with natrolite and scolecite	in cavities in basic flows, (e.g. phonolites, basalts); zeolite, chalcedony, calcite
1.497–1.545	0.020	0°	44°–75°	shows highest birefringence in the zeolite family	in amygdules in basic to ultramafic magmatic rocks, in fractures in metamorphic rocks; natrolite, chabazite, scolecite, analcite, calcite, albite, chalcedony, chlorite or natrolite, thomsonite, stilbite, heulandite, calcite, chlorite, adularia, chalcedony
1.509–1.525	0.012	15°–18° α Λ c	36°–58°		
1.472–1.487	0.005	0°	76°–90°		in cavities and in fractures in acidic volcanic rocks; devitrification product, in sedimentary rocks; heulandite, laumontite, stilbite and other parageneses (see Part B, section 4.11.1.5)
1.502–1.525	0.012	8°–11° γ Λ c	33°–47°	extinction angle dependent on the degree of water loss	in cavities and in fractures in acidic to basic magmatic rocks, in metatuffs and metagreywackes in the zeolite facies; zeolite, apophyllite, albite, quartz, calcite, prehnite, datolite, chlorite, epidote
1.496–1.505	0.006	0°–32° β Λ c	0°–50°	conoscopic images in sections parallel to (010) show crossed dispersion	in cavities and in fractures in basic to acidic volcanic rocks, as devitrification product, in sedimentary rocks and in the zeolite facies; laumontite, analcite, quartz, stilbite
1.486–1.509	0.011	3°–12° α Λ c	30°–49°	twins with subdivisions in grains	in cavities and fractures in basic to acidic volcanic rocks; heulandite, laumontite, calcite, quartz, clay minerals
1.502–1.519	0.014	10° γ Λ c	44°	high birefringence compared to other zeolites	in hydrothermal amygdules in basalts and andesites; stilbite, mordenite, heulandite, chabazite, laumontite, scolecite
1.483–1.514	0.010	11°–30° γ Λ c	60°–80°	interpenetrating twins result in pseudorhombic or pseudocubic symmetry	in cavities and fractures in basic volcanic rocks, in nepheline syenite, as alteration product of rock-glass; analcite, natrolite, thomsonite, chabazite, chalcedony, calcite
1.503–1.514	0.008	28°–32° (→ 82°) β Λ c	79° (→ 32°)	heating during thin-section making changes the optical characteristics	in cavities in basic volcanic rocks, in veins in plutonic rocks; hyalophane, laumontite, natrolite, calcite
1.478–1.490	0.005	0°	0°–30°	anomalous subgrains; also optically biaxial (see Part B, section 3.1.7)	same as harmotome; phillipsite, thomsonite, calcite, analcite

Table 7d *Continued*

No./ *Page*	Mineral	Form and habit	Cleavage	Twinning	Colour	Pleochroism	Opt ch.	Main zone
4.12 *143*	Aenigmatite (cossyrite) tricl.	columnar to acicular	good, intersection angle 66°	polysynthetic twinning	dark brown to opaque	strong in very thin sections	⊕	
4.13 *144*	**Sphene** (titanite) monocl.	idiomorphic, spindle-shaped, granular	clear	simple	colourless, brownish, greenish	clear	⊕	
4.14 *145*	Topaz rhomb.	short columnar, acicular, divergent, lath-shaped, granular	perfect on (001)		colourless		⊕	(+)
4.15 *146*	**Cordierite** rhomb.	short columnar, xenomorphic, granular	poor, not visible under the microscope	simple lamellar, interpenetrating and contact twins	colourless, in thick thin sections bluish to purple	weak	⊖	
4.16.1 *148*	Al_2SiO_5 group: **Andalusite** rhomb.	short columnar, acicular, brush-like, granular	good on (110)		colourless, reddish, yellow, greenish	commonly patchy pink	⊖	(–)
4.16.2 *150*	Al_2SiO_5 group: **Sillimanite** rhomb.	acicular, fibrous, hair-like, brush-shaped, long columnar	perfect on (010)		colourless, rarely brownish	weak	⊕	(+)
4.16.3 *152*	Al_2SiO_5 group: **Kyanite** tricl.	tabular, lath-shaped, rarely radial	good on (100), very good on (010)	simple or lamellar	colourless, pale bluish, pale purple, blue	sometimes patchy blue	⊖	(+)
4.17 *153*	**Staurolite** rhomb.	wide lath-shaped, tabular	clear on (010), often not visible	interpenetrating twins	yellowish, orange, brownish to orange	clear in longitudinal sections	⊕ also ⊖	(+)
4.18 *154*	Wollastonite tricl.	acicular, fibrous, divergent, lath-shaped, platy	perfect on (100), good on ($\bar{1}02$) and (001)	lamellar	colourless		⊖	(+) (–)
4.19 *155*	Chloritoid tricl.	platy, angular, spherical	perfect on (001), good on (110)	simple and multiple twins	colourless, greenish, grey-blue	strong	⊖	(–)

Refraction (n)	Max. Δ	Extinction angle	Axial angle 2V	Special diagnostic features	Occurrence; paragenesis
1.81–1.88	0.07	4° parallel (100) 45° parallel (010) γ Λ c	27°–55°	homoaxial intergrowths with arfvedsonite are common; black to smoky haloes around orthite inclusions	in felsic, Na-rich magmatic rocks; aegirine-augite, arfvedsonite or riebeckite, anorthoclase
1.843–2.110	0.192	36°–51° γ Λ c	20–56°	rhomboidal-shaped cross-sections; patchy colour distribution; common in homogeneous extinction; can cause pleochroic haloes; in metamorphic rocks habit (look like 'insect eggs')	in acidic to intermediary magmatic rocks (absent in gabbro and basalt), in alpine veins, in amphibolites and marbles; K-feldspar, plagioclase, quartz, green hornblende, apatite or nepheline, sanidine, aegirine-augite, apatite
1.606–1.644	0.011	0°	48°–68°	swarms of fluid inclusions, divergent aggregates (pycnite)	in 'greisen' and in granitic contact aureoles; quartz, Li-mica, tourmaline, cassiterite wolframite, beryl, fluorite
1.527–1.578	0.018	0°	35°–106°	commonly alteration around margins and along cracks in orange to yellow pinite; yellow pleochroic haloes around radioactive inclusions; in metamorphic rocks common with inclusions of biotite and quartz or graphite	rare in acidic to intermediary magmatic rocks, in pegmatites, in knobby schist, in cordierite hornfels, in paragneiss, granulite and charnockite; quartz, K-feldspar, plagioclase, andalusite, sillimanite, biotite, garnet, hypersthene or quartz, plagioclase, biotite, muscovite, sillimanite, garnet, hercynite, andalusite
1.633–1.650	0.012	0°	73°–86°	common patchy pink coloration; sieve texture; graphite inclusions (chiastolite); pleochroic haloes are common	in knobby schist and hornfels, andalusite-bearing mica schists, pegmatoidal metatectites; sericite or muscovite, biotite, quartz, cordierite
1.653–1.683	0.022		21°–30° (in most cases cannot be measured)	needle-rich swarms in quartz, cordierite; diverging fibrous aggregates of sillimanite needles (fibrolite)	in mica schist, cordierite gneiss and rocks of the sanidinite facies; cordierite, quartz, K-feldspar, plagioclase, biotite, muscovite, kyanite, andalusite
1.710–1.734	0.017	oblique	78°–83°	patchy blue pleochroic coloration; stress-induced bending	in mica schist and quartzite, in granulites and eclogites; staurolite, almandine, biotite, muscovite, quartz, K-feldspar, plagioclase
1.736–1.761	0.014	0°	80°–90°	typical interpenetrating twins and pleochroism; sieve texture	exclusively in middle-grade metamorphic rocks; kyanite, quartz, biotite, muscovite, albite and almandine
1.616–1.653	0.014	3°–5° β Λ b	36°–60°	nearly square cross-sections; poikiloblastic	in metamorphic siliceous limestones and marbles, rare in phonolites, nephelinites and foyaites; diopside, fassaite, vesuvianite, epidote, grossularite, calcite, quartz
1.705–1.740	0.012	20° β Λ b	36°–70° (124°)	zonar, hourglass texture, sieve texture	typical for low-grade metamorphic rocks; quartz, albite, sericite, chlorite, biotite, almandine, rutile

Table 7d *Continued*

No./ *Page*	Mineral		Form and habit	Cleavage	Twinning	Colour	Pleochroism	Opt ch.	Main zone
4.20.1 *156*	Epidote zoisite group	**Zoisite** (thulite) rhomb.	lath-shaped, hexagonal cross-section, divergent radiating, granular	perfect on (100), poor on (001)		colourless (purple)	(strong)	⊕	(–)
4.20.2 *157*		**Epidote** (piemontite) monocl.			rarely simple	greenish-yellow, patchy or zonar (red-purple)	weak to (strong)	⊖ ⊕	
4.20.3 *158*		**Clinozoisite** monocl.		perfect on (001), clear on (100)	sometimes lamellar	colourless		⊕	(±)
4.20.4 *159*		Orthite (allanite) monocl.	granular, acicular, needle-shaped		commonly simple	pale grey-yellow, orange-brown	quite clear	⊖ also ⊕	
4.21 *160*	Pumpellyite monocl.		lath-shaped, needle-shaped, acicular, fibrous, radial rosettes	perfect on (100), clear on (001)	common	colourless to blue-green	very weak to clear	⊕	(±)
4.22 *160*	Lawsonite rhomb.		platy, lath-shaped	very good on (010), good on (100)	polysynthetic twinning	colourless, rare bluish	in most cases absent	⊕	(–)
4.23 *161*	Anhydrite rhomb.		granular, dense, acicular	perfect on (001), very good on (010) and (100)	polysynthetic	colourless		⊕	(±)
4.24 *162*	Gypsum monocl.		platy, fibrous, granular, dense, spherolitic	perfect on (010), very good on (100) and $\{\bar{1}11\}$	simple	colourless		⊕	(±)
4.25 *163*	Aragonite rhomb.		radial, acicular, short to long columnar	poor, commonly not visible	simple to lamellar	colourless		⊖	(–)
4.26 *164*	Barite rhomb.		flaky, granular, fibrous, dense, columnar, platy, radial	perfect on (001), good on {110} and (010)	polysynthetic interpenetrating twins	colourless		⊕	(–)
4.27 *165*	Goethite rhomb.		needle-shaped, radial fibrous, dense, oolitic	good on (010)		yellow, yellow-orange, orange-brownish, orange	weak to clear	⊖	
4.28 *166*	Prehnite rhomb.		platy, flaky, fan-shaped, in radiating aggregates or dendritic	good on (001)	rare fine lamellar on (110) and (001)	colourless		⊕	(±)

Refraction (n)	Max. Δ	Extinction angle	Axial angle 2V	Special diagnostic features	Occurrence; paragenesis
1.685–1.725	0.008	0°	0°–69°	anomalous blue to brown interference colours; rare normal interference; thulite shows pleochroism	in low-grade metamorphic rocks and siliceous limestones; chlorite, sericite, actinolite, epidote, clinozoisite, albite, prehnite
1.715–1.797	0.051	0° parallel b, in all other cases oblique ≈ 30° γ Λ c	64°–90°	anomalous bright interference colours; piemontite shows pleochroism from yellow to orange to red-purple	in low- to medium-grade regional metamorphic rocks, epidote also in contact aureoles and epidote-bearing magmatic rocks, in blueschist facies; for paragenesis see Part B, section 4.20.2
(1.730–1.829)	(0.073)		(64°–106°)		
1.670–1.734	0.015		40°–90°	also anomalous blue interference colours; in difference to epidote biaxial⊕	
1.690–1.891	0.036		40°–123°	complete metamictic alteration is possible (Δ → 0°)	in low- to high-grade regional metamorphic rocks, in acidic to intermediary magmatic rocks; epidote, sphene, tourmaline
1.665–1.726	0.020	4°–22° (dependent on chemical composition) γ Λ c	7°–110°	commonly anomalous interference colours (blue to brown); zonar, oak-leaf-shaped intergrowth with lawsonite	in greenschist facies, in amygdules, in blueschist; for paragenesis see Part B, section 4.21
1.663–1.686	0.021	0°	76°–87°	parquet floor-like subgrains with undulatory extinction in stressed metamorphic rocks	in lawsonite-glaucophane schist, in greenschist and amphibolites; glaucophane, albite, jadeite, pumpellyite
1.570–1.613	0.044	0°	42°	often bent cleavage planes; with addition of water alteration into gypsum	in evaporites, rare in cavities in volcanic rocks; gypsum, halite, K-salt, quartz, calcite
1.519–1.531	0.010	15° α Λ b	58°	tends to be bent; polysynthetic twins can form during thin-section preparation; simple twins common	in NaCl-K-salt series and sedimentary rocks; anhydrite, halite, K-salt, calcite, quartz
1.530–1.686	0.156	0°	18°	dependent on orientation differences in relief	in cavities and veins in basic volcanic rocks, in organic shell material as thermal deposits; zeolite, calcite
1.636–1.649	0.012	0°	36°–38°	in flaky aggregates, kinking and crenulation possible	as gangue in hydrothermal deposits, in concretions in sandstone and in desert roses (barite-rose); quartz, celestite, sulphide
2.15–2.415	0.140	0°	0°–27°	component of limonite; strong dispersion of optic axes	in weathered/altered Fe-minerals and rocks, in cavities and fractures, in Fe-ore deposits; lepidocrocite, hematite
1.611–1.669	0.039	0°	64°–71°	sometimes anomalous blue to brown interference colours; commonly anomalous subgrains (parquet-floor-like); smaller axial angle 2V = 0° in subgrains	in basic volcanic rocks, rare in gabbros to granodiorite, in greenschists, metabasalts and in metamorphic siliceous limestone; for paragenesis see Part B, section 4.28

Table 8 Reflected colours and habit of opaque and nearly opaque minerals (important minerals are shown in bold)

Number	Mineral	Colour	Form and habit
1.1	**Magnetite**	blue-black	octahedral grains, rare skeletal crystals
1.2	Ilmenite	purple-black	feather-like crystals or irregularly shaped grains, commonly intergrown with magnetite
1.3	Hematite	steel-blue, red or black	at crystal edges and in very thin flakes blood-red translucent
1.4	Pyrite	pale-yellow	idiomorphic with square, rectangular or triangular sections
1.5	Pyrrhotite	bronze-coloured	irregularly shaped aggregates or 'serrated' crystals
1.6	**Graphite**	black	smeared-out margins, flaky or very fine granular
1.7	Carbonaceous substances	black to black-brown	dust-like, in thin flakes brownish to grey translucent
2.2	**Chromite**	iron-black to brown-black	crystal edges dark-brown translucent; small grains are opaque
2.10.1	Limonite	yellow-brown	amorphous, oolitic; translucent edges are isotropic
	Leucoxene	white	fine-grained alteration mineral of primary Ti-minerals (e.g. ilmenite, sphene)

Table 9 Anomalous birefringence in isotropic minerals and substances (important minerals are shown in bold)

Number	Mineral	Anomaly
2.1	Perovskite	lamellar subgrains
2.4	Grossularite	zonar subgrains
2.4	Andradite	cyclic subgrains
2.4	Uvarovite	cyclic subgrains
2.5	**Leucite**	lamellar subgrains (Fig. 51)
2.6	**Sodalite**	inclusions surrounded by tension-induced birefringence
2.7	Analcite	lamellar subgrains (Fig. 58)
2.8	Cristobalite	ball-shaped subgrains with weak birefringence
2.10.2	Opal	tension-induced birefringence due to changes in water content
2.10.3	**Rock-glass**	tension-induced birefringence around inclusions

Table 10 Anisotropic minerals with optical isotropic behaviour (submicroscopic and metamictic minerals respectively) (important minerals are shown in bold)

Number	Mineral	Submicroscopic	Metamictic
1.3	Hematite (crumbly)	+	
	Leucoxene	+	
3.1.3	**Zircon**		+
3.2.6	Apatite (in phosphorites)	+	
	Clay minerals	+	
4.9	**Serpentine**	+	
4.20.4	Orthite		+

Table 11 Rock-forming minerals sorted according to their colours in thin section and pleochroism respectively, viewed in plain polarized light (strongly coloured minerals are shown in bold)

		yellow, yellowish	orange gold-yellow	reddish, red	purple	grey-purple	bluish, blue	greenish, green	brownish, brown
isotropic		orthite perovskite rock-glass	orthite perovskite rock-glass	almandine **hematite** limonite perovskite	fluorite hauyne	perovskite	fluorite hauyne nosean sodalite	fluorite grossularite **hercynite** pleonaste	andradite **chromite** **limonite** **melanite** opal orthite perovskite **picotite** rock-glass
optically uniaxial	positive	cassiterite rutile xenotime zircon	cassiterite	rutile cassiterite xenotime zircon	zircon	rutile		clinochlore penninitee chlorite vesuvianite xenotime zircon	cassiterite rutile vesuvianite xenotime zircon
	negative	anatase cancrinite corundum gehlenite siderite scapolite vesuvianite	**tourmaline**	apatite corundum **hematite** **tourmaline**	corundum **tourmaline**	**tourmaline**	anatase beryl corundum **tourmaline**	beryl **tourmaline** vesuvianite	anatase apatite dolomite gehlenite siderite **tourmaline** vesuvianite
optically biaxial	positive	**piemontite** pumpellyite **sphene** **staurolite** thulite	**piemontite** **sphene** **staurolite**	**aenigmatite** mordenite **piemontite** pigeonite thulite	piemontite thulite titanaugite	titanaugite	chloritoid cordierite **magnesio-riebeckite**	chlorite chloritoid chrysotile pumpellyite pyroxene **sphene**	**aenigmatite** orthite pyroxene sillimanite **sphene** **staurolite**
	negative	**crossite** epidote fayalite **hastingsite** orthite phlogopite **piemontite** **stilpnomelane** **staurolite**	andalusite goethite phlogopite **piemontite** **staurolite**	andalusite goethite hypersthene lepidolite mordenite **oxybiotite** **oxyhornblende** **piemontite**	**crossite** kyanite **glaucophane** lepidolite **piemontite**	**katophorite**	**arfvedsonite** **barroisite** chloritoid cordierite **crossite** kyanite **glaucophane** riebeckite	**aegirine-augite** **barroisite** actinolite andalusite **arfvedsonite** **biotite** bronzite chlorite chloritoid epidote fayalite fuchsite **glauconite** **hastingsite** hypersthene celadonite serpentine smaragdite **stilpnomelane** **tschermakite**	**biotite** cassiterite chlorite goethite **hastingsite** hypersthene **kaersutite** **katophorite** orthite **oxybiotite** **oxyhornblende** phlogopite **stilpnomelane** **titanbiotite**

Table 12 Optically uniaxial minerals with anomalous biaxial behaviour (bold = commonly biaxial)

Anatase	Cancrinite	Nepheline	Vesuvianite
Apatite	Cassiterite	**Quartz**	Zircon
Apophyllite	Chabazite	Rutile	
Beryl	Chalcedony	Tridymite	
Calcite	Corundum	Tourmaline	

Table 13 Optically biaxial minerals with nearly optically uniaxial behaviour (bold = mainly uniaxial)

Biotite	Glauconite	Phlogopite	Talc
Chlorite	Lepidolite	Pigeonite	Zoisite
Clinochlore	Pennine	Sanidine	
Heulandite	Phengite	Stilpnomelane	

Table 14 Minerals with distinct, strong zonar growth

yellowish, yellow	epidote, grossularite
orange, golden-yellow	cassiterite, orthite, tourmaline
reddish, red	andalusite, corundum, piemontite, thulite
purple	titanaugite, tourmaline, zircon
bluish, blue	arfvedsonite, glaucophane, hauyne, corundum, tourmaline
greenish, green	amphibole, aegirine-augite, chlorite, chloritoid, epidote
brownish, brown	anatase, biotite, hornblende, kaersutite, melanite, orthite, oxyhornblende, phlogopite, tourmaline, vesuvianite

Table 15 Minerals with a distinct hourglass structure (bold = very strong)

Aegirine-augite	Oxidized amphibole
Chloritoid	Prehnite
Epidote	**Titanaugite**

Table 16 Minerals with anomalous interference colours (bold = very characteristic)

Aegirine-augite	**Clinozoisite**	Plagioclase	Titanaugite
Anatase	**Epidote**	Prehnite	**Vesuvianite**
Antigorite	**FeMg-chlorite**	Pumpellyite	Zoisite
Apophyllite	Laumontite	Sanidine	
Chloritoid	Melilite	Sphene	

Table 17 Minerals in which pleochroic haloes surrounding radioactive inclusions are common

Andalusite	Cordierite	Lepidolite	Staurolite
Biotite	Hornblende	Muscovite	Tourmaline
Chlorite		Phlogopite	

Table 18 Minerals which cause radioactive haloes in their immediate environment

Cassiterite	Sphene
Orthite	Xenotime
Rutile	Zircon

Table 19 Minerals with a characteristic cleavage

In one direction	In two directions	In three directions
cancrinite	alkali feldspars	anhydrite
chlorite	amphiboles	barite
chloritoid	andalusite	calcite
epidote	mesolite	cancrinite
gypsum	natrolite	corundum
glauconite	plagioclase	dolomite
mica	pyroxene	fluorite
heulandite	rutile	kyanite
clinozoisite	scapolite	lawsonite
corundum	scolecite	magnesite
piemontite	sphene	perovskite
prehnite	wollastonite	rutile
sillimanite		siderite
staurolite		scapolite
stilbite		
stilpnomelane		
thomsonite		
topaz		
zoisite		

Table 20 Mainly idiomorphic minerals

Cubic	Tetragonal	Hexagonal and trigonal	Orthorhombic	Monoclinal	Triclinal
analcite	cassiterite	apatite	andalusite	aegirine-augite	microcline
fluorite	melilite	beryl	hypersthene	amphibole	plagioclase
garnet	rutile	calcite	lawsonite	epidote	
hauyne	scapolite	cancrinite	olivine	jadeite	
leucite	vesuvianite	chabazite	staurolite	orthoclase	
magnetite	zircon	corundum	topaz	pyroxene	
nosean		dolomite	zoisite	sanidine	
perovskite		nepheline		sphene	
pyrite		quartz			
sodalite		tourmaline			
spinel					

Table 21 Common crystal shapes in minerals

Granular	Columnar	Bladed	Fibrous	Acicular	Platy
analcite	alkali feldspars	aegirine-augite	actinolite	aragonite	antigorite
andalusite	amphiboles	actinolite	gypsum	mesolite	chlorite
anhydrite	barite	andalusite	jadeite	natrolite	chloritoid
apatite	beryl	aragonite	magnesio-riebeckite	rutile	mica
barite	cancrinite	barite	mesolite	scolecite	graphite
calcite	chlorite	beryl	natrolite	stilbite	hematite
cassiterite	clinozoisite	biotite	nephrite	thomsonite	stilpnomelane
chalcedony	corundum	clinozoisite	prehnite	tourmaline	talc
chromite	kyanite	epidote	serpentine		
cordierite	mica	feldspars	sillimanite		
dolomite	nepheline	gypsum	thomsonite		
epidote	plagioclase	glaucophane	tremolite		
fluorite	pyroxene	hedenbergite	wollastonite		
gypsum	quartz	ilmenite			
glauconite	scapolite	jadeite			
garnet	staurolite	kyanite			
hauyne	topaz	piemontite			
lawsonite	vesuvianite	prehnite			
leucite	wollastonite	scapolite			
magnesite	zoisite	scolecite			
magnetite		staurolite			
melilite		thomsonite			
nepheline		thulite			
olivine		tremolite			
orthite		tourmaline			
quartz		vesuvianite			
rutile		wollastonite			
sodalite		zoisite			
sphene					
spinel					
topaz					
zircon					

Radiating	Oolitic	Spherulitic	Micrographic intergrowth	Fossil mineral
aragonite chalcedony chlorite natrolite stilbite thomsonite tourmaline	apatite (in phosphorite) calcite chamosite limonite siderite	anorthoclase calcite chalcedony cristobalite orthoclase prehnite sanidine siderite	glass – leucite corundum – andalusite nepheline – feldspar quartz – actinolite quartz – feldspar quartz – staurolite	apatite aragonite calcite chalcedony dolomite glauconite opal quartz

Table 22 Heavy minerals

		colourless	yellow	red	blue	green	brown	opaque (black)
isotropic		fluorite rock-glass grossularite spinel	andradite rock-glass grossularite melanite picotite spessartine	almandine fluorite perovskite picotite pyrope spessartine	fluorite spinel	andradite fluorite grossularite hercynite pleonaste spinel uvarovite	fluorite rock-glass melanite perovskite pictotite spessartine spinel	hematite ilmenite magnetite pyrite pyrrhotite
optically uniaxial	positive	cassiterite quartz xenotime zircon	cassiterite quartz rutile xenotime zircon	rutile xenotime zircon		xenotime zircon	cassiterite quartz rutile xenotime zircon	
	negative	anatase apatite beryl corundum dolomite magnesite siderite tourmaline vesuvianite	anatase beryl corundum dolomite tourmaline vesuvianite	apatite beryl corundum hematite tourmaline vesuvianite	anatase beryl corundum tourmaline vesuvianite	apatite beryl tourmaline vesuvianite	anatase apatite hematite magnesite tourmaline vesuvianite	
optically biaxial	positive	anhydrite augite barite bronzite chlorite chloritoid diopside enstatite lawsonite olivine pigeonite pumpellyite sillimanite sphene staurolite topaz zoisite	barite lawsonite olivine piemontite pigeonite sillimanite sphene staurolite thulite titanaugite topaz	anhydrite piemontite pigeonite sphene thulite topaz	anhydrite chloritoid hedenbergite lawsonite sillimanite sphene topaz	augite chlorite chloritoid diopside hedenbergite olivine pigeonite pumpellyite sphene topaz	bronzite chlorite enstatite olivine piemontite pigeonite pumpellyite sillimanite sphene staurolite titanaugite	
	negative	actinolite andalusite aragonite biotite chlorite chloritoid clinozoisite kyanite muscovite olivine tremolite wollastonite zoisite	actinolite aragonite biotite epidote hornblende hypersthene muscovite olivine orthite piemontite wollastonite	andalusite biotite crossite glaucophane goethite hornblende hyperstene orthite piemontite	arfvedsonite chloritoid glaucophane hornblende kyanite riebeckite	aegirine-augite actinolite andalusite arfvedsonite biotite chlorite chloritoid epidote fayalite glaucophane hornblende hypersthene muscovite orthite riebeckite	biotite chlorite goethite hornblende hypersthene olivine orthite piemontite siderite	

Appendix 2 Diagrams for the classification of magmatic rocks

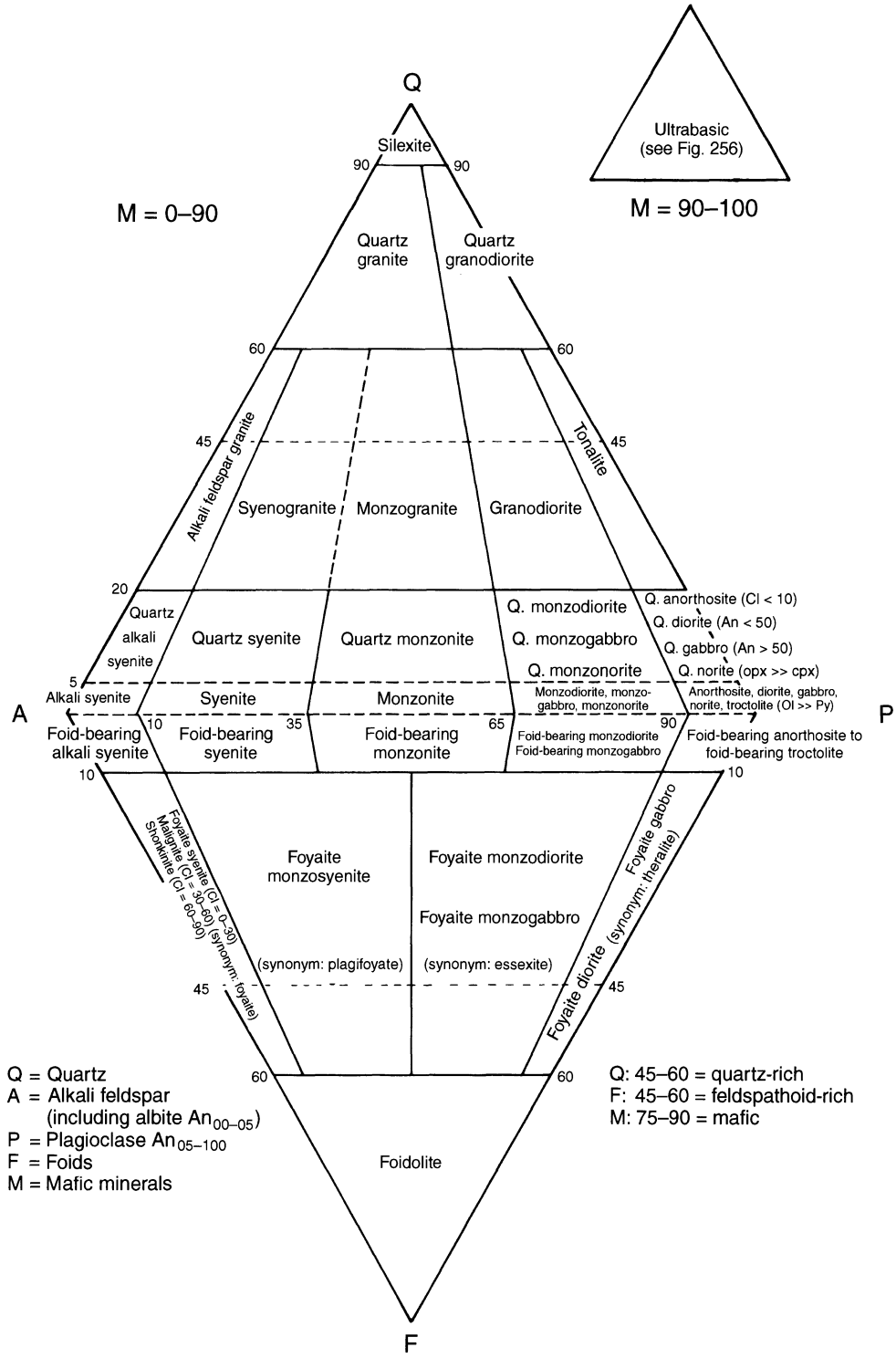

Fig. 254 Classification of plutonic rocks.

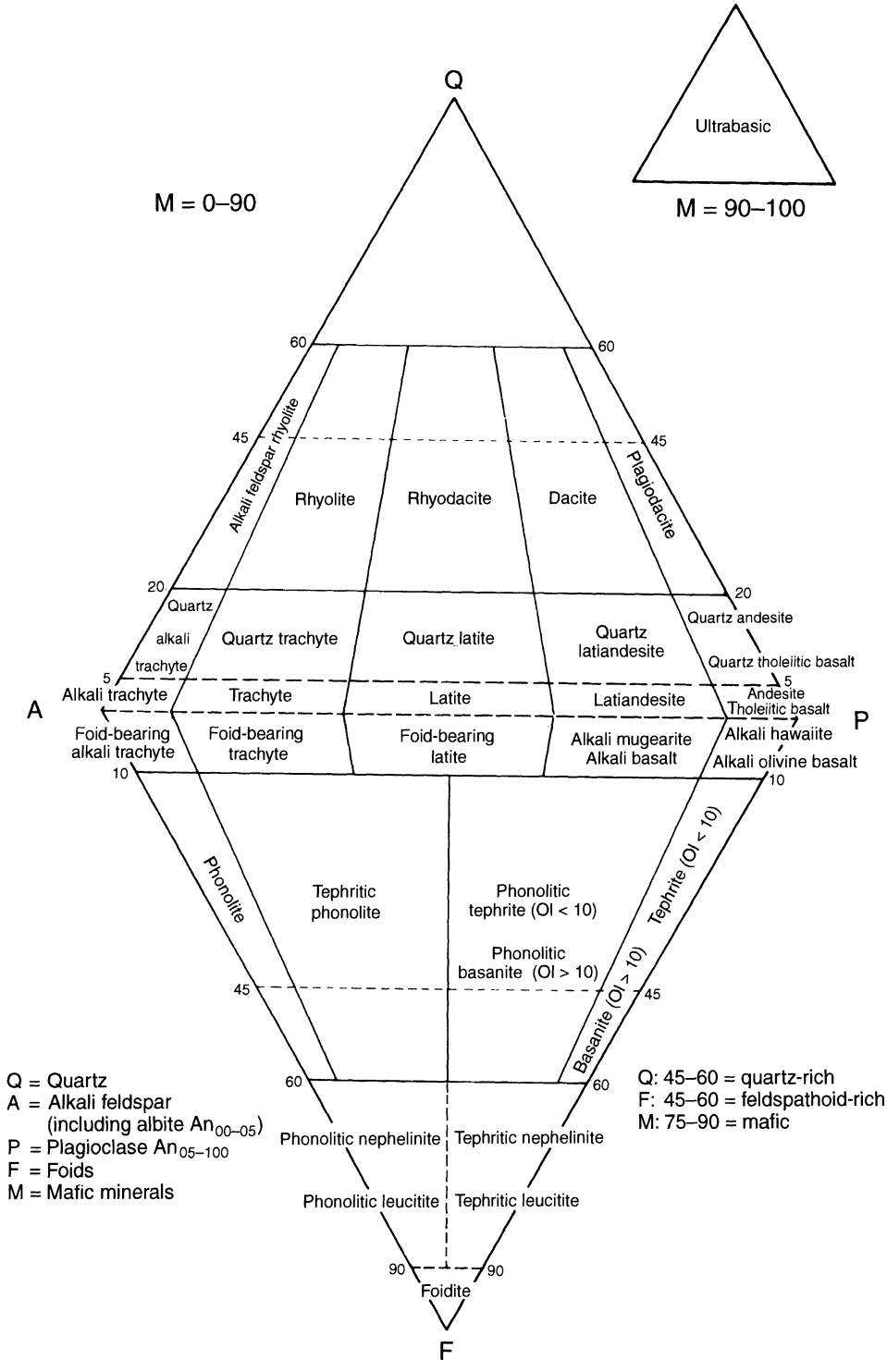

Fig. 255 Classification of volcanic rocks.

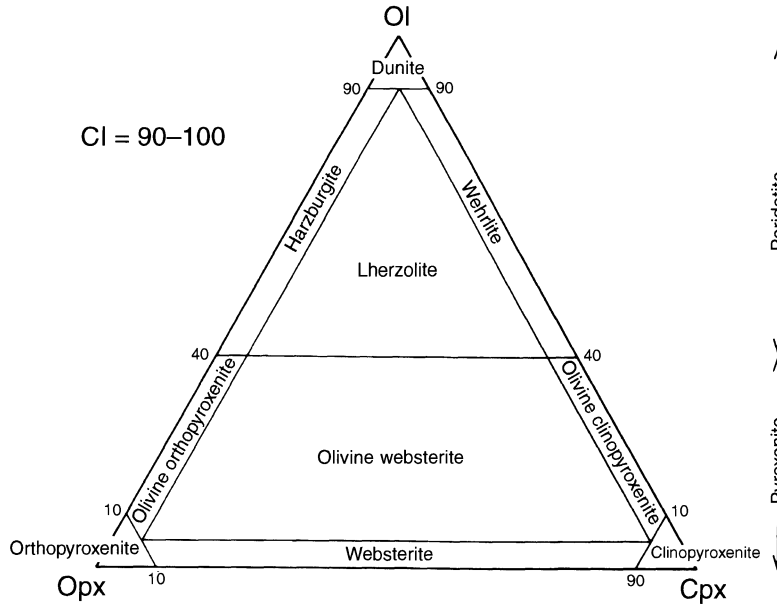

Fig. 256 Classification of part of ultrabasic magmatic rocks (Field 16 of Fig. 254).

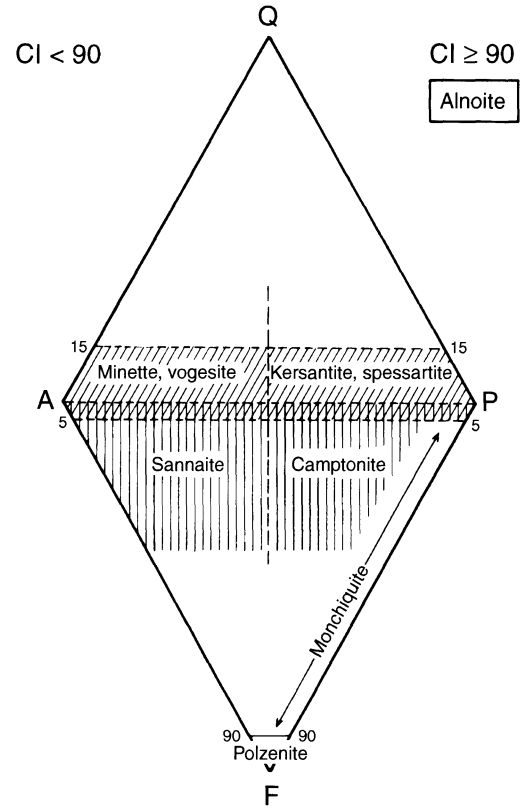

Fig. 257 Classification of lamprophyres. *Calc-alkaline lamprophyres*: minette, vogesite, kersantite, spessartite. *Alkaline lamprophyres*: sannaite, camptonite, monchiquite. *Melilitic lamprophyres*: polzenite, alnoite. (Overlap between minette/vogesite with sannaite and between kersantite/spessartite with camptonite.)

Appendix 3 Diagrams of mineral and rock structures

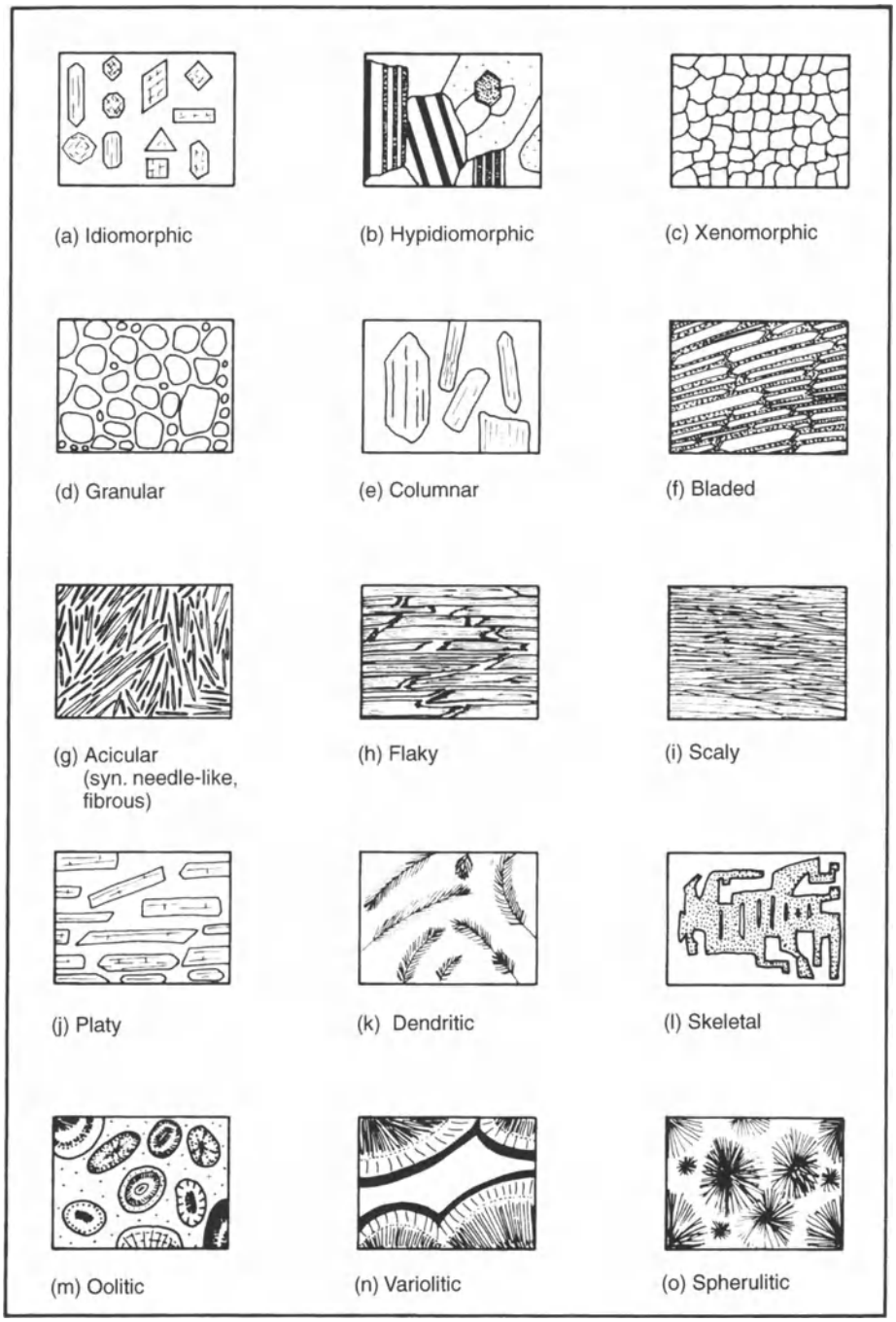

Fig. 258 Various mineral forms and textures.

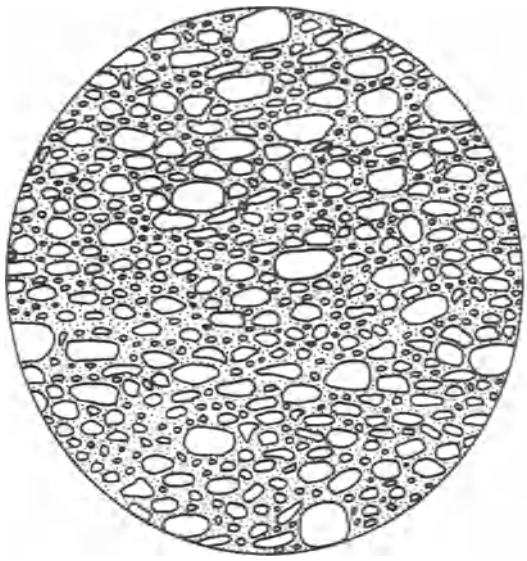

Fig. 259 Hyaline vesicular texture of a pumice without phenocrysts.

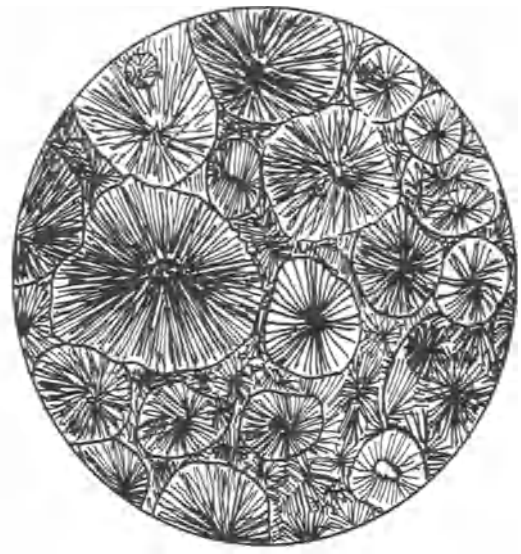

Fig. 260 Spherulitic texture, typical for hyaline volcanic rocks (obsidian). Glass has recrystallized to alkali feldspar and SiO_2 minerals.

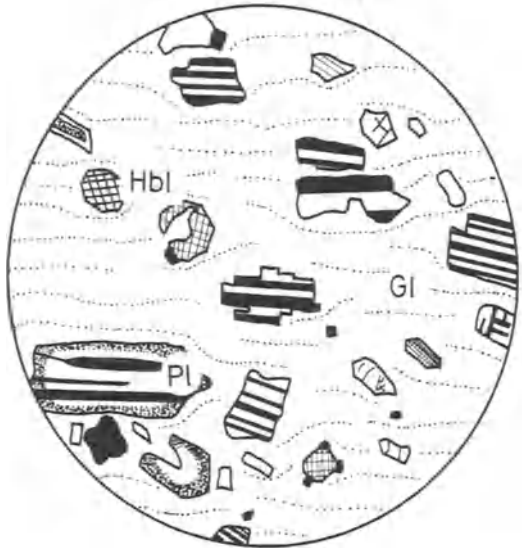

Fig. 261 Vitrophyric texture. Phenocrysts embedded in a glass matrix (dacite).

Fig. 262 Hyaline-porphyric texture in an ignimbrite with quartz, feldspar and biotite phenocrysts.

Fig. 263 Microcrystalline-porphyric texture. Very common in volcanic rocks. Phenocrysts of at least two generations are embedded in a matrix comprised of microlites and glass (dacite).

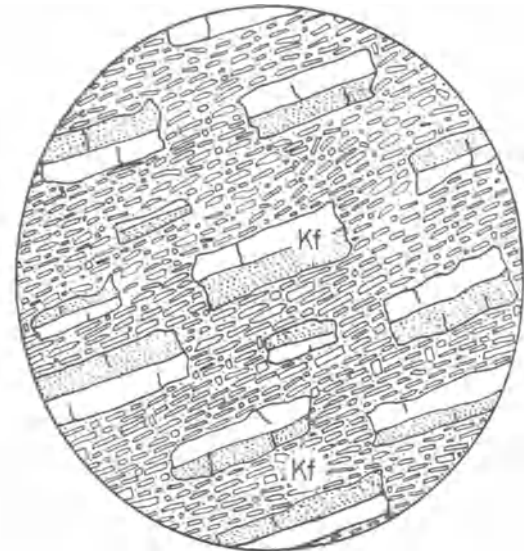

Fig. 264 Hypocrystalline trachytic flow texture with aligned sanidine phenocrysts embedded in a matrix of oriented sanidine microlites and rock-glass (phonolite).

Fig. 265 Intersertal texture. Plagioclase laths randomly oriented embedded in a matrix of pyroxene and rock-glass (basalt).

Fig. 266 Amygdaloidal texture of a volcanic rock. Filling of the amygdules by calcite, zeolite and chalcedony.

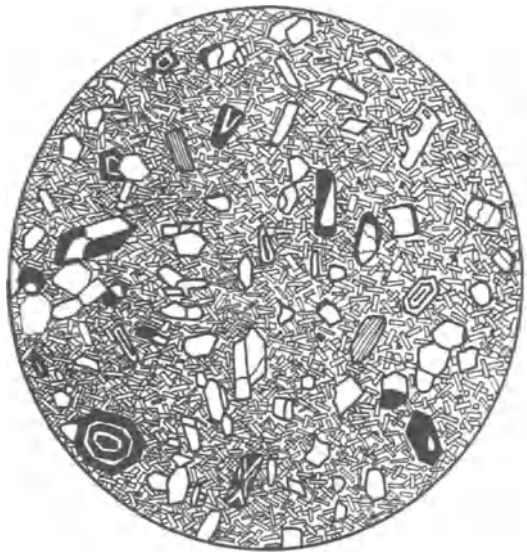

Fig. 267 Microcrystalline-intersertal texture. Abundant small plagioclase laths randomly oriented surrounded by a matrix of pyroxene, plagioclase and rock-glass (basalt). Older generation of various phenocrysts is striking.

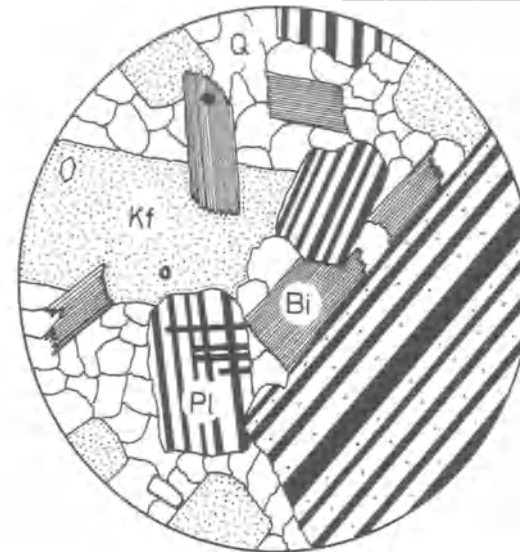

Fig. 268 Holocrystalline-hypidiomorphic (subhedral) texture in a granodiorite.

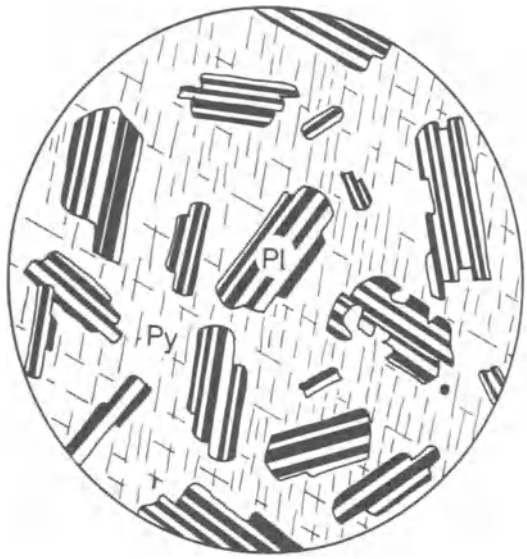

Fig. 269 Ophitic texture: idiomorphic plagioclase phenocrysts surrounded by a matrix of pyroxene (dolerite).

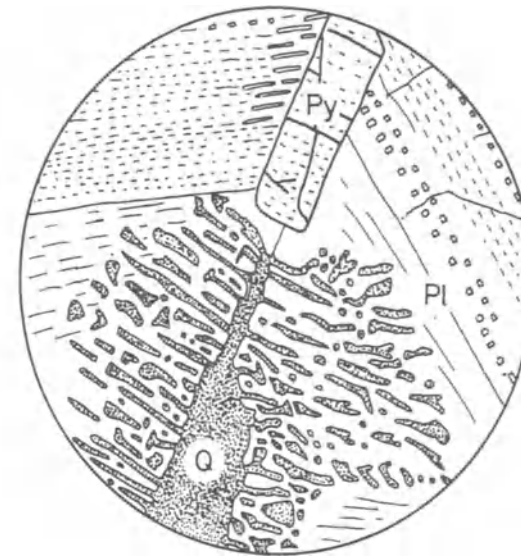

Fig. 270 Intergrowth texture of 'aggressive' quartz with plagioclase (myrmekitic texture).

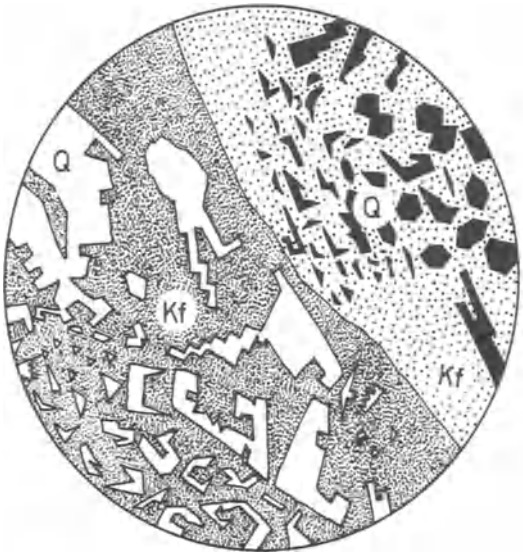

Fig. 271 Intergrowth texture: intergrowth of quartz and alkali feldspar = graphic texture = granophyric texture.

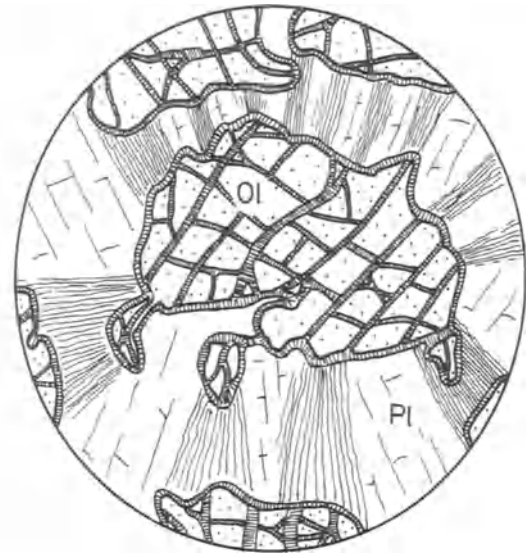

Fig. 272 Corona texture in an olivine gabbro.

Fig. 273 Lepidoblastic texture. Plicated small-scale sericite flakes and fine quartz grains (phyllite).

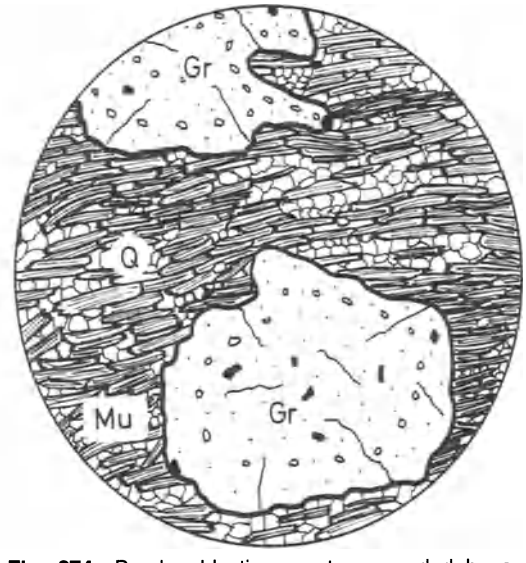

Fig. 274 Porphyroblastic garnet surrounded by a matrix of lepidoblastic muscovite flakes and quartz grains (garnet mica-schist).

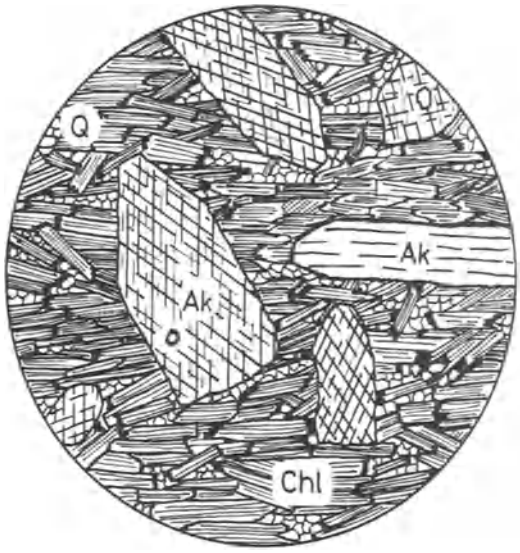

Fig. 275 Nematoblastic-lepidoblastic texture with lath-shaped actinolite phenocrysts in an actinolite-chlorite schist with lepidoblastic chlorite.

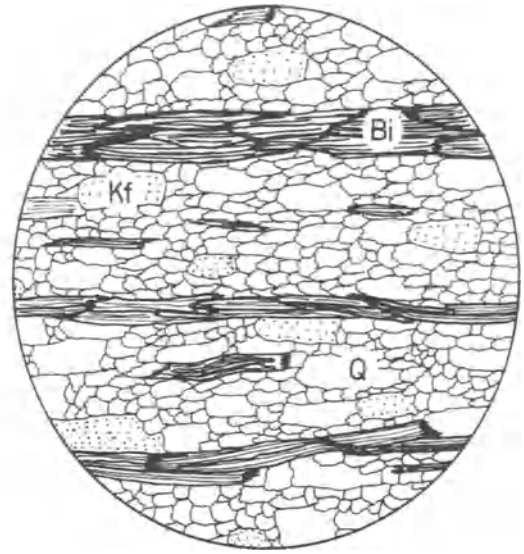

Fig. 276 Granoblastic texture, orthogneiss with mica layers. Polygonal texture with some serrated-grain boundaries between quartz and feldspar.

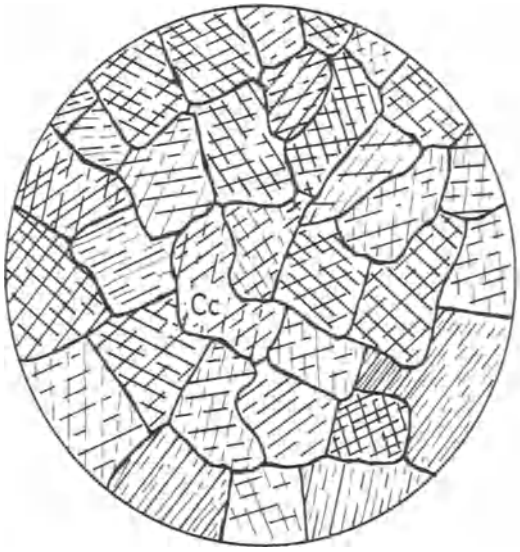

Fig. 277 Granoblastic marble with polygonal grains.

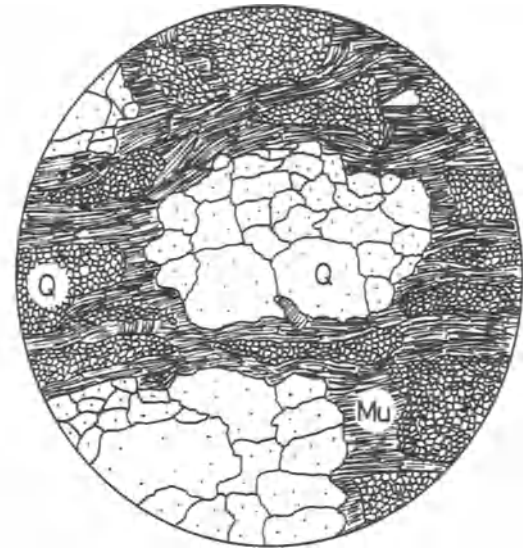

Fig. 278 Porphyroclastic texture. Broken up quartz porphyroblasts surrounded by a matrix of quartz, feldspar and mica (cataclastic gneiss).

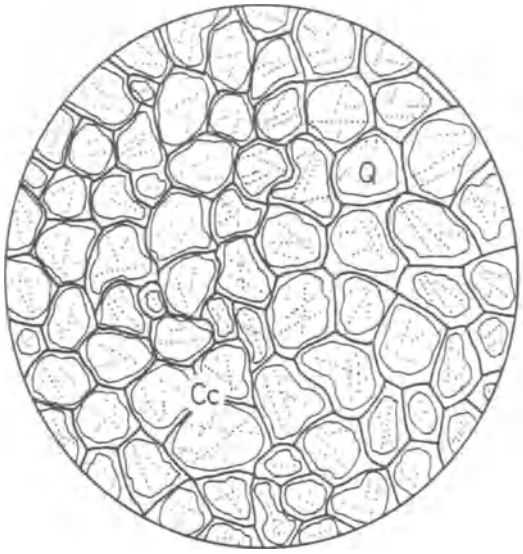

Fig. 279 Granular texture in a calcareous sandstone with carbonate cement.

Fig. 280 Pseudosparitic-cataclastic texture with angular quartz and calcite phenocryst fragments in a carbonate cement.

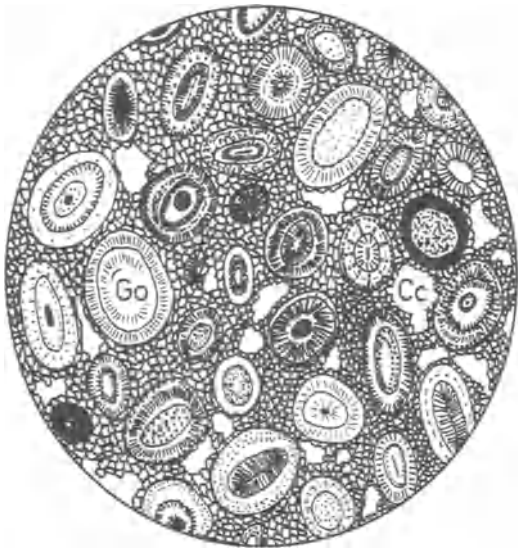

Fig. 281 Oolitic texture. Goethite oolite in a carbonate cement (iron-oolite, middle Jurassic).

Bibliography

Adams, A. E., MacKenzie, W. S. and Guilford, C. (1995) *Atlas of sedimentary rocks under the microscope*, Longman, Harlow.

Chudoba, K. (1932) *Mikroskopische Charakteristik der gesteinsbildenden Mineralien*, Herder & Co., Freiburg i. Br.

Chudoba, K. (1932) *Die Feldspäte und ihre praktische Bestimmung*, Schweizerbart, Stuttgart.

Carozzi, A. V. (1960) *Microscopic sedimentary petrography*, Wiley, London/New York.

Deer, W. A., Howie, R. A. and Zussman, J. (1992) *An introduction to the rock-forming minerals*. 2nd edition, Longman, Harlow.

Fleischer, M., Wilcox, R. E. and Matzko, J. J. (1984) Microscopic determination of the nonopaque minerals. *U. S. Geol. Surv. Bull*, **1627**.

Gribble, C. D. and Hall, A. J. (1985) *A practical introduction to optical mineralogy*. 1st edition Chapman & Hall, London.

Harthorne, N. H. and Stuart, A. (1969) *Practical optical crystallography*, 2nd edition, Arnold, London.

Heinrich, E. W. (1965) *Microscopic identification of minerals*, McGraw-Hill, New York.

Kerr, P. F. (1977) *Optical mineralogy*, 4th edition, McGraw-Hill, New York.

Klein, C. and Hurlbutt, C. S. (1993) *Manual of mineralogy*, 21st edition, Wiley, New York.

Leake, B. E. (1978) Nomenclature of amphiboles. *Mineral. Mag.*, **42**, 533–66.

Le Maitre, R. W. (1989) *A classification of igneous rocks and glossary of terms*, Blackwell Sci. Publ., Oxford.

Lof, P. (1982) *Elsevier's mineral and rock table*, Elsevier, Amsterdam.

MacKenzie, W. S., Donaldson, C. H. and Guilford, C. (1995) *Atlas of igneous rocks and their textures*, Longman, Harlow.

MacKenzie, W. S. and Guilford, C. (1980) *Atlas of rock-forming minerals in thin section*, Longman, Harlow.

MacKenzie, W. S. and Guilford, C. (1993) *Atlas of rock-forming minerals in thin section*, 2nd edition Longman, Harlow.

Mange, M. A. and Maurer, H. F. W. (1991) *Heavy minerals in colour*, Chapman & Hall, London.

Mason, R. (1989) *Petrology of the metamorphic rocks*, 2nd edition, Allen & Unwin, London.

McCrone, W. C., McCrone, L. B. and Delly, J. G. (1978) *Polarized light microscopy*, Ann Arbor Science Publ., Ann Arbor, Michigan.

Michel-Lévy, A. (1894) *Étude sur la détermination des feldspaths dans les plaques minces*, Baudry & Cie., Paris.

Morimoto, N. (1988) Nomenclature of pyroxenes. *Fortschr. Miner.*, **66**, 237–52.

Mücke, A. (1989) *Anleitung zur Erzmikroskopie*, Enke, Stuttgart.

Müller, G. and Raith, M. (1987) *Methoden der Dünnschliffmikroskopie, Clausthaler tektonische Hefte*, **14**, 4th edition, Ellen Pilger, Clausthal-Zellerfeld.

Paltzelt, W. J. (1974) *Polarisationsmikroskopie (Grundlagen, Instrumente, Anwendungen)*, Leitz, Wetzlar.

Phillips, W. R. and Griffen, D. T. (1981) *Optical mineralogy: the nonopaque minerals*, Freeman, San Francisco.

Ramdohr, R. (1980) *The ore minerals and their intergrowths*, 2nd edition, Volume 1, Pergamon Press, Oxford.

Rittmann, A. (1929) Die Zonenmethode. Ein Beitrag zur Methodik der Plagioklasbestimmung mit Hilfe des Theodolithtisches. *Schweiz. mineral. petrogr. Mitt.*, **9**: 1–46, Zurich.

Rittmann, A. (1963) Quantitative Konoskopie. *Schweiz. mineral. petrogr. Mitt.*, **43**: 11–36, Zurich.

Saggerson, E. P. (1975) *Identification tables for minerals in thin sections*, Pergamon Press, London and New York.

Schneiderhöhn, P. (1952) *Erzmikroskopisches Praktikum*, Schweizerbart, Stuttgart.

Schuster, M. (1881) Ueber die optische Orientierung der Plagioklase. *Tscherm. mineral. petrogr. Mitt.*, **3**: 117–284, Vienna.

Shelley, D. (1975) *Manual of optical mineralogy*, 4th edition, Elsevier, Amsterdam.

Stoiber, R. E. and Morse, S. A. (1994) *Crystal identification with the polarizing microscope*, Routledge, London.

Tröger, W. E. (1969) *Optische Bestimmung der gesteinsbildenden Mineral*. Part 2: Textbook, 2nd edition, Schweizerbart, Stuttgart.

Wahlstrom, E. E. (1979) *Optical crystallography*, 5th edition, Wiley, New York.

Williams, H., Turner, F. H. and Gilbert, G. M. (1982) *Petrography: an introduction to the study of rocks in thin sections*, 2nd edition, Freeman, San Francisco.

Winchell, A. N. and Winchell, H. (1961) *Elements of optical mineralogy. Part II: Description of minerals*, 4th edition, Wiley, New York.

Winchell, A. N. and Winchell, H. (1962) *Elements of optical mineralogy. Part III: Determinative tables*, 2nd edition, Wiley, New York.

Yardley, B. W. D., MacKenzie, W. S. and Guilford, C. (1990) *Atlas of metamorphic rocks and their textures*, Longman, Harlow.

Index

Page numbers appearing in **bold** refer to figures and page numbers appearing in *italics* refer to tables.